International PhD Program in Biomolecular Sciences

Department of Cellular, Computational and Integrative Biology – CIBIO

XXXIII Cycle

Insight into the role of complement C1/WNT axis in dystrophic muscles.

Tutor

Prof. Luciano CONTI

University of Trento

Advisor

Prof. Stefano BIRESSI

University of Trento

Dulbecco Telethon Laboratory of Stem Cells and Regenerative Medicine

Ph.D. Thesis of

Francesca FLORIO

University of Trento

Dulbecco Telethon Laboratory of Stem Cells and Regenerative Medicine

Academic Year 2019-2020

Declaration of original authorship

I Francesca Florio confirm that this is my own work and the use of all material from other sources has been properly and fully acknowledged.

Contributions provided by other researchers to the project

Stefano Biressi designed the project, provided general supervision and reviewed this dissertation. The ELISA assays for complement proteins quantification were performed by Annexon Biosciences (California, US).

Table of Contents

Abstract

Duchenne muscular dystrophy (DMD) is the most common inherited muscle disease of childhood. Although under normal conditions muscle stem cells present a very powerful regenerative response, the regenerative potential is progressively lost in patients affected by DMD and fibrotic tissue progressively replaces muscle fibers leading to an impairment of muscle function. Elevated Wnt-signaling has been shown to play a detrimental role in the regenerative process and promotes the accumulation of fibrotic tissue in dystrophic muscles. However, the molecular and cellular pathways responsible for this process are poorly characterized. The C1 protein complex consists of C1q, C1r and C1s and is involved in the innate immunity cascades, specifically the classical complement pathway. C1q has been reported to activate the canonical Wnt-signaling pathway in compromised skeletal muscles (i.e., in aging).

We hypothesized that the C1 complex could be responsible for the enhanced activity of the canonical Wnt-signaling pathway in Duchenne muscular dystrophy.

We present here evidence that the classical complement system expression is increased in dystrophic muscles of the *mdx*^{4Cv} mice compared to the healthy controls and that all the subunits of the C1 complex (i.e., C1q and C1r/s) are locally expressed by muscle-resident cells. Data presented here link the increased expression of the classical complement system to the enhanced canonical Wnt signaling pathway, which is reported in dystrophic muscles. Particularly, we found that specific cells in the stem cell niche (i.e., macrophages and fibro/adipogenic progenitors) are augmented in the dystrophic muscles, secrete distinct subunits of the C1 complex and could act as combinatorial sources of Wnt activity. In keeping with these observations, enhanced C1q protein levels released by macrophages positively correlate with the increased expression of Wnt-target proteins in the dystrophic regenerating areas. We show here that murine cell lines (i.e., macrophages and fibroblasts) recapitulate the expression of all five C1 complex subunits observed *in vivo*. By combining the use of recombinant proteins and conditioned media derived from cultured macrophages and fibroblasts, we found that the C1 complex induces the expression of the canonical Wnt signaling in murine fibroblast and myoblasts. Importantly, we show that the *in vivo* pharmacological inhibition of C1 by targeting C1r/s esterase leads to a reduced expression of canonical Wnt and fibrogenic genes in the dystrophic fibro/adipogenic progenitor cells and to an overall amelioration of the dystrophic muscle phenotype such as a reduced collagen deposition and reduced fibrotic muscle area. The fib-*mdx* mouse model is a dystrophic mouse in which chronic mechanical micro injuries induce augmented levels of muscle fibrosis compared to the *mdx*. Here we present an implemented version of the fib-*mdx* model in which the canonical Wnt-signaling is increased and that better resembles the pathology.

This work supports the idea that enhanced complement levels could be detrimental in the dystrophic environment. By increasing the comprehension of the link existing between the complement system and degenerative diseases like DMD the findings presented here will contribute to open to the definition of novel therapeutic strategies to investigate in the clinical setting.

List of abbreviations

AAV	Adeno-associated virus
AAV-CRISPR	AAV-Clustered Regularly Interspaced Short Palindromic Repeats
AchR	Acetylocholine receptor
Agtr1a	Type-1A angiotensin II receptor
Agtr1b	Type-1B angiotensin II receptor
AIDS	Acquired ImmunoDeficiency Syndrome
ALK5	Activin linked kinase 5
ANOVA	Analysis of Variance
AON	Antisense oligoribonucleotides
APC	Adenomatous Polyposis Coli
Areg	Amphiregulin
AT_1	Angiotensin II type 1
Barx2	BARX Homeobox 2
bFGF	basic fibroblast growth factor
BSA	Bovine Serum Albumin
C1	Complement Component 1
C1-INH	Complement Component 1 inhibitor
C1q	Complement component 1q
C1qa	Complement component 1qa
C1qb	Complement component 1qb
C1qc	Complement component 1qr
C1r	Complement component 1r
C1s	Complement component 1s
C2	Complement component 2
C2a	Complement component 2a
C2b	Complement component 2b
C3	Complement component 3
C3a	Complement component 3a
C3a/C3aR	Complement component 3a/Complement component 3a receptor
C3aR1	Complement component 3a receptor 1
C3b	Complement component 3b
C4	Complement Component 4
C4a	Complement Component 4a

C4b	Complement Component 4b
C5	Complement Component 5
C5a	Complement Component 5a
C5a/C6aR	Complement Component 5a/Complement component 6 a receptor
C5b	Complement Component 5b
C7	Complement Component 7
C8	Complement Component 8
C9	Complement Component 9
CAD	Cold agglutinin disease
CD106	Cluster of Differentiation 106
CD133	Cluster of Differentiation 133
CD25	Interleukin-2 receptor alpha chain
CD31	Cluster of differentiation 31
CD34	Cluster of differentiation 34
CD4	Cluster of differentiation antigen 4
CD45	Cluster of differentiation 45
CD59	Leukocyte cluster of differentiation antigen 59
CK1	Casein Kinase I
CLR	Collagen region
CTGF	Connective Tissue Growth Factor
DAF	Decay-accelerating factor
Daf1	Decay accelerating factor 1
DAMPs	Damage-Associated Molecular Patterns
Dbr	Dystrobrevin
DG	Dystroglycan
DGC	Dystrophin glycoprotein complex
DIA	Diaphragm
DII4	Delta Like Canonical Notch Ligand 4
DM	Dermatomyositis
DMD	Duchenne muscular dystrophy
DMEM	Dulbecco's Modified Eagle's Medium
dpi	days post injury
DR3	Death receptor 3
DRB1	DR Beta 1
DS	Donkey serum
Dvl	Dishevelled

E2F1	E2F transcription factor 1
EAMG	Experimental autoimmune myasthenia gravis
ECM	Extracellular Matrix
ECs	Endothelial Cells
EDL	Extensor Digitorum Longus
EDTA	Ethylenediamine tetraacetic acid
EGFP	Enhanced Green Fluorescent Protein
EMA	European Medicines Agency
FACS	Fluorescence Activated Cell Sorting
FAPs	Fibro/Adipogenic Progenitors
FBS	Fetal Bovine Serum
Fc	Fragment crystallizable
FDA	Food and Drug Administration
FGF	Fibroblasts Growth Factor
FGF2	Fibroblast Growth Factor 2
FGF3	Fibroblast Growth Factor 3
FoxO	Forkhead box O
Foxp3	Forkhead box P3
FSC	Forward scatter
Fzd	Frizzled
Fzd1	Frizzled Class Receptor 1
Fzd2	Frizzled Class Receptor 2
Fzd4	Frizzled Class Receptor 4
Fzd5	Frizzled Class Receptor 5
Fzd6	Frizzled Class Receptor 6
Fzd7	Frizzled Class Receptor 7
Fzd8	Frizzled Class Receptor 8
Fzd9	Frizzled Class Receptor 9
GRMD	Golden Retriever Muscular Dystrophic
gRNA	guide RNA
GSK3β	Glycogen Synthase Kinase 3β
HEA	Hereditary Angiodema
HGF	Hepatocyte Growth Factor
HL	Hindlimb
HLA	Human Leukocyte Antigen
HPRT	Hypoxanthine-guanine phosphoribosyltransferase

IGF-1	Insulin-like Growth Factor-1
IgG	Immunoglobulin G
IgM	Immunoglobulin M
IL-1	Interleukin-1
IL-10	Interleukin-10
IL-12	Interleukin-12
IL-13	Interleukin-13
IL-1β	Interleukin-1β
IL-33	Interleukin-33
IL-4	Interleukin-4
IL-6	Interleukin-6
IL-8	Interleukin-8
INF-γ	Interferon-γ
IP3	Inositol triphosphate
IRI	Ischemia-Reperfusion Injury
Jack/STAT	Janus kinase-Signal Transducer and Activator of Transcription
JDM	Juvenile Dermatomyositis
JNK	c-Jun N-terminal Kinases
Lef1	Lymphoid Enhancer Binding Factor 1
Lgr5	Leucine Rich Repeat Containing G Protein-Coupled Receptor 5
Lin	Lineage
LPS	Lipopolysaccharide
LRP5	Lipoprotein receptor-related protein 5
LRP6	Lipoprotein receptor-related protein 6
Lyz2	Lysozyme2
MAC	Membrane Attack Complex
Mac-1	Macrophage-1 antigen
MASP-1	Mannose-Associated Serine Protease 1
MASP-2	Mannose-Associated Serine Protease 2
MBL	Mannan-Binding Lectin
MBP-1	Major Basic Protein 1
MG	Myasthenia Gravis
MHC	Major Histocompatibility Complex
MMPs	Metalloproteinases
MRFs	Myogenic Regulatory Factors
MuSCs	Muscle Stem Cells

Myf5	Myogenic Factor 5
MyoD	Myoblast Determination protein 1
NMJ	Neuromuscular Junction
nNOS	Neuronal Nitric Oxide Synthase
OCT	Optimal Cutting Temperature
Pax7	Paired Box 7
PBS	Phosphate-Buffered Saline
PCP	Planar Cell Polarity
PDGFαr	Platelet-Derived Growth Factor Receptor α
pSMC	porcine Smooth Muscle Cells
PW1	Paternally expressed gene 3
Q	Quadriceps
RAWm	RAW 264.7 conditioned medium
ROCK	Rho-associated protein kinase
SAMP1	Senescence-accelerated mouse prone 1
Sca1	Stem Cell Antigen 1
SCs	Satellite Cells
Serping1	Serpin Family G Member 1
Setdb1	SET Domain Bifurcated Histone Lysine Methyltransferase 1
Smad2	SMAD Family Member 2
Smad3	SMAD Family Member 3
Smad4	SMAD Family Member 4
SSC	Side Scatter
STOm	STO conditioned medium
Syn	Syntrophin
TA	Tibialis Anterior
TALEN	Transcription Activator-Like Effector Nuclease
TCF/LEF	T-cell Factor/Lymphoid Enhancing Factor
Tcf3	Transcription Factor 3
TCF4	Transcriptional Factor 4
Tcf7l1	Transcription Factor 7 Like 1
TCF7L2	Transcription Factor 7 Like 2
TGFβ1	Transforming growth factor beta 1
TGFβ2	Transforming growth factor beta 2
TGFβ3	Transforming growth factor beta 3
TLRs	Toll-Like Receptors

TNFα	Tumor Necrosis Factor alpha
Tregs	Regulatory T cells
Twist2	Twist Family BHLH Transcription Factor 2
uPA	Urokinase type Plasminogen Activator
VCAM1	Vascular Cell Adhesion Molecule 1
VEGF	Vascular Endothelial Growth Factor
VEGF-A	Vascular Endothelial Growth Factor-A
WISP1	WNT1 Inducible Signaling Pathway Protein
Wnt	Wingless Int-1
Wnt11	Wingless Int-11
Wnt16	Wingless Int-16
Wnt2	Wingless Int-2
Wnt2b	Wingless Int-2b
Wnt3	Wingless Int-3
Wnt3a	Wingless Int-3a
Wnt5a	Wingless Int-5a
Wnt6	Wingless Int-6
Wnt7a	Wingless Int-7a
Wnt9b	Wingless Int-9b
WT	Wild type
YFP	Yellow Fluorescent Protein

List of Figures and Tables

List of Main Figures

List of Supplementary Figures

List of Tables

1. Introduction

1.1 Skeletal muscle in health and disease

1.1.1 Skeletal muscle and muscle stem cell niche

Skeletal muscle. Skeletal muscle, which represents approximately 35% of the total mass of a human, is an organ that fulfils several functions in the body. Skeletal muscle functions include power generation for motion, postural behavior, breathing and temperature homeostasis control [1]. The basic cell unit of skeletal muscle is the myofiber. Myofibers are single elongated multinucleated cells formed during development following proliferation and fusion process of muscle progenitor cells (named myoblasts) [2]. Following injury (single or repeated), and throughout the life of an individual, the skeletal muscle has a remarkable capacity to regenerate and restore its full physiological tissue architecture and functionality. Skeletal muscle regeneration consists of several highly coordinated cellular processes, which lead to the formation of a tissue similar to uninjured muscle. The importance of skeletal muscle regeneration appears clear when considering what happens when it is impaired throughout physiological aging or in pathologies such as muscular dystrophies or heterotopic ossification [3–5]. Muscle regeneration requires the orchestrated contribution of at least three different players in the tissue: 1) the muscle stem cells (also known as satellite cells) which are quiescent in uninjured muscle, but become activated after an injury, proliferate and after several cell division eventually fuse and differentiate into new myofibers; 2) the extracellular matrix (ECM), a scaffold made of collagens, glycoproteins, proteoglycans, laminin and elastin in which muscle fibers reside; 3) support cells, including both tissue-resident cells found in the interstitial spaces between myofibers and cells infiltrating from the circulation.

The muscle stem cell niche. Satellite cells have historically been considered the primary contributors to the regenerative process. Borrowing from and expanding upon the concept of *stem cell niche*, first proposed by Schofield [6] referring to the hematopoietic stem cells, the *satellite cell niche* (or muscle *stem cell niche*) has been defined as the microenvironment in which satellite cells reside. The *satellite cell niche* provides mechanical and chemical cues to promote satellite cells quiescence rather than activation, proliferation, or differentiation [7]. This environment includes the myofibers, the ECM, the support cells, and the blood vessels. The skeletal muscle can exist in different states (i.e., uninjured/injured) and the *satellite cell niche* exhibits differences both in its composition and functionality depending on weather the tissue is in homeostasis or undergoing different stages of regeneration. After muscle injury, inflammation occurs at the injury site and different types of infiltrating immune cells are engaged. Satellite cells become activated and undergo a mitotic phase

followed by differentiation into new myofibers. The *satellite cell niche* may also be referred to as *quiescent niche*, *inflammatory niche*, *mitogenic niche* or *differentiative niche* depending on which state the tissue is at a given moment in time [8] **(Figure 1)**. The dynamics of the *satellite cell niche*, its function during muscle quiescence and regeneration and its components will be described in this thesis.

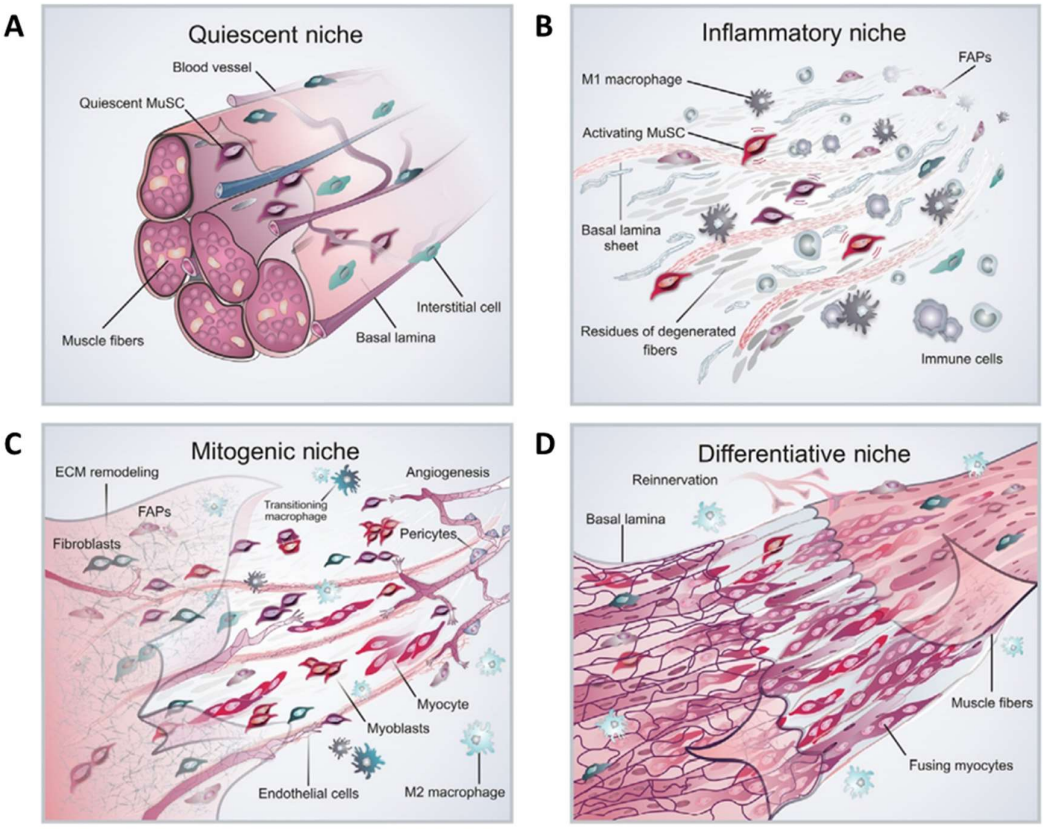

Figure 1. The muscle *stem cell niche* in homeostasis and regeneration. (A) The *quiescent niche* maintains MuSCs in their dormant state in the absence of muscle injury. **(B)** Following injury, the *inflammatory niche* exhibits muscle fibers' debris and a high abundance of inflammatory immune cells. **(C)** Successively, the niche becomes permissive to MuSCs proliferation (*mitogenic niche*). It is characterized by extensive ECM synthesis by fibroblastic cells and angiogenesis. **(D)** In the differentiative phase, anti-inflammatory macrophages become dominant and MuSC-derived myoblasts fuse into new muscle fibers. New myofibers are reinnervated and new membranes mature (*differentiative niche*). Modified from [8].

1.1.2 Muscle Stem Cells or Satellite Cells

Muscle stem cells (MuSCs) are also known as satellite cells (SCs). They have been named like that for the first time by Alexander Mauro in 1961 due to their anatomic location intimately associated

with the muscle fiber. Mauro observed through electro-microscopy that these cells provided with their own plasmalemma shared the basal lamina of a muscle fiber. Given their close association with the myofibers and being the regenerative potential of the skeletal muscle already a known concept, he predicted that SCs could have contributed to the myofiber repair [9]. Several *in vitro* and *in vivo* studies, throughout different stages of development, have elucidated the stem cell nature of these cells, revealing their contribution to muscle regeneration, and confirming the Mauro hypothesis.

During homeostasis adult MuSCs exist in a cellular state outside of the replicative cell cycle (G0 phase) in a quiescent phase characterized by a low metabolic activity and mitotic inactivity [10]. MuSCs quiescence is regulate by different mechanisms of the *quiescent niche*, such as the ECM interactions on their apical pole and the muscle fiber interactions on their basal pole. Different components of the ECM (i.e. laminin α2, β1, γ1 and collagen IV), blood vessels, vessel-associated smooth muscle cells and pericytes play a role to the maintenance of the MuSCs quiescence [11–14]. The Notch signaling supports MuSCs quiescence by inhibiting cell differentiation and inducing the expression of extracellular components of the niche [15–17]. The Notch-induced microRNA-708 regulates MuSCs quiescence and self-renewal by antagonizing cell migration [18]. Moreover, the proximity of MuSCs to the blood vessels and the capacity of MuSCs to recruit vessel cells has recently shed light on the contribution of endothelial cells in maintaining MuSC quiescence likely through the endothelial cells-derived Notch ligand DII4 [19]. The heparan sulfate on the basal lamina of both fibers and MuSCs sequesters growth factors from the environment, also contributing to MuSCs dormant state [20].

Muscle injury or trauma is followed by a regenerative response that consists of three phases: 1) inflammation of the site of damage, occurring immediately after the injury; 2) a mitogenic phase, in which MuSCs exit the G0 phase, enter the cell cycle and undergo extensive mitosis; in this phase also support cells proliferate significantly; 3) a final differentiation phase, during which myoblasts produced in the mitogenic stage fuse and differentiate into new fibers restoring the muscle initial composition and functionality. Importantly, given their stem cell nature, a set of MuSCs is capable of self-renew ensuring maintenance of the satellite cells pool [21].

Muscle regeneration is finely regulated by MuSC expression of myogenic regulatory factors (MRFs) [22–28]. Among the MRFs of note are Myf5, MyoD and myogenin. Myf5 is the first activation marker expressed after an injury and enables a transient myoblast amplification [29,30]; MyoD is an activation and differentiation marker [24,31,32]; myogenin is expressed in association with irreversible cell cycle exit and terminal differentiation [25,27,28]. In quiescence and up to the beginning of the differentiation process, all MuSCs express the transcriptional factor Paired Box 7 (Pax7) [33]. Pax7 is not expressed in other cellular types in adult muscle and its absence leads to severe impairment of muscle regeneration [34]. Studies on isolated MuSCs from the skeletal muscle of adult mice have been possible thanks to several protocols based on both positive and negative selection of cell surface markers combined to the

Fluorescence Activated Cell Sorting (FACS) technique [35]. Moreover, the mouse strain $Pax7^{CreER}$;$R26R^{YFP}$, which is generated by crossing Pax7-$CreER^{tm}$ to $R26R^{YFP/YFP}$ mice and has the CreER knocked into the Pax7 locus, has enabled the *in vivo* tracing of MuSCs progeny using the yellow fluorescent protein (YFP) reporter gene after tamoxifen administration [36]. A mouse strain (i.e., Tg(Pax7-EGFP)#TAjb) in which the Pax7 mouse promoter drives the expression of a nuclear localized EGFP [37] and a mouse strain carrying a Cre-ER^{T2} knock-in allele at the Pax7 locus, the $Pax7^{CE}$ allele [38] also represent robust tools for the study of the dynamic behaviors of MuSCs. Isolation of MuSCs using either the YFP expression of $Pax7^{+ve}$ cells in $Pax7^{CreER}$;$R26R^{YFP}$ mice or the expression of vascular cell adhesion molecule 1 (VCAM1; also known as cluster of differentiation 106 (CD106)) on the MuSCs surface [35] has been used in the experiments presented in this thesis.

1.1.3 Extra cellular matrix

The extra cellular matrix (ECM) is defined as the non-cellular component present within all tissues and organs in the body. In the skeletal muscle, the ECM coats and surrounds the muscle fibers, providing essential physical scaffolding for all the components of the *satellite cell niche*, nerves, and vessel. The ECM is important for the fiber force transmission and it takes part in crucial biochemical and biomechanical processes required for tissue morphogenesis, homeostasis, and differentiation [39]. A wide range of syndromes arise from genetic abnormalities of its components [40]. Collagens, glycoproteins (i.e. fibronectin), proteoglycans, and elastin are the major components of muscle ECM [39]. However, given the complexity of the environment in which fibers exists, several other proteins, ECM regulators and secreted factors interacting with core ECM proteins have to be taken into account when considering the extracellular space at any given time of muscle physiology as well as muscle pathology [41]. Within the 28 different members of collagen superfamily, types I, III, IV, V, VI, XII, XIII, XIV, XV, XVIII, and XXII have been reported to be present in skeletal muscle at gene and/or protein level [39]. Among them, types I and III collagen are by far the most abundant, accounting together for ~75% of total muscle collagens [42].

Fibrosis. The abnormal deposition and accumulation of ECM components within a tissue is referred to as fibrosis. Fibrosis can interfere with the functional parenchyma of several organs and it can either be the primary or the secondary cause of several degenerative and inflammatory conditions [43]. In addition, fibrosis-related conditions are particularly challenging to treat due to the poor penetrability of several drugs into the scar-like fibrotic tissue [44]. In skeletal muscle, fibrosis development occurs in response to acute or chronic injury, it is associated with an impairment of muscle regeneration and can be particularly harmful as it interferes with proper muscle contraction and functionality. This happens with different extent of severity in a variety of muscle pathologies, including muscular dystrophies [4]. In addition, the aged muscle is generally infiltrated by fibrotic tissue [45].

1.1.4 Interstitial cells

As suggested by their name, the interstitial cells are cells that are found in the interstitial space (i.e., between myofibers) of skeletal muscle. These cells are essential components of the *satellite cell niche* and provide critical support to MuSCs both at rest and during regenerative processes. Fibro/adipogenic progenitors, macrophages, immune cells, endothelial cells, pericytes, fibroblasts and interstitial cells with myogenic potential are all members of this category.

FAPs. Fibro/adipogenic progenitors (or FAPs) are multipotent progenitors that gained their name from being capable to differentiate in both adipose and fibrotic tissue within the muscle [46,47]. However, as they have been shown to differentiate also in other cell types (i.e. chondrocytes and osteogenic cells), these cells are also broadly referred to as mesenchymal cells [48,49]. FAPs are characterized by the expression of the cell surface markers platelet-derived growth factor receptor α (PDGFαr) and stem cell antigen 1 (Sca1) [46,50,51]. These markers have been used in experiments presented in this thesis to trace FAPs cells *in vivo* (PDGFαr) or to FACS isolate them (Sca1). FAPs have been directly involved in the secretion and remodeling of the ECM upon muscle injury and play a central role in the accumulation of fibrotic tissue in both aging and muscular dystrophies [52]. Interestingly, the canonical Wnt pathway has been implicated in the increased proliferation of $Sca1^{+ve}$ resident cell population in muscles of dystrophic mice and in the subsequent augmentation of collagen deposition [53]. In addition to their contribution to the fibrosis development, some studies have suggested that FAPs may be involved in regenerative processes. Joe and colleagues have shown that FAPs increase myogenic differentiation of MuSCs-derived myoblasts, supporting the satellite cells-mediated regeneration [46]. FAPs number during regeneration is regulated by cytokines released from inflammatory macrophages. This underlies the crosstalk existing between FAPs and immune cells that infiltrate the injury site during the first phases of muscle regeneration [54].

Macrophages. Macrophages are innate immune cells specialized in the detection, phagocytosis and destruction of bacteria and pathogens in tissues. Additionally, they play critical roles in various physiological and pathological cell process, including homeostasis, tissue development and regeneration [55]. Macrophages present in a tissue are derived from monocyte progenitors and consist of two groups: 1) resident macrophages and 2) infiltrating macrophages. These two types of macrophages emerge at different points during development and adulthood [56]. From the mouse embryonic development stages E10 to E19/P1 (birth) the fetal liver starts generating all immune cells and tissue-resident macrophages colonize their respective tissues in different organs including skeletal muscle [56]. After birth, hematopoiesis shifts to the bone marrow [56]. Monocytes originate in the bone marrow from multipotent stem cells and migrate throughout the blood circulation. Once they leave the blood, monocytes mature into macrophages which eventually replace a percentage of tissue-resident macrophages over time [56]. Another currently used classification divides macrophages into pro-

inflammatory and anti-inflammatory type, based upon their different response to microenvironment signals (known as macrophage polarization) [55,57]. Pro-inflammatory macrophages are typically activated by INF-γ or lipopolysaccharide (LPS), secrete pro-inflammatory cytokines (i.e., IL-6, IL-12, TNFα) and direct host-defense response against pathogens through phagocytosis. Anti-inflammatory macrophages, also known as regenerative or restorative type, respond to IL-4, IL-10 or IL-13 and secrete anti-inflammatory cytokines (i.e., IL-10), thereby contributing to tissue healing. Importantly, it has been described that pro-inflammatory to anti-inflammatory phenotype transition represents more likely a continuum of phenotypes rather than a distinct shift between two distinct phenotypes and functions [58].

Macrophages represent the major inflammatory cell type found in the degenerating skeletal muscle both after injury and in chronic conditions like dystrophies. Pro-inflammatory macrophages are the first to appear in the degenerative environment, they secrete pro-inflammatory cytokines (ADAMTS1, IGF-1, IL-6, IL-β1, TNFα), phagocyte cell debris present at the injury site and stimulate MuSCs proliferation [59]. TNFα secreted by macrophages during muscle regeneration has been shown to target FAPs for apoptosis, thereby reducing the number of these cells that are available for the formation of detrimental fibrosis [54]. In a second phase of muscle response to injury, anti-inflammatory macrophages become predominant in the damaged tissue. Restorative macrophages mediate MuSCs' proliferation at first (by releasing high levels of IGF-1) and myogenic differentiation at second (by releasing low level of TNFα and growth differentiation factor 3). Shifts in macrophages' balance may affect muscle regeneration at different levels: if pro-inflammatory phenotype is prolonged, the persistence of pro-inflammatory cytokines leads to an impaired myogenesis; on the other hand, anti-inflammatory abundance progressively increase with age in the diaphragm of dystrophic mice [60]. The accumulation of a subtype of anti-inflammatory macrophages has been associated with increased fibrosis in the aging muscle and dystrophy [61,62].

Neutrophils. Neutrophils are immune cell types taking part in the first pro-inflammatory phase of muscle regeneration. Muscle-resident neutrophils are activated immediately after injury and secrete pro-inflammatory cytokines (TNFα, IFNγ, IL-1β). These cytokines, together with the pro-inflammatory factors derived from the activation of complement system which occur after injury, recruit peripheral neutrophils leading to a massive infiltration of both neutrophils and additional immune cell at the injury site (IL-1 and IL-8 mediated) [63]. After injury neutrophils are also the major source of reactive oxygen species, which contribute to a temporary degradation and necrosis of muscle fiber at the injury site, followed by tissue repair. This underlies a dual role played by these cells during muscle regeneration [63,64]. To date, muscle regeneration has not been extensively studied in a neutrophils-depleted environment. Thus, it is not yet known whether these cells directly affect MuSCs activation and/or proliferation due to the release of one or more of their cytokines.

Tregs. The acronyms Tregs indicates a subset of regulatory T cells expressing CD4, CD25 and the lineage-specific transcription factor forkhead box P3 (Foxp3) [65,66]. Tregs are normally present in lymphoid organs but they are recruited in different tissues upon damage, including skeletal muscle. IL-33 secreted from FAPs is thought to be the attractive factor of Tregs within the muscle damaged environment [67]. This is consistent with the accumulation dynamics of both populations: FAPs peak in the regenerative niche around 3 days post injury (dpi), just prior to Treg accumulation [46]. Once engaged, Tregs serve their role in the immune response during muscle regeneration by promoting pro-inflammatory-to-anti-inflammatory macrophages switch [68]. Moreover, there is evidence of these cells promoting tissue repair by acting on parenchymal cells [69]. Burzyn and colleagues reported a negative effect of *in vivo* Tregs ablation on muscle regeneration (increased inflammation, fibrosis, and collagen deposition) and hypothesized a role of the growth factor amphiregulin (Areg) in supporting MuSCs survival and differentiation [68]. Areg is expressed by Tregs, its receptor is expressed by MuSCs and Tregs accumulate in the niche around the same time point in which MuSCs proliferation peaks and become ready to terminally differentiate (~ 4 dpi). Also, MuSCs proliferation is enhanced when MuSCs are cocultured with activated Treg cells [70].

Eosinophils. Eosinophils are immune cells which have been detected in muscle injury sites in both dystrophic mice and patients [71–74]. Following glucocorticoid treatment of dystrophic mice eosinophils number decreases in the lesion areas of the muscle [71,72]. Eosinophils' cytotoxicity has been historically widely explored and their primary secreted mediator MBP-1 has been reported to promote muscle cell lysis *in vitro* [73]. However, a recent study in dystrophic mice has suggested that eosinophils, despite their prominent presence at injury sites, do not drive muscle damage and that eosinophils infiltration alone does not promote muscle deterioration [75]. Little is known on the direct contribution of eosinophils in respect to muscle regeneration, but it has been shown that they have an indirect impact on the process, mediated by their IL-4 secretion. Indeed, IL-4 promotes FAPs proliferation after injury at the expense of their fibro/adipogenic conversion positively regulating muscle repair [76].

Fibroblasts. Fibroblasts are the most common cell type of the connective tissue, which connects, separates and support all other tissue throughout the body. They produce a great variety of ECM proteins including structural proteins (i.e., collagen and elastin), adhesive proteins (i.e., laminin and fibronectin), glycosaminoglycans and glycoproteins [77]. Fibroblasts reside in the interstitial space between myofibers and serve important roles not only in ECM production, but also in its maintenance, wound healing and inflammation [77]. As major producers of ECM fibroblasts are critical contributors to both physiological and pathological fibrotic processes. Numerous studies have provided significant knowledge on fibroblast functions in skeletal muscle in both health and disease [77]. However, to date these cells lack a unique molecular signature defined by a single marker expression. For this reason *in vitro* studies of fibroblasts have been historically conducted using a functional approach: the identification of isolated cells that had the highest ability to quickly adhere to plastic tissue culture

dishes [78]. Using this strategy, Mathew and colleagues have demonstrated that myoblasts fusion is increased when cocultured with fibroblasts suggesting a role of fibroblasts in controlling MuSCs differentiation [79]. This observation was supported by the defective regeneration observed *in vivo* after transcriptional factor 4^{+ve} (TCF4) cell depletion. However, a causal relation cannot be defined as fibroblasts are not the only cell type expressing TCF4 within the muscle [79]. While FAPs are known to be one of the lineage precursors of fibroblasts and they share with these cells the capacity of secreting ECM components, further investigations will be necessary in the future in order to define a clear lineage relationship between fibroblasts, FAPs and the other cell type in the skeletal muscle [80].

Endothelial cells. An extensive network of vasculature enwraps both myofibers and the *satellite cells niche* providing the muscle with oxygen and nutrients at any given time. Angiogenesis occurs during muscle repair after the first inflammatory phase, when the *niche* becomes permissive for regeneration [81,82]. The actual role of endothelial cells (ECs) in muscle regeneration is still not well defined but some observations suggest the existence of a crosstalk between ECs and MuSCs. For instance, a reduced number of vessels in skeletal muscle correlates with a reduced number of MuSCs in the human disorder amyopathic dermatomyositis [13,83]. IGF-1 [13], hepatocyte growth factor (HGF) [84] and vascular endothelial growth factor (VEGF) [85] have emerged from i*n vitro* coculture of ECs and MuSCs as ECs secreted factors that may influence both MuSCs proliferation and differentiation. Moreover, an attempt to address the role of ECs in muscle regeneration has been done by Latroche and colleagues. After identifying factors that enhance either MuSCs differentiation (periostin) or MuSCs proliferation and differentiation (apelin and oncostatin) they depleted their expression *in vivo* through blocking antibodies and inhibitors. The resulting reduction of both myofibers cross sectional area and myogenin expression suggests a role of ECs in muscle regeneration. However, other cells in the regenerative milieu can express the same proteins and could be responsible of the observed phenotype [86].

Pericytes. Pericytes are cells found in close spatial and functional relation to endothelial cells with whom they share a basal lamina. Their contribution to normal physiology and homeostasis of tissues is well documented [87]. The kinetic of pericytes accumulation during muscle regeneration is not clear and isolation of these cells is to date challenging due to a not well-defined cell surface molecular signature. However, pericytes have gained increased interest in the study of muscle regeneration due to their interaction to the vasculature ECs and to their myogenic potential [88]. Kostellari and colleagues have suggested a potential role of pericytes in MuSCs activation through the expression of Ang-1 and in MuSCs differentiation through the expression of IGF-1 [14].

Interstitial cells with myogenic potential. Throughout the years different cell populations of the interstitial space not belonging to any of the aforementioned categories have been identified and have been reported to have myogenic potential. PW1 interstitial cells [89], myoendothelial cells [90],

muscle-derived stem cells [91], CD133^{+ve} cells [92], Twist2^{+ve} progenitors [93] and muscle side population cells [82] are all part of this group. Despite their myogenic potential these cells are not able to restore the muscle following injury without MuSCs contribution and their specific role in the tissue regeneration is still elusive [94–96]. Nevertheless, these cells are receiving growing interest as they represent potential myogenic cells to use in transplantation studies and therapies, especially considering the poor rate of success that MuSCs transplantation has reached so far [88,97].

1.1.5 Muscle injury and physiologic regeneration

To date, our knowledge on skeletal muscle regeneration following acute injury originates from experimental damage induced in animal models (mostly rodents). Numerous different methods have been established to induce muscle injury and are associated with different dynamics of MuSCs activation, support cells' engagement and completion of regeneration [98]. Despite differences existing among different protocols, common aspects of the regenerative process are presented here.

The Inflammatory Niche. Injury or trauma of a muscle caused by external factors leads muscle fibers to undergo a severe detrimental process usually resulting in premature death of the cells. This process is known as necrosis and differs from apoptosis which is the programmed cell death often associated with beneficial effects to the organism. During necrosis muscle fibers usually hyper contract within their basal lamina [99] . The remaining basal lamina emptied of its fiber, also called "ghost fiber", guides the myogenesis of new fibers by serving as a template for the correct organization and orientation of myotubes [100,101]. Studies on necrosis occurring in chronic muscle injury during diseases (i.e., inflammatory myopathies and dystrophies) have reported the role of the complement system in this process. Components of the membranolytic complement membrane attack complex (MAC) have been detected in necrotic fibers [102]. Moreover, while the MAC can directly damage muscle fibers, some products of the complement cascade reactions can stimulate cellular infiltration and phagocytosis of the necrotic fibers. For example, complement component 5a (C5a) is chemotactic for macrophages and neutrophils [103]; complement component 3b (C3b) can enhance phagocytosis by interacting with macrophage receptors through opsonization [104]. Increased complement component 4 (C4) concentration in rat serum following muscle stimulation with a modified hindlimb muscle loading (obtained through the technique of Morey-Holton and Wronski [105]) have shown the activation of the classical complement cascade within the first 2 hours after stimulation [106].

Immediately after muscle injury, the earliest events of the immune response in the *inflammatory niche* are orchestrates by a cascade of both chemical and biological molecules. While circulating fibrinogen is immediately converted into fibrin and accumulates at the injury site, damage-associated molecular patterns (DAMPs) leak from the disrupted fibers into the surrounding ECM and then in the blood

circulation [63,107]. Both fibrin deposit and DAMPs contribute to immune cell recruitment and infiltration at the injury site. The former binds to the integrin receptor Mac-1 on pro-inflammatory macrophages providing a scaffold for the engagement of infiltrating immune cells [60]. The latter recruits immune cells through interaction to their toll-like receptors (TLRs) [108]. In addition, early inflammation following muscle injury is triggered by pro-inflammatory cytokines released from muscle-resident mastocytes and macrophages, which sense DAMPs [109].

Once inflammation has been triggered neutrophils are the earliest immune cells, which massively infiltrate the skeletal muscle. Their number peaks within 24 hours from muscle injury and they initiate the phagocytosis of cellular debris present at the damage site [63]. Neutrophils generate reactive oxygen species and secrete pro-inflammatory cytokines (i.e. IFNγ, IL-1β, TNFα, IL-1 and IL-8) that further stimulate immune cell infiltration [63,64]. After neutrophils, circulating monocytes migrate form the blood flow into the degenerative muscle environment, maturing into pro-inflammatory macrophages [110]. Pro-inflammatory macrophages contribute to the phagocytic removal of necrotic debris and to maintenance of a pro-inflammatory environment within the degenerating muscle site [111,112]. Eosinophils also take part to the early immune response. They infiltrate the injury site with a similar dynamic to pro-inflammatory macrophages. They peak in number within 1.5 dpi and secrete IL-4. IL-4 promotes the proliferation of FAPs, which have also been shown to contribute to the clearance of muscle fiber debris [76].

The Mitogenic Niche. After the inflammatory phase, the *niche* environment becomes permissive for both MuSCs and support cells proliferation. Events occurring at this stage include: 1) proteolytic modifications at the injury site; 2) changes of the structure and composition of the ECM; 3) immune cell-mediated regulation of the regenerating environment and 4) angiogenesis.

1) The pro-inflammatory fibrin clots built up to stabilize the tissue as an immediate response to muscle damage are resolved by plasmin and proteolytic enzymes (i.e. matrix metalloproteinases (MMPs) and uPA) [113,114]. 2) Fibroblasts- and FAPs-mediated synthesis and deposition of new ECM components are upregulated to ensure the correct architecture and mechanical properties of the *stem cell niche* [46,95]. Fibronectin, a ubiquitous extracellular matrix glycoprotein, is produced by FAPs, fibroblasts and MuSCs [115]; collagen VI, which is important for mechanical proprieties and for the elasticity of the ECM, is released by fibroblasts and MuSCs [116]; FAPs secrete also promyogenic cytokines that support MuSCs pool expansion [117]. Several growth factors (i.e. FGF2, IGF1) are released from both the ECM and muscle cells [118]. 3) At this stage of muscle regeneration, immune cells regulate myogenesis and support cell proliferation. Macrophages, after being recruited as immature monocyte from activated MuSCs, inhibit apoptosis through a cell-cell contact mechanisms, supporting cell amplification [119]. INFγ, released by pro-inflammatory macrophages, lymphocytes and natural killer cells, repress myogenic differentiation through a process mediated by MHC Class II transactivator expression [120].

TNFα released from both macrophages and neutrophils at this stage curbs the expression of Pax7 and notch in MuSCs to levels permissive for cell expansion [121,122]. When the number of MuSCs reaches its peak in the niche (~ 3 dpi), muscle regulatory T cells (Treg) accumulate in the regenerating area [67,68]. Starting from this phase macrophages shift their phenotype from pro-inflammatory to anti-inflammatory. This event is crucial and finely regulated. Pro-inflammatory deactivation is mediated by IGF1, which if genetically ablated impairs muscle regeneration due to dysregulation of cytokines levels [123]. On the other side, aberrant amplification of pro-inflammatory macrophages at the expenses of anti-inflammatory macrophages leads to premature differentiation of MuSCs [124]. When the MuSCs pool is mature and ready to start differentiation the restorative macrophages are dominant over the pro-inflammatory macrophages and start to express ECM-related genes contributing to the structural remodeling of the regenerating niche [110]. 4) Finally, while all the aforementioned events are occurring in the *mitogenic niche*, new vessel formation also takes place [125]. Angiogenesis is mediated by endothelial cells derived from their circulating progenitors. Endothelial cells and cycling MuSCs colocalize and crosstalk in the regenerating *niche*. MuSCs release the proangiogenic factor VEGF, while endothelial cells support MuSCs amplification through growth factors release (i.e., IGF1 and FGF3) [13,126].

The Differentiative Niche. After extensive proliferation, myoblast eventually fuse to each other, differentiate in multinucleated new myofibers and give rise to a restored tissue, which is similar in both composition and functionality to the uninjured skeletal muscle. Myogenin expression in myoblasts correlates at this stage with irreversible cell cycle exit and activation of terminally differentiation [22].

During terminal differentiation different cell types within the *niche* crosstalk and exhibit their role. In particular, pericytes serve different functions: 1) together with smooth muscle cells, they stabilize the vessel organization embracing the basal lamina of newly generated fibers [98,125,127]; 2) they express and release angiotensin 1, which activate Tie2 receptor on MuSCs that resisted myogenic commitment. This promotes MuSCs exit from the cell cycle and their return to a quiescent state, where they remain available for future regenerating events [12,14,128]. 3) Pericytes reportedly can take part to muscle fiber formation [129]. In this phase of muscle regeneration macrophages express mostly an anti-inflammatory phenotype and secrete cytokines (i.e. IL-10) that aids tissue repair [124]. The transcriptional growth factor 3 released by macrophages has been shown to have a role in promoting myoblast fusion by inhibiting cell proliferation [110]. In addition, FAPs boost myogenic differentiation by releasing IL-6 [46]. Then, once newly formed myofibers are mature, FAPs undergo apoptosis induced by TNFα secreted from macrophages [54].

In conclusion, all stages of muscle regeneration from the moment the traumatic event occurs until muscle is completely repaired relies on finely regulated events that involve all the *niche* components:

muscle fibers, ECM, immune cells, satellite cells and support cells. All these elements extensively communicate to each other and coordinate their functions to ensure a correct muscle healing. When one or more of these processes are perturbated or deregulated muscle regeneration can be impaired. This can happen in both physiological conditions such as aging and pathologies such as muscular diseases.

1.1.6 Impaired Muscle Regeneration

1.1.6.1 Aging

Sarcopenia is an age-related condition characterized by loss of skeletal muscle mass and function, which correlate with decrease of muscle strength, physical disability, and poor quality of life. Sarcopenic muscles exhibit an impaired regenerative capacity and increased baseline levels of ECM [130]. Research on age-related regenerative defects on skeletal muscles has mostly focused on investigating the altered phenotype of MuSCs. Recent studies have shed light also on the contribution of other *stem cell niche* components including fibroblasts, FAPs and immune cells.

MuSCs and stem cell niche in aging. Tissue integrity and function of aged muscles is impaired due to an aberrant behavior of MuSCs [131]. The implication of MuSCs in aging has been historically explained through two theories: 1) according to the *numerical stem cell aging theory* the reduced number of MuSCs in aged muscle is responsible for impaired muscle maintenance and regeneration [132–134]; 2) the *functional stem cell aging theory*, on the other side, correlates the regenerative failure of skeletal muscle to MuSCs intrinsic aberrant mechanisms and to environmental changes. However, as of present the research community agrees not only in supporting the existence of links between the two hypotheses, but also in the influence of the *niche* milieu on mechanisms of aging cells which have been traditionally considered intrinsic MuSCs properties [135]. For instance, telomere length is susceptible of environmental stimuli-mediated modifications and epigenetic differences in young and old MuSCs have been reported [136,137].

The fact that the *stem cell niche* environment is significantly altered with aging and that such changes affect the regenerative capacity of skeletal muscle has been extensively proven both *in vitro* and *in vivo* studies. In 1989 Carloson and colleagues observed that transplantation of the extensor digitorum longus (EDL) muscle from either a young or old donor rat to and old recipient rat led to impaired regeneration [138]. Subsequently, it was observed that the replacement of the systemic environment of old mice with that of young mice through heterochronic parabiosis improved the muscle regenerative capacity [139]. Initial studies showed that MuSCs isolated from young and old mice have some similar proliferation and differentiation behavior *in vitro*, but when explanted from the muscle with a portion of their *niche* (i.e. the associated myofiber and part of the ECM) the proliferation of old MuSCs is impaired, confirming the influence of environmental factors on age-related phenotypes [140,141]. Heparan

sulfate chains composition of the ECM has also been related to aging-dependent modification. In physiological conditions heparan sulfate acts like the major binders of growth factors in the ECM. In aged muscle it fails to bind signaling molecules leading to a break of MuSCs quiescence [142]. Heparan sulfate also binds Wnt signaling ligands (i.e. Wnt3a) and stabilizes their activity [143]. Finally, a distinction must be made regarding the ECM present in the muscle during homeostasis and the ECM formed in the *stem cell niche* after injury. The former is increased in aged muscles and is associated with an augmented fibrosis. The latter, which is transient and associated with the regenerative attempt after a traumatic event, is reduced in aging [115].

FAPs and fibroblasts in aging. Both fibroblasts and FAPs contribute to the augmented baseline levels of ECM components and to increased fibrosis in old muscles [144]. Some recent studies have shed light on the role of FAPs in muscle regeneration and aging-related phenotypes, investigating both their abundance and their interaction with the *stem cell niche*. Reduced FAPs proliferation has been linked to attenuated fibrosis in aged muscles [52]. In addition, an impaired interplay between FAPs and Tregs in aging has been described [67]. The aging-associated loss of FAPs-secreted WNT1 Inducible Signaling Pathway Protein 1 (WISP1) has been reported to affect MuSCs function and to impair myogenesis in aged skeletal muscles [145]. On the other side, restoration of WISP1 through either young FAPs transplantation or systemic treatment with the recombinant molecule mimics rejuvenation effects such as the rescue of myogenic dysfunction and regenerative capacity of aged MuSCs [145]. FAPs are therefore emerging as a promising cellular target for the treatment of aged-associated skeletal muscle defects.

Aberrant characteristics of the aged environment. An altered microvascular structure and function, the increased production of reactive oxygen species and a chronic state of mild inflammation are interconnected phenomena characteristic of the aged skeletal muscle [146,147]. Altered levels of several cytokines are associated with chronic inflammation [148]. Among these TNFα has been reported to decrease myoblast differentiation in aged muscles and to impair regeneration. IL-6 and its downstream signaling Jack/STAT are also increased in aging and MuSCs self-renewal and myogenic potential have been reported to be rescued following Jack/STAT pathway inhibition [149,150]. Inhibition of osteopontin, another inflammation-related factor, also improves muscle regeneration in aged muscles [151]. Finally, an altered polarization of macrophages is reported in both mice and human aged muscles. Anti-inflammatory macrophages are elevated in aged mouse skeletal muscle and they are associated with increased levels of fibrosis [61]. Similarly, the restorative macrophages, which are the most abundant type of macrophages in homeostatic human skeletal muscle, are increased during aging, while the pro-inflammatory macrophages abundance declines [152].

Several cellular factors and signaling pathways are altered in MuSCs of aged muscle and contribute to their impaired proliferation or function [153]. Among these, Notch signaling and TGFβ have been widely

explored [141,154–156]. Fibronectin, fibroblast growth factor (FGF)-2, oxytocin and apelin altered levels affect cellular pathways in aging muscles thereby contributing to impaired MuSCs function [115,142,157,158]. Importantly, Wnt signaling pathway has been reported to enhance muscle aging-related phenotypes. The activation of canonical (β-catenin-dependent) Wnt signaling leads to a reduction of the myogenic properties of aged MuSCs that acquire fibrotic features instead. As a result of this change of fate an increased number of fibroblasts is produced at the expenses of myoblasts with a consequent increase of fibrosis [159]. This tissue regeneration decline is promoted by the complement component C1q, which levels are increased in serum of aged mice. C1q is a protein complex that together with C1r and C1s forms the C1 complex and takes part to the innate immune response. Macrophages-secreted C1q activates the canonical Wnt signaling pathway through direct interaction with the Wnt receptors Frizzled followed by C1s- dependent cleavage of the ectodomain of Wnt coreceptor low-density lipoprotein receptor-related protein 6 (LRP6) **(Figure 2)**. Both C1s inhibition through a blocking antibody and C1qa gene ablation have been shown to rescue the aging-related impairment of muscle regeneration[160].

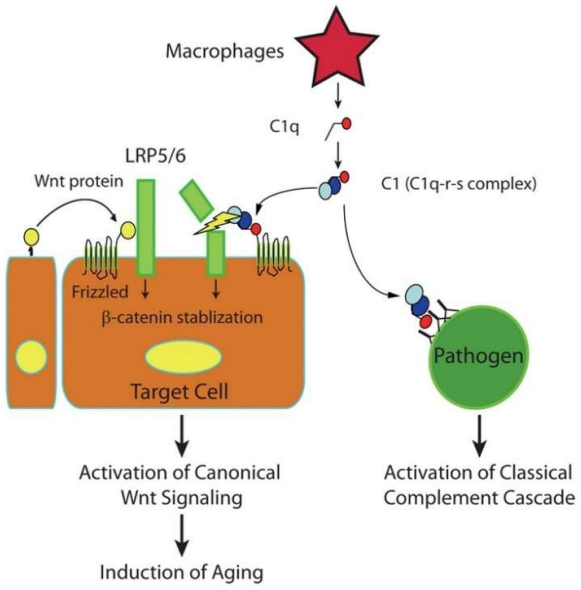

Figure 2. C1q induced activation of canonical Wnt signaling pathway. C1 complex is formed by C1q, C1r and C1s. Once C1 is assembled, C1q binds to Wnt receptor Frizzled, induces the cleavage of Wnt coreceptor LRP5/6 (C1s-mediated) and activates the canonical Wnt signaling. Adapted from [160].

1.1.6.2 Muscle diseases

Muscle diseases and chronic inflammation. The muscle *stem cell niche* is altered in several diseases referred to as myopathies. Myopathies are primary caused by genetic mutations. Duchenne Muscular Dystrophy (DMD), the most common myopathy, is caused by a mutation in dystrophin gene (*DMD*) that leads to a lack of dystrophin, a protein that connect the cytoskeleton of the muscle fiber to

the ECM [161]. A different mutation in the same gene is related to the production of an altered form of dystrophin, which is partially functional and causes a milder form of myopathy named Becker Muscular Dystrophy. Other components of the protein complex that connects the intracellular cytoskeleton to the external matrix (named dystrophin glycoprotein complex, or DGC) can be defective due to mutations of several genes and can result in different types of dystroglycanopathies [162]. Mutations of other components of the ECM lead to congenital muscular dystrophy type 1A, Ulrich muscular dystrophy and Walker-Warburg syndrome [163]. The muscle *stem cell niche* is also affected in other conditions, such as neuromuscular disorders, metabolic disorders (i.e. diabetes mellitus), inflammatory disorders and cachexia (massive loss of skeletal muscle mass occurring in severe conditions such as cancer, AIDS, sepsis, heart failure and chronic obstructive pulmonary disease) [164].

The common denominator of all muscular dystrophies and muscle-related diseases is the presence of weak and fragile fibers that are easily prone to rupture under mechanical stress (i.e., contraction) [165]. The proteins leaking from the damaged fibers and the continuous and asynchronous occurrence of numerous foci of injury within the muscle are responsible for a chronic inflammatory response [112,148]. Due to the constant state of inflammation, the *niche* is enriched in signaling molecules that contribute to an impaired regeneration. Many studies have reported increased levels of prostaglandins in dystrophic muscles of mice and humans [166,167]. Several cytokines and chemokines (i.e. TNFα, IL-1β, IL-4, IL-6, INFγ) are increased in the dystrophic environment and influence myoblasts survival, proliferation, differentiation and fusion [168]. Consistently with these inflammation-related modifications in the dystrophic *stem cell niche* glucocorticoids-based immunosuppressive therapy has been proven to improve muscle strength in patients and animal models of dystrophy [72,169,170].

ECM alteration. The chronic presence of pro-inflammatory stimuli in the dystrophic *niche* alters the stiffness of the ECM and leads to the accumulation of ectopic adipose tissue [171]. The ECM undergoes important alterations in muscle pathologies in terms of its composition, abundance and structural arrangement. Heparan sulfate proteoglycans are increased in dystrophic muscles [172,173]. The proteolytic system is impaired and the chronic deposition of fibrinogen further enhances inflammation through leukocyte activation [174]. Moreover, fibrotic proteins (i.e. fibrinogen) promote an increased secretion of TGFβ2 by macrophages, which leads to further ECM deposition [60]. The altered bioavailability of growth factors and cytokines (i.e. TGFβ, IL-1, IL-6) promotes fibrosis accumulation at the expenses of myogenesis [175]. Augmented levels of collagen I, III, IV and V are reported in both mice and human dystrophic muscles [176–178].

Muscle cells' aberrant behavior. FAPs likely represents the major cellular source of fibrosis in muscular dystrophies [46,47]. Their number is elevated in dystrophic muscles and their presence is associated with increased collagen production and increased number of fibroblasts, which also contribute to exacerbate ECM secretion [54,179]. Macrophages have also been shown to have a role in

fibrosis accumulation. Other than being increased in the degenerating foci as they are part of the inflammatory response to the damage, they promote epithelial to mesenchymal transition in injured muscles [180,181]. Moreover, anti-inflammatory macrophages accumulation in damaged areas leads to higher levels of TGFβ1 production. TGFβ1 decreases the FAPs apoptosis by competing with TNF-α. Thus, it corroborates to FAPs accumulation and to the consequent fibrosis increase [54]. MuSCs isolated from dystrophic patients and mice exhibit functional defects *in vitro* [182,183]. In addition, myogenic cells from dystrophic patients secrete increased levels of collagen *in vitro*, suggesting their involvement in muscle fibrosis [184]. Importantly, MuSCs contribution to the severity of dystrophy has been confirmed *in vivo*. The canonical Wnt signaling, which is increased in the dystrophic environment similarly to the aged muscle, enhances the expression of TGFβ2, which in turn promotes a fibrogenic program in MuSCs at the expenses of their regeneration commitment [180,181] **(Figure 3)**. Aberrant interactions of MuSCs to an altered ECM further impairs MuSCs function [185]. While attempting the regeneration process, myogenic cells eventually are not able to compensate for the dystrophic muscle fiber's degeneration. This leads to the deterioration of the tissue and to the progressive loss of muscle strength and functionality. Endothelial and hematopoietic cells have also been shown to gain a fibrogenic phenotype in the dystrophic mice via TGFβ signaling pathway, which leads to the production of high levels of ECM proteins and negatively impacts regeneration [180]. Finally, a subset of pericytes contributes to augmented levels of collagen secretion after injury in dystrophic muscles, supporting fibrotic phenotypes [186,187]. To note, the controlled and coordinated recruitment of all the aforementioned cells promote myogenesis and regeneration after a traumatic event in the muscle of a healthy person. However, the uninterrupted activity of these cells is detrimental in dystrophic muscles [76].

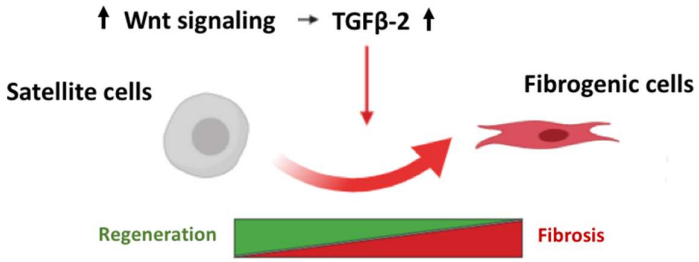

Figure 3. A Wnt-TGFβ2 axis induces a fibrogenic program in MuSCs from dystrophic mice. Canonical (β-dependent) Wnt signaling enhances TGFβ2 in dystrophic muscle. In turn, TGFβ2 effects satellite cell fate promoting fibrosis at the expenses or regeneration.

1.1.7 Duchenne Muscular Dystrophy

Duchenne muscular dystrophy (DMD) is the most frequent and severe hereditary childhood myopathy, caused by mutations of dystrophin gene (*DMD*) [188]. *DMD* is located on the X chromosome, which

consists of 79 exons and is the largest known gene of the human genome. DMD disease is characterized by the completely absence or presence in very small amounts (< 3% of physiological levels) of dystrophin protein mainly due to frameshifts mutations (**Figure 4**). In-frame mutations of the same gene lead to the production of reduced quantities of a truncated yet partially functional dystrophin protein in Becker Muscular Dystrophy, which is associated with a later onset and a milder disease [189]. Dystrophin is a cytoplasmic protein and part of the dystrophin glycoprotein complex (DGC), that connects the cytoskeleton of a muscle fiber to the ECM through the cell membrane [190] (**Figura 5**). Therefore, the absence of dystrophin in patients causes abnormal mechanical properties of muscle fibers. Muscles of dystrophic patients exhibit continue cycles of degeneration, caused by the absence of structural integrity and regeneration attempted by MuSCs and by their support network as a response to the damage. In physiologic conditions MuSCs ensure a highly effective muscle regeneration, but with the progression of a chronic disease like DMD they lose their regenerative potential and both fibrotic and adipose tissue progressively replace muscle fibers [191]. Newly regenerated fibers are also prone to degeneration as they share the same molecular defect and this further contributes to muscle fiber fragility and to chronic inflammation at the damage sites. [63,192,193]. The numerous regenerating foci typical of DMD muscles are evident in histological sections, which are characterized by less uniform fibers compared to healthy controls, increased number of centrally nucleated fibers resulting from regeneration, clustered nuclei and an overall increased number of cells [194] (**Figure 6**). DMD affects today 1 in 5000 male newborns worldwide that face progressive muscle wasting and weakness from when they are 2 or 3, they become wheelchair bound by the age of 12-13 and eventually die within their second to third decade of life due to respiratory or cardiovascular failure [195].

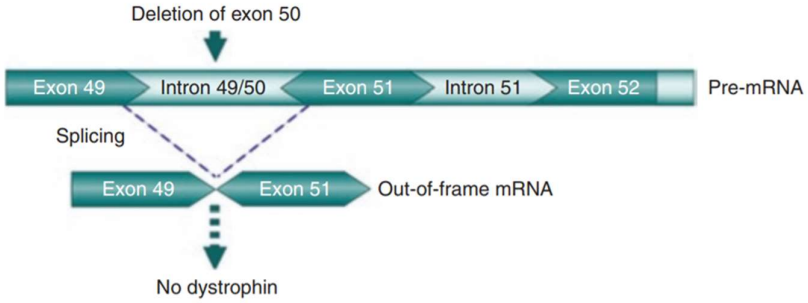

Figure 4. Frameshift mutations in DMD gene lead to the absence of dystrophin in DMD patients. The deletion of exon 50 in DMD gene generates an out-of-frame mRNA transcript in which exon 49 is spliced to exon 51. This creates a premature stop codon in exon 51 and the subsequent abortion of dystrophin synthesis during translation. Modified from [196].

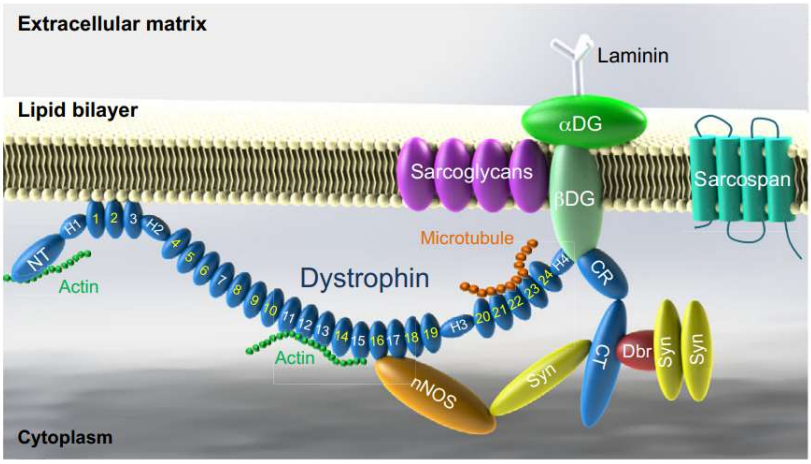

Figure 5. Dystrophin and the dystrophin glycoprotein complex (DGC). DGC consists of dystrophin, α and β dystroglycan (DG), sarcoglycans, sarcospan, syntrophin (Syn), dystrobrevin (Dbr) and neuronal nitric oxide synthase (nNOS). The cytoplasmic protein dystrophin connects the cytoskeleton (actin filaments and macrotubules) of a muscle fiber to laminin in the extracellular matrix. NT: N-terminal; CR: cysteine-rich; CT: C-terminal; 1-24: spectrin-like repeats; H1-H4: hinges. Adapted from [197].

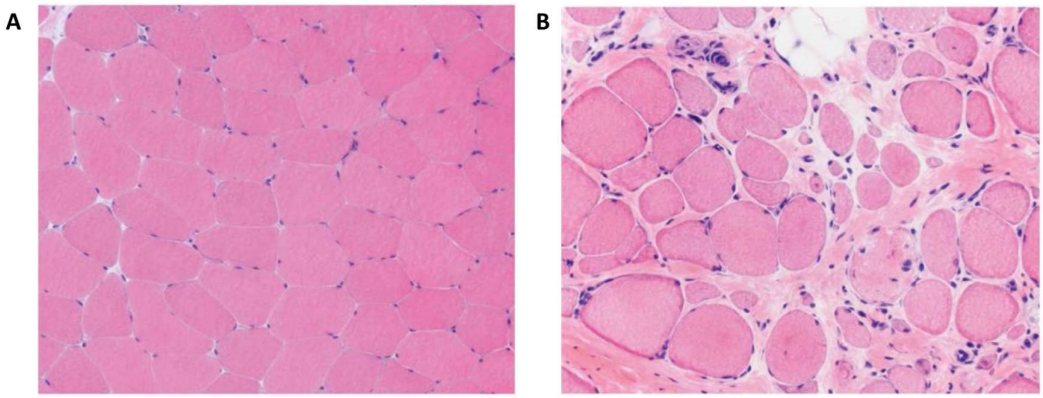

Figure 6. Histological sections of healthy and DMD muscle. (A) A normal muscle presents myofibers that are uniform in size and shape, evenly spaced and with little connective tissue between them. **(B)** A DMD muscle is characterized by myofibers that are variable in size and shape, clustered nuclei, necrosis, fibrosis and fat tissue replacement. Hematoxylin and eosin staining. Adapted from [189].

1.1.7.1 Signaling Pathways involved in Duchenne Muscular Dystrophy

The primary cause of muscular dystrophies is genetic and directly leads to myofibers' mechanical defects due to the disruption of structural proteins. However, several signaling pathways are also implicated in the pathogenic processes and in fibrosis development. Dystrophin connects to multiple proteins within the DGC, and it has a major role in regulating signaling pathways involved in nitric

oxide production, Ca^{2+} uptake and reactive oxygen species production. The impairment of these membrane-associated pathways has been associated to early stages of dystrophy pathology [198,199]. One the other side, in later stages of dystrophy development, profibrotic molecular effectors have a critical role in promoting inflammation and disease's progression. Among them TGFβ is the most potent fibrogenic factor [200]; Wnt signaling interplays with TGFβ and is another important pathway involved in the disease [201].

1.1.7.1.1 TGFβ pathways

TGFβ is a multifunctional cytokine that includes three different isoforms (TGFβ1, TGFβ2, TGFβ3), stored in the ECM as latent precursors [202]. Following specific growth signals or tissue damage, TGFβ is activated, binds to a heterodimeric complex consisting of TGFβ type I (also called activin linked kinase 5, or ALK5) and TGFβ type II receptors and activates its downstream signaling pathway in a *canonical* or *alternative* fashion. In the *canonical* TGFβ pathway, ALK5, after binding its ligand, phosphorylates the transcription factors Smad2 and Smad3, which bind Smad4 and then translocate to the nucleus. In the nucleus the Smad-complex activates transcription of profibrotic genes, resulting in the production of ECM proteins such as collagen and fibronectin by fibroblasts [43,203]. *Alternative* TGFβ signaling pathway involves different intracellular transducers than Smad2 and Smad3 (i.e. Ras/MEK/ERK pathways) and has a role in collagen type I expression and ECM contraction [203]. TGFβ can also boost fibrosis accumulation by modulating ECM degrading enzymes: it reduces these enzymes production while increasing the production of their inhibitors [204]. Importantly, TGFβ promotes the conversion of MuSCs into fibrogenic cell *in vitro* and *in vivo* in injured and dystrophic muscles [180,181,205]. In dystrophic mice the canonical Wnt signaling has been shown to act upstream the TGFβ pathway, inducing its enhanced expression which promotes the synthesis of profibrotic genes (i.e., collagen and fibronectin) in MuSCs [181]. A large body of evidence has demonstrated that Tgfβ signaling is a potent inhibitor of muscle cells terminal differentiation [206,207]. Moreover, it has been recently reported that the activation of TGFβ signaling impairs myoblasts fusion *in vitro* leading to a strong reduction of myotube formation [208]. Tgfβ inhibition has been reported to lead to the amelioration of the *mdx* mice phenotype. Mice treated with neutralizing antibody against TGFβ1 resulted in reduces connective tissue proliferation in the diaphragm [209]. The angiotensin receptor antagonist drug losartan, which antagonizes Tgfβ signaling in the *mdx* mice, leads to reduced muscle fibrosis and increased hindlimb grip strength [210]. Inhibiting Tgfβ activity has also been reported to lead to decreased serum creatine kinase levels, increased diaphragm muscle fiber density and decreased hydroxyproline levels which overall highlighted an improved muscle function after treatment [211]. Finally, the pharmacological inhibition of the Tgfβ pathway reduced the expression of fibrogenic gene in the *mdx* satellite cells [181]. Other than being stored as latent precursor in the ECM, TGFβ is produced by several cell types, including inflammatory cells, T cells, mesenchymal cells and MuSCs [154,212,213].

TGFβ expression by anti-inflammatory macrophages inhibits TNFα-mediated effects on fibrogenic progenitors. Under physiological condition TNFα induces FAPs apoptosis, preventing their differentiation into fibroblasts and ensuring the return to their baseline number after a regenerative event. However, the disruption of this process mediated by TGFβ leads to accumulation of FAPs in the dystrophic muscle and to consequent fibrosis deposition [54]. Moreover, FAPs enzymes can activate latent TGFβ1 produced by pro-inflammatory macrophages, ultimately contributing to collagen production by fibroblasts [57]. TGFβ detrimental effect on tissue regeneration in muscular dystrophies is amplified by its crosstalk to CTGF, a non-structural ECM regulatory protein that, similarly to TGFβ, inhibits myogenesis and enhances fibrotic process [214].

1.1.7.1.2 Wnt signaling pathways

Wnt signaling pathways are a group of signal transduction pathways essential to a wide variety of evolutionary conserved biological process [215]. The molecular effectors of these pathways consist in a group of secreted growth factors (Wnt proteins, expressed by 19 Wnt genes in the human genome) belonging to a family of cysteine-rich glycoproteins [216]. Wnt signaling pathways are classified in two main categories depending on the involvement of the intracellular protein β-catenin: *canonical* (or β-catenin-dependent) Wnt signaling and *non-canonical* (or β-catenin-independent) Wnt signaling.

Canonical Wnt pathway. β-catenin exist in the cytoplasm in its phosphorylated form associated to a cytoplasmic complex consisting of Axin, Adenomatous Polyposis Coli (APC), Casein Kinase I (CKI) and Glycogen Synthase Kinase 3β (GSK3β). In this status, phosphorylated β-catenin is ubiquitinated and recruited from the proteasome for degradation [217]. When Wnt proteins bind their receptor Frizzled (Fzd, a 7-transmembrane domain protein belonging to the Frizzled family) and coreceptor low-density lipoprotein receptor-related protein 5/6 (LRP5/6), the transient formation of Wnt-Fzd-LRP5/6 complex leads to the recruitment of Dishevelled (Dvl) protein to the membrane. Dvl provides a site for Axin and its associated proteins to migrate to the membrane. When Axin finally binds to the phosphorylated tail of LRP5/6, its association with APC, CKI and GSK3β is disrupted with subsequent inhibition of β-catenin ubiquitination. β-catenin, which is no longer engaged by the proteasome, accumulates in the cytoplasm and translocate to the nucleus, where it interacts to transcriptional factors (i.e., T-cell factor/lymphoid enhancing factor: TCF/LEF) and drives target genes expression [201,218]. Axin2, Lgr5 and Tgfβ2 are some of the best defined canonical Wnt target gene and their expression is widely used as a readout of the activation of this pathway [181,201,218,219] **(Figure 7)**.

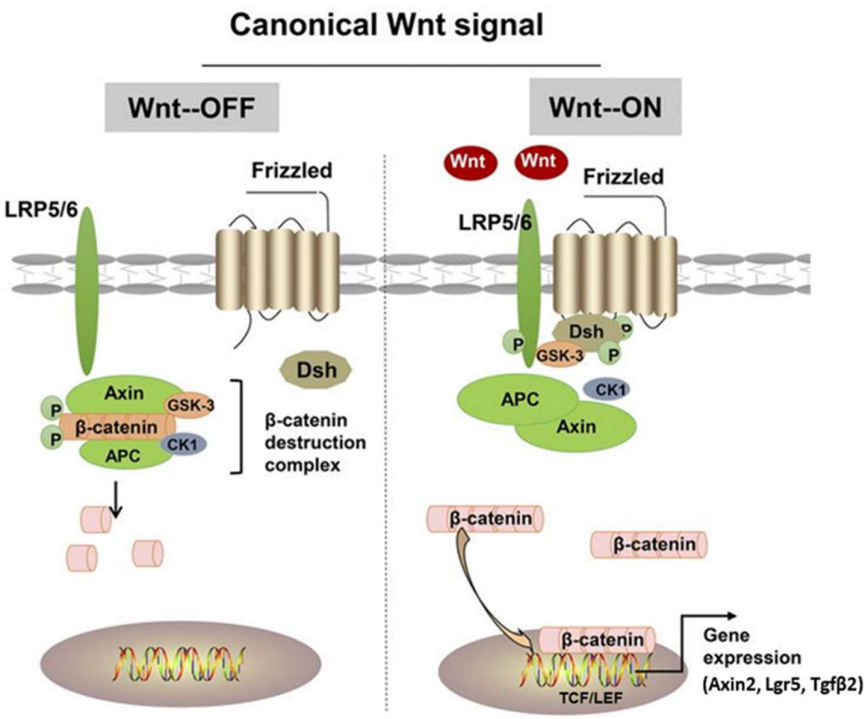

Figure 7. Canonical Wnt pathway. Schematic representation of Wnt canonical pathway in the absence (left, Wnt-OFF) or in the presence (right, Wnt-ON) of Wnt ligand. APC: adenomatous polyposis; CKI: Casein Kinase I; GSK3: glycogen synthase kinase 3; Dsh/Dvl: dishevelled. Modified from [218].

Non-canonical Wnt pathways. Within the non-canonical Wnt signaling pathways, which do not involve β-catenin, two different pathways have been identified: the Planar Cell Polarity (Wnt/PCP) pathway and the calcium-dependent (Wnt/Ca^{2+}) pathway [201]. Wnt/PCP pathway leads to either cytoskeleton rearrangements or target genes transcription through a phosphorylation cascade triggered by two kinases (Rho-associated protein kinase or ROCK and c-Jun N-terminal kinases or JNKs), which are activated after Wnt-Fzd interaction. In Wnt/Ca^{2+} pathway the transcriptional activation is mediated by Wnt-Fzd-dependent increase of inositol triphosphate (IP3). IP3 triggers the release of intracellular calcium (Ca^{2+}) and the subsequent activation of kinase proteins.

Wnt signaling in embryonic myogenesis and development. Numerous studies have demonstrated that Wnt signaling is highly active during embryonic myogenesis. Indeed, the expression of multiple Wnt ligands and receptors is finely regulated during this period. These factors, together with many other molecular pathways and process, drive the formation and the development of skeletal muscle [201]. During development, the Wnt signaling has also been reported to modulate the heterogeneity of fibers, which in mammalian muscles can be of four different types, one slow (type 1) and three fast (types 2A, 2X and 2B) [79,220].

Wnt signaling in muscle regeneration and disease. To date, several molecular details of Wnt contribution to muscle regeneration are still elusive. Still, it is well known that both the canonical and non-canonical Wnt pathways are activated during muscle repair and that their timely regulation is critical [201]. Wnt signaling is not active in quiescent MuSCs [201]. However, after injury and following MuSCs activation, Wnt7a activates Wnt/PCP pathways and stimulates MuSCs symmetric cell division [201]. At this time, the canonical Wnt signaling is inhibited by Axin, ensuring myoblasts proliferation [201]. Later on, the canonical Wnt signaling inhibits the Notch signaling, which in turn triggers MuSCs differentiation at the expense of their proliferative state [201]. Both MuSCs differentiation and myoblasts fusion are promoted by canonical Wnt signaling. Canonical Wnt signal activates Barx2, a protein that promotes myogenic differentiation gene expression [201]. Moreover, it triggers the expression of myogenin and follistatin, which positively regulate myogenic differentiation. Finally, the canonical Wnt signaling drives the translocation into the cytoplasm of the chromatin modifier histone lysine methyltransfaerase (Setdb1), a potent inhibitor or terminal differentiation [201]. Once the repair process is completed and newly regenerated myofibers are mature, Wnt7a regulates muscle size and strength through modulation of Akt/TOR pathway [201]. Lastly, Wnt activity returns to its basal low levels [201].

Numerous studies have shown that the canonical Wnt signaling is activated in several pathologies. In particular, it has a major role in promoting ECM gene expression and collagen deposition of stromal cells, supporting fibrosis accumulation in multiple tissues [221]. Augmented levels of canonical Wnt signal have been found in the serum of aged mice [159,160]. In the skeletal muscle this systemic upregulation of Wnt or Wnt-like molecules has been associated to the conversion of MuSCs from a myogenic to a fibrogenic lineage and subsequent reduction of MuSCs regenerative potential [159]. Wnt canonical activation is increased in the serum of dystrophic mice compared to aged-matched controls [53]. This upregulation is associates with an increased collagen deposition of $Sca1^{+ve}$ resident stromal cells. While Wnt3a muscle injections in wild type mice were reported to increase stromal cells number and collagen levels, injections of the Wnt antagonist Dickkof protein in dystrophic muscles led to a reduction of collagen deposition [53]. A recent study has demonstrated that the canonical Wnt signaling is a crucial pathway in modulating FAPs adipogenesis [222]. β-catenin protein expression and Lgr5 gene expression have been reported to be increased in dystrophic diaphragm and hindlimb, respectively, compared to the wild type [181]. Moreover, MuSCs cells expressing β-catenin and Lgr5 proteins are elevated in dystrophic mice hindlimb muscles compared to the wild type [181]. TGFβ2 expression was found to be induced in response to elevated canonical Wnt signaling in dystrophic muscles and to promote fibrotic gene expression in MuSCs. This phonotype was rescued following *in vivo* pharmacological inhibition of TGFβ [181].

Muscle sources of Wnt. Canonical Wnt proteins expression (i.e., β-catenin and Lgr5) has been reported in MuSCs and it is enhanced in dystrophic mice [181]. Wnt receptors (Fzd1, Fzl2, Fzd4, Fzd6, Fzd7, Fzd8, Fzd9) and coreceptors (LRP5 and LRP6) gene expression has been reported in both

young and aged MuSCs, with Fzd1 being the only one among these genes upregulated in aging [223]. Following skeletal muscle injury, macrophages have been described to be a primary source of Wnt ligands (i.e., Wnt2b, 3, 5a, 6, 9b 11 and 16). Macrophages-secreted Wnt proteins act in an autocrine fashion to stimulate macrophages' VEGF-A production and in turn to regulate endothelial permeability after damage [224]. A recent study has integrated single-cell transcriptomes of murine limb muscles (from Tabula Muris consortium) and mononuclear muscle cell populations [225]. From this integrated analysis, FAPs have been reported as the main muscle cell population expressing Wnt ligands (especially Wnt2, Wnt5a and Wnt11). Different Wnt ligands (i.e. the non-canonical Wnt5a) appear to be downregulated in dystrophic muscles compared to wild type, whereas MEST, a negative regulator of β-catenin signaling and LRP6, is upregulated in dystrophic muscles [222]. The expression of the canonical Wnt Tcf/Lef transcriptional factors has been recently reported in PDGFα^{+ve} cells of skeletal muscle (FAPs) and cardiac tissue. *Tcf7l1* (*Tcf3*) has been identified as a Tcf/Lef gene with high expression in PDGFa^{+ve} muscle cells and both *Tcf7* and *Lef1* have been shown to be strongly upregulated by tissue damage and TGFβ [226]. Importantly, Wnt transcriptional factor TCF7L2^{+ve} MuSCs are increased in fibrotic muscles of dystrophic mice and DMD [179,227].

1.1.7.2 DMD Therapies

Several promising therapeutical strategies for DMD (and for other muscular dystrophies) are currently under investigation. The aim of the research is to restore dystrophin and/or to ameliorate the pathogenic processes resulting from dystrophin absence (i.e., inflammation, myofibers necrosis, fibrosis).

1.1.7.2.1 Biotechnology-based approaches for dystrophin restoration

Different biotechnologies have been used in the past decades to restore dystrophin and to improve the structural integrity of muscle fibers. These include 1) gene delivery, 2) mRNA splice modifications and 3) gene editing.

Gene delivery. Gene delivery has been mostly carried out using adeno-associated viruses (AAVs), gene vectors with high inflection efficiency and the ability to specifically target multiple tissues, including muscle [228]. However, their transgene carrying capacity (up to 5kb) is too limited to accommodate the full-length DMD transcript consisting of 14kb. For this reason, truncated yet partially functional forms of dystrophin called mini- or micro-dystrophins have been generated [229]. AAV delivery of microdystrophins has been reported to improve muscle strength in mouse and dog models [230,231]. However, patients failed to express the synthetic protein during the first mini-dystrophin clinical trial likely due to the dosage-dependent immune response triggered by the therapy [232]. To date, three further clinical trials using micro-dystrophins are ongoing in the US [233]. AAVs-mediate gene therapy has been used also for the delivery of micro-utrophin. Utrophin is a homologue of dystrophin,

less immunogenic yet highly functional. Systemic administration of AAV-micro-utrophin has led to a reduction of myofibers necrosis without evidence of a cell-mediated enhanced immune response in neonatal dystrophic mice [234]. Finally, the so-called *surrogate gene therapy* does not replace DMD gene itself, but it delivers the gene for the enzyme β-1,4 N-acetylgalactosaminyltransferase 2 (*GALGT2*). GALGT2 overexpression in animal models has been associated to functional improvement of the disease despite the absence of dystrophin [235,236]. AAV-GALGT2 is currently undergoing a clinical trial.

Cell-based therapy is another gene delivery approach that aims to introduce normal copies of *DMD* gene into myofibers using cells as a carrier. Both genetically normal and autologous defective cells can be used for transplantation, but the latter require a gene correction (i.e., through gene editing) before being used as a vehicle. Myogenic cells including MuSCs, myoblasts, mesangioblasts (cells associated with blood vessels and able to differentiate into mesodermal linages, including skeletal muscle) and cell populations with myogenic potential from muscle interstitium (i.e., muscle side population cells, $PW1^{+ve}PAX7^{-ve}$ interstitial cells) have been investigated for this approach [97]. Moreover, cells derived from non-skeletal muscle tissue (i.e., mesenchymal stem cells, cardiac stromal cells, bone marrow-derived cells) and pluripotent stem cells (i.e., embryonic stem cells and induced pluripotent stem cells) have been tested in cell therapy approaches. Preclinical studies of the aforementioned cells have shown positive results such as dystrophin expression, improved muscle morphology and function. However, only few cell types (i.e., MuSC-derived myoblasts, mesenchymal stem cells, mesangioblasts, cardiac stromal cells) are currently evaluated in clinical trials [97]. The major challenges for successful cell therapies are to date the partial loss of MuSCs regenerative potential after *ex-vivo* expansion, the poor cell engraftment during transplantation, the lack of an effective systemic delivery and the host immune response following transplantation [97,237,238].

mRNA splice modifications. mRNA splice modifications rely for the most part on the exon skipping approach. Exon skipping consists in the omission (or skip) from the cellular machinery of an exon of the spliced *DMD* mRNA during translation. It is obtained using short nucleic acid molecules (called antisense oligoribonucleotides, or AONs) which bind to the mutated exon causing its exclusion from the mature mRNA and thus from the translation into protein. Exon skipping strategy to restore dystrophin in DMD is based on two notions: 1) the internal region of dystrophin protein, which consists of a rod-shaped domain, is tolerant to some extent to in-frame deletions that do not compromise its function completely (as it happens in Beker Muscular Dystrophy patients) [239]; 2) dystrophin protein can be rescued to some extent due to internal spontaneous exon skipping in DMD patients; this was observed from the first time in 1993 in studies that described the revertant fibers events [240,241]. The first attempts of AON-mediated therapies had to face major challenges related to the specificity of AONs to the target exon, critical to minimize off-targets effects, and the stability of these molecules that are subjected to RNAse degradation. Chemical modifications have enormously improved the stability of AONs and several modified AONs are currently undergoing clinical trials [233].

Eteplirsen and golodirsen are two chemically modified AON which restore the translational reading frame of DMD though skipping of exon 51 and exon 53, respectively. Eteplirsen can be used to treat about 14% of DMD cases and has been approved in 2016 as an orphan drug by the US Food and Drug Administration (FDA), whereas golodirsen was approved in 2019 and it can be used to treat about 9% of the DMD patients [242–244]. While these two drugs represent the first targeted treatments for DMD, there is still very limited evidence of their clinical efficacy and their usage is still far to be represent a definitive treatment [245].

Gene editing. Gene editing studies, in particular AAV-CRISPR approach, have been conducted to correct endogenous mutations in *DMD* gene and to restore its normal reading frame. CRISPR/Cas9 genome editing is based on the use of a guide RNA (gRNA) that directs the Cas9 endonuclease to create a double-strand break on a specific chromosome target site. Following repair mechanisms carried out by the cellular machinery, a new mutation is created, specifically designed to correct the gene of interest [246]. AAV-CRISPR genome editing can efficiently excise the mutation in exon 23 of *DMD* gene in dystrophic mice and enhances the expression of a truncated yet functional dystrophin in myofibers, cardiomyocytes and MuSCs [247–249]. Restored dystrophin expression (up to 80% of wild type levels) and improved muscle histology has been observed in canine model of DMD following a single-cut genome editing after a 8-weeks-long treatment [250]. Longer-term benefits of AAV-CRISPR therapy such as dysrophin restoration and reduction of fibrosis have been reported in mice up to one year following a single administration [251,252]. Although the preclinical studies are promising in terms of both dystrophin production and persistence of gene modification, to date no clinical trial based on the AAV-CRISPR approach is ongoing. This is due to the lack of sufficient evidence of the absence of severe side effects such as unwanted genome-editing (off-targets effects) and the uncontrolled immune response to the vectors.

1.1.7.2.2 Pharmacological strategies

Ataluren is a small molecule approved by the European Medicines Agency (EMA) in 2014 for the treatment of DMD pathology resulting from nonsense mutations, which represent the minority of DMD mutations causing the pathology, whereas deletions of one or more exons and duplications are the most common mutations in the dystrophin gene [253]. Nonsense mutations in DMD gene lead to the generation of premature stop codons and the consequent synthesis of a truncated/not-functional protein. Ataluren can bypass to some extent the premature stop codons via a mechanism known as *ribosomal read-through of nonsense mutations in mRNA*, which might allow the restoration of a full-length functional dystrophin [254]. Studies published so far have reported a slower evolution of the disease in patients with nonsense mutations treated with ataluren and promising data are emerging also in refer to respiratory and cardiac parameters [255].

Several pharmacological approaches are used to target the secondary effects of the DMD such as calcium dysregulation, oxidative stress, mitochondria disfunction, myofiber necrosis, inflammation and fibrosis. Among these drugs, glucocorticoids (i.e., prednisone and deflazacort) represent currently the pharmacotherapeutic of care for DMD patients as they can slow the disease progression and restore to some extent ambulation in patients [256,257]. However, to date there is no cure for DMD patients who for the most part do not live beyond age 30.

1.1.7.3 Animal Models for DMD

The dystrophin gene is highly conserved among species and *DMD* homologues have been identified in both vertebrates (mammals, birds, fishes) and invertebrates (i.e., *C. elegans, D. Melanogaster*). Several experimental models of DMD have been discovered or established throughout the years. These include mice, dogs, cats and non-mammalian models. The Golden Retriever Muscular Dystrophic (GRMD) dog is probably the most closely homologous model of the human disease. Just like patients, GRMD dogs exhibit muscle fibrosis that increases in time, enhanced levels of creatinine kinase (a commonly used diagnostic biomarker for DMD) and usually die at a young age due to respiratory or cardiovascular failure [258]. However, GRMD dogs' use is extremely limited in preclinical studies due to the maintenance expenses of the colonies and the small number of available animals that makes it difficult to address statistically significant results. Murine models' genome is highly similar to humans' (99%) and their relatively small size allows cost-efficient large scale and high throughput studies. Moreover, a wide variety of molecular and genetic tools is available to engineering their biology. For these reasons murine models are the most widely used models of DMD.

Generation of dystrophic mice. Generation of a dystrophic mouse strain can occur in two ways: 1) following a spontaneous mutation; this case makes up for the minority of available models and includes the *mdx* mouse which is the most used mouse model for DMD; 2) following genetical engineering; most mouse models have been generated by either overexpression of a mutated gene or replacement of the wild-type gene through *non-targeted* or *targeted* gene disruption. *Non-targeted* gene editing is obtained using chemicals that randomly generate mutations within the animal's genome. The offspring of mutated mice is then screened for creatinine kinase blood levels and muscle pathology. Finally, their genome is sequenced to identify the specific mutation. This approach led to the generation of mdx^{2cv}, mdx^{3cv}, mdx^{4cv}, mdx^{5cv} models [259]. On the other side, gene *targeted* strategy is performed through different approaches (i.e., targeted gene disruption [260,261], TALEN technology [262], CRISPR/Cas9 technology[263,264]) and led to the development of the majority of knockout mouse models available for muscular dystrophies [259].

The mdx model. The *mdx* strain was originally derived from a naturally occurring mutant within a C57Bl/J colony, identified from his atypically high creatin kinase blood level [265]. *Mdx* and its

genetic variants *mdx*^{2cv}, *mdx*^{3cv}, *mdx*^{4cv} and *mdx*^{5cv} are affected by the absence of dystrophin starting from the 3rd week post birth as continue cycles of muscle fibers necrosis and regeneration occur during the growth period. Around the 12th week of age most of the myofibers appear centrally nucleated indicating the recent regeneration events within the muscle [266]. After this acute phase, the pathology stabilizes and adult mice exhibit a chronic increasing fibrosis yet milder than patients throughout the rest of their life [267]. The diaphragm is the most severely affected muscle in *mdx* mice [268]. Fibrosis is present in all the *mdx* skeletal muscles, but fat infiltrates are less commonly seen in the *mdx* mice compared to DMD patients. Cardiomyopathy can occur in *mdx* mice from around 6 months of age, but these mice have a lifespan that is only slightly reduced (~25%) compared to patients (~75%) [197].

Double knockout dystrophic models. To overcome the *mdx* model limitations associated to its mild pathological phenotype, different double knockout mice have been generated introducing a second mutation in the *mdx* background. Double knockout mouse models for DMD include the *mdx-utrn*$^{-/-}$ strain, the *mdx/Cmah*$^{-/-}$ strain and the *mdx*^{4cv}*/mTR*^{ko} strain. The *mdx-utrn*$^{-/-}$ mouse lacks both dystrophin and its homologue utrophin. It is more severely affected by the disease and it dies within 13 weeks of age due to muscle weakness and respiratory failure mimicking overall the human pathology better compared to the *mdx* [269]. However, when using this strain, it is impossible to link any effect observed after drug treatment or other experiments to dystrophin rather than utrophin absence. *Mdx/Cmah*$^{-/-}$ mouse was generated to introduce a human mutation (a deletion in the *CMAH* gene) which is absent in mice [270]. Some features of this double knockout mouse are more similar to patients', such as the impaired life span (50% survival rate before one year of age), abundant fibrosis levels from 6 weeks of age and the impaired cardio functionality. However, *mdx/Cmah*$^{-/-}$ mouse growth and bone development does not mimic the typical DMD growth pattern and this led to a limited usage of this tool for studying growth and skeletal development in DMD [271]. The *mdx*^{4cv}*/mTR*^{ko} model combines dystrophin-deficiency with telomere dysfunction/shortening. Since telomeres length dictate the lifespan of cells, the hypothesis behind the generation of this strain was that the long telomeres of *mdx* mice were partially responsible of their MuSCs regenerative capacity, which is indeed reduced in the *mdx*^{4cv}*/mTR*^{ko} mouse. This strain is also characterize by skeletal muscle fibrosis from ~8 weeks of age and severe hearth dysfunctions [272,273].

The fib-mdx model. Genetic manipulation led to the generation of useful models to study DMD. However, double knockout generation is relatively expensive and time-consuming. To overcome these limitations, Isabelle Desguerre and colleagues developed the so-called fib-*mdx* model by performing daily micro-mechanical injuries in the tibialis anterior (a muscle of the hindlimb) of *mdx*^{4cv} mice for 2 weeks. Starting from 1 week post injury and up to 3 months post injury they observed an increased expression of factors involved in fibrogenesis (i.e., α-smooth muscle actin), connective tissue growth factors and collagen deposition. Moreover, a reduction of the muscle maximal specific force was observed in the same time period. This model requires a relatively short

time (3 weeks) and effort to be generate and allows accessibility to a fibrotic muscle which better resemble the human pathology, which makes it a particularly useful tool for DMD research [274].

The D2-mdx model. Crossing *mdx* mice onto a different genetic background has been reported to worsen the myopathology of the *mdx*. D2-*mdx* strain, which has been generated by breeding *mdx* mice on the DBA2/J background, better recapitulates several human characteristics of DMD, including muscle weakness, increased fibrosis, inflammation and myofibers' atrophy [275].

The experiments presented in this thesis have been carried out using the mdx^{4cv} model, in which the dystrophin gene has a mutation in exon 53. This mutation is associated with a relatively rare number of revertant fiber events compared to the *mdx* strain [276]. Revertant fibers are sporadic occurring dystrophin-positive myofibers found in animals whose dystrophin gene has a null mutation. Dystrophin production likely arise from an alternative splicing event followed by a mutation that corrects the original DNA defect. This could represent a confounding element in DMD studies. An implementation of the fib-*mdx* model was performed and used in some of the experiments presented here, in which microinjury-induced fibrosis was triggered in the entire hindlimb of mdx^{4cv} animals.

1.2 The complement system in skeletal muscle

1.2.1 The complement system: an overview

The immune system enables all living organisms to protect themselves from harm caused by pathogens. This process is ensured through the following two ways: 1) the so-called innate immunity, which an organism is born with and does not change during an individual's lifetime; 2) the adaptive immunity, that is acquired following exposure to pathogens and is highly specific for each antigen the organism has encountered. The adaptive immunity includes both the humoral immunity and the cell-mediated immunity. The humoral immunity is primarily driven by B lymphocytes and relies on the generation of antibodies. The cell-mediated immunity does not depend on antibodies and is primarily driven by mature T cells, macrophages and release of cytokines in response to a foreign antigen. The complement system (or complement cascade) consists of over 40 proteins and is a critical effector mechanism of the innate immune system. It enhances (or complements) the ability of antibodies and phagocytic cells to rapidly mediate the clearance of pathogens, apoptotic cells and cellular debris. Moreover, the complement system modulates various steps of inflammation that occur during the immune response. While being part of the innate immunity, the complement system also participates in the adaptive immune response, contributing to antibody-mediated pathogen disruption and clearance [277]. Three different recognition pathways activate the complement system leading to sequential protein

cleavage and enzymatic activation: the classical pathway, the mannose-lectin pathway and the alternative pathway.

The classical complement pathway. The classical pathway is initiated by antibody-antigen complexes binding to C1. C1 (or complement component 1, or C1 complex) is composed of the C1q sensing unit and the hetero-tetramer $C1r_2C1s_2$ (ref. *C1 complex* paragraph). C1q recognizes the antigen-bound antibody and binds the Fc portion of IgG and IgM, while the two C1s and C1r serine proteases trigger the catalytic function of the complex. Upon the binding of C1 to an activating surface, each C1r molecule cleaves and activates the other C1r. Active C1r cleaves C1s, which in turn cleaves C4 and C2 into larger (C4b, C2a) and smaller (C4a, C2b) fragments. The larger fragments associate on pathogenic surfaces forming C4bC2a complex, also called C3 convertase due to its ability to cleave C3 into sub fragments C3a and C3b. The formation of C3 convertase is the event at which all the three complement activation pathways converge. While C3a plays a role in the recruitment of inflammatory cells (anaphylatoxin), C3b binds to the C4bC2a complex to form C5 convertase (C4bC2aC3b). C5 convertase cleaves C5 into C5a and C5b. C5a is an anaphylatoxin, C5b combines with other complement components (C5, C7, C8 and C9) to form the Membrane Attack Complex (MAC) on the surface of pathogens' cell membranes. MAC assembly and bound to membrane's phospholipids induce irreversible membrane lesions causing the lysis and death of the target cell [278].

The mannose-lectin complement pathway. The mannose-lectin pathway is triggered by the mannan-binding lectin (MBL) protein. MBL binds specifically to mannose or other carbohydrate residues present on many pathogens' surfaces. MBS is a six-headed molecule that forms a complex (named MBL complex) with two protease zymogens (MASP-1 and MASP-2, close homologous of C1r and C1s) [279]. After MBL complex binds to a pathogen surface, MASP-1 and MASP-2 are activated and cleave C4 and C2. From this point onwards the complement cascade proceeds in a similar way as the classical pathway, forming a C3 convertase from fragments C2a and C4b [278].

The alternative complement pathway. The alternative pathway was discovered after the classical pathway as another "alternative" for complement activation. Its initiation differs from both the classical and the mannose-lectin pathways. Indeed, the alternative pathway is triggered by the spontaneous hydrolysis of C3 and does not depend on the presence of an antibody or a specific pathogen-binding protein. Despite this, several mechanisms ensure that the activation of this pathway proceed only on pathogens surfaces. The spontaneous hydrolysis of the thioester bond in C3 leads to $C3(H_2O)$ formation. This molecule can bind the plasma protein factor B and this binding directs another plasma protease (factor D) to cleave factor B into Ba and Bb fragments. Bb fragment remains associated with $C3(H_2O)$ to form the $C3(H_2O)Bb$ complex. $C3(H_2O)Bb$ is the fluidic-phase C3 convertase of this pathway. It can cleave C3 into C3a and C3b. C3b, if not hydrolyzed, can attaches covalently to pathogens surfaces and can form the C3 convertase C3b,Bb through steps mediated by

both factor B and factor D. Other regulators of the alternative pathway include the plasma proteins factor I, factor H and factor P. Complement factor I is a serine protease that cleaves and inactivates C3b, factor H binds C3b and compete with factor B, factor P act as a positive regulator by stabilizing the convertase on microbial surfaces [278].

1.2.2 C1 complex

C1 is the first component of the classical complement pathway. It consists of a large (~800 kDa) multimeric protease complex assembled from two functional entities: the recognition protein C1q and the catalytic Ca^{2+}-dependent heterotetramer C1s/C1r/C1r/C1s (or C1r2C1s2). C1q is a ~460 kDa glycoprotein composed of 18 polypeptide chains: six C1qA chains, six C1qB chains, and six C1qC (γ) chains [280]. In mice the three polypeptides are 223, 226 and 217 residues long, respectively, and are encoded by three genes (*C1qA, C1qB, C1qC*) located on the same locus on chromosome 4. The three genes are arranged on a 19 kb stretch of DNA in the 5' to 3' orientation A-C-B and each one of them consists of two exons separated by one intron [281]. Each chain contains a N-terminal collagenous tail domain and a C-terminal globular head domain. Both the N-terminal and C-terminal domains of each chain interact with the equivalent regions of the other two chain. As a result, the A, B and C chains associate in six heterotrimers, each containing one A chain, one B chain and one C chain. The mature functional C1q configuration is often referred to as "bouquet of tulips"-like configuration (**Figure 8**). The main "stem" of the "bouquet" is constituted by the cylinder-shaped structure formed by the N-terminal domains and stabilizes C1q through interchain disulfide bridges. This structure diverges into six separated collagen "stems" due to an imperfect Gly-X-Y collagen sequence pattern in C1qA and C1qC [282]. The "tulips" are constituted by the C-terminal globular head domains and are responsible for the pathogens or other activators' recognition [283]. C1r and C1s are structurally homologous multidomain serine proteases zymogens [284]. Electron microscopy studies have shown that both C1r and C1s dimerize and form an elongated S shape tetramer with two central C1r molecules flanked by C1s molecules (**Figure 9**) [285]. The C1s/C1r/C1r/C1s tetramer then folds into a compact structure and forms a complex with C1q by interacting with the diverging "stems" of the "bouquet" structure. The binding of C1q to an activator element via its globular heads results in autolytic activation of each C1r molecule. This marks the beginning of the classical complement cascade events (ref. *The classical complement pathway* paragraph).

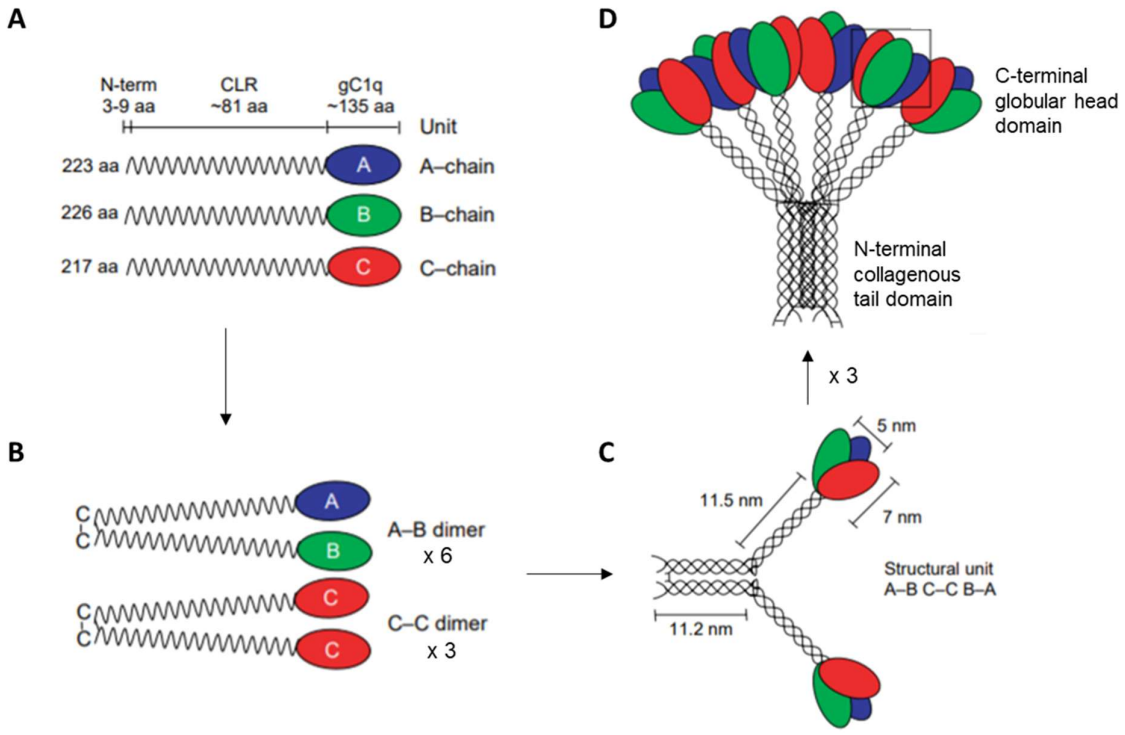

Figure 8. Structural organization of the C1q molecule. (A) C1q (460 kDa) is composed of 18 polypeptide chains (6A, 6B and 6C). Each A, B and C chain has a short N-terminal region (involved in interchain disulfide bond formation), a collagen region (CLR) and a C-terminal globular region (gC1q domain). **(B)** Interchain disulfide bonds generates 6 A–B dimers and 3 C-C dimers. **(C)** The two collagen regions of the A–B dimer and one of the C–C dimer form an ABC-CBA unit held together by covalent and non-covalent bonds. **(D)** Three of these units interact though strong non-covalent bonds in the collagenous portions to form the hexameric C1q molecule with a "bouquet of tulip"-like structure. Modified from [286].

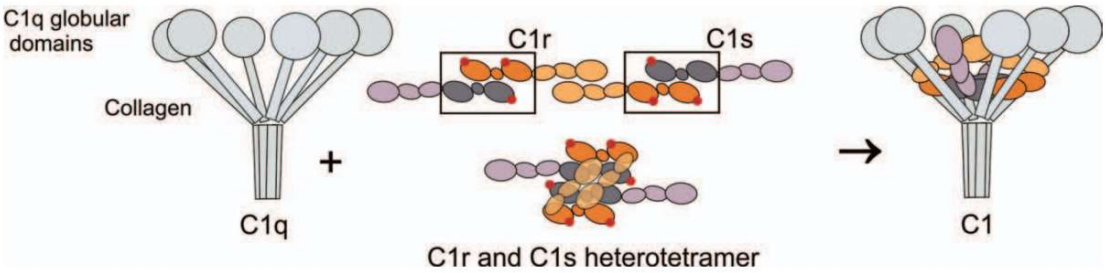

Figure 9. Formation of the C1 complex. Initially C1r/C1s/C1s/C1r tetramer is in an extended conformation (top center). When the two central C1r molecules dimerise the outer C1s molecules

interact with $C1r_2$ and the tetramer folds into a compact structure (bottom center). Then C1q subcomponents bind to C1s/C1r/C1r/C1s generating the C1 complex. Adapted from [284].

1.2.3 Non-canonical functions of complement

The first discovered and most widely documented function of the complement system is the protection against pathogens and against external or autologous antigens through both the innate and the adaptive immune response. However, evidence has shed light to the existence of additional roles of the complement system in different organs in both physiological conditions and diseases. These functions are usually referred to as *non-canonical. Non-canonical* complement functions have been reported in cell metabolism diseases, inflammatory conditions, thrombo-inflammation, cardiovascular diseases, neutrophil-mediated sepsis and neutrophil-mediated autoimmune inflammation (review in [287]). Complement system has been shown to have a role not only in detrimental processes, but also in brain and bones' development, in intestine's homeostasis maintenance and in bones' regenerative processes following injury or infections (review in [287]). Complement proteins exert control over several stem cell populations (i.e., in the bone, liver, gut, heart and brain) by controlling their proliferation, differentiation, survival and regeneration [288]. Complement is also involved in embryogenesis and post-natal development [288]. Complement factors have been identified on both sperm and oocyte, they are secreted into the female reproductive tract, contribute to blastocyst, gastrulation and neurulation stages [288]. Complement contribution to neurogenesis, neural migration and synapse pruning has been associated with the correct brain development and defects in complement activity have been linked with some neurodevelopmental disorders (i.e., autism and schizophrenia) [287]. Moreover, the absence of complement factors (i.e., C1q) results in defective placenta formation and a predisposition to the development of preeclampsia in mice [289]. Finally, whereas complement has been traditionally used in anti-cancer therapy mostly to increase the cytotoxic effect of immunotherapies, it has emerged throughout the years that it can act as a positive as well as a negative regulator of tumorigenesis. For this reason targeting complement-mediated immunoregulation is a strategy currently considered as a potential anti-cancer therapeutic option [288].

With respect to the skeletal muscle, the interplay of complement system and Wnt/β-catenin signaling represent a *non-canonical* complement function that has gained attention in the past years. Increased serum levels of C1q protein have been shown to enhance aging-related phenotypes in skeletal muscle [160]. This mechanism is mediated by the activation of the canonical Wnt signaling (ref. *Complement in skeletal muscle aging* paragraph). Importantly, both the genetic loss of C1qa and the blocking antibody-mediated ablation of C1s, but not the inhibition of the canonical complement pathway (through anti-C5 antibody), lead to a rescue of aging-related impairment of muscle regeneration. In addition, C1q treatment of young mice results into increased canonical Wnt signaling and impaired muscle regeneration following cryoinjury. Finally, both Wnt/β-catenin signaling and fibrosis increases

were observed also in C3-deficient mice [160]. The C1q-mediated increased activity of the Wnt/β-catenin pathway (i.e., C1q-Wnt/ β-catenin pathway) has also been proposed in the skeletal muscle of old adults [290] (ref. *Complement in skeletal muscle aging* paragraph). Altogether, these observations have revealed a new function of complement, suggesting that C1q role in skeletal muscle regeneration might be independent of the classical complement cascade activation [160].

1.2.4 Synthesis of complement components

The liver hepatocytes are responsible of the production and secretion of the bulk of complement proteins found in serum [291]. However, the serum does not reach all the body sites in which complement is needed and complement components can be locally produced and activated in a variety of other cell types, such as monocytes, macrophages, and dendritic cells [292]. Local complement production not only contributes to the pool of complement proteins in the circulation, but it also regulates local process in a paracrine or autocrine fashion [292].

Synthesis of complement components in muscle cells. Expression of complement components in human myoblasts was first observed *in vitro* by Jocelyne Legoedec and colleagues. Classical pathway's (C1q, C1r, C1s, C2 and C4) and alternative pathway's (C3, factor B, factor H and factor I) components were detected at both the RNA and protein level. Human myoblasts were shown to constitutively produce and secrete these proteins, which are structurally and functionally similar to their serum counterparts, and this synthesis was reported to be regulated by inflammatory cytokines (i.e. INF-γ and IL-1β) [293,294]. C1qa, C1r and C1s mRNAs have been detected in tibialis anterior muscles of *senescence-accelerated mouse prone 1* (SAMP1) mice. C1q protein has also been detected in the same muscles, but the circulation contribution of this presence cannot be excluded considering that muscles were collected and processed without prior blood removal through perfusion [295]. C1s mRNA was detected in cultured human dermal fibroblasts and porcine smooth muscle cells (pSMC) through northern blot, and C1r and C1s proteins were found in serum-free conditioned media of the same two types of cells [296]. Naito and colleagues have reported that C1r and C1s genes are expressed in the gastrocnemius of 2 months old mice and that their expression is upregulated following muscle cryoinjury [160]. Moreover, the same authors have observed macrophages expression of C1qa protein in several tissues, including skeletal muscle, and they have shown that this expression increases with aging [160]. However, *in vivo* expression of complement proteins in other muscle-resident cells (i.e., myofibers, *stem cell niche* and interstitial cells) is, to date, not extensively documented.

1.2.5 Complement system in skeletal muscle: protective and detrimental roles

Complement system activation is beneficial during development and defense process, but it can be detrimental during chronic inflammation and diseases [297]. Thus, a fine regulation of complement activation is crucial in all cells at any given time. Complement activation occurs in the skeletal muscle during the first phases of successful regeneration after injury. At the same time differential expression of several complement proteins has been involved in a number of muscle diseases and conditions.

1.2.5.1 Protective roles of complement system in skeletal muscle

As an effector of the immune response the complement system ensures the clearance of cellular debris and pathogens, substantially contributing to the homeostasis of all tissues, including skeletal muscle. Following muscle injury, or after muscle stimulation achieved by removing weight-bearing from rats' hindlimbs for 10 days followed by reloading through normal ambulation, the complement system is activated immediately within seconds and contributes to the recruitment of inflammatory cells [63,106]. Desmin is a muscle-specific protein that rapidly leaks from muscle fibers following tissue disruption and has been reported to act as a signaling molecule to promote complement activation [63,298]. Moreover, some evidence has shown that the complement system can directly participate to the remodeling and differentiation process during tissue regeneration [299,300]. These mechanisms involve mostly C3, the protein at which the three complement pathways converge prior to the membrane attack complex formation. C3 expression both at transcriptional and protein levels has been reported initially in amphibians' (urodeles) regenerating limb. C3 was not observed during limb development, which suggests the specificity of its expression during regeneration. C3 was equally expressed in all mesenchymal cells during the early phases of regeneration but became mainly localized in muscle cells during differentiation [299]. C3 and C5 transcripts and proteins have been reported to exist in the regenerative milieu of the limb and eye tissue in amphibians (axolotls) and to contribute to the regeneration of both organs [300]. Long and colleagues have hypothesized a role for C3 in cellular debris removal during muscle regeneration. Indeed, Sca1-deficient mice have a defective capacity to recruit soluble IgM and C3 complement at the muscle injury sites and they display defects in muscle regeneration and increased fibrosis [301]. The reduced IgM and C3 recruitment at the damage site leads to a lack of complement deposition [301]. This can cause a reduced debris clearance and an impaired or delayed macrophages infiltration and phagocytosis, that could likely be the main cause of Sca-1 knockout defective phenotype [301,302]. In another study, C3b deposition has been observed in skeletal muscle in mice following cardiotoxin injury [303]. C3 genetically deficient mice exhibited impaired regeneration (i.e., reduced cross sectional area of newly formed myofibers) after injury. However, when C3 was depleted 2 days after injury, impaired muscle regeneration was no longer observed,

suggesting the critical role of complement activation during the early phase of muscle injury and regeneration [303]. C4-deficient mice did not show impaired muscle regeneration, whereas complement factor B genetical depletion led to the reduction of C3b deposition at the injury site and to defective tissue regeneration [303]. This phenotype was rescued in the presence of wild type mouse serum and these findings suggested that the contribution of complement system during muscle regeneration is mainly restricted to the alternative pathway [303]. Finally, C3a/C3aR (C3aR: C3a receptor) but not C5a/C5aR (C5aR: C5a receptor) signaling was shown to be critical for macrophage infiltration into muscle and therefore for muscle regeneration [303]. C3 has also been reported to promote myogenic differentiation. This was suggested by cell culture experiments with conditioned media or media supplemented with C3 and by the observation that complement C3 secreted by muscle-resident pre-adipogenic cells ($CD34^{+ve}/Sca1^{+ve}$) rapidly internalizes within the cytoplasm of myogenic progenitor cells prior to their differentiation [304].

1.2.5.2 Detrimental roles of complement system in skeletal muscle

Complement in Duchenne Muscular Dystrophy. The involvement of complement system in DMD has been historically related to the late steps of myofiber necrosis and initial studies on DMD biopsies did not support the role of complement-mediated process in promoting muscle fiber injury [102,305,306]. In 1982 Engel and colleagues reported the presence of the membrane attack complex (MAC) in the necrotic fibers of 100% of the biopsies of patients analyzed in their study (n=66). C3 and C9 were also detected in necrotic fibers, while the presence of either C1q or C4 was reported only in few necrotic fibers [102]. However, C1q binding is reversible and C4 can undergo proteolytic degradation. Thus, even suggesting that the alternative pathway is involved in fiber necrosis, this study does not preclude the participation of the classical pathway in the process. Complement was not observed in nonnecrotic fibers of any of the biopsies [102]. Muscle fiber necrosis is associated with a massive inflow of extracellular material that under physiological conditions does not enter the cell. The plasma protein albumin was used as endogenous marker of extracellular fluid penetration following the disruption of DMD fibers' membrane. C3 and C9 were reported to colocalize with albumin in all necrotic DMD fibers, but complement was not found in nonnecrotic albumin-positive DMD fibers [305]. A possible explanation of the absence of complement components in the nonnecrotic albumin-positive cells could be that the plasma membrane discontinuities in these fibers let albumin through but excluded the complement components, which have a higher molecular weight. This study suggested that plasma membrane lesions in DMD triggers molecular events that lead the fiber to necrosis and that complement cascade occurs in the late steps of cell necrosis. Moreover, consistently with the activation of the alternative pathway, C1q was not observed in DMD fibers [305]. In addition, Spuler and colleagues did not report the presence of either MAC or C3 on nonnecrotic DMD fibers. However, they contemplated the hypothesis of proteolytic process-mediated removal of C3 from chronic lesions sites [306].

The first hint on the possible role of complement in promoting muscle damage in DMD came in 1987 from Swery and colleagues' immunocytochemical studies on patients' biopsies [307]. Differently from what was previously reported, C9 was detected in different abundance in both necrotic and nonnecrotic fibers. Moreover, C8 was observed in both types of fibers. The possibility of MAC to be formed on the surfaces of fibers also in the absence of necrosis suggested that complement may be involved in early muscle fiber damage in muscular dystrophies [307]. Interestingly, a DNA microarray-based analysis has led to the identification of 6 complement genes differently expressed in the *mdx* mouse hindlimb (8 weeks old) compared to the wild type control [308]. The most upregulated of these genes are the classical pathway components *C1qb* (25.5 fold change compared to the control) and *C1qa* (7.7 fold change), followed by *C3aR1* (: C3a receptor 1 - 6,9 fold change), the positive regulator of the alternative pathway *properidin* (or factor P – 6.6 fold change), *C3* (2.8 fold change) and the complement related-gene *Serping1* (serine or cysteine proteinase inhibitor – 1.8 fold change). Another study carried on 19 DMD patient younger than 2 years old revealed that the expression of *C1qa*, *C1qb*, *C1r*, *C1s*, *C3*, *CFH* (Complement Factor H) and *CFHL1* (Complement factor H-related 1) is upregulated during the initial or "presymptomatic" phase of the disease [309]. This molecular signature has suggested that the complement activation could be involved in the pathology of DMD. Indeed, while dystrophin deficiency is the primary cause of DMD, secondary mechanisms may be key contributors to the disease pathogenesis. For example, secondary mechanisms including complement activation may be critical to explain how different muscles are more (i.e., diaphragm) or less (i.e., extraocular muscle) heavily affected and to elucidate the reasons underling different extent of severity of the disease (i.e., in DMD vs in the *mdx*) [308].

Complement in skeletal muscle aging. To date, our knowledge of complement activation in skeletal muscle during aging is mostly related to the crosstalk existing between the classical complement pathway and the canonical Wnt/β-catenin signaling (ref. also to *Non-canonical functions of complemen*t paragraph). In 2012 Naito and colleagues reported from the first time that complement system can promote skeletal muscle aging in mice via activation of Wnt/β-catenin pathway [160]. The expression of the classical complement protein C1q is upregulated in serum and in various tissues with age, including skeletal muscle. C1q activates Wnt signaling by binding to Wnt receptor Frizzled and subsequently inducing C1s-mediated cleavage of Wnt coreceptor LPR6 [160]. This leads to aberrant behaviors of cells of the *stem cell-niche* in the aged muscle, such as the inhibition of satellite cell proliferation and the stimulation of fibroblasts proliferation. It also leads to collagen accumulation and increased levels of muscle fibrosis [160]. The intuition that complement could be the activator of Wnt signaling in aging came from two preceding observations. First, the canonical Wnt signaling was already known to be enhanced in mammalian aging from studies on a mouse model of accelerating aging [310]. Moreover, the inhibition of canonical Wnt signaling was known to rescue aging-related skeletal muscle phenotypes and Wnt activation in aging was attributed to substances in the serum that

bind Frizzled extracellular domain and promote Wnt cascade in an endocrine fashion [159]. Second, Wnt ligands were known to act in a spatially short-range fashion, within two or three cell diameters from the secreting cell and to bind to the cell surface and/or to the extracellular matrix [311,312]. For these reasons, a Wnt-unrelated protein was assumed and then proved to be the substance activating Wnt signaling in aging [160]. Following the initial finding of complement and Wnt/β-catenin signaling interplay in aged skeletal muscle, this new pathway has been investigated in other studies. Yabumoto and colleagues reported the contribution of C1q in aging-related muscle impairment caused by the absence of angiotensin II type 1 (AT_1) receptor [313]. AT_1 is encoded in mice by *Agtr1a* and *Agtr1b* genes and its excessive activation is detrimental and promotes aging process both *per se* and in aging-related diseases [314,315]. Aging-related decline in skeletal muscle was shown to be milder in *Agtr1a*-deficient mice, which also have a prolonged life span [316]. Systemic administration of AT_1 receptor inhibitor to wild type mice downregulated C1qa (a subunit of C1q protein) expression in macrophages and led to lower C1q serum concentration after cryoinjury. Moreover, the AT_1 receptor blocker (irbesartan)-mediated downregulation of C1q-Wnt/β-catenin pathway led to an improved muscle growth in AT_1 receptor inhibitor-treated mice [313]. C1q-induced activation of Wnt signaling has been also related to the activation of forkhead box O (FoxO) signaling and subsequent muscle proteins degradation in C2C12 myoblasts [317]. Finally, in aged mice it has been shown that levels of C1q mRNA and protein in skeletal muscle and levels of C1q in circulation are reduced after resistance training [295]. In the same study the number of satellite cells and fibroblast positive for β-catenin staining was decreased after resistance training of mice. This suggests a reduction of Wnt activation in both cell types [295]. Interestingly, increased serum levels of C1q have also been associated with aging in humans [290]. Enhanced C1q serum levels in old adults have been shown to negatively correlate with muscle mass and muscle strength. The Wnt/β-catenin target gene Axin2 has been reported to be enhanced in older adults. Progressive resistance training has been associated to reduced C1q serum levels and C1q decrease correlates with an increased muscle cross sectional area. Moreover, both Axin2 and the profibrotic gene collagen1a1 expression is reduced after resistance training [290]. These observations have suggested a reduction of muscle regeneration capacity mediated by C1q-Wnt/β-catenin pathway and the possibility to use C1q as a biomarker of sarcopenia in humans [290].

Complement in Dysferlinophaties. Dysferlinopathies are a class of autosomal recessive myopathies caused by the complete or partial absence of dysferlin. Dysferlin is a 230 kDa protein involved in membrane fusion [318]. Its absence is associated with defective plasma membranes repair and leads to a constant leakage of cytoplasmic material in the extracellular environment [319,320]. Consequently, patients experience muscle weakness and wasting usually by their age 30 to 40. Muscle biopsies of dysferlin-deficient patients exhibit massive immune cells infiltration and MAC deposition on fibers indicates complement activation [319,320]. Other than being involved in the immune response following muscle damage it is possible that complement has a role in inducing muscle damage *per se*

in dysferlinopathies. Indeed, complement activation and MAC deposition was observed on both necrotic and nonnecrotic muscle fibers on human dysferlin-deficient skeletal muscle [306,320,321]. Microarray data have reported a differential expression of classical complement pathway genes in quadriceps of dysferlin-deficient mice (SJL) of 2-month and 9-month-old [322]. The three C1q subunits (*C1qa*, *C1qb*, *C1qc*) and *C4* genes are upregulated with the progression of the disease [322]. Moreover, the negative regulator of the classical pathway decay accelerating factor 1 (*Daf1*) is downregulated in both 2 months and 9 months old SJL mice compared to healthy controls [322]. An independent study reported decay-accelerating factor reduction at both RNA and protein levels in skeletal muscle of dysferlin-deficient mice and patients [323]. RNA levels of classical components C1qa and C4 and the alternative pathway component complement factor B increase in quadriceps of 8 months old dysferlin-deficient mice compared to 2 months old, while the expression of the complement inhibitor gene *CD59* decreases with the progression of the disease [324]. Finally, genetic disruption of C3 but not C5 in mice led to an amelioration of muscle pathology in dysferlin-deficient mice (i.e., reduction of inflammation, percentage of centrally nucleated fibers, fibrosis and fat infiltration) [324]. This has suggested a central role of C3 in promoting muscle injury in dysferlinopathy. Therefore, the inhibition of complement cascade upstream to C3 or at the C3 level has the potential to be a therapeutic option for this condition.

Complement in Autoimmune Muscle Diseases. Complement system contributes to the pathogenesis of dermatomyositis (DM, and its children form juvenile dermatomyositis, JDM). DM is a degenerative autoimmune disorder that belongs to the heterogeneous class of inflammatory myopathies and affects mostly muscles and skin. It is characterized by an autoimmune attack against the endothelium of the capillaries. Deposited autoantibodies activate the complement cascade, leading to the formation of MAC complexes on the vasculature surfaces [83,325]. Consequently, capillaries exhibit extended damage and necrosis, resulting in an insufficient blood supply to the muscle. Complement-mediated necrosis has been observed in muscle fibers biopsies from DM patients and circulating immune complexes, IgG, IgM, C3 and MAC have been detected in DM muscle and skin biopsies [83,325–329]. Complement activity is considered a diagnostic measure for DM and the detection of MAC in patients differentiate DM from other inflammatory myopathies at both early and advanced stages [330]. Moreover, complement represents together with other immune components (i.e., cytokines, T- and B-cell activating factors, adhesion molecules) a promising candidate for future DM therapeutic strategies [331]. One case of a C2 hereditary deficient individual having DM has been reported [332]. Finally, C4A genetic deficiency has been related to JDM. HLA (Human Leukocyte Antigen) class II gene DRB1 allele *0301 (also known as *DR3* gene) is known to be the major immunogenetic risk factor for JDM [333]. A study reported C4A deficiency to be independent of DR3 in association with JDM. Moreover, it was shown that deficiency of both *C4A* and *DR3* leads to a higher risk of JDM [334].

Myasthenia gravis (MG) is a chronic autoimmune neuromuscular disease. It is characterized by the production of autoantibodies that target the acetylocholine receptor (AchR) at the neuromuscular junction (NMJ) [335]. Patients exhibit weakness and fatigability that involves ocular, bulbar and skeletal muscle [335]. Antibodies directed towards the AchR are mostly IgG, which are able to activate the classical complement pathway by binding C1q on the Fc domain [336]. Complement activation represents the main effector of MG and its detrimental role in the pathology is well established [336]. Initial studies have reported C3 and MAC deposition at the NMJ in absence of inflammation [336]. C3 and C4 levels are decreased in patients' sera, while complement terminal components levels are increased [336]. Moreover, when cultured in the presence of patients' sera, rat myoblasts were reported to undergo cell lysis and release AChR-immunoglobulin complexes in the medium [337]. IgG and complement proteins are detected also at the degenerating NMJs of mice with experimental autoimmune myasthenia gravis (EAMG) [338]. EAMG mice have allowed the investigation of several complement components through both genetic-mediated depletion experiments and pharmacological complement blockage [336]. As a consequence of these studies, many EAMG preclinical studies have been carried out to investigate the effect of the modulation of classical complement components (i.e., C1q, C2), terminal complement components (i.e., C5, C6) and complements regulators (i.e., complement receptor 1, DAF) (reviewed in [336]). Importantly, there is currently an approved antibody (eculizumab) directed towards C5 for the treatment of MG and other complement inhibitors are undergoing a phase III study [336,339].

Complement in skeletal muscle ischemia-reperfusion injury. Skeletal muscle ischemia-reperfusion injury (IRI) is the tissue damage caused by the restoration of the blood flow to the muscle (reperfusion) after a period of ischemia. IRI is characterized by tissue inflammation, oxidative stress and complement system activation. Studies with C3 and C4 genetically deficient mice have shown that the classical complement pathway is crucial to the initiation of inflammation following reperfusion in skeletal muscle [340]. C1 depletion through the human C1-esterase inhibitor and through a synthetic C1qA chain peptide have resulted in increased contractile force of the reperfused EDL muscle in rat [341]. Terminal complement components are also involved in IRI. Indeed, C5-deficient mice are protected from IRI, which is restored in the presence of wild type serum. Moreover, neutrophils and MAC have been reported to act additively to mediate skeletal muscle IRI [342]. Finally, the mannose-lectin complement pathway has been involved in IRI and MBL-deficient mice have been reported to be protected after skeletal muscle reperfusion injury [343].

1.3 Aim of the thesis

The complement system has been involved in the necrosis process occurring in muscle fibers during the progression of DMD and few studies have also reported the role of complement in promoting muscle damage before necrosis. C3 and some components of the alternative complement system have been reported to directly participate to tissue regeneration. However, the role of the classical complement pathway in the progression of DMD is poorly documented and its participation in muscle regeneration to date is not known.

Altered serum levels of complement proteins have been reported in aging and muscle diseases, but the local production of complement components in the skeletal muscle has not been extensively investigated neither in physiological nor in pathological conditions.

The experiments presented here are based on two premises: 1) The canonical Wnt signaling is increased in skeletal muscles of dystrophic mice. It enhances the expression of TGFβ2 and the Wnt-TGFβ2 pathway induces a fibrogenic program in dystrophic muscles [181]. 2) The classical complement component C1q activates the canonical Wnt signaling in aging and promotes aging-related skeletal muscle phenotypes [160].

The overall goal of this thesis is to get insights into the cellular and molecular events responsible for the enhanced Wnt signaling in dystrophic muscles and to validate the model described in **Figure 10** by pursuing the following specific aims:

1) Evaluate the complement expression levels in the skeletal muscles of both healthy (i.e., wild type) and dystrophic mouse models. In particular, we aimed to evaluate the classical complement pathway levels, with a focus on C1 complex.

2) Investigate the C1q-Wnt/β-catenin pathway activity *in vitro* in murine muscles cells (i.e., fibroblasts and myoblasts).

3) Investigate whether the C1q-Wnt/β-catenin pathway is aberrantly upregulated and can promote fibrosis in dystrophic muscles. This has been achieved through different complementary approaches: (*i*) gene expression analysis of the muscles' cell populations which express C1 complement components (refer to aim 1) and might contribute to the enhanced Wnt signaling expression in the dystrophic muscles. We also quantified the same cells in the muscles and we studied their localization within the dystrophic regenerating areas; (*ii*) a histological analysis of the coexpression of canonical Wnt target proteins and complement proteins in dystrophic muscles; (*iii*) the *in vivo* pharmacological C1 inhibition.

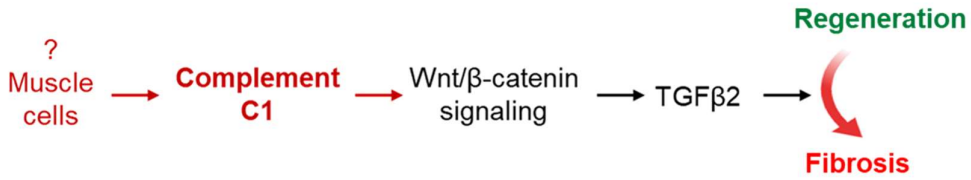

Figure 10. The biological question of this thesis. The aims of this study are to investigate whether the muscle–resident cells are sources of complement proteins and to investigate whether the C1q-Wnt/β-catenin pathway is aberrantly upregulated and promotes fibrosis in dystrophic muscles.

2. Materials and Methods

2.1 Mice

Animal care and experimental procedures were conducted in accordance with the Ethical Committee of the University of Trento and were approved by the Italian Ministry of Health (D. Lgs no. 2014/26, implementation of the 2010/63/UE). Animals were maintained with access to food and water ad libitum and kept at a constant temperature (19–22°C) on a 12:12 h light/dark cycle. C57BL/6J mice (Charles River Laboratories, no. 000664) were used as wild type (WT) animals. B6Ros.Cg-D^{md}*mdx-4Cv*/J mice (Charles River Laboratories, no. 002378, herein referred to as *mdx*^{4Cv}) were used as MDX mice. B6.129S4-PDGFRα$^{tm11(EGFP)Sor}$/J were purchased by The Jackson Laboratories (Stock No: 007669) and B6.129S4-PDGFRα$^{tm11(EGFP)Sor}$/J;*mdx*^{4Cv} mice were obtained after breeding B6.129S4-PDGFRα$^{tm11(EGFP)Sor}$/J males with *mdx*^{4cv} homozygous females [52]. For experiments with C1r/s inhibitor, Pax7-CreER^{tm} males [36] were crossed to R26R$^{YFP/YFP}$ females (The Jackson Laboratory, no. 006148) to obtain Pax7Cre$^{ER/WT}$; R26R$^{YFP/WT}$ males. These breeders were crossed to *mdx*$^{4Cv/4Cv}$ female to obtain the male experimental animals (Pax7Cre$^{ER/WT}$; R26R$^{YFP/WT}$; *mdx*^{4Cv}). Tamoxifen (T5648 Sigma) was dissolved at 50 mg/ml in 92.5% corn oil/7.5% ethanol, and 2.5 mg was administrated intraperitoneally to 5-week-old experimental mice (i.e., male Pax7Cre$^{ER/WT}$; R26R$^{YFP/WT}$; *mdx*^{4Cv}) every day for 8 days. For Lyz2Cre$^{+/-}$; C1qa$^{FL/FL}$; *mdx*^{4Cv} generation, C1qa$^{FL/FL}$ (The Jackson Laboratory, no. 031261) males were crossed to C1qa$^{WT/WT}$; *mdx*$^{4Cv/4Cv}$ females to obtain C1qa$^{FL/WT}$; *mdx*^{4Cv} males. These males were crossed to C1qa$^{WT/WT}$; *mdx*$^{4Cv/4Cv}$ females to obtain C1qa$^{FL/WT}$; *mdx*$^{4Cv/4Cv}$ females, that were crossed to C1qa$^{FL/WT}$; *mdx*^{4Cv} males to obtain C1qa$^{FL/FL}$; *mdx*$^{4Cv/4Cv}$ females. Lyz2Cre$^{+/+}$ (The Jackson Laboratory, no 004781) males were crossed to Lyz2Cre$^{-/-}$; *mdx*$^{4Cv/4Cv}$ females to obtain Lyz2Cre$^{+/-}$; *mdx*^{4Cv} males. These breeders were crossed to C1qa$^{FL/FL}$; *mdx*$^{4Cv/4Cv}$ females to obtain Lyz2Cre$^{+/-}$; C1qa$^{FL/WT}$; *mdx*^{4Cv} males. Finally, C1qa$^{FL/FL}$; *mdx*$^{4Cv/4Cv}$ females were crossed to Lyz2Cre$^{+/-}$; C1qa$^{FL/WT}$; *mdx*^{4Cv} males to obtain the male experimental animals (Lyz2Cre$^{+/-}$; C1qa$^{FL/FL}$; *mdx*^{4Cv}). Genotyping was performed with primers listed in **Table 1**.

Gene	**Forward Primer 5' → 3'**	**Reverse Primer 5' → 3'**	**T_{Ann}**
C1qa	tgcatcctgccatctcct	gaaagtgcttaaagaaaccactg	60 °C
Cre	gcatttctggggattgctta	cccggcaaaacaggtagtta	53.7 °C
YFP	aagttcatctgcaccaccg	tccttgaagaagatggtgcg	53.7 °C

Table 1. Primer list for genotyping PCR

2.1.1 Muscle injury

2.1.1.1 Acute muscle injury

Mice were anesthetized with 2.5% isoflurane, hindlimb skin was shaved and disinfected with 70% ethanol. 29-gauge needles were disinfected with 70% ethanol and used to make several injuries. Punctures were performed deep into the muscle (7-8 mm), randomly but close enough to each other to cover the whole muscles surface. Skin was cleaned, disinfected with 70% ethanol and an analgesic (Altadol) was administered at the end of the procedure according to the manufacturer's instructions. Muscles were dissected and analyzed 2.5 days after the injury.

2.1.1.2 Chronic muscle injury

Micromechanical muscle chronic injury protocol was adapted from Isabelle Desguerre and colleagues previously published protocol [274]. Mice were anesthetized with 2.5% isoflurane, hindlimb skin was shaved and disinfected with 70% ethanol. 150 µm diameter micropins (Kabourek, Czechoslovakia) were disinfected with 70% ethanol and handled with forceps. Fifteen micro punctures in the tibialis anterior, thirty micro punctures in the right side of the gastrocnemius, thirty micro punctures in the left side of the gastrocnemius and thirty micro punctures in the posterior side of the gastrocnemius were made daily for 14 days. Punctures were performed deep into the muscle (7-8 mm), randomly but close enough to each other to cover the whole muscles surface. No bleeding was observed due to the small diameter of the pins. Skin was disinfected with 70% ethanol and an analgesic (Altadol) was administered at the end of the procedure according to the manufacturer's instructions. Muscles were dissected and analyzed 1 week after the last injury.

2.1.1.3 Muscle injury and C1r/s inhibitor treatment

For experiments with C1r/s inhibitor, mice were processed as described in *"Chronic muscle injury"* paragraph. ~30 minutes after micro injury, 15 UI of human plasma derived C1r/s esterase inhibitor were administered to mice through intraperitoneally (i.p) or intravenous (i.v) injections on alternate days. C1r/s esterase inhibitor was administered daily for 7 more days after the last micro injury (15 UI, i.p or i.v. injection on alternate days). Muscles were dissected and analyzed 1 week after the last injury.

2.1.2 Behavioral test

Before behavioral tests, mice were handled on a regular basis from the same operator to limit stress levels. Tests were consistently performed at the same time of the day during the mice dark phase hours.

2.1.2.1 1.2.1 Four limbs hanging test

Four limbs hanging test protocol was adapted from *Treat-NDM Neuromuscular Network SOP DMD_M2.2.1.005* (https://treat-nmd.org/wp-content/uploads/2016/08/MDX-DMD_M.2.1.005.pdf). Prior the test, mice were weighed to allow normalization for body weight. A 40 cm x 30 cm metallic grid was placed 40 cm above a desk with sufficient bedding (i.e., papers and wood chips) to ensure a soft landing. Mice were placed on the grid and were allowed to acclimate to this environment for 3 to 5 seconds before the grid was inverted and held at 40 cm of height. Mice were given a fixed maximum hanging time (900 secs). If mice fell off the grid before the time limit, they were immediately given two more tries; if mice hung for 900 seconds they were placed back in the cage. The total hanging time was recorded. The test was repeated after 2 days. Only data referred to the second day of test was analyzed as the first day was used as an acclimatization period.

2.1.2.2 Open field test

Open field test protocol was adapted from *Treat-NDM Neuromuscular Network SOP DMD_M2.2.1.002* (http://www.treat-nmd.eu/downloads/file/sops/dmd/MDX/DMD_M.2.1_002.pdf). Immediately after the four limb hanging test, mice were placed into a 40 cm x 40 cm arena and allowed to move freely and explore for 6 minutes. The test was recorded and movement data was analyzed using ANY-maze software. The test was repeated after 2 days. Only data referred to the second day of test were analyzed as the first day was used as an acclimatization period.

2.1.3 Sera collection and preparation

Mice were heated under a lamp for few minutes to increase the blood flow. The area of the submandibular vein was pierced with the tip of a needle and the blood flow from the cheek was collected in a tube. Blood samples were incubated at room temperature for 1 hour, centrifuged at 10.000 g for 10 minutes at 4°C. The supernatant (serum) was collected.

2.2 Cell Isolation and culture

2.2.1 Single fibers isolation

Single myofibers were isolated from the extensor digitorum longus (EDL) muscles as previously described [24,344] . EDL muscles were dissected and digested using 0.2% type II collagenase (Worthington Biochemical Corporation) in DMEM (GIBCO) for 70 minutes at 37°C with agitation (70 rpm). Muscles were placed in DMEM containing 10% horse serum (GIBCO) and repeatedly triturated with a micropipette to liberate single fibers. Samples were washed 5 times, centrifuged (500g, 10 minutes at 4°C) and the cell pellet was processed for RNA extraction and RT-PCR.

2.2.2 Muscle single cells isolation

Muscles (hindlimbs and diaphragm) from adult wild type and *mdx*^{4Cv} mice were dissected, weighed and processed as previously described to obtain mononucleated cells [35]. Muscles were washed in Wash Medium (Ham's F-10 supplemented with 10% FBS, 1% L-glutamine and 1% penicillin-streptomycin), added to Muscle Dissociation Buffer (700-800 U/ml collagenase II (Worthington Biochemical Corporation) prepared in Ham's F-10 supplemented with 1% L-Glutamine and 1% penicillin-streptomycin) (16 ml/hindlimb, 8 ml/diaphragm), minced with scissor, incubated in a 37° C water bath with agitation (70 rpm) for 40 minutes. After incubation samples were centrifuged at 500g for 5 minutes, dispase (11 U/ml, GIBCO) and collagenase II (235 U/mg) (1,5 ml/hindlimb, 0.5 ml/diaphragm) were added to induce enzymatic digestion and the pellet was resuspended and triturated with a 10-ml serological pipette. Samples were incubated in a 37° C water bath with agitation (70 rpm) for 20 minutes, then passed through 18- and 19-gauge needles by using a 10 ml syringe to allow mechanical dissociation of the cell suspension into single cells. Samples were centrifuged at 500g for 10 minutes at 4°C, the pellet was resuspended and filtered through a 40 µm nylon cell strainer (Euroclone), centrifuged (500g, 10 minutes at 4°C), then resuspended in Wash Medium. Cells were counted and incubated on a rotating wheel (10 rpm) for 45 minutes at 4° C with primary antibodies to mark macrophages, fibro-adipogenic progenitors, satellite cells, hematopoietic and endothelial cells. A list of primary antibodies used is enclosed in **Table 2**. Samples were washed, APC Streptavidin (1:100, BioLegend) was added and samples were incubated on a rotating wheel (10 rpm) for 20 minutes at 4°C, then washed and resuspended in a sorting buffer (Wash Medium + (PBS with 1,5 mM EDTA, 2% BSA, 1% L-glutamine and 1% penicillin-streptomycin), 1:1 ratio). Samples were finally filtered through cell strainer cap tubes (Thermo Fisher Scientific).

Antibody	Company	Dilution
APC/Fire 750 anti-mouse CD45	BioLegend (103154)	1:100
APC/Fire 750 anti-mouse CD31	BioLegend (102434)	1:100
FITC anti-mouse F4/80	BioLegend (123107)	1:100
Brillant Violet 421 anti-mouse Ly-6A/E (Sca1)	BioLegend (108127)	1:100
Biotin anti-mouse CD016 (Vcam)	BioLegend (105704)	1:100

Table 2. Primary antibodies used to FACS isolate muscle cells.

FACS Aria™ II cell sorter (BD Biosciences) was used to separate cell populations. Physical parameters as forward scatter (FSC) and side scatter (SSC) were used to exclude cell clumps, debris, dead cells and to isolate single cells. Satellite cells were purified by negative selection with anti-CD31, anti-CD45, anti-Sca1 antibodies and positive selection with anti-Vcam antibody [35], fibro-adipogenic progenitors were purified by negative selection with anti-CD31 and anti-CD45 antibodies and positive selection with anti-Sca1 antibody (Judson et al., 2017), macrophages were purified by positive selection with anti-CD45 and anti-F4/80 antibodies. In experiments with C1r/s inhibitor satellite cells were purified by sorting YFP^{+ve} cells from $Pax7Cre^{ER/WT}$; $R26R^{YFP/WT}$; mdx^{4Cv} mice. After sorting, cells were processed for RNA extraction and RT-PCR. For immunostaining with anti-C1q cells were resuspended in Ham's F-10 supplemented with 20% FBS and allowed to adhere overnight on glass ECM-coated slides (Merck) before fixation.

2.2.3 Cell Culture

C2C12 (myoblasts, ATCC), RAW 264.7 (macrophages, ATCC), HEK 293 (embryonic kidney cells, ATCC), C3H/10T1/2 (fibroblasts, ATCC), NIH 3T3 (fibroblasts, ATCC) and STO (fibroblasts, ATCC) were maintained in DMEM supplemented with 10% FBS (GIBCO, decomplemented for 30 minutes at 56°C), 1% L-Glutamine and 1% penicillin-streptomycin and grown at 37°C with 5% CO_2. C57 primary myoblasts were isolated from C57 (Jacksoon Laboratory, no. 000664) mice, as previously described [181,345]. Primary cultures were plated on 5 ug/ml laminin/collagen coated dishes and amplified in Ham's F-10 (Euroclone) medium supplemented with 20% FBS (GIBCO, decomplemented for 30 minutes at 56°C), 1% L-glutamine and 1% penicillin-streptomycin and grown at 37°C with 5% CO_2. Every 24 hours, 2.5 ng/ml basic fibroblast growth factor (bFGF, LSBio) was added to the culture to maintain the cells in a proliferation state. All cell lines were mycoplasma-free.

In the experiment with mice sera, C2C12 cells were cultured for 24 hours in DMEM supplemented with 5 % mice serum collected from ~7-month-old wild type, ~7-month-old mdx^{4Cv} or ~31-month-old wild type mice, 1% L-glutamine and 1% penicillin-streptomycin. After 24 hours, cells were processed for RNA extraction and RT-PCR.

In experiments with conditioned media, STO and RAW 264.7 cells were plated, allowed to reach confluence and kept in 5% CO_2 incubator at 37°C for 4.5 days. Media were collected and filtered through a 0.42 µm filter prior C2C12 treatment. STO and RAW 264.7 media were combined in 8:1 ratio, which was previously calculated from *in vivo* analysis of the proportion of macrophages and FAPs in *mdx*^{4Cv} muscles (**Supplementary Figure 5**). 24 hours after treatment, C2C12 cells were processed for RNA extraction and RT-PCR.

In specific experiments C2C12 cells were treated with XAV-939 (100 µM, Sigma) for 6 hours, Wnt3A (100ng/ml or 50 ng/ml, Sigma), C1q (100 µg/ml, Sigma), C1r (25 µg/ml, BIOPUR), C1s (25 µg/ml, BIOPUR), C1r/s inhibitor (100 µg/ml, Merck) for 24 hours. After treatment, cells were processed for RNA extraction and RT-PCR.

2.3 Real-time PCR

Prior to RNA extraction, muscles were homogenized using a mortar and pestle on dry ice under liquid nitrogen. Total RNA was extracted from muscles, from FACS isolated cells and from cultured cells using TRIzol® Reagent (Invitrogen) according to manufacturer's instructions. RNA was quantified using NanoDrop spectrophotometer and reverse transcribed using High Capacity cDNA Reverse Transcription Kit (Thermo Fisher Scientific) according to manufacturer's instructions. Gene expression was measured by quantitative RT-PCR using SYBR Green Master Mix (Thermo Fisher Scientific) and a C1000 Touch thermocycler - CFX96 Real Time System (Biorad). The thermo protocol used for RT-PCR is indicated in **Table 3**. Primers spanning exon-exon junctions were used (**Table 4**). The level of each transcript was measured using mouse HPRT (hypoxanthine-guanine phosphoribosyltransferase) mRNA levels as normalizer.

Step	Temperature (°C)	Time (min)
1	50.0	2.00
2	95.0	5.00
3	95.0	0.15
4	60.0	1.00
5	72.0	0.30 (Plate read)
6	Go to step 3 (39x)	
7	65.0 – 95.0	0.05 – 0.5 (Plate read)

Table 3. RT-PCR thermo protocol.

Gene	Forward Primer 5'→3'	Reverse Primer 5'→3'	T_{Ann}
mAxin2	cagagggacaggaaccactc	tgccagtttctttggctctt	60 °C
mC1qa	tctcagccattcggcagaac	tggttggtgaggaccttgtca	60 °C
mC1qb	gggaatccactgctgtccggc	ctcagcctcaggggcttcctgt	60 °C
mC1qc	agagccaggaatcccagccgtcc	gcatgccaggctcgccctt	60 °C
mC1r	aaccatattacaagatgctgacca	ccttgggctgtgcaggta	60 °C
mC1s	gaccagaggcaggagaggaggc	gctcagtgtcaccttcaggagc	60 °C
mE2F1	gaggctggatctggagactg	cccggagatttcacacctttc	60 °C
mCol1a1	tccggctcctgctcctctta	gtatgcagctgacttcagggatgt	60 °C
mCol3a1	gcccacagccttctacac	ccagggtcaccatttctc	60 °C
mFn1	tgcctcgggaatggaaag	atggtaggtcttcccatcgtcata	60 °C
mLgr5	tcgccttccccaggtcccttc	gccgtggtccacaccccgat	60 °C
mTgfβ2	cgagcggagcgacgaggagt	tgggcgggatggcattttcgg	60 °C
mHPRT	tcagaccgctttttgccgcga	atcgctaatcacgacgctgggac	60 °C
h/mHPRT	aactggaaagaatgtcttgattgt	gaatttcaaatccaacaaagtctgg	60 °C
mLrp6	tcctcgagctctggcact	cctccccactcagtccaata	60 °C

Table 4. Primer list for SYBER Green RT-PCR

2.4 Tissue Lysis and Complement Proteins Quantification

All tissues (e.g., diaphragms, quadriceps, tibialis anterior) were weighed and resuspended in 1:10 w/v of lysis buffer (BupH™ Tris Buffered Saline (Thermo Scientific 28379) + protease inhibitor cocktail (Thermo Scientific A32963) + 10mM EDTA) by homogenizing with 7mm steel bead in Qiagen TissueLyser for 2 minutes at 30Hz. Lysates were then spun at 17,000 x g for 20 minutes. Supernatants were used for ELISA assays. Total protein was measured using the PIERCETM BCA Protein Assay kit (ThermoFisher 23225). The levels of free C1q, total C1q, C1s, C4, C3 and C3d proteins were measured in plasma and tissue lysates using sandwich ELISAs. Black 96 well plates (Costar #3925) were coated with 75 µL of respective capture antibody (**Table 5**) in bicarbonate buffer (pH 9.4) overnight at 4° C. Next day, the plates were washed with dPBS pH 7.4 (Dulbecco's phosphate-buffered saline) and then blocked with dPBS buffer containing 3% bovine serum albumin (BSA). Standard curves were prepared with purified proteins in assay buffer (dPBS containing 0.3% BSA, 0.1% Tween20, 10mM EDTA). The blocking buffer was removed from the plate by tapping. Standards and samples were added at 75 µL per well in duplicates and incubated with shaking at 300

rpm overnight at 4° C. Plates were washed thrice with wash buffer (dPBS containing 0.05% Tween20) and 75 µL of alkaline-phosphatase conjugated secondary antibodies (**Table 5**) were added to all wells. Plates were incubated at room temperature with shaking for 1h. Plates were washed thrice with wash buffer and developed using 75 µL of alkaline phosphatase substrate (Life Technologies, T2214). After 20 minutes at room temperature, plates were read using a luminometer. Standards were fit using a 4PL logistic fit and concentration of unknowns determined. Analyte levels were corrected for dilution and then plotted using GraphPad Prism. Tissues for proteins quantification were collected at CIBIO (Trento, Italy). Tissue lysis and ELISA assays were performed by Annexon Biosciences (California, US).

Assay	**Capture Antibody**	**Secondary Antibody**
C1q Free	anti-C1q (JL1, abcam 71940)	anti-C1q-AP (M1, Annexon)
C1q Total	anti-C1q (JL1, abcam 71940)	anti-C1q-AP (7H8, abcam 11861)
C1s	polyclonal anti-C1s (Annexon)	polyclonal anti-C1s-AP (Annexon)
C4	anti-C4 (LSBio C374031)	anti-C4-AP (Invitrogen MA1-40047)
C3	anti-C3d (Dako A063)	anti-C3-AP (MPBio 0855444)
C3d	anti-C3d (Dako A063)	anti-C3-AP (Novus Bio NB200-540)

Table 5. Antibodies used in ELISA assays.

2.5 Immunofluorescence

Cells were fixed with 4% paraformaldehyde for 10 minutes at room temperature, washed 4 times with PBS + 1% BSA + 0.2 % Triton, incubated with 10% donkey serum (DS, GIBCO) in PBS for 30 minutes, then incubated overnight at 4°C with primary antibodies in PSB with 1.5% DS. After incubation, samples were washed 4 times with PBS + 1% BSA + 0.2% Triton, incubated with Alexa Fluor® conjugated secondary antibodies in PBS with 1% BSA for 45 minutes at room temperature, washed 4 times with PBS + 0.2% Triton. Samples were incubated for 10 minutes with 10 µg/mL Hoechst in PBS, washed 3 times with PBS and mounted using Fluroshield histology mounting medium (Sigma).

Dissected muscles were fixed for 4-6 hours with 0.5% paraformaldehyde, then transferred to 30% sucrose overnight. Muscles were frozen in optimum cutting temperature compound (OCT), cryosectioned at 8 µm on glass and processed as cells. Alternatively, muscles were mounted on a small mound of 10% Gum Tragacanth (Alfa Aesar) placed on a cork disk. Muscles were frozen in nitrogen-

cooled isopentane, cryosectioned at 6 µm on glass and processed as cells. The acquisition of images was done with a Zeiss Axio Observer Z1 optical microscope equipped with a monochrome camera (AxioCam 503 mono D).

A list of primary and secondary antibodies is enclosed in **Table 6** and **Table 7**, respectively.

Antibody	**Specie**	**Company**	**Dilution**
Axin2	Rabbit	Abcam (32197)	1:20
TGFβ2	Rabbit	Santa Cruz Biotechnology (sc-90)	1:30
C4	Rat	Santa Cruz Biotechnology (16D2)	1:50
C1q	Rabbit	Abcam (182451)	1:80
C1q	Rat	Abcam (11861)	1:50
Laminin2α	Rat	Abcam (11576)	1:1000
Collagen1	Rabbit	Cederlane (CL50151AP)	1:200
Alexa Fluor 594 anti-mouse F4/80	Rat	BioLegend (123140)	1:50

Table 6. Primary antibody list for immunofluorescence

Antibody	**Specie**	**Company**	**Dilution**
Alexa Fluor 488 α rabbit	Donkey	Thermo Fisher Scientific	1:1000
Alexa Fluor 488 α rat	Donkey	Thermo Fisher Scientific	1:1000
Alexa Fluor 594 α rabbit	Donkey	Thermo Fisher Scientific	1:1000
Alexa Fluor 647 α rat	Donkey	Thermo Fisher Scientific	1:1000

Table 7. Secondary antibody list for immunofluorescence

2.5.1 Immunofluorescence analyses

The analysis of distance between macrophages and FAPs was performed on B6.129S4-PDGFRα$^{tm11(EGFP)Sor/J}$ and B6.129S4-PDGFRα$^{tm11(EGFP)Sor/J}$;*mdx*^{4Cv} muscles using two different approaches: 1) measuring the distance of each macrophage from its closest FAP within the image field (580 µm^2); for each biological replicate 60 to 200 macrophages were selected in at least twenty different sections, and the corresponding distance from their closest FAP was measured using the "distance" tool in Zen 2 software. 2) Measuring the distance of each FAP from its closest macrophage; for each biological replicate 100 to 350 FAPs were selected into a fixed portion of the image field (100 µm^2) in at least four different sections, and the corresponding distance from their closest macrophage

within the entire image field (580 μm^2) was measured using the "distance" tool in Zen 2 software. If no macrophage was present in the entire image field, distance was estimated as the distance between a FAP and the image edge. Refer also to **Supplementary Figure 6**.

The average collagen 1 pixel intensity was calculated for each biological replicate in 17 to 27 regions within the muscle sections excluding myofibers using Zen 2 software (Zeiss). The background pixel intensity measured on sections stained only with the secondary antibody was subtracted. The cross sectional area (CSA) was measured in 201 to 372 randomly selected myofibers for each biological replicate using Zen 2 software and the median of these measurements was calculated for each replicate. The percentage of fibrotic area was calculated by measuring for each biological replicate the area of 201 to 372 randomly selected myofibers in 3 to 6 different muscle sections and by using the following formula: [(total muscle area – total myofibers area)/total muscle area)] * 100.

2.5.2 Analysis of correlation of complement and Wnt-Tgfβ2 expression

The correlation between the expression of C1q and Wnt-related genes (Axin2 and Tgfβ2) was determined by quantifying the average pixel intensity of C1q, Axin2 and Tgfβ2 signals using Zen 2 software. For each biological replicate ≥ 106 randomly selected regions of 1017 μm^2 (for C1q and Axin2 correlation) or 102 μm^2 (for C1q and Tgfb2 correlation) were analyzed within the regenerating areas of the muscle. The background pixel intensity measured on sections stained only with the secondary antibody was subtracted. Normal or non-normal distribution of data set, Spearman (*r*) and Pearson coefficient (*r*) were determined with GraphPad Prism 8 software. Refer also to **Supplementary Figure 8**.

2.6 Statistical Analysis

Unless otherwise stated, experiments presented here were repeated at least three times. Unless otherwise stated, data are presented as mean ± SEM. Statistical analysis was performed using GraphPad Prism 8. One-way ANOVA test was performed for multiple comparison; parametric Student-t test or non-parametric Mann-Whitney test was performed for comparison between two groups. The number of biological replicates and the use of specific tests has been reported in each figure legend. Statistical significance was expressed with p-value (p): $p > 0.05$: ns; $p \leq 0.05$: *; $p < 0.01$: **; $p < 0.001$: *** and $p < 0.0001$: ****.

3. Results

3.1 Skeletal muscles express the classical complement pathway's components and their expression is enhanced in dystrophy.

Enhanced levels of the canonical Wnt signaling are reported in both dystrophic and aged mice [159,160,181]. At first, in the aged mice it was shown that serum components may account for the enhanced Wnt signaling [159]. Later on, increased levels of complement proteins in the serum have been reported to lead to an increased Wnt signaling in the old mice's muscles [160]. In order to evaluate whether the factors that contribute to an enhanced canonical Wnt signaling in the dystrophic mice have a serum origin, C2C12 myoblasts were cultured for 6 hours in DMEM supplemented with 5% of serum collected from ~7 months old wild type, ~7 months old *mdx*^{4Cv}, ~31 months old wild type mice or Wnt3a and Axin2 mRNA expression was evaluated as a readout of the canonical Wnt signaling expression (**Figure 11 A**). *Axin2* expression was increased in cells cultured with the serum collected from old mice compared to cells cultured with the serum collected from wild type and *mdx*^{4Cv} mice. However, *Axin2* expression in cells cultured with the *mdx*^{4Cv} serum was not significantly different to its expression in cells cultured with the wild type serum, suggesting that the factors that lead to an increased Wnt signaling in the dystrophic muscles are not likely found in the serum (**Figure 11 A**).

C1q has been previously shown to lead to an increased expression of the canonical Wnt signaling in the skeletal muscles of aged mice [160]. We hypothesized that C1q could enhance the expression of the canonical Wnt signaling in the dystrophic muscles as well. The serum collected from *mdx*^{4Cv} mice did not lead to an enhanced expression of the canonical Wnt signaling in C2C12 myoblasts compared to cells cultured with the serum from the wild type (**Figure 11A**); thus, we evaluated the classical complement cascade proteins' levels in the skeletal muscles in order to test whether the muscles could locally produce complement proteins. The levels of the classical complement proteins C1q, C1s, C3, C3d and C4 were evaluated through ELISA in diaphragms, quadriceps and tibialis anterior of ~1 month, ~3 months and ~1 year old wild type and *mdx*^{4Cv} mice (**Figure 11 B-F and Supplementary Figure 1**). Importantly, mice were perfused with PBS prior to muscle dissection and ELISA with the aim of restricting the evaluation to the muscles and excluding the serum protein components from the analysis. C1q, C1s, C3, C3d and C4 were expressed in all the analyzed wild type and *mdx*^{4Cv} muscles (**Figure 11 B-F and Supplementary Figure 1**). C1q (**Figure 11 B and Supplementary Figure 1 A-E**), C1s (**Figure 11 C and Supplementary Figure F-G**), C3 (**Figure 11 D and Supplementary Figure 1 H-I**) and C3d (**Figure 11 E and Supplementary Figure J-K**) protein expression was higher in the ~1 month, ~3 months and ~1 year old dystrophic muscles compared to the wild type in the diaphragm, quadriceps and tibialis anterior, reaching statistical significance in most cases. C4 protein expression was higher in the dystrophic tibialis anterior **(Figure 11 F)** and quadriceps

(Supplementary Figure 1 L) of ~1 month old mice compared to the wild type, in the diaphragm of ~3 months old dystrophic mice compared to the wild type **(Figure 11 F)** and in the tibialis anterior of ~1 year old dystrophic mice compared to the wild type (**Figure 11 F**).

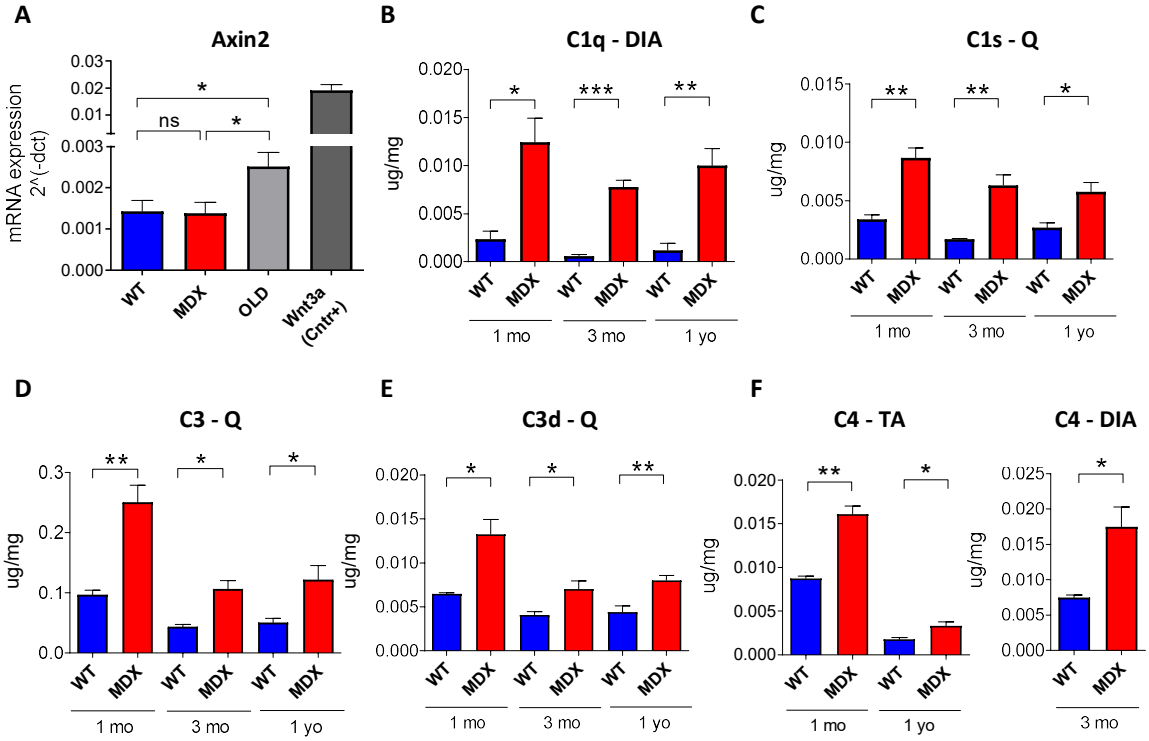

Figure 11. The classical complement pathway is enhanced in muscles of dystrophic mice. (A) qPCR analysis of Axin2 expression of C2C12 cells cultured for 6 hours in DMEM supplemented with 5% serum collected from ~7 months old wild type (WT), ~7 months old *mdx*^{4Cv} (MDX), ~31 months old wild type (OLD) mice or with 50 ng/ml Wnt3a (Cntr+). N=8 (WT), N=7 (MDX), N=6 (OLD), N=4 (Cntr+). Data are expressed as mean with SEM. One-way Anova test was applied. **(B-F)** ELISA assay of proteins of the classical complement pathway: C1q (**B**), C1s (**C**), C3 (**D**), C3d (**E**), C4 (**F**). C1q protein level was assessed using anti C1qJL1-7H8 antibody. Refer also to **Supplementary Figure 1** for ELISA performed on the same muscles using anti C1qJL1-M1 antibody. Diaphragm (DIA), quadriceps (Q) and tibialis anterior (TA) muscles from ~1 month (1 mo), ~3 months (3 mo) or ~1 year old (1 yo) wild type (WT) and *mdx*^{4Cv} (MDX) mice (as indicated on the graphs) were used. N=3 (WT 1 mo, WT 3 mo), N=4 (WT 1 yo, MDX 1 mo, MDX 3 mo, MDX 1 yo). Data are expressed as mean with SEM. Two-tailed unpaired t-test was applied. $p > 0.05$: ns; $p \leq 0.05$: *; $p \leq 0.01$: **; $p \leq 0.001$: ***; $p \leq 0.0001$: ****. Refer also to **Supplementary Figure 1**.

The same dystrophic and wild type mice analyzed for complement proteins expression (**Figure 11**) exhibited a differential muscle resistance during behavioral tests performed before muscle dissection and ELISA, in keeping with the reported motor deficit occurring in the *mdx* mice compared to healthy controls [346,347]. Dystrophic mice were less resistant during the 4 limbs hanging wire test compared to the age-matched wild type at ~3 months and ~1 year old (**Figure 12 A**). In the open field test, ~3 months old dystrophic mice walked a shorted distance at a lower speed and spent more immobile time compared to the wild type (**Figure 12 B**), whereas no differences were observed among ~1-months and ~1 year old dystrophic mice compared to the age-matched wild type (**Supplementary Figure 2 B, C**).

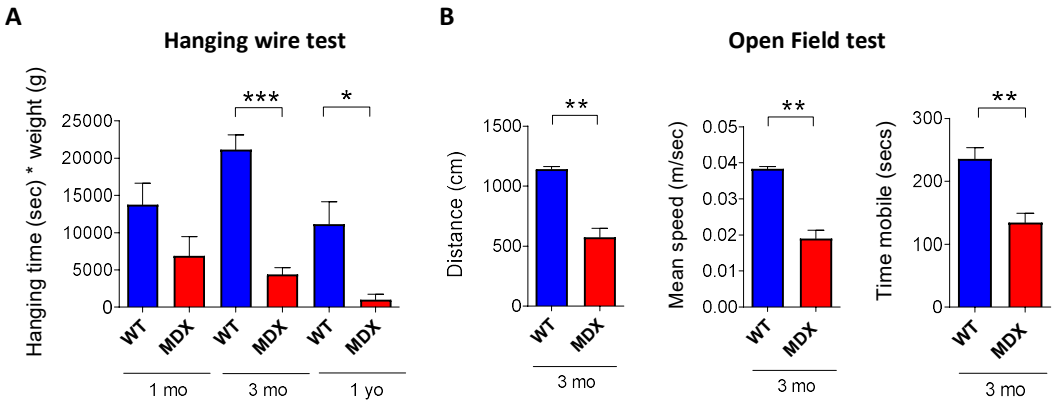

Figure 12. Dystrophic mice are less resistant to physical activity compared to the wild type. (A) Hanging test performed on ~1 month (1 mo), ~3 months (3 mo) and ~1 year (1 yo) old wild type (WT) and *mdx*^{4Cv} (MDX) mice. N=3 (WT 1 mo, WT 3 mo), N=4 (WT 1 yo, MDX 1 mo, MDX 3 mo, MDX 1 yo). Data are expressed as mean with SEM. Two-tailed unpaired t-test was applied. **(B)** Open field test performed on ~3 months (3 mo) old wild type (WT) and *mdx*^{4Cv} (MDX) mice. N=3 (WT 3 mo), N=4 (MDX 3 mo). Refer also to **Supplementary Figure 2**. Data are expressed as mean with SEM. Two-tailed unpaired t-test was applied. $p > 0.05$: ns; $p \leq 0.05$: *; $p \leq 0.01$: **; $p \leq 0.001$: ***; $p \leq 0.0001$: ****.

We performed immunofluorescence studies, which revealed C4, C1q and C1s protein expression in the interstitial space of *mdx*^{4Cv} muscles (**Figure 13**). Moreover, C1s and C1q protein expression resulted higher in the ~1 year old dystrophic muscles compared to the wild type (**Figure 13 B-C** and **Supplementary Figure 3**).

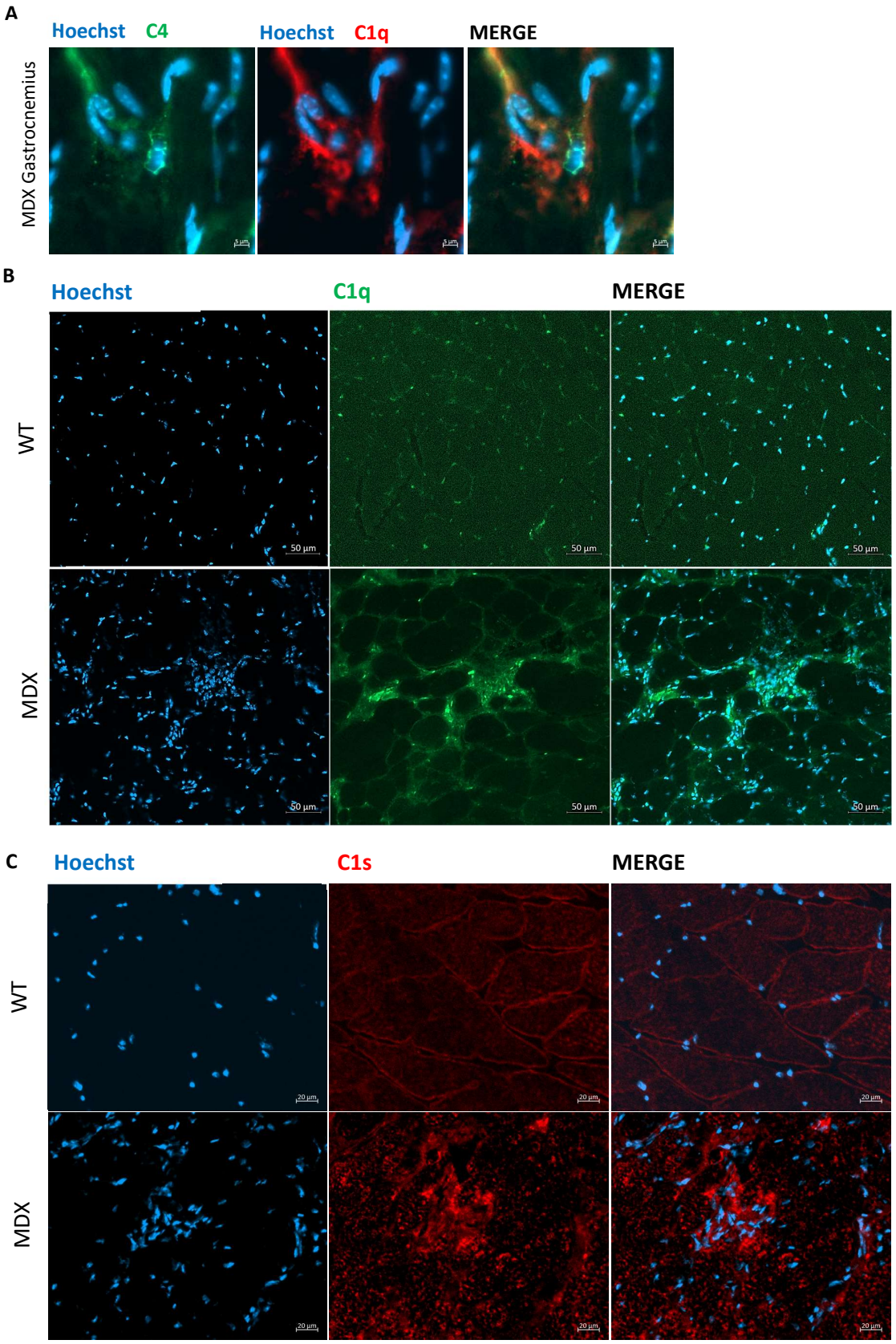

Figure 13. C4, C1q and C1s proteins expression in muscles. (A) Representative immunofluorescence of gastrocnemius of ~ 5 months old *mdx*^{4Cv} (MDX) stained with anti-C4 (green),

anti-C1q (red) and Hoechst (blue). Scale bar: 5 µm. **(B)** Representative immunofluorescence of gastrocnemius of ~ 1 year old wild type (WT) and *mdx*^{4Cv} (MDX) stained with anti-C1q (green) and Hoechst (blue). Note that C1q expression is higher in *mdx*^{4Cv} muscles compared to the wild type. Scale bar: 50 µm. **(C)** Representative immunofluorescence of gastrocnemius of ~ 1 year old wild type (WT) and *mdx*^{4Cv} (MDX) stained with anti-C1s (red) and Hoechst (blue). Note that C1q expression is higher in *mdx*^{4Cv} muscles compared to the wild type. Scale bar: 20 µm.

Having assessed that the classical complement proteins are more expressed in dystrophic muscles compared to the wild type (**Figure 11, 13** and **Supplementary Figure 1, 3**), we focused our study on the first component of the pathway, C1 complex, which triggers the complement cascade activation after the pathogens' recognition. C1 complex comprises the C1q sensing unit, which consists of C1qa, C1qb and C1qc chains, and the heterotetramer C1s/C1r/C1r/C1s (**Figure 14 A**). We found that the mRNA levels of all C1 complex components (i.e., *C1qa*, *C1qb*, *C1qc*, *C1r* and *C1s*) are increased in the hindlimb muscles of ~1 year old dystrophic mice compared to the wild type supporting the idea of a local production of all C1 components (**Figure 14 B**).

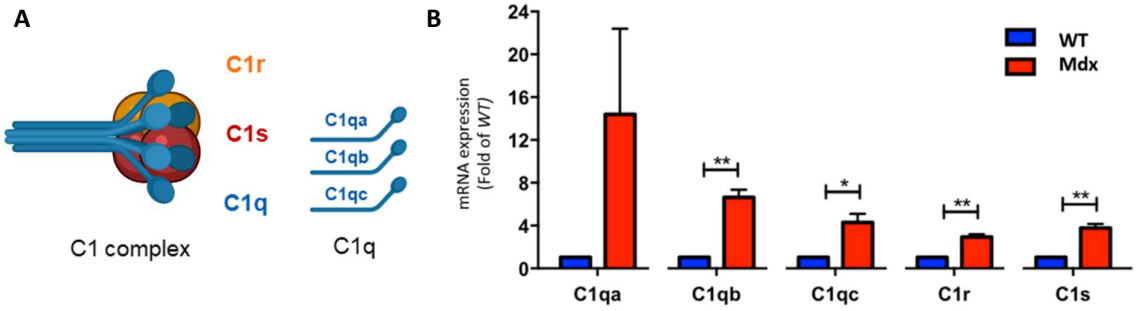

Figure 14. C1 complex components' expression is enhanced in dystrophic muscles. (A) Schematic representation of C1 protein complex, composed of the subcomponents C1q, C1s and C1r. C1q consists of six A-chains, six B-chains and six C-chains. Created with BioRender.com. **(B)** mRNA expression of C1 complex subunits C1qa, C1qb, C1qc, C1r, C1s in hindlimb muscles of ~ 1 year old wild type (WT) and *mdx*^{4Cv} (Mdx) mice. N=3. Data are expressed as mean with SEM. Two-tailed unpaired t-test was applied. $p > 0.05$: ns; $p \leq 0.05$: *; $p \leq 0.01$: **; $p \leq 0.001$: ***; $p \leq 0.0001$: ****.

Taken together, these data indicate that: 1) the expression of an enhanced Wnt signaling in the *mdx*^{4Cv} mice compared to the wild type is likely not caused by factors found in the serum; 2) proteins of the classical complement cascade are produced in skeletal muscles; 3) the expression of most of the classical complement pathway proteins (i.e. C1q, C1s, C3, C3d, C4) is overall increased in dystrophic

muscles compared to the wild type; 4) dystrophic mice which have a higher muscle expression of the classical complement proteins are also overall less resistant to physical activity; 5) the gene expression of all the C1 complex components is increased in the dystrophic muscles compared to the wild type suggesting their local production.

3.2 C1 complex's components are expressed by distinct cell types in the skeletal muscles and they are differentially expressed in homeostatic and injured tissues.

After having assessed that the classical complement proteins are locally expressed by muscles and that their expression is higher in the dystrophic mice compared to the wild type (**Figures 11, 13, 14** and **Supplementary Figures 1-3**), we aimed to establish which cell type/s express C1 complex's components within the skeletal muscles. Moreover, we wanted to compare C1 complex components' expression in two different types of muscle injuries: the chronic injury which characterize the dystrophic muscles and the acute injury performed through needle punctures. Hindlimb muscles were collected from ~1 year old wild type mice, ~1 year old *mdx*^{4Cv} mice and ~1 year old wild type mice 2.5 days after muscle injury. Five different cell populations were FACS isolated (**Figure 15**): CD45^{+ve}F4/80^{+ve} (macrophages, MAC), CD45^{-ve}CD3^{-ve}Sca^{+ve} (fibro-adipogenic progenitors, hereinafter referred to as FAPs) [348], CD45^{-ve}CD31^{-ve}Sca1^{-ve}Vcam^{+ve} (satellite cells, SC) [35], CD45^{-ve}CD31^{-ve}Sca1^{-ve}Vcam^{-ve} (hereinafter referred to as Lin^{-ve}Sca1^{-ve}Vcam^{-ve}, Lin^{-ve}: CD45^{-ve}CD31^{-ve}), CD45^{+ve}CD31^{+ve}F4/80^{-ve} (hereinafter referred to as Lin^{+ve}F4/80^{-ve}, Lin^{+ve}: CD45^{+ve}CD31^{+ve}). Single fibers from the same animals were also isolated as previously reported [344].

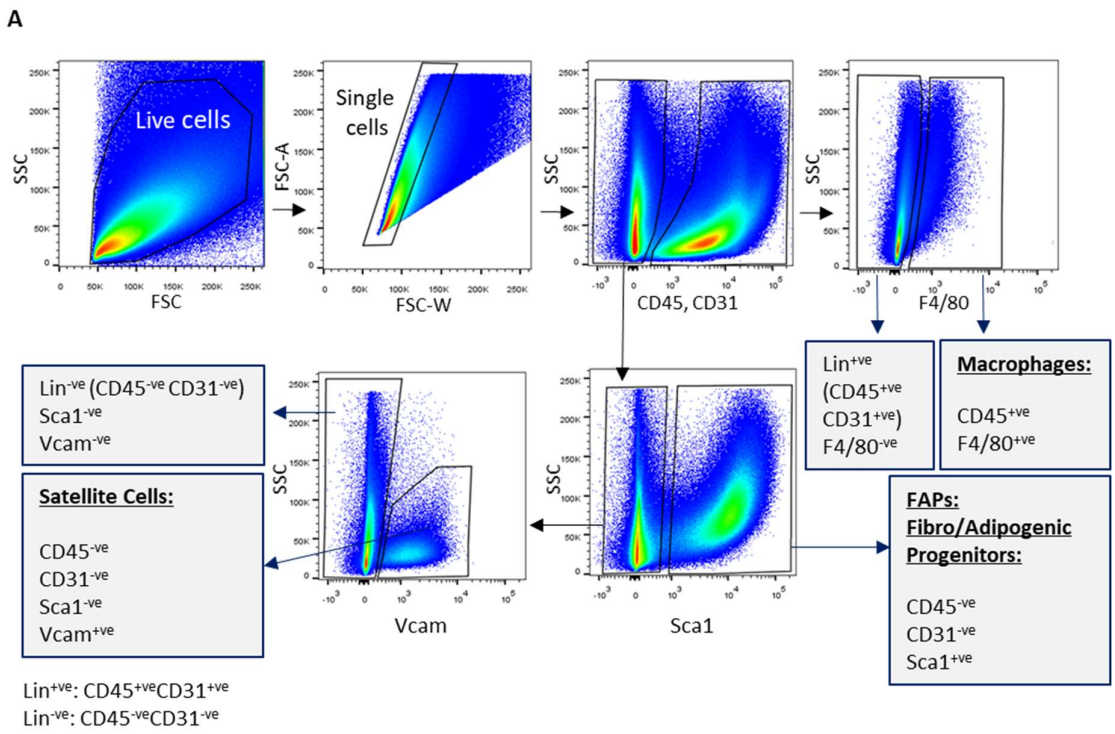

Figure 15. Sorting strategy of muscle cell populations. (A) Representative gating and sorting strategy used to FACS isolate macrophages (MAC: $CD45^{+ve}F4/80^{+ve}$), fibro/adipogenic progenitors (FAPs: $CD45^{-ve}CD31^{-ve}Sca1^{+ve}$), satellite cells (SC: $CD45^{-ve}CD31^{-ve}Sca1^{-ve}Vcam^{+ve}$), $Lin^{+ve}F4/80^{-ve}$ (Lin^{+ve}: $CD45^{+ve}CD31^{+ve}$) and $Lin^{-ve}Sca1^{-ve}Vcam^{-ve}$ (Lin^{-ve}: $CD45^{-ve}CD31^{-ve}$) cell populations from wild type (WT) and *mdx*^{4Cv} (MDX) hindlimb muscles.

The mRNA analysis of *C1qa*, *C1qb*, *C1qc*, *C1r* and *C1s* performed in cells isolated from wild type, *mdx*^{4Cv} and injured tissues showed that: 1) *C1qa* (**Figure 16 A**), *C1qb* (**Figure 16 B**) and *C1qc* (**Figure 16 C**) are mostly expressed by macrophages in the wild type, *mdx*^{4Cv} and injured muscles, whereas all the other cell types exhibit negligible *C1qa* (**Figure 16 A**), *C1qb* (**Figure 16 B**) and *C1qc* (**Figure 16 C**) levels. 2) *C1r* (**Figure 16 D**) and *C1s* (**Figure 16 E**) are mostly expressed by FAPs in the wild type, *mdx*^{4Cv} and injured muscles. $Lin^{-ve}Sca1^{-ve}Vcam^{-ve}$ represent the second type of cells expressing *C1r* (**Figure 16 D**) and *C1s* (**Figure 16 E**) in the wild type, *mdx*^{4Cv} and injured muscles, whereas all the other cell types exhibit negligible *C1s* (**Figure 16 D**) and *C1r* (**Figure 16 E**) levels. 3) The *mdx*^{4Cv} macrophages and FAPs express higher levels of *C1qb* (**Figure 16 B**) and *C1r* (**Figure 16 D**), respectively, compared to the wild type muscles. Furthermore, the gene expression analysis of C1 complex components in wild type, *mdx*^{4Cv} and injured muscles showed that: 1) The expression of C1q cluster genes is lower in the macrophages isolated from injured muscles compared to the *mdx*^{4Cv}, with *C1qa* and *C1qb* expression reaching statistical significance and *C1qc* exhibiting a similar trend (**Figure 16 A-C**). 2) The expression of *C1r* and *C1s* is lower in FAPs isolated from injured muscles compared to the *mdx*^{4Cv} (**Figure 16 D-E**). 3) *C1s* is less expressed in the FAPs isolated from the

injured muscles compared to the wild type (**Figure 16 E**). These data lead to the conclusion that the five C1 complex's components are expressed by different cell types within the skeletal muscles and that they are differentially expressed in homeostatic and injured tissues. Moreover, C1 complex gene expression is overall higher in dystrophic muscles which are characterized by a chronic state of inflammation and injury compared to muscles undergoing the regeneration process following a single acute injury event.

Homeostatic and injured muscles exhibit different proliferative states. The former exist in a quiescent state characterized by mitotic inactivity [10]. The latter undergo the regenerative process which includes both satellite cells and support cells proliferation [2]. In order to investigate whether the observed differential expression of C1 complex components in the wild type, dystrophic and wild type muscles after injury (**Figure 16 A-D**) was related to the different proliferative cells state in the muscles, we analyzed in the same muscles' cells the expression of *E2F transcription factor 1 (E2F1)*, a widely known marker of cell proliferation [349]. *E2F1* expression was increased in the satellite cells of injured muscles compared to the wild type, with this being in line with the proliferative activity of satellite cells during the regeneration process [2]. *E2F1* expression was not significantly different between macrophages and FAPs isolated from wild type muscles, dystrophic muscles and wild type muscles 2.5 days after acute injury, suggesting that C1 complex expression in these cells might not depend on the differential proliferative state existing in the homeostatic and regenerative conditions (**Figure 16 F**).

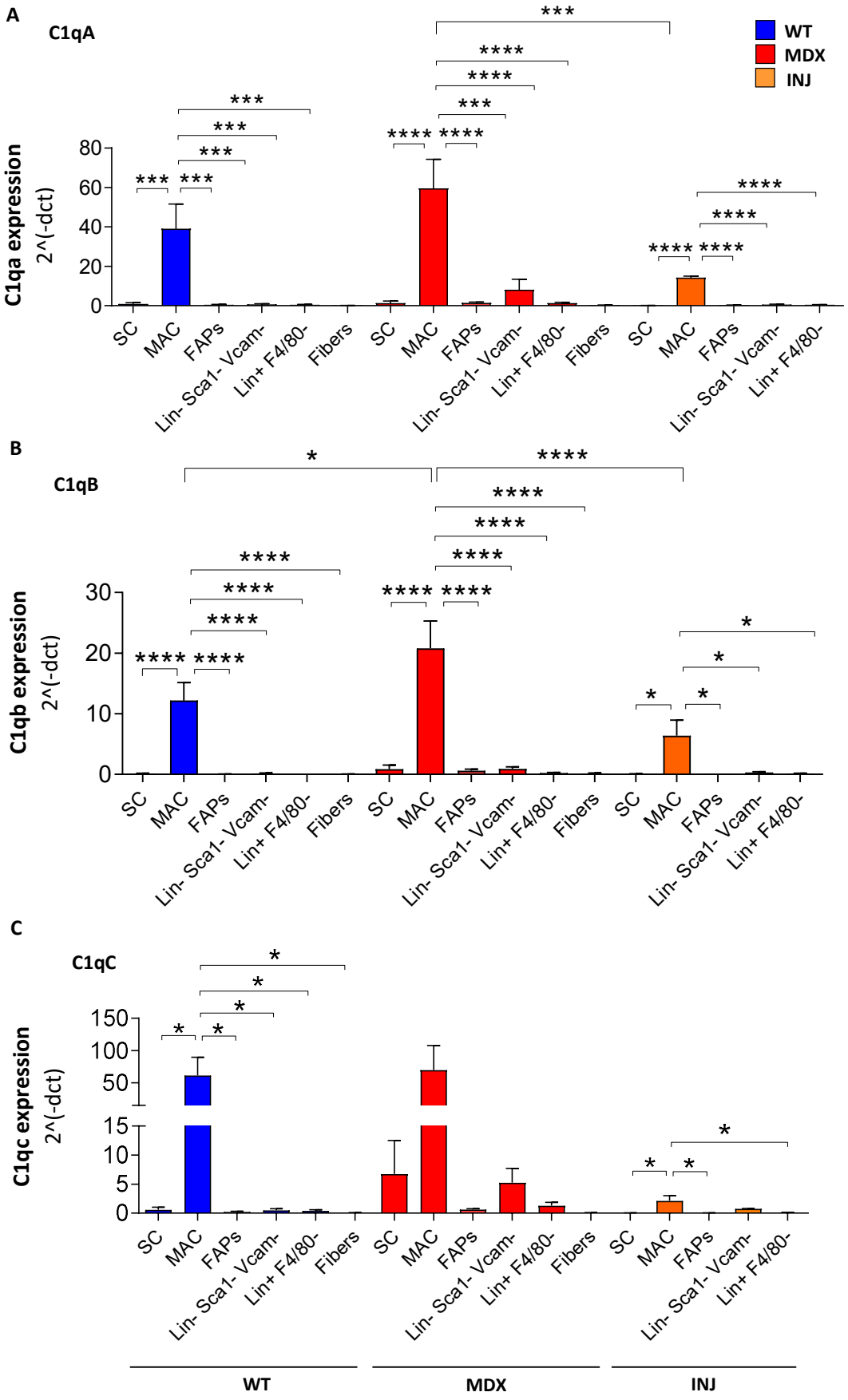
A
C1qA
WT
MDX
INJ
C1qa expression
2^(-dct)
B
C1qB
C1qb expression
2^(-dct)
C
C1qC
C1qc expression
2^(-dct)
SC
MAC
FAPs
Lin- Sca1- Vcam-
Lin+ F4/80-
Fibers
WT
MDX
INJ

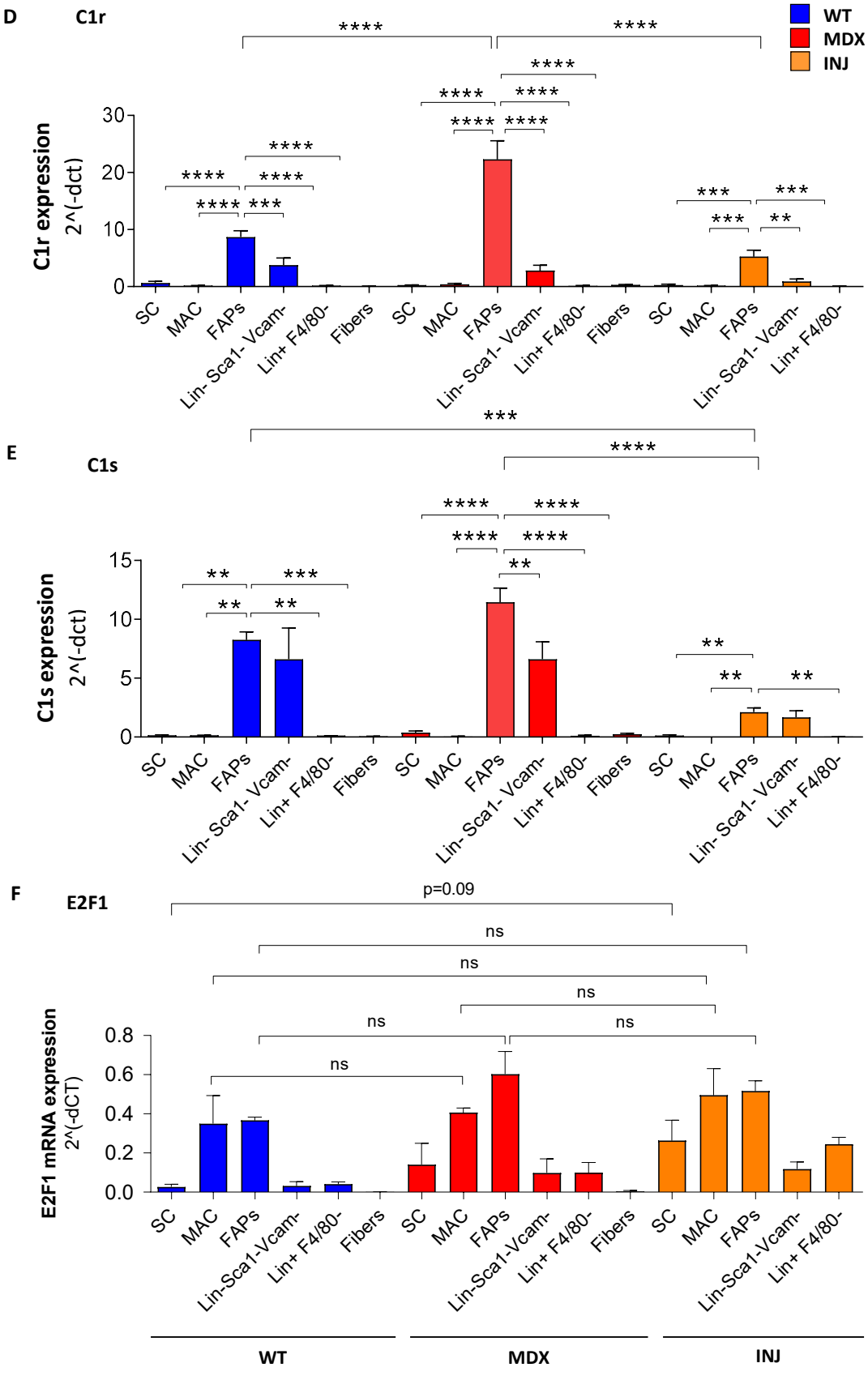

Lin-: CD45^{-ve}CD31^{-ve}
Lin+: CD45^{+ve}CD31^{+ve}

Figure 16. C1 complex's components are expressed by distinct cell types in the skeletal muscles and they are differently expressed in homeostatic and injured tissues. (A-E) qPCR analysis of C1qa **(A)**, C1qb **(B)**, C1qc **(C)**, C1r **(D)**, C1s **(E)** and E2F1 **(F)** expression in satellite cells (SC), macrophages (MAC), fibro/adipogenic progenitors (FAPs), $Lin^{+ve}F4/80^{-ve}$, $Lin^{-ve}Sca1^{-ve}Vcam^{-ve}$ and single fibers (Fibers) isolated from hindlimb muscles of ~ 1 year old wild type (WT), *mdx*^{4Cv} (MDX) and wild type 2.5 days after acute injury (INJ). N=5 (C1qa, C1qb, C1qc, C1r in WT and MDX SC, MAC, FAPs, $Lin^{+ve}F4/80^{-ve}$, $Lin^{-ve}Sca1^{-ve}Vcam^{-ve}$); N=3 (C1s in WT and MDX SC, MAC, FAPs, $Lin^{+ve}F4/80^{-ve}$, $Lin^{-ve}Sca1^{-ve}Vcam^{-ve}$; C1qa, C1qb, C1qc; C1r and C1s in INJ SC, MAC, FAPs, $Lin^{+ve}F4/80^{-ve}$, $Lin^{-ve}Sca1^{-ve}Vcam^{-ve}$); N=4 (C1qa, C1qb, C1qc, C1r and C1s in Fibers); N=3 (E2F1 in all samples). Data are expressed as mean with SEM. One-way Anova test was applied. Two-tailed unpaired t-test was applied between WT SC and INJ SC. $p > 0.05$: ns; $p \leq 0.05$: *; $p \leq 0.01$: **; $p \leq 0.001$: ***; $p \leq 0.0001$: ****. SC: $CD45^{-ve}CD31^{-ve}Sca1^{-ve}Vcam^{+ve}$; MAC: $CD45^{+ve}F4/80^{+ve}$; FAPs: $CD45^{-ve}CD31^{-ve}Sca1^{+ve}$; Lin^{+ve}: $CD45^{+ve}CD31^{+ve}$; Lin^{-ve}:$CD45^{-ve}CD31^{-ve}$.

C1q protein expression was observed in $F4/80^{+ve}$ cells (macrophages) of *mdx*^{4Cv} muscles' (i.e. diaphragm and gastrocnemius) cryosections through immunofluorescence (**Figure 17 A** and **Supplementary Figure 4**). Moreover, C1q expression was observed in FACS isolated macrophages from dystrophic muscles but not in FAPs nor in satellite cells isolated from the same muscles, further underling that C1q is selectively expressed by macrophages in the muscle (**Figure 17 B**).

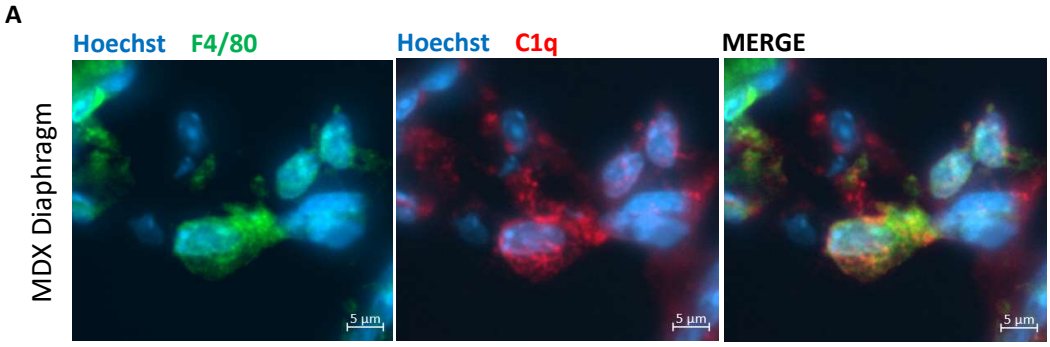

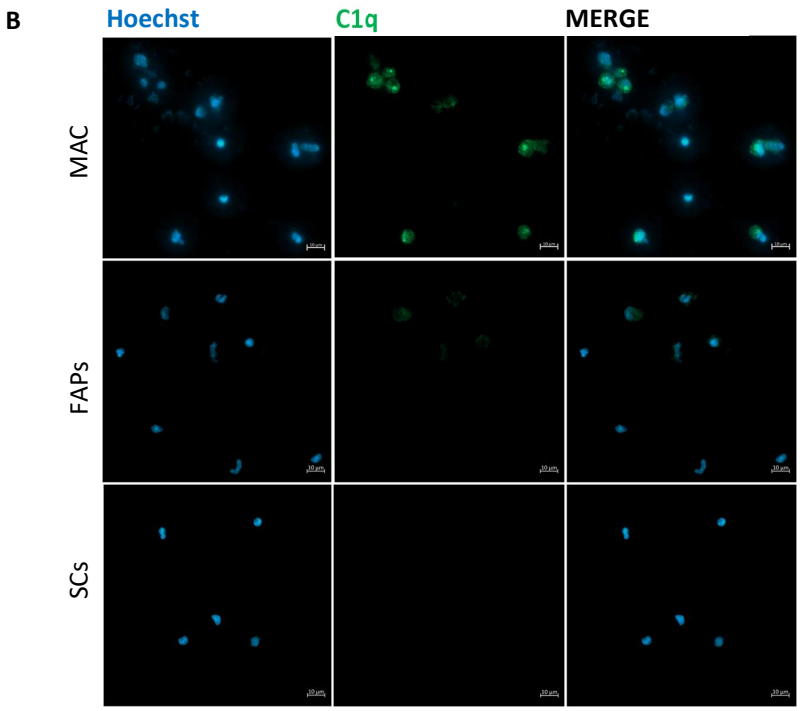

Figure 17. C1q protein is selectively expressed by macrophages in dystrophic muscles. (A) Representative immunofluorescence of a cryosection of ~ 5 months old *mdx*^{4Cv} (MDX) diaphragm stained with anti-F4/80 (green), anti-C1q (red) and Hoechst (blue). Scale bar: 2 µm. **(B)** Representative immunofluorescence image of FACS isolated satellite cells (SCs), fibro/adipogenic progenitors (FAPs) and macrophages (MAC) from ~ 1 year old *mdx*^{4Cv} (MDX) hindlimb muscles stained with anti-C1q (green) and Hoechst (blue). Scale bar: 10 µm.

3.3 Macrophages and fibro/adipogenic progenitors are increased in dystrophic muscles.

We observed that the classical complement pathway levels, including C1 complex components' levels, are increased in dystrophic muscles compared to the wild type (**Figure 11, 13, 14, 16** and **Supplementary Figure 1, 3**). Moreover, we observed that macrophages and FAPs are the main cellular sources of C1 complex components within the skeletal muscle (**Figure 16 A-D** and **Figure 17**). In order to assess whether an increased amount of these two cell types may account for the enhanced expression of complement levels in the dystrophic muscles we quantified macrophages and FAPs in the diaphragm and in hindlimb muscles of ~1 year old wild type and dystrophic mice. We found that the number of macrophages is increased in both the diaphragm and the hindlimb muscles of the dystrophic mice compared to the wild type when calculated both as percentage of $CD45^{+ve}CD31^{+ve}$ cells (**Figure 18 A**) as well as total number of cells per mg of tissue (**Figure 18 B**). Similarly, the

number of FAPs is increased in both the diaphragm and the hindlimb muscles of the dystrophic mice compared to the wild type when calculated both as percentage of CD45^{-ve}CD31^{-ve} cells (**Figure 18 C**) as well as total number of cells per mg of tissue (**Figure 18 D**).

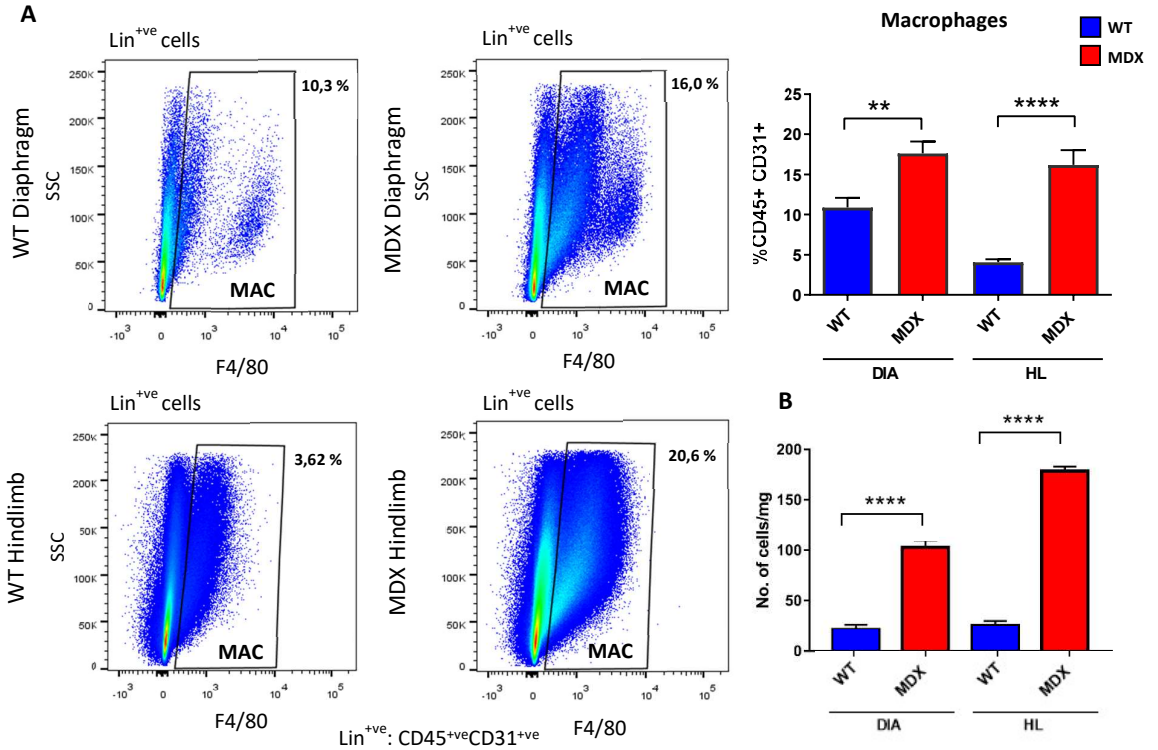

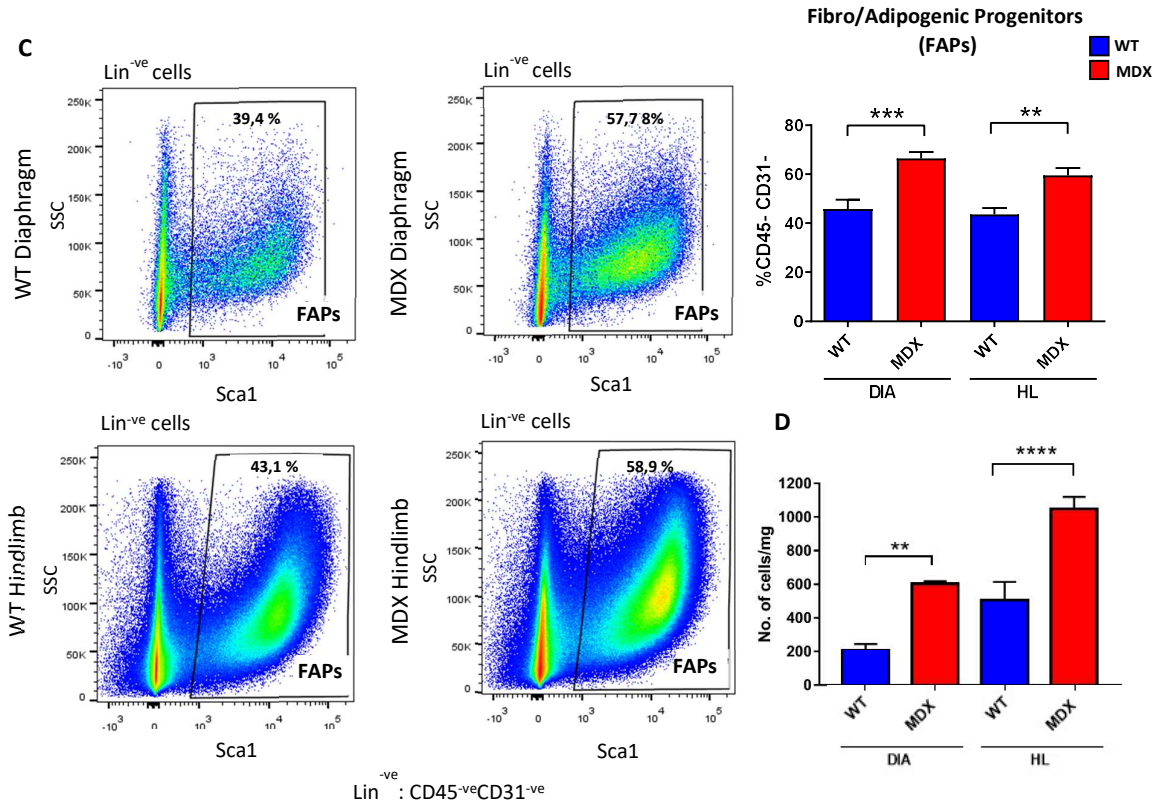

Figure 18. Macrophages and fibro/adipogenic progenitors are increased in dystrophic muscles. **(A)** Representative FACS plot (left) and quantification (right) of macrophages (MAC: $CD45^{+ve}F4/80^{+ve}$) expressed as percentage of Lin^{+ve} cells (Lin^{+ve}: $CD45^{+ve}CD31^{+ve}$) in diaphragm (DIA) and hindlimb (HL) muscles of ~ 1 year old wild type (WT) and *mdx*^{4Cv} (MDX) mice. N=7 (WT DIA, MDX DIA); N=8 (WT HB, MDX HB). **(B)** Number of macrophages (MAC: $CD45^{+ve}F4/80^{+ve}$) per mg of tissue in diaphragm (DIA) and hindlimb (HL) muscles of ~ 1 year old wild type (WT) and *mdx*^{4Cv} (MDX) mice. N=7 (WT DIA, MDX DIA); N=8 (WT HL, MDX HL). **(C)** Representative FACS plot (left) and quantification (right) of fibro/adipogenic progenitors (FAPs: $CD45^{-ve}CD31^{-ve}Sca1^{+ve}$) expressed as percentage of Lin^{-ve} cells (Lin^{-ve}: $CD45^{-ve}CD31^{-ve}$) in diaphragm (DIA) and hindlimb (HL) muscles of ~ 1 year old wild type (WT) and *mdx*^{4Cv} (MDX) mice. N=7 (WT DIA, MDX DIA); N=8 (WT HB, MDX HB). **(D)** Number of fibro/adipogenic progenitors (FAPs: $CD45^{-ve}CD31^{-ve}Sca1^{+ve}$) per mg of tissue in diaphragm (DIA) and hindlimb (HL) muscles of ~ 1 year old wild type (WT) and *mdx*^{4Cv} (MDX) mice. N=7 (WT DIA, MDX DIA); N=8 (WT HL, MDX HL). Data are expressed as mean with SEM. Two-tailed unpaired t-test was applied. $p > 0.05$: ns; $p \leq 0.05$: *; $p \leq 0.01$: **; $p \leq 0.001$: ***; $p \leq 0.0001$: ****.

Taken together our evaluations of the complement amount in muscles both at the protein and gene levels suggests that the increased C1 complex expression observed in the dystrophic muscles compared to the wild type (**Figure 11, 13, 14, 16** and **Supplementary Figure 1, 3**) is due to a combination of two factors: 1) an increased number of macrophages and FAPs in the dystrophic muscles compared to the wild type (**Figure 18**), with these two cell types being the main cellular sources of C1q (C1qa, C1qb and C1qc) and C1s/r, respectively (**Figure 16**); 2) at least for specific C1 complex components (i.e., C1qb and C1r) an increased transcriptional activity of macrophages (for *C1qb*) and FAPs (for *C1r*) in the dystrophic muscles compared to the wild type (**Figure 16**).

3.4 C1 complex components are selectively expressed by different cell lines.

The complement component C1q has been reported to activate the canonical Wnt signaling in the aged mice [160]. In the dystrophic mice we observed that C1 complex components are expressed mostly by macrophages (C1q) and FAPs (C1r/s) (**Figure 16, 17**). In order to establish an *in vitro* model that recapitulates the differential expression of the C1 complex components observed *ex vivo* we tested the gene expression of C1 complex in the following murine cell lines: STO (fibroblasts), C3H/10/T1/2 (fibroblasts), NIH 3T3 (fibroblasts), RAW 264.7 (macrophages), C2C12 (myoblasts), primary myoblasts derived from C57BL/6J mice (hereinafter referred to as C57). Similarly to our gene expression analysis of freshly isolated dystrophic cells (**Figure 16**), we observed that: 1) *C1qa*, *C1qb* and *C1qc* are mostly expressed by macrophages (**Figure 19 A-C**); 2) *C1s* and *C1r* are mostly expressed by fibroblasts (**Figure 19 D-E**); 3) myoblasts (C2C12 and C57) express negligible to

undetectable levels of all C1 complex components (**Figure 19 A-E**). C1q protein expression was observed through immunofluorescence in RAW 264.7 macrophages, but no C1q staining was detected neither in STO fibroblasts nor in C2C12 myoblasts (**Figure 19 F**), further underling that C1q is selectively expressed by macrophages within the tested cell lines.

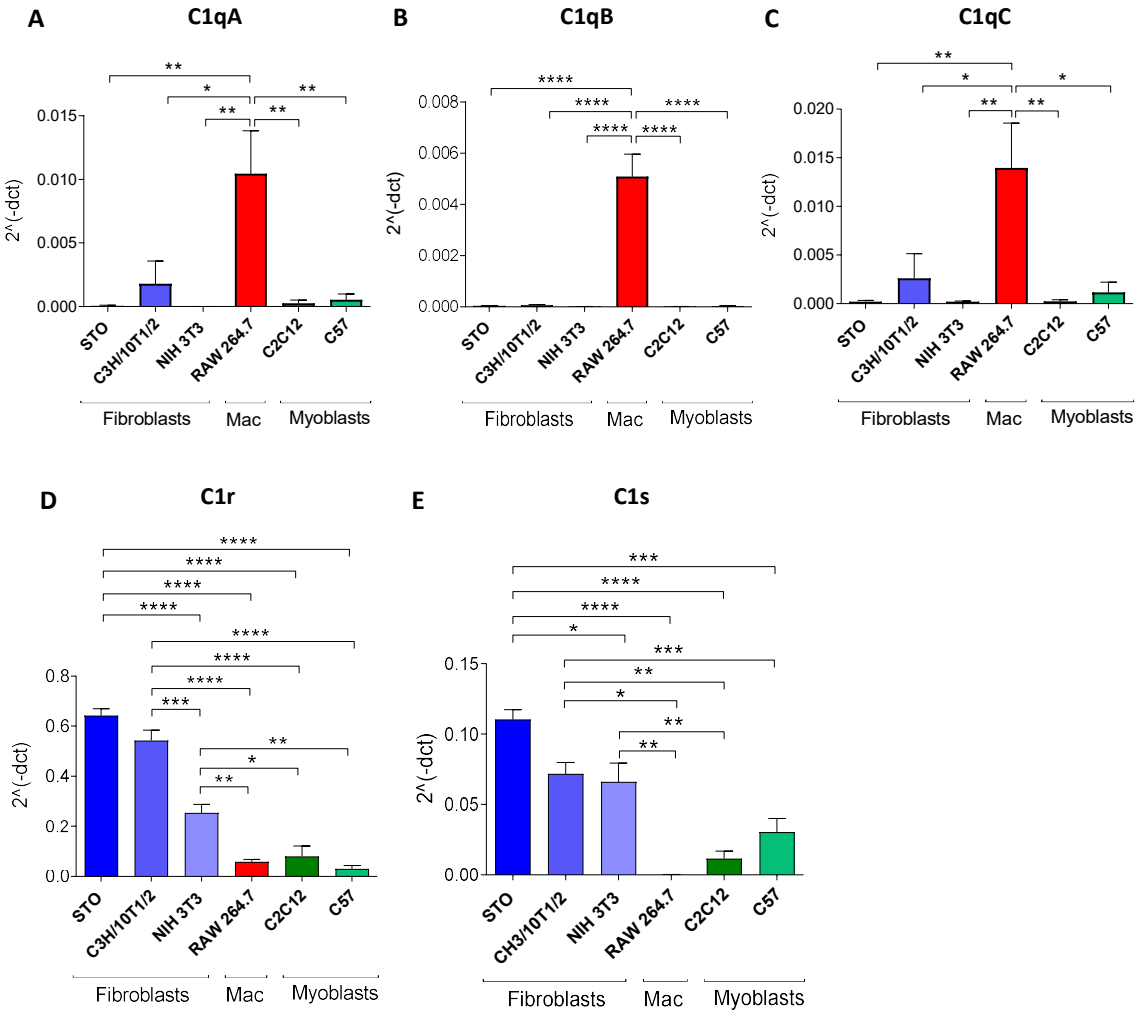

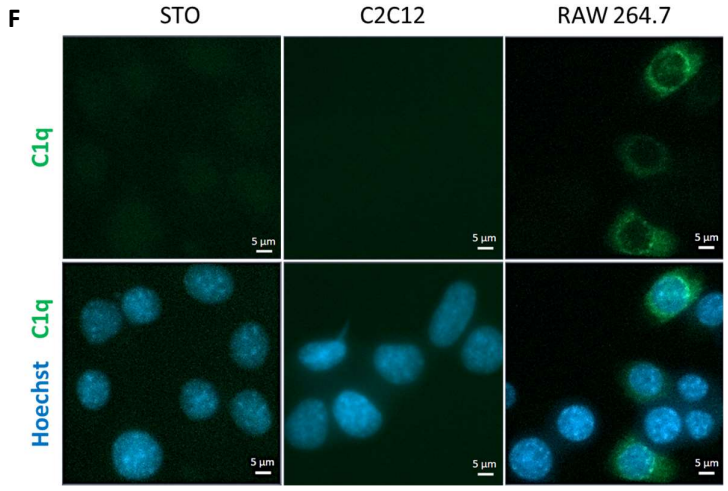

Figure 19. C1 complex subunits are selectively expressed by different cell lines. (A-E) qPCR analysis of C1qa (A), C1qb (B), C1qc (C), C1r (D) and C1s (E) in fibroblasts (STO, CH3/10/T1/2), macrophages (Mac, RAW 264.7) and myoblasts (C2C12, C57). Data are expressed as mean with SEM. N=3. One-way Anova test was applied. $p > 0.05$: ns; $p \leq 0.05$: *; $p \leq 0.01$: **; $p \leq 0.001$: ***; $p \leq 0.0001$: **** **(F)** Representative immunofluorescence image of STO, C2C12 and RAW 264.7 cells stained with anti-C1q (green) and Hoechst (blue) showing that C1q protein is expressed selectively by macrophages. Scale bar: 12 µm.

3.5 C1 complex induces the expression of the canonical Wnt signaling *in vitro* in murine fibroblasts and myoblasts.

Our gene expression and immunofluorescence analysis on murine cell lines revealed a differential expression of C1 complex components, with C1q cluster genes being mostly expressed by macrophages and C1r/s being mostly expressed by fibroblasts (**Figure 18, 19**). C1q-induced activation of Wnt signaling has been previously reported in the aged mice [160]. Upon binding to Frizzled receptors, C1q activates C1r/C1s, which results in Lrp5/6 cleavage and activation of canonical Wnt signaling [160]. We wanted to study if and how C1 complex modulates the canonical Wnt signaling *in vitro* in two different cell types: 1) in cells that express high levels of C1s and C1r similarly to the FAPs in muscles (**Figure 16**), and STO cells were used for this purpose (**Figure 20**); 2) in cells that express negligible levels of C1 complex components similarly to the other muscle resident cells, including satellite cells and fibers (**Figure 16**), and C2C12 cells were used for this purpose (**Figure 21**). C1qa, C1qb, C1qc, C1r and C1s are all secreted proteins [350]. Thus, we used STO and RAW 264.7 cells' conditioned media which are enriched in C1r/C1s and C1q proteins, respectively, to treat STO and C2C12 cells.

First, STO conditioned medium was used alone or in combination with C1q recombinant protein to treat STO cells (**Figure 20**). An increased expression of the canonical Wnt signaling target gene *Axin2* was observed in cells treated with STO medium and C1q compared to cells treated with STO medium alone or cultured with unconditioned medium (**Figure 20 B** and **Supplementary Figure 5 A**).

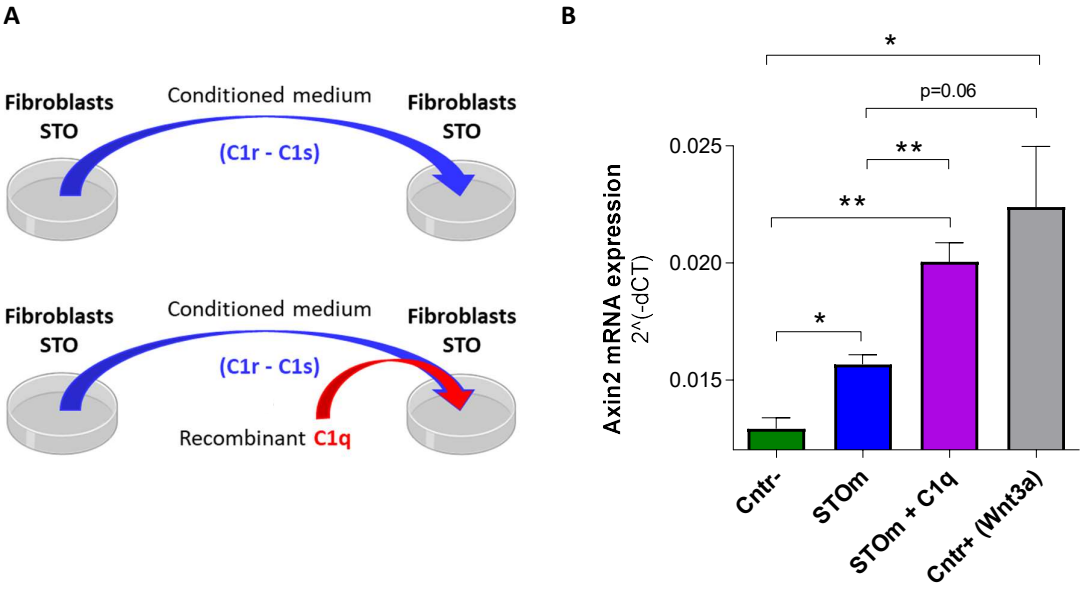

Figure 20. C1 complex induces the canonical Wnt signaling in fibroblasts *in vitro*. (A) Scheme of the experiment. Fibroblasts' (STO cells') conditioned medium (rederred to as STOm in **B**) was used alone or in combination with C1q recombinant protein to treat STO cells. **(B)** qPCR analysis of Axin2 expression in STO cells cultured with STO conditioned medium (STOm) or STOm + C1q recombinant protein (100 ug/ml) for 6 hours. Cntr-: STO cultured in DMEM. Cntr+: STO cultured in DMEM + 50 ng/ml Wnt3a. Data are expressed as mean with SEM. N=3. Two-tailed unpaired t-test was applied. $p > 0.05$: ns; $p \leq 0.05$: *; $p \leq 0.01$: **; $p \leq 0.001$: ***; $p \leq 0.0001$: ****

Second, STO and RAW 264.7 conditioned media were used alone or in combination in a 8:1 ratio (STO:RAW 264.7) to treat C2C12 cells (**Figure 21 A**). STO:RAW 264.7 ratio was calculated as 8:1 considering two factors: 1) the *ex vivo* analysis of the proportion of macrophages and FAPs in *mdx*^{4Cv} muscles; 2) the number of cultured STO and RAW 264.7 cells per area (**Supplementary Figure 5 B**). An increased *Axin2* expression was observed in C2C12 myoblasts treated with the combination of STO and RAW 264.7 media compared to the same cells treated with just one of the two media or cultured with the unconditioned medium (**Figure 21 B**). The augmented *Axin2* expression observed in the copresence of STO and RAW 264.7 media was rescued in C2C12 cells treated with XAV939, a well-known inhibitor of the canonical Wnt signaling (**Figure 21 C**). Next, we treated C2C12 cells with

recombinant C1q, C1r and C1s proteins and we observed an augmented *Axin2* expression compared to the cells cultured with the unconditioned medium, further suggesting that C1 complex might be the factor leading to the increase of the canonical Wnt signaling (**Figure 21 D**). Finally, in order to demonstrate that *Axin2* increase in the copresence of STO and RAW 264.7 media is specifically caused by the C1 complex components secreted in the media rather than by other components of the media, we used an inhibitor of C1r and C1s proteases which led to a reduced *Axin2* expression compared to cells treated with STO and RAW 264.7 media (**Figure 21 E**). Altogether, these data suggest that the formation of C1 complex that is made of C1s, C1r and C1q enhances the *in vitro* expression of the canonical Wnt signaling in murine fibroblasts which express C1s and C1r but do not express significant levels of C1q and in murine myoblasts, which do not express significant levels of any C1 complex components.

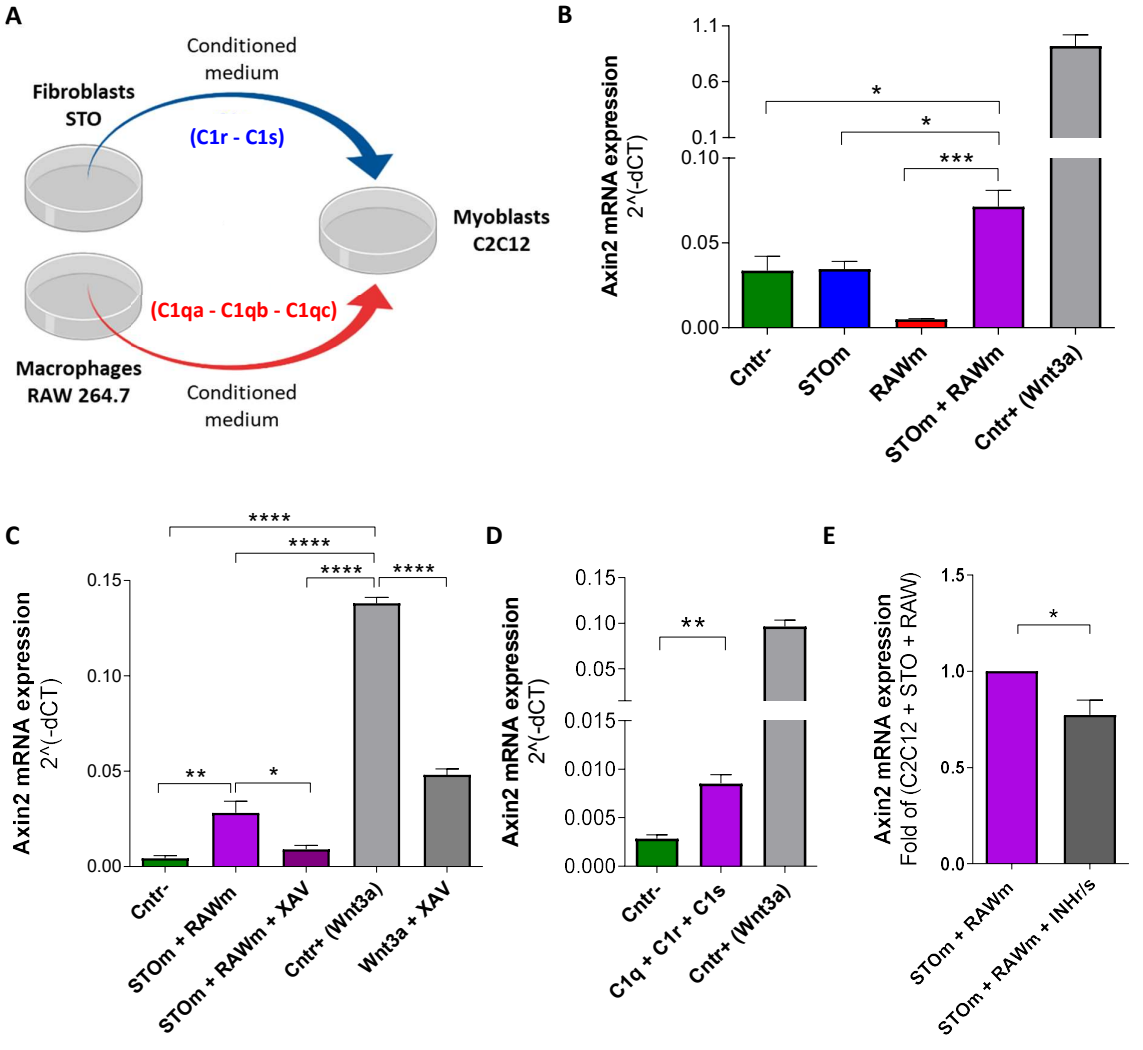

Figure 21. C1 complex induces the canonical Wnt signaling in myogenic cells *in vitro*. (A) Scheme of the experiment. Fibroblasts (STO cells), macrophages (RAW 264.7 cells) and myoblasts (C2C12

cells) were cultured separately. STO medium (referred to as STOm in **B, C, E**) and RAW 264.7 medium (referred to as RAWm in **B, C, E**) were used alone or in combination as conditioned media to culture C2C12 cells. **(B)** qPCR analysis of Axin2 expression in C2C12 cultured with STO, RAW 264.7 or STO+RAW 264.7 media for 24 hours. Cntr-: C2C12 cultured in DMEM. Cntr+: C2C12 cultured in DMEM + 100 ng/ml Wnt3a. Data are expressed as mean with SEM. N=3. One-way Anova test was applied. $p > 0.05$: ns; $p \leq 0.05$: *; $p \leq 0.01$: **; $p \leq 0.001$: ***; $p \leq 0.0001$: ****. **(C)** qPCR analysis of Axin2 expression in C2C12 cultured with STO+RAW 264.7 media or with STO+RAW 264.7 media and 100 µM XAV939 (indicated as XAV, inhibitor of the canonical Wnt signaling) for 6 hours. Cntr-: C2C12 cultured in DMEM; Cntr+: C2C12 cultured in DMEM + 50 ng/ml Wnt3a. Data are expressed as mean with SEM. N=4 (Cntr-), N=2 (Cntr+ and Wnt3a + XAV), N=3 (STOm + RAWm and STOm + RAWm + XAV). One-way Anova test applied. $p > 0.05$: ns; $p \leq 0.05$: *; $p \leq 0.01$: **; $p \leq 0.001$: ***; $p \leq 0.0001$: ****. **(D)** qPCR analysis of Axin2 expression in C2C12 cultured with recombinant C1q (100 µg/ml), C1s (25 µg/ml) and C1s (25 µg/ml) for 24 hours. Cntr-: C2C12 cultured in DMEM; Cntr+: C2C12 cultured in DMEM + 50 ng/ml Wnt3a. Data are expressed as mean with SEM. N=3 (Cntr-), N=2 (C1q + C1r + C1s and Cntr+). Two-tailed unpaired t-test applied. $p > 0.05$: ns; $p \leq 0.05$: *; $p \leq 0.01$: **; $p \leq 0.001$: ***; $p \leq 0.0001$: ****. **(E)** qPCR analysis of Axin2 expression in C2C12 cultured with STO medium or STO medium + 100 µg/ml C1r/s inhibitor (INHr/s) for 24 hours. Data are expressed as mean with SEM. N=3. Two-tailed unpaired t-test was applied. $p > 0.05$: ns; $p \leq 0.05$: *; $p \leq 0.01$: **; $p \leq 0.001$: ***; $p \leq 0.0001$: ****.

3.6 Macrophages and fibro/adipogenic progenitors are close in the regenerating areas of dystrophic muscles which exhibit an increased expression of C1q.

C1r and C1s are mostly expressed by FAPs in the muscle and by fibroblasts *in vitro*, whereas C1qa, C1qb and C1qc are mostly expressed by macrophages both *in vivo* and *in vitro* (**Figure 16, 17, 19**). Moreover, the copresence of C1q, C1r and C1s enhances the expression of the canonical Wnt signaling in fibroblasts and myoblasts *in vitro* (**Figure 20, 21**). In the aged mice it has been shown that the canonical Wnt signaling is enhanced in muscle by C1q binding to Frizzled receptors and inducing C1s-dependent cleavage of Wnt coreceptor Lrp5/6 [160]. We wanted to assess whether C1 complex, which includes C1q (i.e., C1qa, C1qb and C1qc) and C1r/s can induce the canonical Wnt signaling expression in the dystrophic muscles. First, we studied the localization of FAPs and macrophages within the muscle. Being both these cell types required for the formation of C1 complex as they respectively release C1r/s and C1q, we expected them to be physically close to each other in the dystrophic muscles. We used for this study B6.129S4-PDGFRα$^{tm11(EGFP)Sor/J}$ and B6.129S4-PDGFRα$^{tm11(EGFP)Sor/J}$;*mdx*^{4Cv} mice which have an enhanced green fluorescent protein (eGFP) fusion protein knocked into the *Pdgfrα* locus (Jackson stock number: 7669). These mice have been previously

validated and used to mark and study specifically FAPs in both homeostatic and injured muscles [52]. Our FACS analysis revealed that the GFP^{+ve} cells from B6.129S4-PDGFRα$^{tm11(EGFP)Sor/J}$;*mdx*^{4Cv} mice exhibited the same staining signature as FAPs (CD45^{-ve}CD31^{-ve}Sca1^{+ve}) (**Supplementary Figure 6 A**). Moreover, cryosections of the B6.129S4-PDGFRα$^{tm11(EGFP)Sor/J}$;*mdx*^{4Cv} mice's muscles stained with anti-laminin2α antibody showed the presence of the majority of the GFP^{+ve} cells in the interstitial space (i.e., between myofibers) where FAPs are known to be found. (**Supplementary Figure 6 B**). Therefore, we concluded that the GFP^{+ve} population in B6.129S4-PDGFRα$^{tm11(EGFP)Sor/J}$;*mdx*^{4Cv} muscles largely overlap with the FAPs cell population. Muscles from B6.129S4-PDGFRα$^{tm11(EGFP)Sor/J}$;*mdx*^{4Cv} and B6.129S4-PDGFRα$^{tm11(EGFP)Sor/J}$ mice were cryosectioned and stained with anti-F4/80 antibody to mark macrophages and the distance between macrophages and FAPs was measured (**Figure 22**). As DMD is a recessive X-linked disease, female B6.129S4-PDGFRα$^{tm11(EGFP)Sor/J}$;*mdx*^{4Cv} mice which are carrier for the dystrophin mutation but do not exhibit the disease-related phenotypes were used as control. A muscle collected from a B6.129S4-PDGFRα$^{tm11(EGFP)Sor/J}$ was also used as an additional healthy control (**Figure 22**). Clusters of macrophages and FAPs were observed mostly in the male *mdx*^{4Cv} regenerating areas compared to other areas of the tissue (**Figure 22 C** and **Supplementary Figure 7 B**). Macrophages to FAPs and FAPs to macrophages distances were measured with two different approaches: 1) by measuring the distance of each macrophage from its closest FAP within each image field (**Supplementary Figure 7 A**); 2) by measuring the distance of each FAP from its closest macrophage within a fixed portion of each image field (**Supplementary Figure 7 B, C**). Similar results were obtained from both analysis: macrophages and FAPs are closer to each other in muscles collected from male B6.129S4-PDGFRα$^{tm11(EGFP)Sor/J}$;*mdx*^{4Cv} mice compared to the female and wild type controls (**Figure 22 A, B**). Moreover, muscles from male B6.129S4-PDGFRα$^{tm11(EGFP)Sor/J}$;*mdx*^{4Cv} mice showed a higher percentage of macrophages and FAPs direct contacts (distance between macrophages and FAPs = 0 μm) compared to the controls (**Figure 22 C, D**) and a higher percentage of macrophages and FAPs close to each other 30 μm or less compared to the controls (**Figure 22 E**).

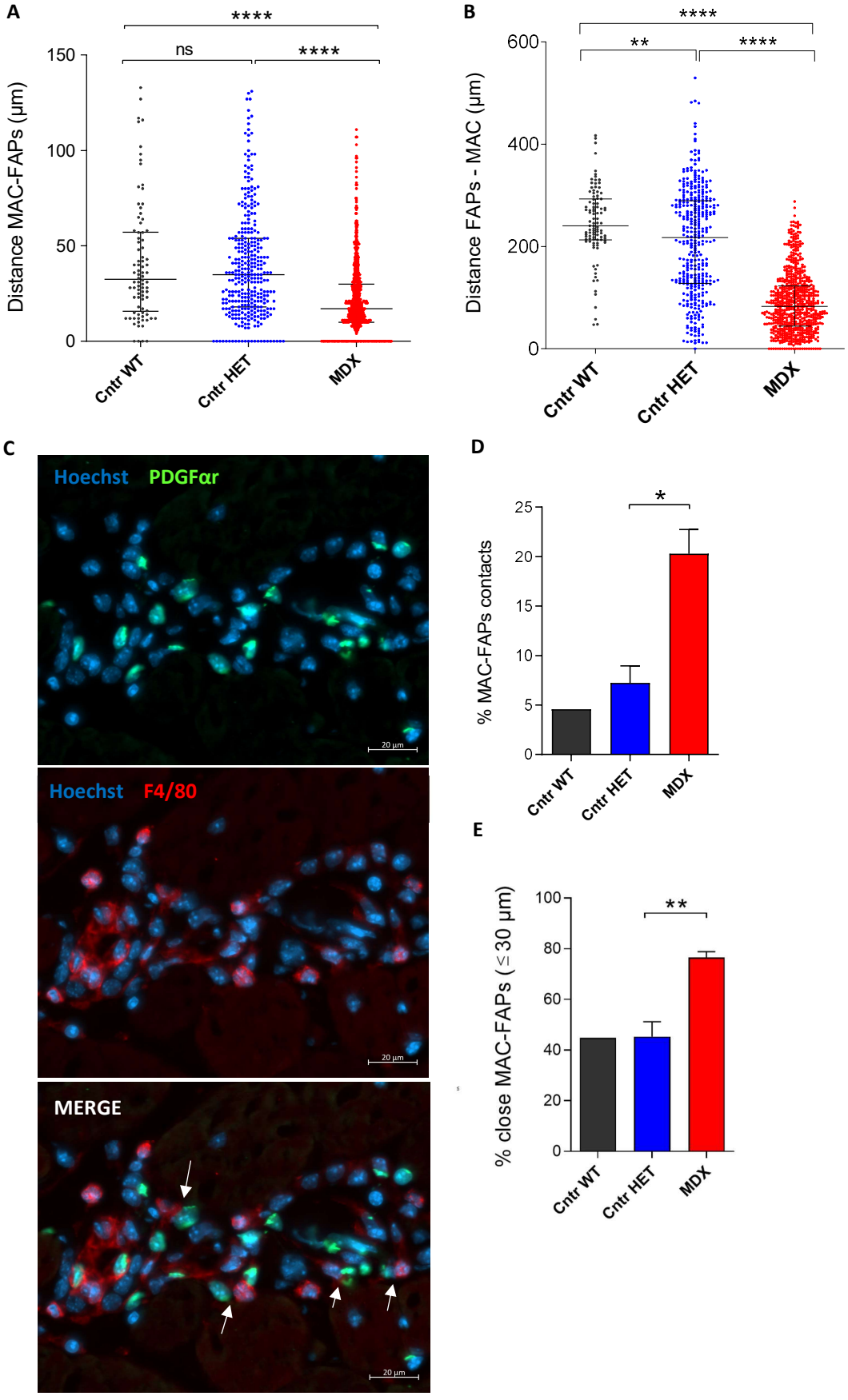
A
****
ns
****
Distance MAC-FAPs (µm)
150
100
50
0
Cntr WT
Cntr HET
MDX
B
****
**
****
Distance FAPs - MAC (µm)
600
400
200
0
Cntr WT
Cntr HET
MDX
C
Hoechst PDGFαr
20 µm
Hoechst F4/80
20 µm
MERGE
20 µm
D
*
% MAC-FAPs contacts
25
20
15
10
5
0
Cntr WT
Cntr HET
MDX
E
**
% close MAC-FAPs (≤ 30 µm)
100
80
60
40
20
0
Cntr WT
Cntr HET
MDX

Figure 22. Macrophages and fibro/adipogenic progenitors are close in the regenerating areas of dystrophic muscles. (A) Distance (μm) between macrophages (MAC) and fibro/adipogenic progenitors (FAPs) in gastrocnemius of ~ 12 months old male B6.129S4-PDGFRα$^{tm11(EGFP)Sor/J}$ (Cntr WT), ~ 18 months old female B6.129S4-PDGFRα$^{tm11(EGFP)Sor/J}$;*mdx*^{4Cv} (Cntr HET) and ~ 18 months old male B6.129S4-PDGFRα$^{tm11(EGFP)Sor/J}$;*mdx*^{4Cv} (MDX) mice. The analysis was performed measuring the distance of each macrophage in the image field from its closest FAP. Refer also to Material and Methods section and to **Supplementary Figure 7 A**. N=1 (Cntr WT), N= 3 (Cntr HET), N=3 (MDX). Data are expressed as median with interquartile range. Mann-Whitney test was applied. $p > 0.05$: ns; $p \leq 0.05$: *; $p \leq 0.01$: **; $p \leq 0.001$: ***; $p \leq 0.0001$: ****. **(B)** Distance (μm) between fibro/adipogenic progenitors (FAPs) and macrophages (MAC) in same muscles as in **(A)**. The analysis was performed measuring the distance of each FAP in the image field from its closest macrophage. Refer also to Material and Methods section and to **Supplementary Figure 7 B**. Data are expressed as median with interquartile range. Mann-Whitney test was applied. $p > 0.05$: ns; $p \leq 0.05$: *; $p \leq 0.01$: **; $p \leq 0.001$: ***; $p \leq 0.0001$: ****. **(C)** Representative immunofluorescence of a regenerating area in the gastrocnemius of a ~ 18 months old male B6.129S4-PDGFRα$^{tm11(EGFP)Sor/J}$;*mdx*^{4Cv} (MDX) mouse stained with anti-F4/80 (red) and Hoechst (blue). White arrows in merge panel indicate contacts between macrophages (F4/80^{+ve}, red) and FAPs (PDGFαr^{+ve}, green). Scale bar: 20 μm. **(D)** Percentage of contacts between macrophages and FAPs calculated in same muscles as in **(A)**. Data are expressed as mean with SEM. Two-tailed unpaired t-test was applied. $p > 0.05$: ns; $p \leq 0.05$: *; $p \leq 0.01$: **; $p \leq 0.001$: ***; $p \leq 0.0001$: ****. **(E)** Percentage of macrophages and FAPs which are close to each other 30 μm or less, calculated in same muscles as in **(A)**. Data are expressed as mean with SEM. Two-tailed unpaired t-test was applied. $p > 0.05$: ns; $p \leq 0.05$: *; $p \leq 0.01$: **; $p \leq 0.001$: ***; $p \leq 0.0001$: ****.

The regenerating areas are widely studied in the dystrophic muscles as they exhibit all the phenotypical muscles' features of the disease, including the presence of myofibers which are variable in size and shape, clustered nuclei, necrosis, fibrosis and fat tissue replacement [189]. We showed that macrophages and FAPs which release C1 complex proteins are increased in dystrophic muscles (**Figure 18**). We performed an immunofluorescence analysis in order to test whether the increased presence of these cells types correlates with the enhanced activity of the canonical Wnt signaling, previously reported in the regenerative portions of dystrophic muscles [181]. Cryosections of muscles collected from male B6.129S4-PDGFRα$^{tm11(EGFP)Sor/J}$;*mdx*^{4Cv} mice and non-dystrophic controls were stained with anti-F4/80 and anti-Tgfβ2 antibodies (**Figure 23 A**). We found an increased expression of Tgfβ2 in the regenerating areas of dystrophic males which were also characterized by an increased number of macrophages and FAPs (marked as GFP^{+ve} cells) compared to the controls (**Figure 23 A** and **Supplementary Figure 8**). We found that the staining of the canonical Wnt signaling effector/target proteins β-catenin and Tgfβ2 colocalize with F4/80^{+ve} (i.e., macrophages) cells in the

regenerating areas of *mdx*^{4cv} muscles (**Figure 23 B, C**). Moreover, regions within the regenerating areas of *mdx*^{4cv} muscles that were characterized by strong expression of Axin2 or Tgfβ2 also exhibited a strong expression of C1q protein (**Figure 24 A, B and Supplementary Figure 9, 10**).

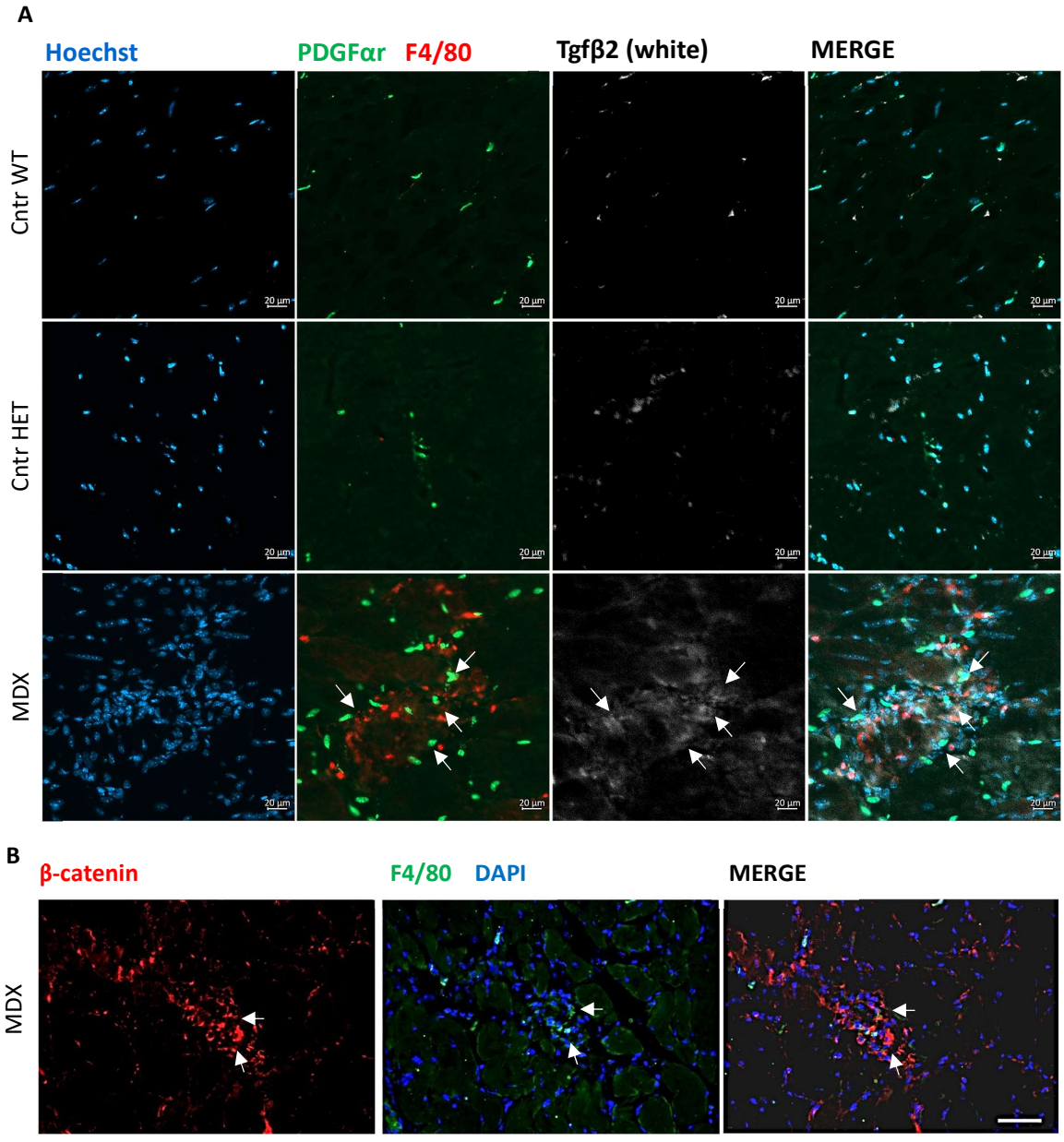

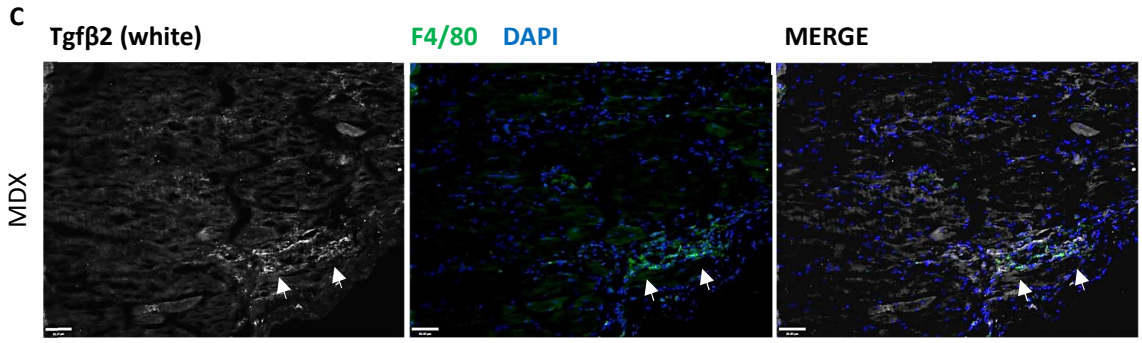

Figure 23. Expression of canonical Wnt signaling target proteins in the dystrophic regenerating areas. (A) Representative immunofluorescence image of gastrocnemius of ~ 12 months old male B6.129S4-PDGFRα$^{tm11(EGFP)Sor/J}$ (Cntr WT), ~ 18 months old female B6.129S4-PDGFRα$^{tm11(EGFP)Sor/J}$;*mdx*^{4Cv} (Cntr HET) and ~ 18 months old male B6.129S4-PDGFRα$^{tm11(EGFP)Sor/J}$;*mdx*^{4Cv} (MDX) mice stained with anti-F4/80 (red), anti-Tgfβ2 (white) and Hoechst (blue). Both the number of cells (macrophages and FAPs) and the Tgfβ2 protein expression are increased in the MDX muscles compared to the controls. White arrows in MDX sample indicate Tgfβ2 signal that colocalizes with macrophages (F4/80^{+ve} cells) and FAPs (PDGFαr^{+ve} cells) within the regenerating area of the muscle. Scale bar: 20 µm. **(B)** Representative immunofluorescence image of a diaphragm of a ~12 months old male *mdx*^{4Cv} (MDX) stained with anti-β-catenin (red), anti-F4/80 (green) and DAPI (blue). White arrows indicate the colocalization of β-catenin and F4/80 stainings. Scale bar: 50 µm **(C)** Representative immunofluorescence image of a diaphragm of a ~12 months old male *mdx*^{4Cv} (MDX) stained with anti-Tgfβ2 (white), anti-F4/80 (green) and DAPI (blue). White arrows indicate the colocalization of Tgfβ2 and F4/80 stainings. Scale bar: 50 µm.

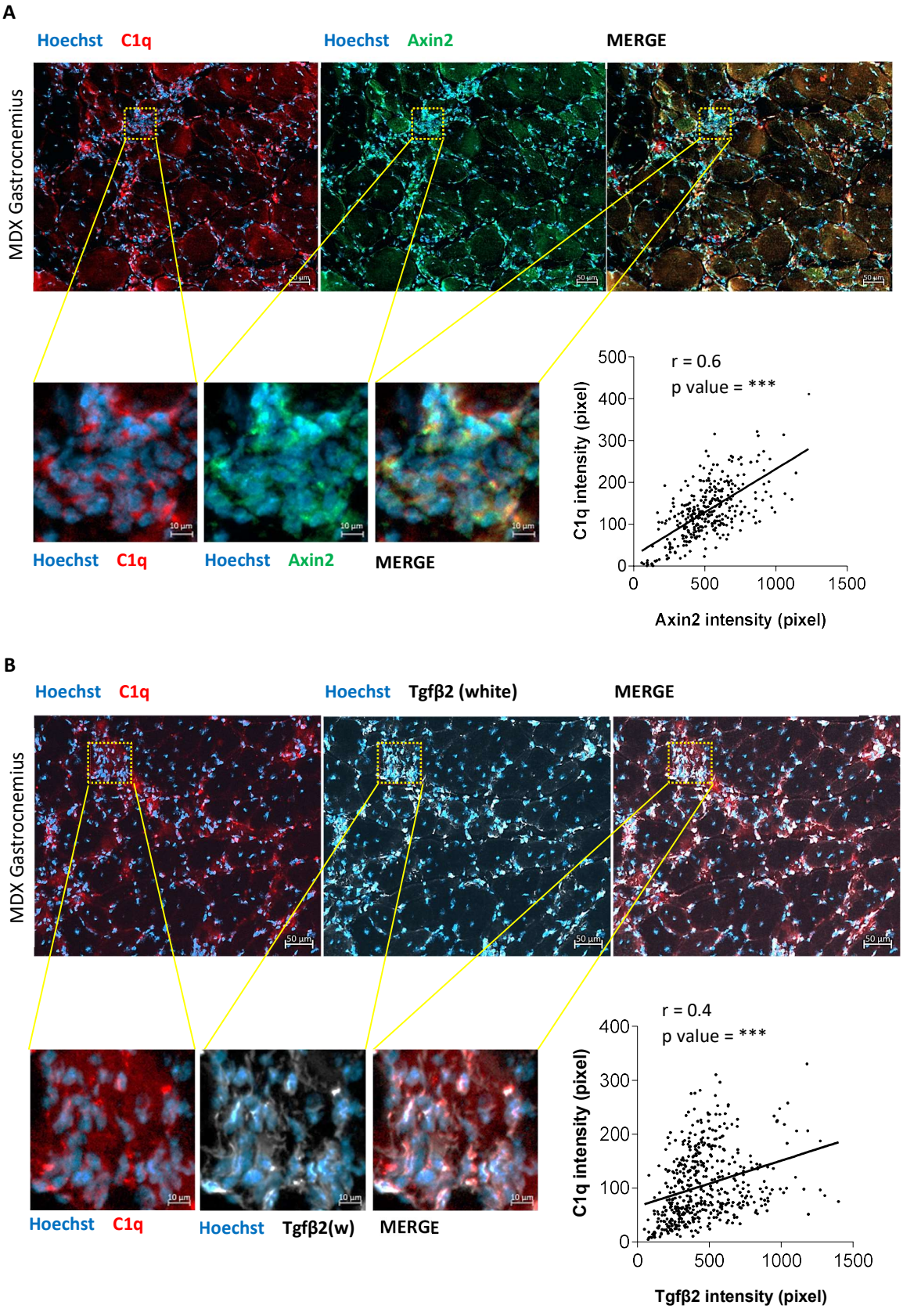
A
Hoechst C1q
Hoechst Axin2
MERGE
MDX Gastrocnemius
50 µm
10 µm
Hoechst C1q
Hoechst Axin2
MERGE
r = 0.6
p value = ***
C1q intensity (pixel)
Axin2 intensity (pixel)
0
100
200
300
400
500
0
500
1000
1500
B
Hoechst C1q
Hoechst Tgfβ2 (white)
MERGE
MDX Gastrocnemius
50 µm
10 µm
Hoechst C1q
Hoechst Tgfβ2(w)
MERGE
r = 0.4
p value = ***
C1q intensity (pixel)
Tgfβ2 intensity (pixel)
0
100
200
300
400
0
500
1000
1500

Figure 24. Enhanced C1q correlates with an increased Wnt-Tgfβ2 activity in dystrophic muscles. **(A)** Representative immunofluorescence of gastrocnemius of ~ 12 months old *mdx*^{4Cv} (MDX) stained with anti-C1q (red), anti-Axin2 (green) and Hoechst (blue). Scale bar (top images): 50 μm; scale bar (bottom images): 10 μm. The average pixel intensity of each signal was evaluated in ≥ 109 randomly selected regions per biological replicate within the regenerating areas of the muscle (refer to Materials and Methods section). The correlation between C1q and Axin2 intensity values in each region is shown. N=3. Positive correlation is indicated. Spearman r = 0.6 ($p<0.001$, two-tailed t test). **(B)** Representative immunofluorescence of gastrocnemius of ~ 12 months old *mdx*^{4Cv} (MDX) stained with anti-C1q (red), anti-Tgfβ2 (white) and Hoechst (blue). Scale bar (top images): 50 μm; scale bar (bottom images): 5 μm. The average pixel intensity of each signal was evaluated in ≥ 106 randomly selected regions per biological replicate within the regenerating areas of the muscle (refer to Materials and Methods section). The correlation between C1q and Tgfβ2 intensity values in each region is shown. Positive correlation is indicated. Spearman r = 0.4 ($p<0.001$, two-tailed t test).

Altogether these data indicate: 1) that FAPs and macrophages are physically close to each other in the dystrophic muscles; 2) the copresence of the canonical Wnt signaling downstream proteins (β-catenin, Tgfβ2, Axin2), FAPs and macrophages in the regenerating areas of dystrophic muscles and 3) the copresence of C1q, Axin2 and Tgfβ2 in the same areas. The positive correlation between the signals intensities of C1q and Axin2 and C1q and Tgfβ2 is in line with the possibility that the augmented level of C1q in dystrophic muscles contributes to the increased Wnt/Tgfβ axis reported in dystrophy [181].

3.7 The fib-*mdx* mouse model exhibits an increased canonical Wnt signaling and an increased fibrosis which better mimic human DMD compared to the *mdx*^{4Cv}.

The *mdx* mouse model exhibits some limitations associated to its mild pathological phenotype compared to the human disease [197]. With the aim of getting access to muscles which closely recapitulate the severity of the human pathology, we tested a modified version of the fib-*mdx* mouse model [274]. The fib-*mdx* model is generated by performing daily micro-mechanical injuries in the tibialis anterior of 8 weeks old *mdx*^{4cv} mice for 2 weeks [274]. While using the same injury protocol for the generation of the fib-*mdx* model, we performed daily microinjuries in the entire hindlimb (i.e., tibialis anterior, EDL, soleus, gastrocnemius) of 4 to 6 months old *mdx*^{4cv} mice for 2 weeks; we used the same protocol also to injury wild type aged-matched mice (**Figure 25 A**). 1 week after the last injury FACS isolated FAPs and satellite cells were analyzed for the expression of both canonical Wnt signaling (i.e., *Axin2*, *Tgfβ2* and *Lgr5*) and fibrosis-related (i.e., *collagen1a1*, *collagen3a1* and *fibronectin*) genes. Interestingly, collagen1a1, collagen3a1, Axin2, Lgr5 and fibronectin gene

expression was increased in the FAPs of the fib-*mdx* muscles compared to the uninjured *mdx*^{4Cv} muscles (**Figure 25**) and a similar trend (not statistically significant) was observed in the expression of *collagen1a1*, *collagen3a1*, *fibronectin* and *Tgfβ2* in satellite cells (**Supplementary Figure 11**). Moreover, we found that both the number of macrophages and FAPs were increased in the fib-*mdx* compared to the uninjured *mdx*^{4Cv} muscles, suggesting an augmented state of inflammation and an increased ECM production in this mouse model **(Supplementary Figure 12)**.These results further describe the fib-*mdx* model, pointing out that both the canonical Wnt signaling and the fibrotic process are enhanced in the FAPs from 4 to 6 months old fib-*mdx* mice compared to the uninjured aged-matched *mdx*^{4Cv} muscles. Thus, we concluded that the fib-*mdx* mice might be a useful tool to study the FAPs in dystrophy.

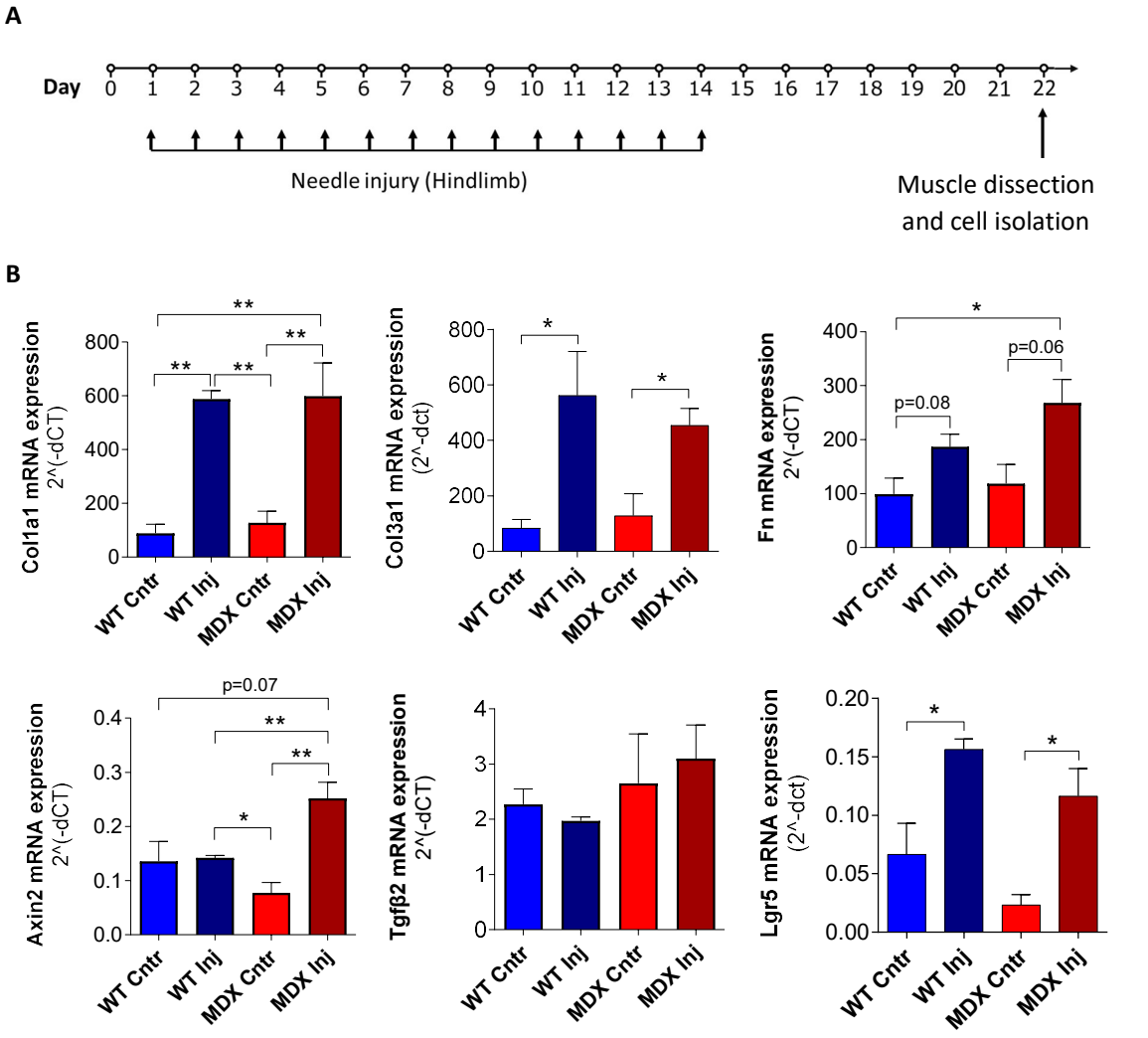

Figure 25. The fib-*mdx* mouse model exhibits an increased canonical Wnt signaling and an increased fibrosis compared to the *mdx*^{4Cv}. (A) Scheme of the experiment. Hindlimb muscles of 4 to 6 months old wild type (WT) and *mdx*^{4Cv} (MDX) were micro injured every day for 14 days. 7 days

after the last day of injury muscles were collected. The protocol was adapted from Deseguerre et al.[274]. Fibro/adipogenic progenitors (FAPs) and satellite cells (SCs) were FACS isolated. **(B)** qPCR analysis of collagen1a1, collagen3a1, fibronectin, Axin2, Tgfβ2 and Lgr5 expression in FAPs FACS isolated from 4 to 6 months old wild type (WT) and *mdx*^{4Cv} (MDX). WT Cntr and MDX Cntr were not injured. WT Inj and MDX Inj were processed as indicated in **(A)**. Data are expressed as mean with SEM. N=3. Two-tailed unpaired t-test was applied. $p > 0.05$: ns; $p \leq 0.05$ (*), < 0.01 (**), < 0.001 (***), < 0.0001 (****).

3.8 Wnt coreceptor Lrp6 is highly expressed from fibro/adipogenic progenitors in the dystrophic muscles and in murine fibroblasts.

Previous studies have reported that the canonical Wnt signaling is increased in both dystrophy and aging [53,159,160,181]. In the dystrophic muscles, a Sca1^{+ve} cell population (likely overlapping with FAPs) and satellite cells have been shown to contribute to the enhanced canonical Wnt signaling [53,181]. In aged muscles the molecular events leading to the activation of the canonical Wnt signaling have been described: C1q binding to the Wnt receptor Frizzled induces the C1s-mediated cleavage of the Wnt coreceptor Lrp5/6 [160]. We tested the gene expression of Wnt coreceptor Lrp6 in order to assess whether muscle cells in dystrophy could be responsive to the C1q-mediated induction of the Wnt signaling (i.e., C1/Wnt axis) through a mechanism similar to the one described in aging [160]. All cells that are found in the muscle were analyzed: single fibers, satellite cells, macrophages, FAPs, Lin^{-ve}Sca1^{-ve}Vcam^{-ve} (Lin^{-ve}: CD45^{-ve}CD31^{-ve}) and Lin^{+ve}F4/80^{-ve} (Lin^{+ve}: CD45^{+ve}CD31^{+ve}) (**Figure 15**). While Lrp6 mRNA was expressed in all the tested cells both in the wild type and dystrophic muscles, we found that the FAPs isolated from dystrophic muscles have the highest expression of *Lrp6* among all the tested cells, suggesting the contribution of FAPs to the enhanced canonical Wnt signaling in dystrophic muscles (**Figure 26 A**). Moreover, the enhanced expression of *Lrp6* in the dystrophic FAPs compared to the wild type FAPs is in line with the reported enhanced canonical Wnt signaling in dystrophy [53,181]. We analyzed the gene expression of Lrp6 in murine myoblast (C2C12) and fibroblasts (STO and C3H10T1/2). While Lrp6 mRNA was expressed in all the three cell lines, fibroblasts had the highest expression of *Lrp6* among the tested cells, with this result being in line with the *Lrp6* expression analysis performed in cells directly isolated from muscles (**Figure 26 B**).

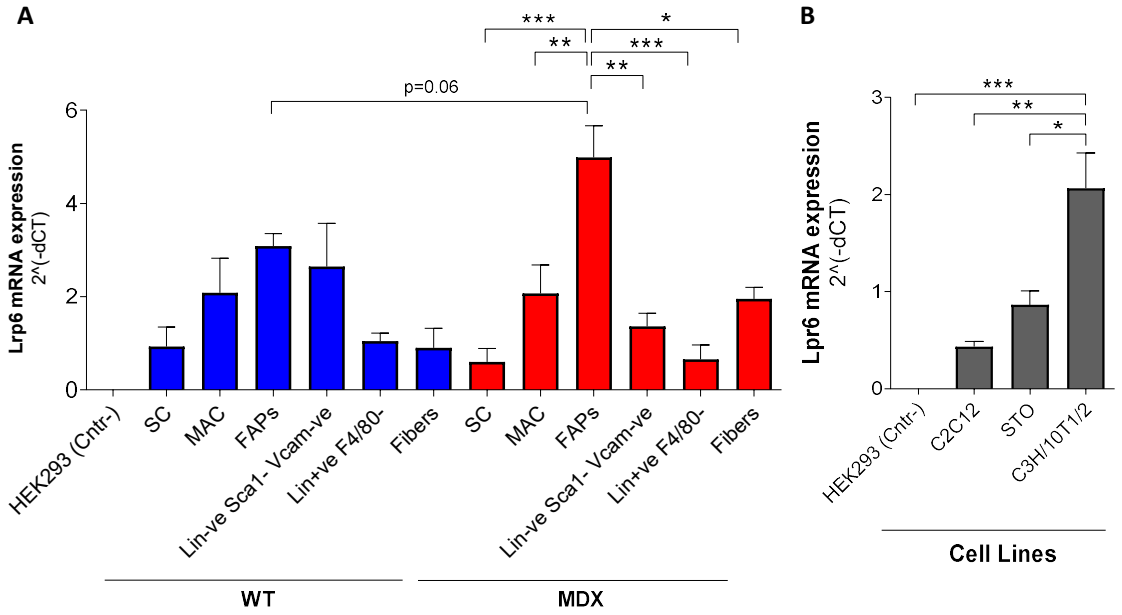

Figure 26. Wnt co-receptor Lrp6 is highly expressed in fibro/adipogenic progenitors of dystrophic muscle. (A) qPCR analysis of Lrp6 expression in satellite cells (SC: $CD45^{-ve}CD31^{-ve}Sca1^{-ve}Vcam^{+ve}$), macrophages (MAC: $CD45^{+ve}F4/80^{+ve}$), fibro/adipogenic progenitors (FAPs: $CD45^{-ve}CD31^{-ve}Sca1^{+ve}$), $Lin^{+ve}F4/80^{-ve}$ (Lin^{+ve}: $CD45^{+ve}CD31^{+ve}$), $Lin^{-ve}Sca1^{-ve}Vcam^{-ve}$ (Lin^{-ve}: $CD45^{-ve}CD31^{-ve}$) and single fibers (Fibers) isolated from hindlimb muscles of ~ 12 months old wild type (WT) and *mdx*^{4Cv} (MDX) mice. Data are expressed as mean with SEM. N=3 (all samples except MDX Fibers, N=2). One-way Anova test was applied. Two-tailed unpaired t-test was applied between WT FAPs and MDX FAPS. **(B)** qPCR analysis of Lrp6 expression in HEK293, C2C12, STO and C3H/10T1/2 cells. HEK293 (human cells) were used as negative control as Lrp6 primers were designed to specifically amplify only the murine isoform of the gene. Data are expressed as mean with SEM. N=3. One-way Anova test was applied. $p > 0.05$: ns; $p \leq 0.05$ (*), < 0.01 (**), < 0.001 (***), < 0.0001 (****).

3.9 *In vivo* inhibition of FAPs cell fate by blocking complement C1r/s in the fib-*mdx* mouse model.

The canonical Wnt signaling is enhanced in dystrophic muscles and it corroborates to the promotion of fibrogenic phenotypes [181]. FAPs likely represents the major cellular source of fibrosis in muscular dystrophy [46,47]. We have observed that in our implemented version of the fib-*mdx* model both the canonical Wnt signaling target gene *Axin2* and the fibrotic genes (i.e., *collagen1a1* and *fibronectin*) are enhanced in the FAPs compared to the wild type and to the *mdx*^{4Cv} (**Figure 25**). Moreover, we have shown that FAPs are the cells with the highest gene expression of the canonical Wnt coreceptor Lrp6 among all muscle cells (**Figure 26 A**). The complement system component C1q has been reported to contribute to the promotion of fibrosis-related phenotypes in the skeletal muscle of aged mice [160].

Altogether these observations suggest that inhibiting the first component of the classical complement pathway C1 might be a way to counteract the aberrant behavior of FAPs in muscles of dystrophic mice. To test this possibility, we treated the fib-*mdx* mice for 21 days with a C1r/s esterase inhibitor (**Figure 27 A**). The gene expression analysis of FACS isolated FAPs from the hindlimb muscles revealed a reduced expression of both the canonical Wnt signaling target genes (i.e., *Axin2*, *Lgr5* and *Tgfβ2*) and the fibrogenic genes (i.e., *collagen1a1*, *collagen3a1*) in the fib-*mdx* mice treated with the C1r/s esterase inhibitor compared to the controls (**Figure 27 B-G**). These data support the notion that enhanced complement levels enhance a fibrogenic program in the FAPs and may therefore participate to the accumulation of fibrotic tissue in dystrophic muscles. Moreover, the histological analysis revealed a decreased collagen 1 average pixel intensity in the interstitial space between myofibers in the muscles treated with the C1r/s esterase inhibitor compared to the controls (**Figure 28 B**). The cross sectional area of myofibers was increased in the muscles treated with the C1r/s esterase inhibitor compared to the controls (**Figure 28 C**), whereas the fibrotic muscle area resulted decreased in the muscles treated with the C1r/s esterase inhibitor compared to the controls (**Figure 28 D**). Altogether, these data highlight an overall amelioration of the dystrophic phenotype following the inhibition of the classical complement pathway (**Figure 28**).

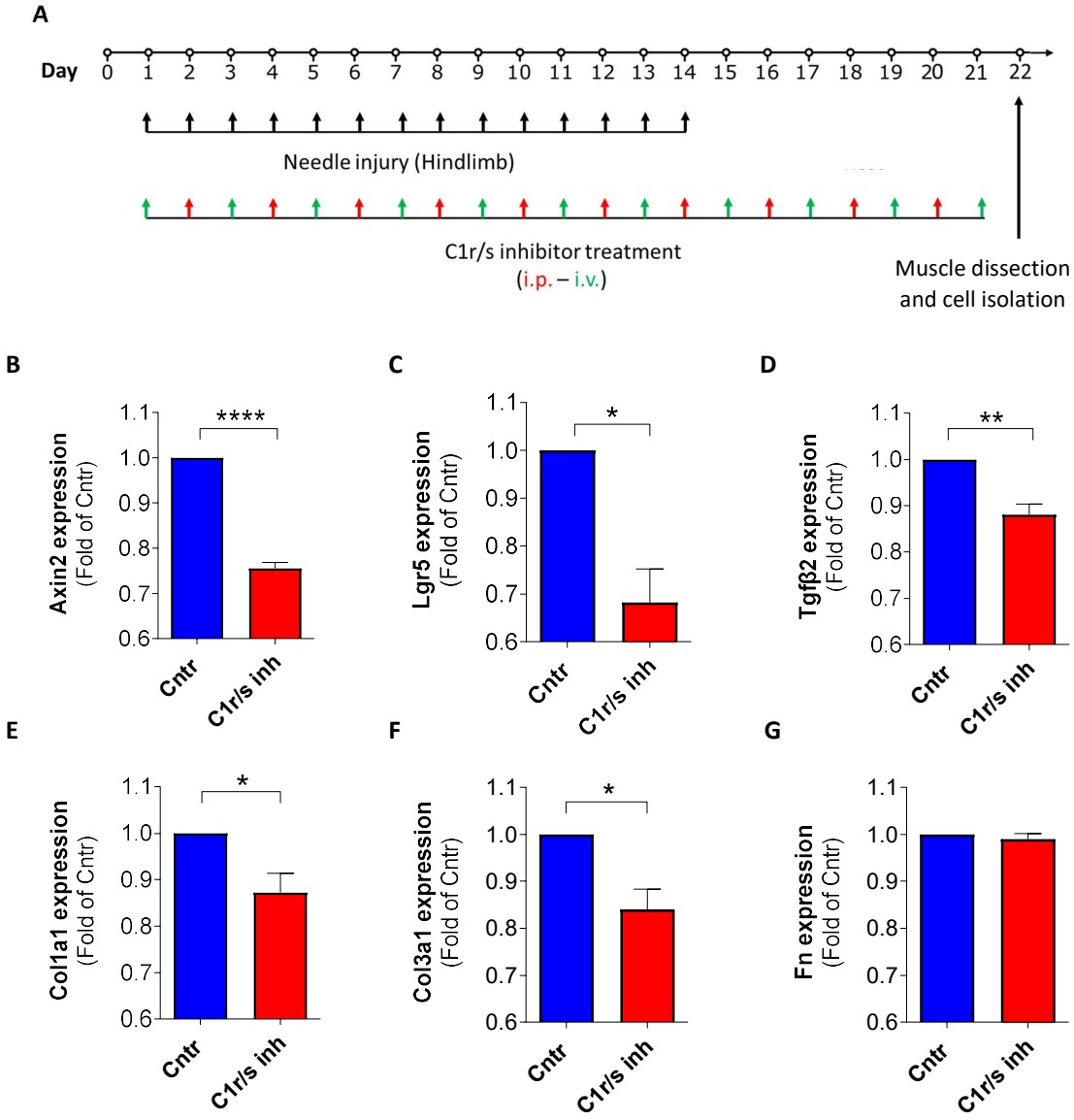

Figure 27. Inhibiting FAPs cell fate in fib-*mdx* mice by inhibiting the classical complement pathway. (A) Scheme of the experiment. Hindlimb muscles of ~ 14 months old *mdx*^{4Cv} mice were micro injured every day for 14 days and mice were treated with C1r/s inhibitor (C1r/s inh) or with the control solution (Cntr) for 21 days starting from the first day of injury. 7 days after the last injury muscles were collected, and fibro/adipogenic progenitors (FAPs) were FACS isolated. **(B-G)** qPCR analysis of Axin2 **(B)**, Lgr5 **(C)**, Tgfβ2 **(D)**, collagen1a1 **(E),** collagen3a1 **(F)** and fibronectin **(G)** in FACS isolated FAPs from ~ 14 months old *mdx*^{4Cv} mice processed as in **(A)**. Data are expressed as mean with SEM. N=3. Two-tailed unpaired t-test was applied. $p > 0.05$: ns; $p \leq 0.05$ (*), < 0.01 (**), < 0.001 (***), < 0.0001 (****).

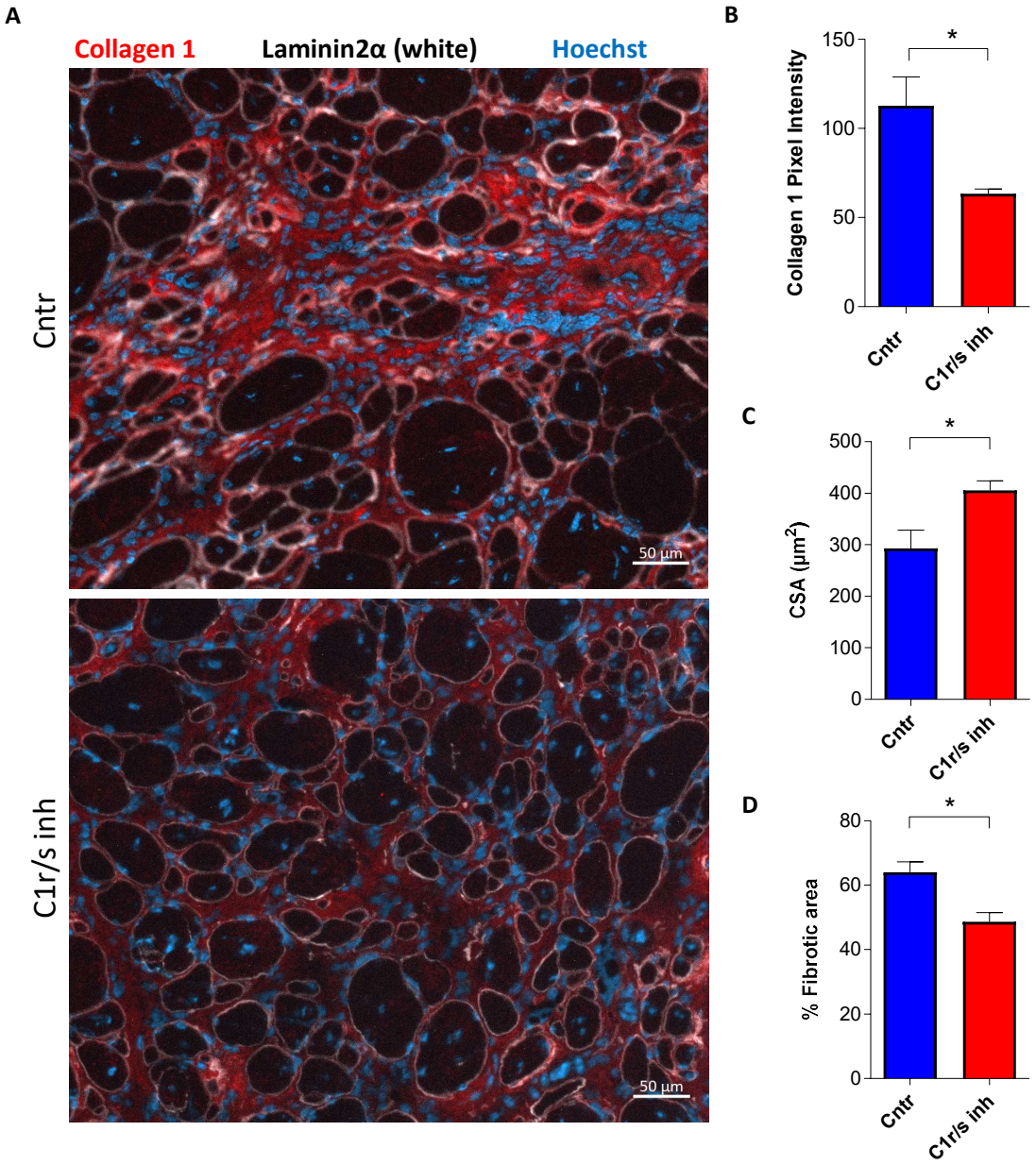

Figure 28. Inhibiting the classical complement pathway ameliorates the dystrophic phenotype. **(A)** Representative immunofluorescence of gastrocnemius muscles from ~ 14 months old *mdx*^{4Cv} mice micro injured for 14 days and treated with C1r/s inhibitor (C1r/s inh) or with the control solution (Cntr) for 21 days starting from the first day of injury. 7 days after the last injury muscles were collected, mounted on cork, cryosectioned and stained with anti-collagen 1 (red), anti-laminin2α (white) and Hoechst (blue). Note that collagen 1 intensity is reduced in the muscles treated with the C1r/s inhibitor compared to the controls and that the fibrotic area is reduced in the muscles treated with the C1r/s inhibitor compared to the controls. Scale bar: 50 µm. **(B)** Quantification of collagen 1 pixel intensity in the interstitial space between myofibers of the same muscles as in **(A)**. **(C)** Quantification of the cross sectional area (CSA) of the muscle fibers of the same muscles as in **(A)**.

(D) Quantification of the fibrotic area in the same muscles as in **(A)**. Refer also to Materials and Methods section. Data are expressed as mean with SEM. N=3. Two-tailed unpaired t-test was applied. $p > 0.05$: ns; $p \leq 0.05$ (*), < 0.01 (**), < 0.001 (***), < 0.0001 (****).

4. Discussions

In this work we present evidence that the classical complement system is increased in dystrophic muscles of the *mdx*^{4Cv} mice and that all the components of the C1 complex (i.e., C1q and C1r/s) are locally expressed by muscle cells. Our data link the increased expression of the classical complement to the enhanced canonical Wnt signaling which is reported in dystrophic muscles [53,181]. Importantly, we suggest here that inhibiting C1 in dystrophic mice could be a strategy to reduce the collagen deposition in compromised dystrophic muscles and to counteract the aberrant behavior of the FAPs which are reported to be one of the main cellular sources of fibrosis [46,49].

4.1 Insight in the complement levels of skeletal muscles

Muscular dystrophy and aging are two conditions characterized by defective regenerative potential of muscles, chronic inflammation, and fibrosis [351]. Furthermore, both aged and dystrophic muscles exhibit increased levels of canonical Wnt signaling [53,159,160,181]. In the aged mice it was initially reported that serum components may account for the enhanced Wnt signaling [159]. Later on, Naito and colleagues reported that increased levels of complement proteins in the serum might lead to the increased Wnt signaling in the old mice's muscles [160]. Here we show that the dystrophic muscles are characterized by increased complement levels similarly to the aging condition [160] (**Figures 11, 13, 14** and **Supplementary Figures 1, 3**). Moreover, we propose a local production of most of the classical complement pathway proteins (i.e., C1q, C1s, C3, C3d, C4) in the skeletal muscles (**Figures 11, 13, 14, 16** and **Supplementary Figures 1, 3**). With respect to C1 complex we show that both its components (i.e., C1q and C1r/s) are expressed in muscles both at mRNA and protein levels (**Figures 16, 17** and **Supplementary Figures 3, 4**). Our data are in keeping with a DNA microarray-based analysis that led to the identification of complement genes differently expressed in the *mdx* mouse skeletal muscles compared to the wild type, with C1qb and C1qa being the two most upregulated among these genes in the *mdx* [308]. As we did not observe increased levels of the canonical Wnt signaling after treating murine myoblasts with the *mdx*^{4Cv} serum, we propose that the enhanced complement levels observed in dystrophy have for the most part a muscle origin rather than a systemic origin (**Figure 11**). It is possible that the local expression of complement proteins in muscles occurs in the aging as well and that it contributes to the promotion of aged-related phenotypes similarly to what has been observed for the enhanced C1q serum levels in the aged mice [160]. This hypothesis is in line with the reported gene expression of C1qa, C1r and C1s in the skeletal muscles of the *senescence-accelerated mouse prone 1* (SAMP1) mice [295].

Our data highlight the cellular sources of C1 and are in keeping with the previously reported macrophages expression of C1q protein in the skeletal muscle [160]. Importantly, we have extended the analysis to all the other muscle-resident cells (i.e., myofibers and interstitial cells) and we have shown that C1q is almost exclusively produced by the macrophages while C1r/s are mostly produced by the

FAPs (**Figure 16, 17**). In addition, our data suggest that the increased expression of C1 in the skeletal muscles is due to a combination of an increased number of macrophages and FAPs which release C1q and C1r/s, respectively, and, at least for specific C1 components (i.e., C1qb and C1r) an increased transcriptional activity of macrophages (for *C1qb*) and FAPs (for *C1r*) in the dystrophic muscles compared to the wild type (**Figure 16, 18**). While the expression of some of the classical complement components (including C1 complex) has been previously described in mice's skeletal muscles [160,295,308], this is to our knowledge the first work that compares C1 complex components' expression in the dystrophic and wild type muscles at the single cell population level.

In this study we have compared C1 complex gene expression in purified cells from dystrophic muscles and muscles undergoing the regeneration process following a single acute injury event (**Figure 16 A-E**). In a previous work the gene expression of C1r and C1s in the whole unfractioned hindlimb muscles of young wild type mice (2 months old) resulted upregulated 2 days after cryoinjury compared to the uninjured muscles [160]. Interestingly, our data show a reduced expression of both C1q cluster genes and C1r/s in in isolated cells from the hindlimb of wild type mice 2.5 days after acute needle injury compared to dystrophic muscles, a reduced expression of C1s in cells from the wild type injured muscles compared to the uninjured and a similar expression of C1r and C1q between cells from injured and uninjured wild type muscles (**Figure 16 A-E**). Moreover, our experiment suggests that the number of cells secreting C1 complement components is increased in the injured muscles compared to the uninjured (data not showed). An increased number of FAPs (which secrete C1r and C1s) in the injured muscles could explain the apparent discrepancy between the two studies with respect of C1r/s. A similar reasoning can be made for macrophages (which secrete C1q). In addition, some other factors might have to be taken into account when considering these data. First, both the abundancy and the transcriptional activities of the FAPs might be different in the time points used in the two studies even though their difference consists of only 12 hours. In keeping with this hypothesis, another study in which the notexin injury was used to induce the muscle damage has shown that FAPs peak in the regenerative milieu 2 days after the muscle damage, while their amount starts to decrease right after the second day post injury to finally be back at the basal level (i.e., uninjured muscle) by the fourth day post injury [46]. Second, it is well documented that different methods used to induce muscle injury are associated with different dynamics of cells engagement and regeneration [98]. This might also result in a different FAPs transcriptional activity. Last, the different age of mice used for the analysis (2 months old in [160] and 1 year old in our study) could also play a role in the observed differential gene expression. Our data suggest that the proliferative state of the dystrophic and injured muscles is not likely linked to the differential C1 complex expression in macrophages and FAPs (**Figure 16 E**). It would be interesting to investigate whether the same differences in C1 expression between the dystrophic and injured muscles persist at different time points after injury, and to explore the

possibility that the C1/Wnt axis that we have highlighted in this work in the dystrophic muscles is active also in muscles undergoing regeneration after acute injury.

4.2 Detrimental role of C1/Wnt axis in dystrophic mice

While the most widely documented function of the complement system is the protection against pathogens through the activation of the innate immunity [278], the existence of several additional complement functions has been reported in different organs in both physiological and pathological conditions [287]. In aged muscles the classical complement C1q has been linked to the activation of the canonical Wnt signaling: C1q binding to the Wnt receptor Frizzled induces the C1s-mediated cleavage of the Wnt coreceptor Lrp5/6 [160]. Data presented in our work suggest that in the dystrophic muscles the canonical Wnt signaling activation is induced by the C1 complex as well (**Figure 27**). Our Lrp6 gene expression analysis indicates that FAPs and other cells within the dystrophic muscles can be responsive to the C1q-induced activation of the canonical Wnt signaling (i.e., C1/Wnt axis [181]) (**Figure 26**). Therefore, we speculate that the molecular events leading to the C1q-dependent Wnt activation in the dystrophic muscles are similar to the ones described in the aging [160] (**Figure 29**).

In physiological conditions the activation of the canonical Wnt signaling occurs following to the binding of the Wnt ligands to the Frizzled receptors and Lrp5/6 coreceptors and it contributes to different biological processes, including cell proliferation, differentiation and tissue regeneration [216] (**Figure 29**). In aged tissues the C1q-mediated increase of the canonical Wnt signaling has not been reported to be dependent on the Wnt ligands [160]. Moreover, data from the same work have described how the role of C1q in the promotion of the C1q/Wnt pathway in the skeletal muscles is independent of the classical complement cascade activation [160]. Other than the enhanced complement levels in the aged serum, both the increased expression of Wnt ligands and receptors and the decreased expression of Wnt signaling inhibitors has been associated to the enhanced Wnt signaling in aging [223,310,352]. Similarly to the aging condition, increased levels of the canonical Wnt signaling in dystrophic muscles have been described [53,159,181]. However, no evidence on the possible upstream mechanism leading to this upregulation has been reported so far. To our knowledge this work is the first study which highlights a possible cause of the enhanced canonical Wnt signaling in muscular dystrophy.

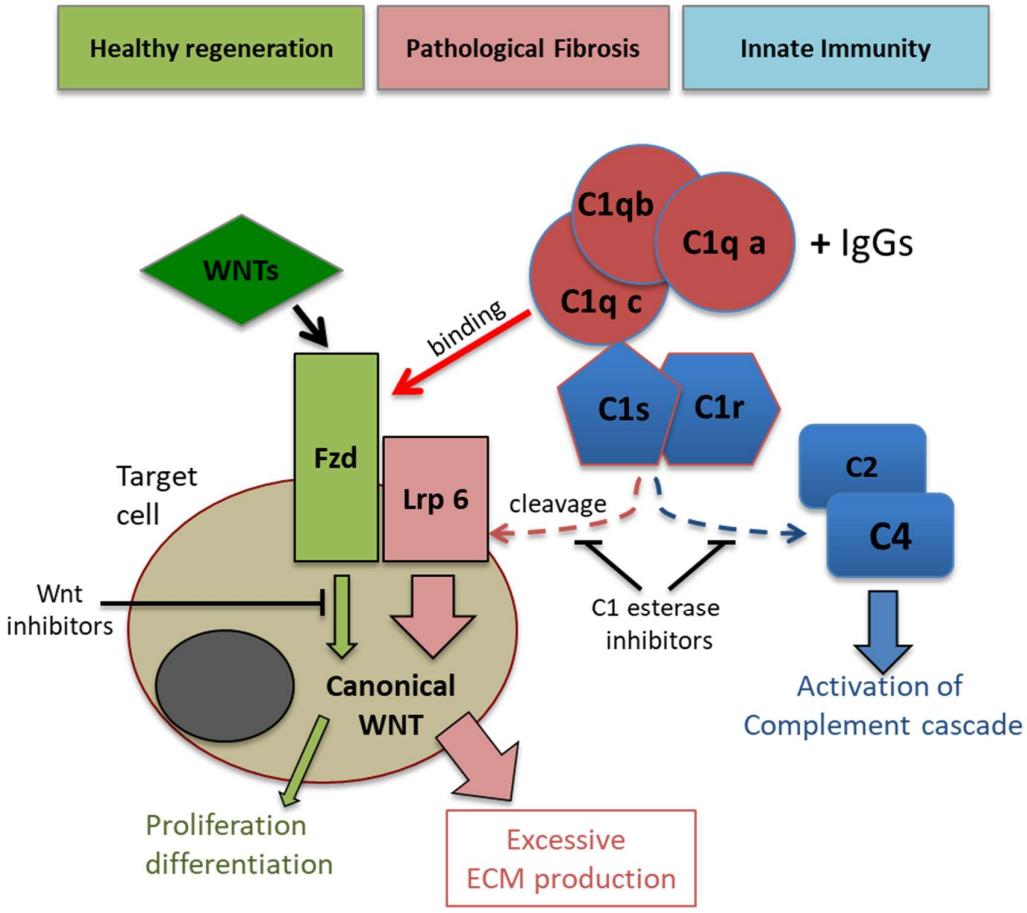

Figure 29. Schematic representation of the signaling pathways activated by C1q. C1q-induced activation of the Wnt signaling pathway is depicted in red, the Wnt ligand-dependent canonical Wnt signaling pathway in green, and the complement cascade that participate in innate immunity in blue. We propose that C1q released by macrophages determines fibrosis by excessively activating the canonical Wnt signaling pathway.

Our data suggest that the increased expression of the classical complement component C1 corroborates to the enhanced detrimental canonical Wnt signaling in the dystrophic muscles. In a previous study the canonical Wnt pathway has been linked to the increased proliferation of a $Sca1^{+ve}$ resident cell population in muscles of dystrophic mice and to the subsequent increase of collagen deposition [53]. The evidence presented here and by others support a primary active role of FAPs in the production of the ECM in dystrophic muscles which is in line with the notion that FAPs aberrant behavior actively contributes to the dystrophic phenotype [46,49]. In keeping with this view, our pharmacological inhibition of C1r/s counteracted the canonical Wnt signaling expression and led to a reduction of the fibrogenic genes expression in the FAPs of dystrophic muscles (**Figure 27**) and to a reduction of collagen deposition and fibrosis in dystrophic muscles (**Figure 28**). Given its upstream position in inflammation, complement C1-targeting drugs are in use for a variety of rare diseases, and some of

them hold orphan drug status [353]. Sanofi and Annexon have clinical programs for C1s and C1q blocking antibodies for the treatment of cold agglutinin disease (CAD), Guillain-Barre' Syndrome and Huntington disease [354] (https://annexonbio.com/pipeline/anx005). Of note, inhibitors of C1s (C1-INH) obtained from human plasma or as recombinant proteins are available in the clinic with a primary indication for the treatment of Hereditary Angiodema (HEA), a life-threatening inherited disease affecting 1:50.000 people [355]. This would likely represent an advantage in future clinical studies on C1 inhibition as the safety requirements of the active molecule have been already proved to be satisfied. C1 primarily function in the organism is the recognition of the antibody-antigen complexes and the activation of the classical complement pathway in response to pathogens [278] (**Figure 29**). Therefore, immunosuppression might be a serious concern to take into account when considering a future C1 inhibition in patients. On the other side, some clinical trials for DMD have shown that immunosuppression might be required in combination to other approaches (i.e., cell-based therapies) in order to minimize the immune response against transplanted allogenic cells or autologous cells expressing a foreign therapeutic gene [97]. In our 21 days long *in vivo* treatment with C1r/s inhibitor (i.v. and i.p. injections on alternate days) we did not observe any evident side effect or hallmarks of toxicity in mice following the drug administration. This could be a relevant indication for other preclinical studies which aim to use C1 inhibition alone or in combination to other approaches. Finally, considering the severity of DMD, the poor quality of life of patients and their short life expectancy, while complement inhibition must be applied cautiously, if proven to be even partially effective it could represent a valid approach to use in future clinical trials.

Other than FAPs, other cell types, including fibroblasts, pericytes, endothelial and satellite cells have been proposed as sources of ECM proteins in muscles diseases and regeneration [46,60,95,180,181,186,356]. The idea that C1 complex is assembled due to the copresence of C1q and C1r/s which are released by macrophages and FAPs in the regenerating foci of the dystrophic muscles is supported by our analysis of these two cell types localization in the dystrophic B6.129S4-PDGFRα$^{tm11(EGFP)Sor/J}$;*mdx*^{4Cv} mice (**Figure 22 and Supplementary Figure 7**). We observed that macrophages and FAPs are physically close in the regenerating areas which are characterized by an increased expression of both complement and canonical Wnt target proteins (i.e., Axin2 and Tgfβ2) (**Figure 23, 24 and Supplementary Figure 8-10**). The satellite cells are also physically close to the interstitial space between myofibers and directly interact with the ECM on their apical pole while remaining in close association to the muscle fibers on their basal pole [9]. Given their localization in the proximity of FAPs and macrophages, and the reported expression of Wnt coreceptor Lrp6 in MuSCs (**Figure 26** and [223]) we are currently investigating the possibility that the C1/Wnt pathway induced in the regenerative milieu of the dystrophic muscle can enhance a fibrogenic program in MuSCs similarly to what we have observed in the FAPs.

Macrophages represent the major inflammatory cell type found in the degenerating skeletal muscle in chronic conditions like dystrophy. We show in this work that macrophages abundance is increased in dystrophic muscles compared to healthy muscles (**Figure 18**) and that they have a pivotal role in the production of complement C1q (**Figure 16, 17**). We noticed in our immunofluorescence analysis that while the great majority of $C1q^{+ve}$ cells were also positive for the macrophages' marker F4/80 (as expected and in keeping with our gene expression analysis), not all the $F4/80^{+ve}$ cells exhibited C1q staining as well (**Figure 17 A**). Macrophages are an heterogenous population of cells consisting of subpopulations (i.e., pro-inflammatory and anti-inflammatory macrophages and different subtypes within the anti-inflammatory fraction) characterized by different responses to the microenvironment signals [55,57]. It would be interesting to further investigate these cells, using markers to identify specific subpopulation and to determine whether the complement secretion and the mechanism that we have described here are related to the preferential expression of one or more subpopulations.

4.3 *In vitro* and *in vivo* models used to investigate the C1/Wnt signaling pathway

Our analysis of the C1 complex on different cell lines allowed us to establish an *in vitro* system that recapitulates the differential expression of the C1 complex components observed in the freshly isolated cells (**Figure 19**). Our *in vitro* experiments and our Lrp6 gene expression analysis suggest that the C1/Wnt pathway which was previously described in the aged muscles [160] is also active in both murine fibroblasts and myoblasts (**Figure 20, 21, 26**). The use of cell lines allows the reproducibility of our data in a relatively easy and cost-effective way, which could be useful to gain further insight in the molecular events that are operating downstream of the C1/Wnt pathway. Indeed, while it has been reported that in dystrophic mice a Wnt-Tgfβ2 axis affects the behavior of muscle satellite cells, the molecular events occurring downstream of Tgfβ2 signaling are unknown [181].

Another relevant tool that we have used and implemented in this study is the mouse model fib-*mdx*, which has been established for the first time by Desguerre and colleagues and is generated by performing micro mechanical injuries for 2 weeks in muscles of young *mdx* mice [274]. The *mdx* mouse is the most used mouse model for DMD as it lacks dystrophin protein similarly to what happens in patients, but its pathological phenotype is overall milder compared to the patient especially at a young age of mice [266]. The fib-*mdx* model on the other side allows to get access to muscles that exhibit increased levels fibrosis and collagen deposition compared to the uninjured *mdx* starting from a young age of the animals (i.e., 2 months old) [274]. Data presented here highlight previously unappreciated features of the fib-*mdx* mouse model. Our fib-*mdx* model is characterized by an overall increased number of macrophages and FAPs compared to the uninjured mice suggesting an augmented state of inflammation and ECM deposition, respectively, which are more in line with the dystrophic phenotype (**Supplementary Figure 12**). We show in this work that the levels of the canonical Wnt signaling are increased in the FAPs of our fib-*mdx* model compared to the uninjured mice, which makes it a useful tool to investigate these cells' functions in the context of dystrophy while optimizing time and costs of

experiments (i.e., working with mice which are younger than one year) (**Figure 25**). Moreover, we have observed encouraging trends suggesting that the Tgfβ2 and fibrotic genes expression might be increased also in the MuSCs of the fib-*mdx* mice compared to the uninjured *mdx*^{4cv} (**Supplementary Figure 11**). Therefore, we are currently further investigating this model with the aim of using it for MuSCs studies as well.

5. Concluding remarks

Data presented in this work support a key role of C1/Wnt axis in controlling the behavior of FAPs in dystrophic muscles. The mechanism by which complement might induce dystrophic-related phenotypes is depicted in **Figure 30**. In the regenerating foci of dystrophic muscles augmented levels of C1q (i.e., C1qa, C1qb and C1qc) secreted by an increased number of macrophages and augmented levels of C1r/s secreted by an increased number of FAPs lead to the formation of the C1 complex. Once formed, the C1 complex induces the expression of the canonical Wnt signaling (i.e., Wnt/Tgfβ axis [181]) in responsive cells like FAPs. This results into an increased expression of fibrogenic genes and ECM production by FAPs which eventually leads to fibrosis deposition and to the worsening of the dystrophic phenotype [46,49]. In keeping with this model, our data show that the pharmacological inhibition of C1 rescues to some extent the increased gene expression of both the canonical Wnt signaling and fibrogenic genes in FAPs and ameliorates the dystrophic muscle phenotype.

We do not exclude the possibility that other cells within the stem cell *niche* which have previously been proposed as sources of ECM proteins can be responsive to the C1/Wnt axis described in this work [46,60,95,181,186,356]. These include the satellite cells in which augmented levels of canonical Wnt signaling in dystrophic muscles have been already reported [181].

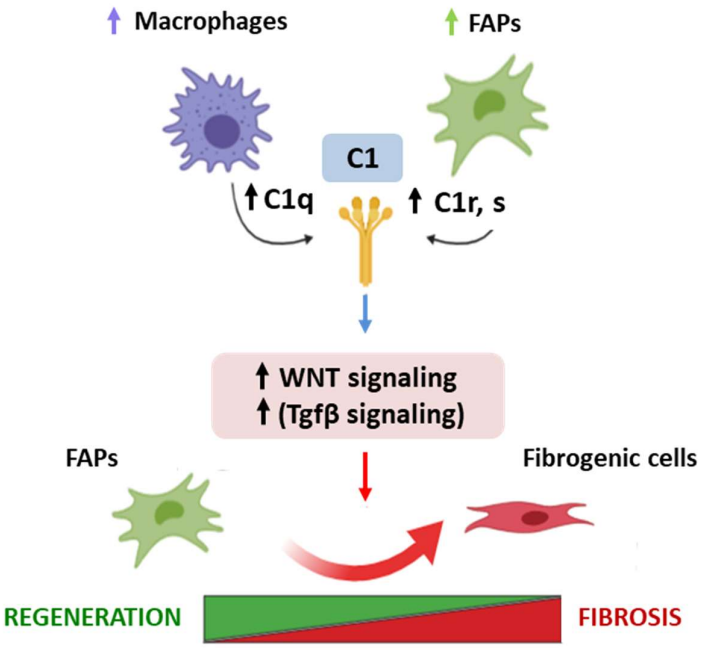

Figure 30. Model of mechanism through which the C1/Wnt axis may affect FAPs fate in dystrophic muscles. The regenerating foci of dystrophic muscles are characterized by increased levels of C1q (i.e., C1qa, C1qb, C1qc) and C1r/s which are secreted by augmented macrophages and FAPs, respectively. C1q and C1r/s combine to form the C1 complex, which leads to an enhanced Wnt/Tgfβ

activity in FAPs. This results in an augmented expression of fibrogenic genes in FAPs and subsequent increase of fibrosis levels in the muscles.

The increased complement levels described here in dystrophic muscles might suggest that the complement activation could be involved in the pathology of DMD. Indeed, while dystrophin deficiency is the primary cause of DMD, secondary mechanisms may be key contributors to the disease pathogenesis and may be critical to elucidate the reasons underling different extent of the severity of the disease [308]. Also, it would be interesting to explore the possibility that C1 complement complex could play a detrimental role in the context of other conditions characterized by increased Wnt signaling and FAPs dysfunction [357].

Finally, understanding the mechanisms that contribute to the development of muscle fibrosis is relevant for muscular dystrophies as well as for other degenerative and inflammatory diseases. Fibrosis is a primary process that strongly contributes to the symptomatology of DMD, but it also represents a physical barrier which makes treatments in both DMD and other conditions particularly challenging due to the poor penetrability of drugs into the scar-like fibrotic tissue [44]. The work presented here provides previously unreported insights into the cellular and molecular mechanisms leading to fibrosis. Modulation of C1-dependent activation of the canonical Wnt signaling may represent a step toward the development of effective therapeutic approaches for muscular dystrophies and other tissues' degenerative conditions.

6. Future perspectives

In this study we have presented evidence that all the C1 complex components (i.e., C1q and C1r/s) are increased in dystrophic muscles of the *mdx*^{4Cv} mice compared to the wild type. We have shown that the pharmacological inhibition of C1 by targeting C1r/s esterase leads to a reduced expression of canonical Wnt and fibrogenic genes in FAPs in the fib-*mdx* model (**Figure 27**) and to a reduced collagen deposition and fibrosis in the fib-*mdx* model (**Figure 28**). The formation of C1 complex requires the interaction of C1r/C1s/C1s/C1r tetramer and C1q (which includes C1qa, C1qb and C1qc) [284]. In order to evaluate the effect of *C1qa* loss in dystrophic muscles, we crossed female C1qa$^{FL/FL}$;*mdx*^{4Cv} (FL: floxed) to male Lzy2Cre$^{+/-}$;C1qa$^{FL/WT}$;*mdx*^{4Cv} and we generated Lyz2Cre$^{+/-}$;C1qa$^{FL/FL}$;*mdx*^{4Cv} (hereafter referred to as C1qa^{KO};*mdx*^{4Cv}) mice **(Figure 31 A)**. In these mice exon 3 excision of *C1qa* leads to the *C1qa* deletion specifically in the myeloid cell lineage (i.e., monocytes, mature macrophages and granulocytes), which express the Lyz2Cre recombinase under the control of the endogenous Lyz2 promoter/enhancer elements (Jackson stock number: 4781). We observed ~ 93% reduction of C1qa in the macrophages of C1qa^{KO};*mdx*^{4Cv} mice compared to the controls **(Figure 31 B)** and 96-97% reduction of *C1qa* in the gastrocnemius and in the diaphragm of the C1qa^{KO};*mdx*^{4Cv} mice compared to the controls (**Figure 31 C, D**), which indicates that *C1qa* was effectively ablated in our C1qa^{KO};*mdx*^{4Cv} mice.

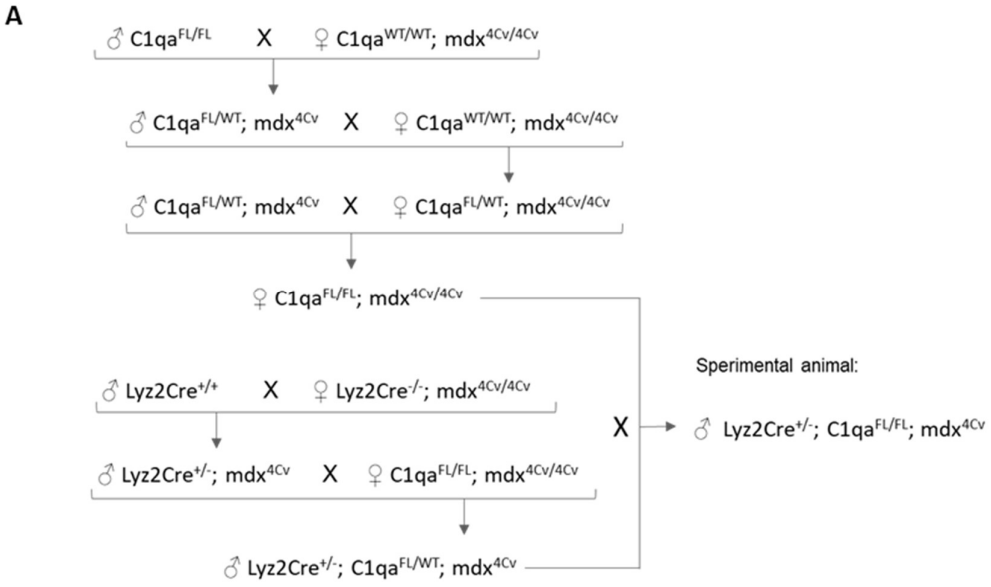

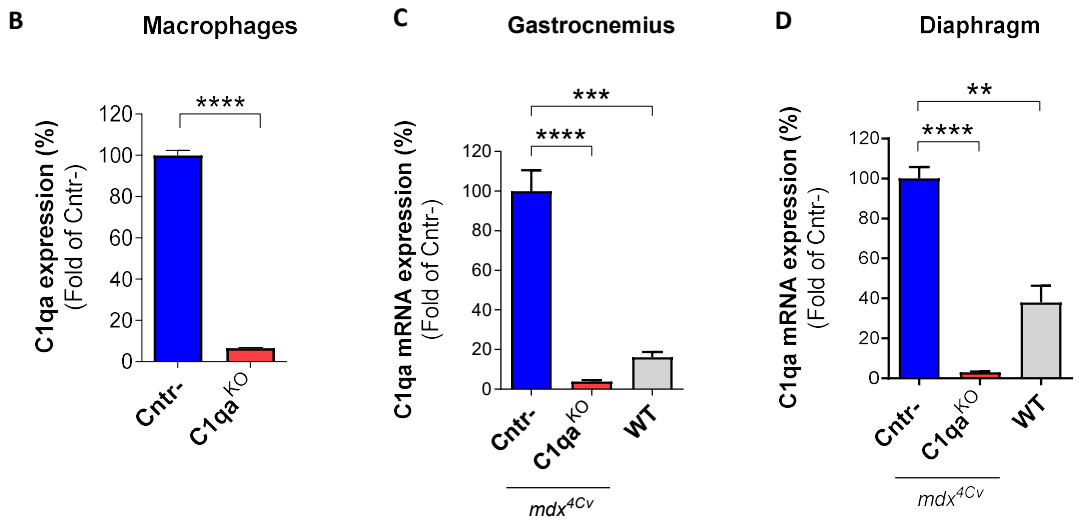

Figure 31. C1qa ablated expression in the C1qa^{KO};*mdx*^{4Cv} mice. (A) Mice crossing strategy used to generate C1qa knockout animals Lyz2Cre$^{+/-}$; C1qa$^{FL/FL}$; *mdx*^{4Cv} (i.e., C1qa^{KO}; *mdx*^{4Cv}) FL: floxed. **(B)** qPCR analysis of C1qa expression in FACS isolated macrophages (CD45^{+ve}F4/80^{+ve}) from hindlimb muscles of ~ 3 months old Lyz2Cre$^{-/-}$C1qa$^{KO/WT}$;*mdx*^{4Cv} or Lyz2Cre$^{-/-}$C1qa$^{KO/KO}$;*mdx*^{4Cv} (Cntr-) and Lyz2Cre$^{+/-}$C1qa$^{KO/KO}$;*mdx*^{4Cv} (C1qa^{KO}). N=3 (Cntr-), N=4 (C1qa^{KO}). Data are expressed as mean with SEM. Two-tailed unpaired t-test applied. **(C-D)** qPCR analysis of C1qa expression in gastrocnemius **(C)** and diaphragm **(D)** of ~ 3 months old Lyz2Cre$^{+/-}$C1qa$^{WT/WT}$;*mdx*^{4Cv} (Cntr-, N=6), Lyz2Cre$^{+/-}$C1qa$^{KO/KO}$;*mdx*^{4Cv} (C1qa^{KO}, N=5) and wild type (WT, N=3). Data are expressed as mean with SEM. One-way Anova test was applied. $p > 0.05$: ns; $p \leq 0.05$ (*), < 0.01 (**), < 0.001 (***), < 0.0001 (****).

We are currently using our C1qa^{KO};*mdx*^{4Cv} mice to study how C1qa levels can modulate the Wnt signaling and fibrosis in dystrophy. These findings together with data presented in this work will increase our understanding on the link existing between complement levels and degenerative disease like DMD and will suggest effective therapeutic strategies to investigate in the clinical setting.

7. Supplementary Figures

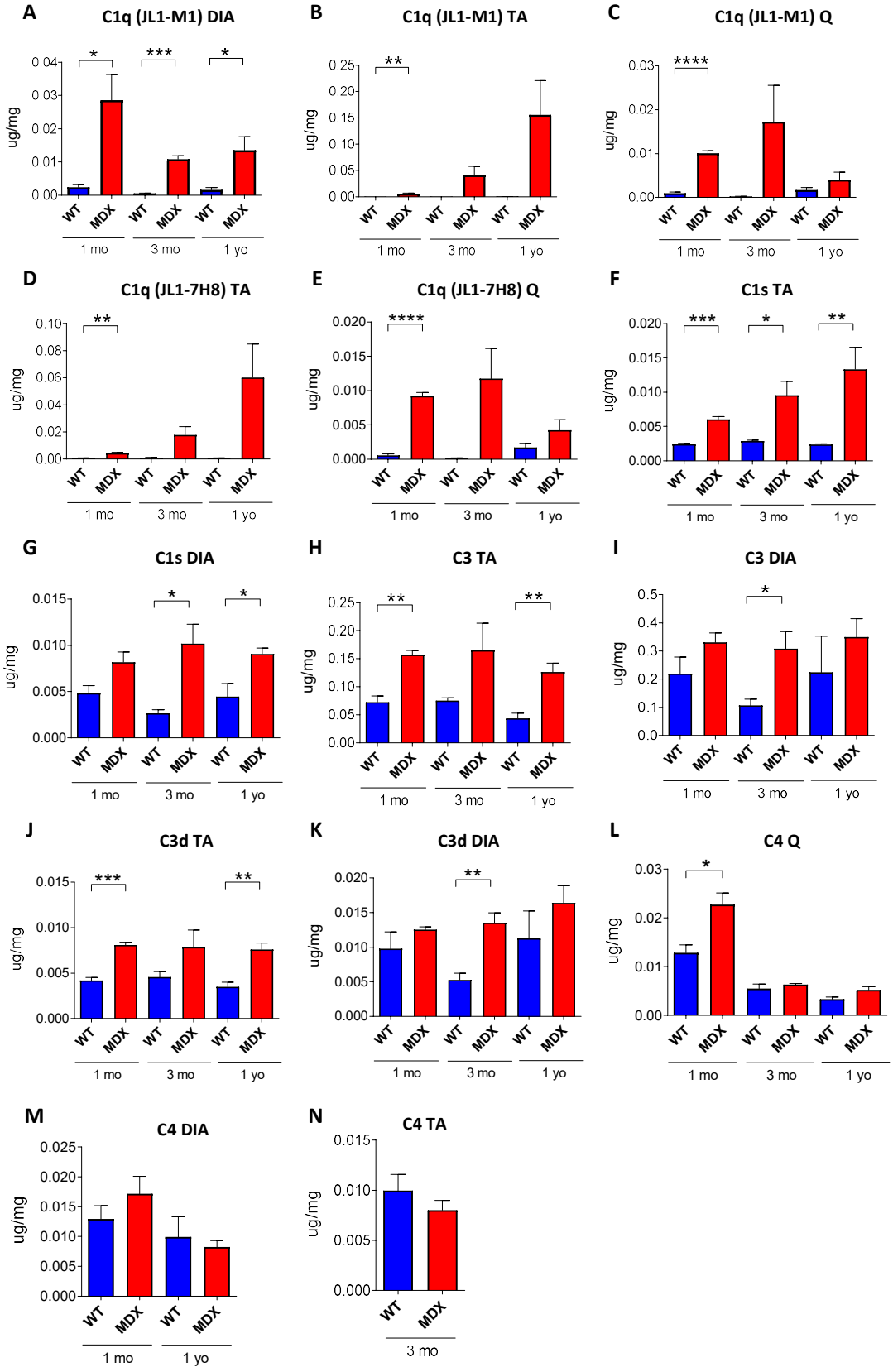

Supplementary Figure 1. The classical complement pathway is enhanced in muscles of dystrophic mice. ELISA assay of proteins of the classical complement pathway: C1q (**A-E**), C1s (**F-G**), C3 (**H-I**), C3d (**J-K**), C4 (**L-N**). Diaphragm (DIA), quadriceps (Q) and tibialis anterior (TA) muscles from ~ 1 month (1 mo), ~ 3 months (3 mo) or ~ 1 year old (1 yo) wild type (WT) and *mdx*^{4Cv} (MDX) mice (as indicated on the graphs) were used. N=3 (WT 1 mo, WT 3 mo), N=4 (WT 1 yo, MDX 1 mo, MDX 3 mo, MDX 1 yo). C1q protein level was assessed using two different antibodies (anti C1qJL1-M1 and anti C1qJL1-7H8. Refer also to Materials and Methods section). Data are expressed as mean with SEM. Two-tailed unpaired t-test was applied. $p > 0.05$: ns; $p \leq 0.05$: *; $p \leq 0.01$: **; $p \leq 0.001$: ***; $p \leq 0.0001$: ****.

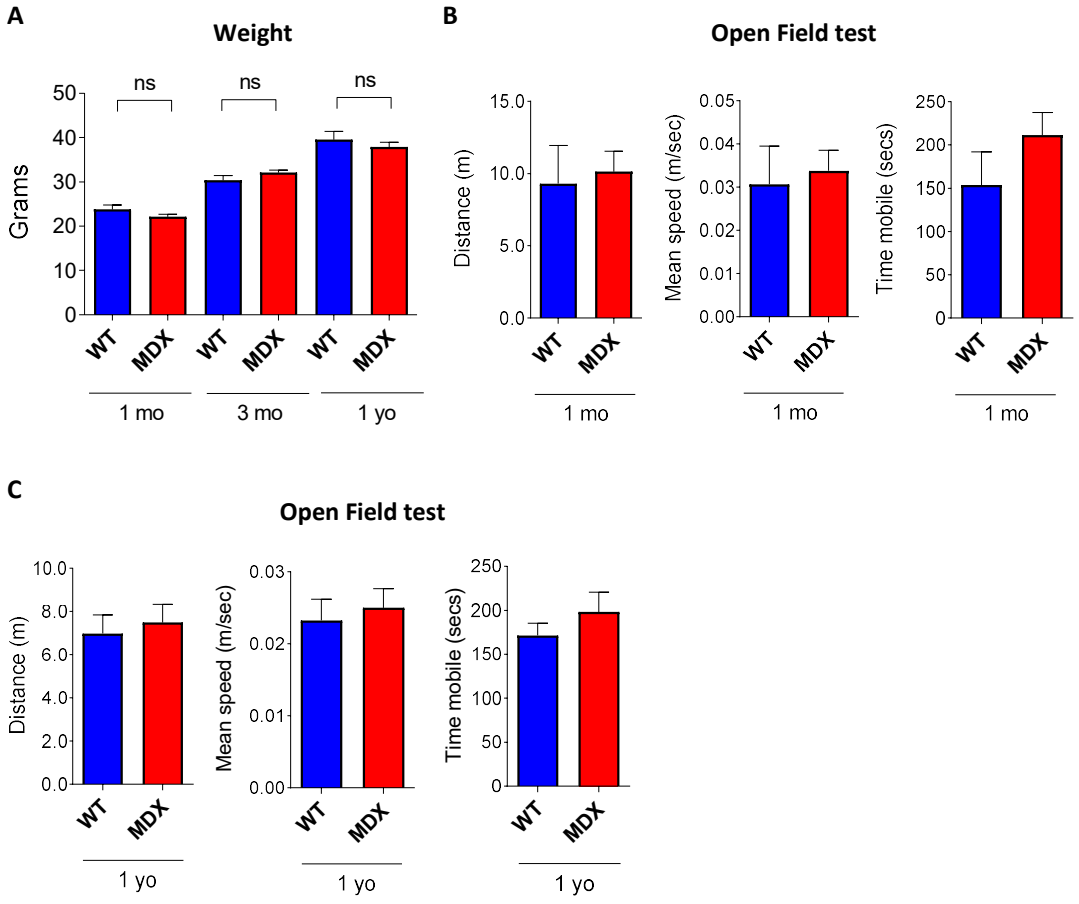

Supplementary Figure 2. Open Field test on wild type and dystrophic mice. (A) Mice weight (grams) of ~1 month (1 mo), ~3 months (3 mo) and ~1 year old (1 yo) wild type (WT) and *mdx*^{4Cv} (MDX) mice used in behavioral test shown in **(B)**, **(C)** and in **Figure 12. (B)** Open Field test performed on ~ 1 month old (1 mo) wild type (WT) and *mdx*^{4Cv} (MDX) mice. N=3 (WT 1 mo), N=4 (MDX 1 mo). **(C)** Open Field test performed on ~ 1 year old (1 yo) wild type (WT) and *mdx*^{4Cv} (MDX)

mice. N=4. Data are expressed as mean with SEM. Two-tailed unpaired t-test was applied. $p > 0.05$: ns; $p \leq 0.05$: *; $p \leq 0.01$: **; $p \leq 0.001$: ***; $p \leq 0.0001$: ****.

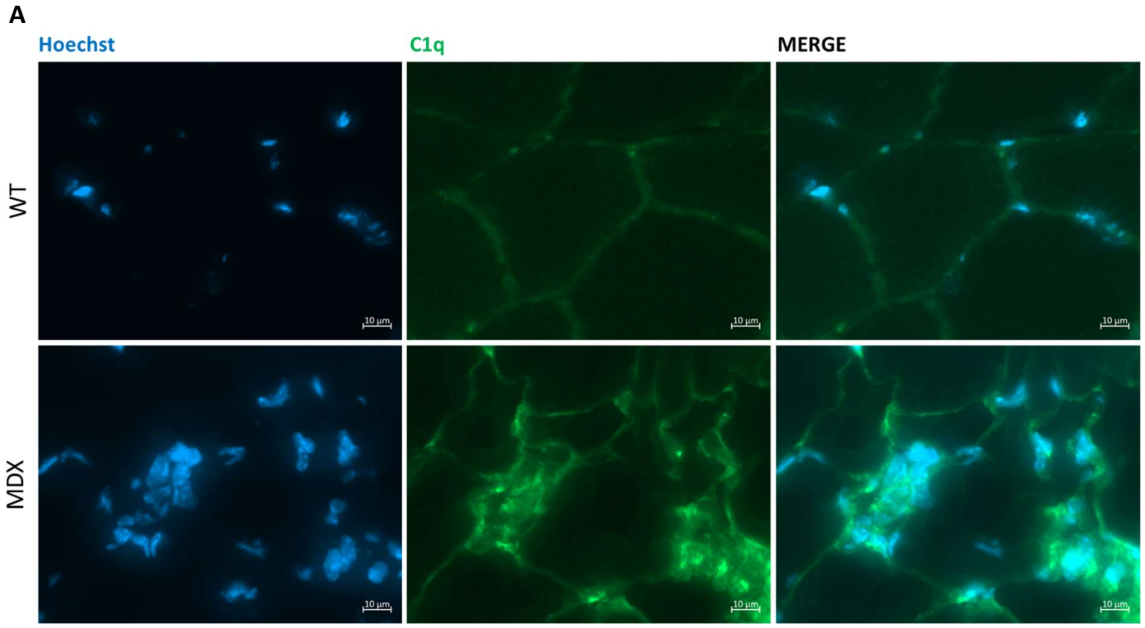

Supplementary Figure 3. C1q proteins expression in tibialis anterior muscles. (A) Representative immunofluorescence of tibialis anterior of ~ 1 year old wild type (WT) and *mdx*^{4Cv} (MDX) stained with anti-C1q (green) and Hoechst (blue). C1q expression is higher in *mdx*^{4Cv} muscles compared to the wild type. Scale bar: 10 µm.

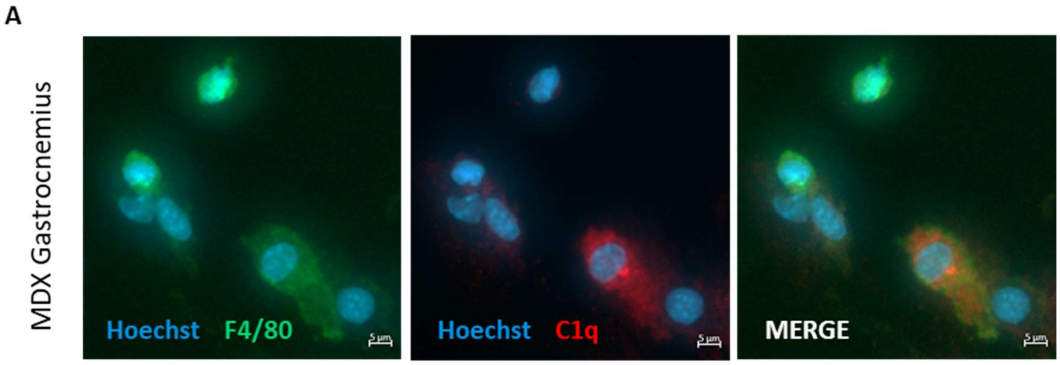

Supplementary Figure 4. C1q protein is expressed by macrophages in dystrophic muscles. (A) Representative immunofluorescence image of cryosection from ~ 1 year old *mdx*^{4Cv} (MDX) gastrocnemius stained with anti-F4/80 (green), anti-C1q (red) and Hoechst (blue). Scale bar: 5 µm.

A

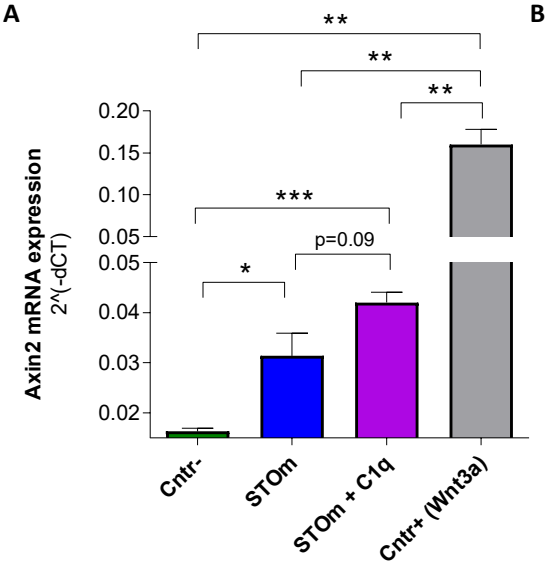

B

Hindlimb Muscles MDX ~ 1 year old	Macrophages (MAC)	Fibro/Adipogenic Progenitors (FAPs)
	% of total cell number	
Biological replicate 1	3.60	9.60
Biological replicate 2	3.30	13.70
Biological replicate 3	3.39	10.4
Average	3.43	11.2
SD	0.15	2.17

FAPs/MAC = 11.2/3.43 = 3,27
Numbers of cells per area = RAW 264.7/STO = 2,5

Final ratio = **STO/RAW 264.7 = 8,16/1**

Supplementary Figure 5. C1 Complex induces the canonical Wnt signaling in fibroblasts *in vitro*. **(A)** qPCR analysis of Axin2 expression in STO cells cultured with STO conditioned medium (STOm) or STOm + C1q recombinant protein (100 ug/ml) for 24 hours. Cntr-: STO cultured in DMEM. Cntr+: STO cultured in DMEM + 50 ng/ml Wnt3a. Data are expressed as mean with SEM. N=3. Two-tailed unpaired t-test was applied. $p > 0.05$: ns; $p \leq 0.05$: *; $p \leq 0.01$: **; $p \leq 0.001$: ***; $p \leq 0.0001$: ****. Refer also to **Figure 20**, in which similar results after a shorter (6 hours) incubation are reported. **(B)** STO/RAW 264.7 conditioned media ratio used to treat C2C12 cells was calculated considering the *in vivo* proportion of macrophages and fibro/adipogenic progenitors in dystrophic mice and the number of STO and RAW 264.7 cells counted per area. Refer also to **Figure 21**.

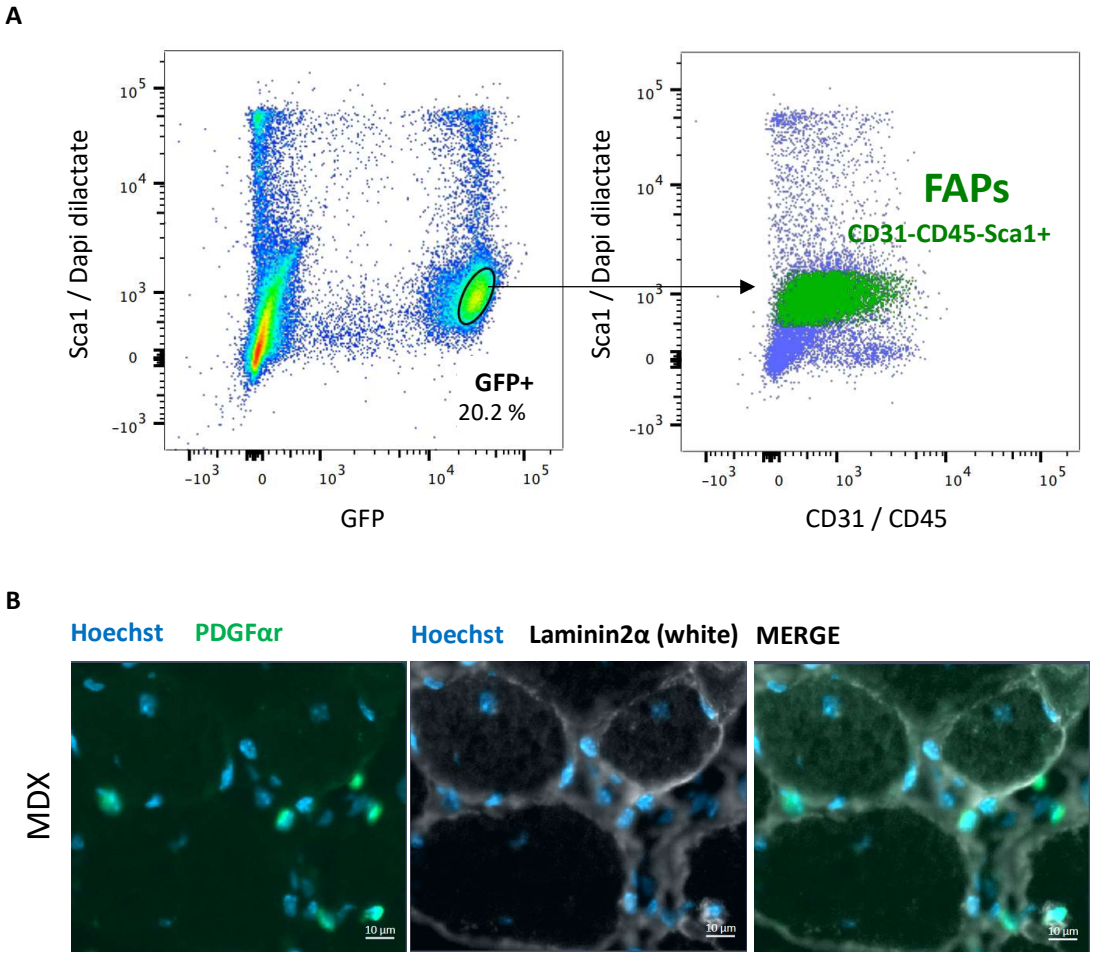

Supplementary Figure 6. Fibro/adipogenic progenitors are selectively marked in B6.129S4-PDGFRα$^{tm11(EGFP)Sor/J}$ mice. (A) Representative FACS plot of hindlimb muscles of a ~ 1 year old male B6.129S4-PDGFRα$^{tm11(EGFP)Sor/J}$;*mdx*^{4Cv} (MDX) showing that GFP^{+ve} cells have the same staining signature as fibro/adipogenic progenitors (FAPs): CD31^{-ve}CD45^{-ve}Sca1^{+ve}. **(B)** Representative immunofluorescence of gastrocnemius of a ~ 18 months old male B6.129S4-PDGFRα$^{tm11(EGFP)Sor/J}$;*mdx*^{4Cv} (MDX) mouse stained with anti-laminin2α (white) and Hoechst (blue). PDGFαr^{+ve} cells (GFP^{+ve}, green) do not localize underneath the basal lamina (laminin2α^{+ve}, white), showing that PDGFαr^{+ve} cells are not satellite cells. Scale bar: 10 µm.

A MAC – FAPs distance analysis

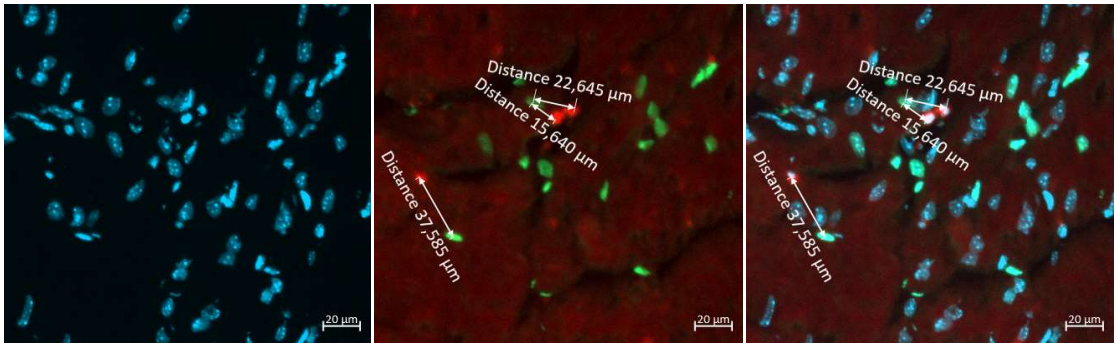

B FAPs – MAC distance analysis. Case 1: Macrophages are present in the image field.

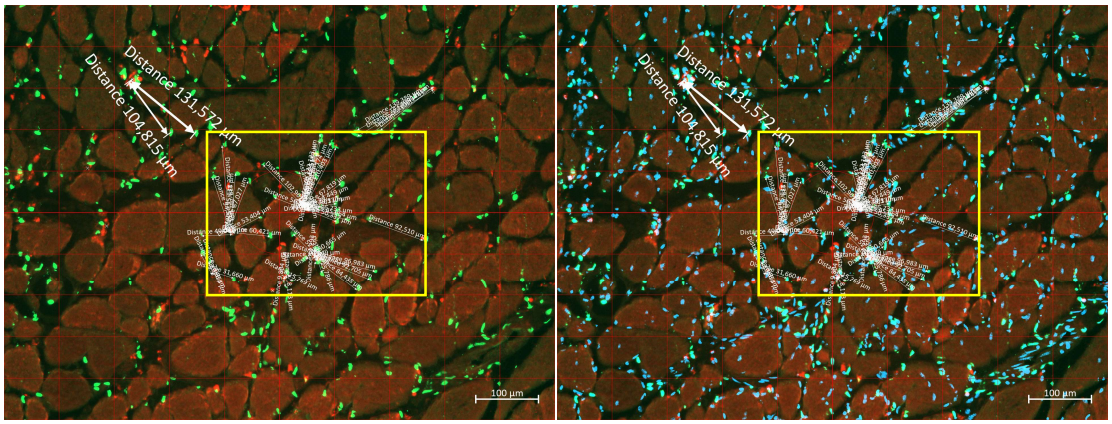

C FAPs – MAC distance analysis. Case 2: No macrophage is present in the image field.

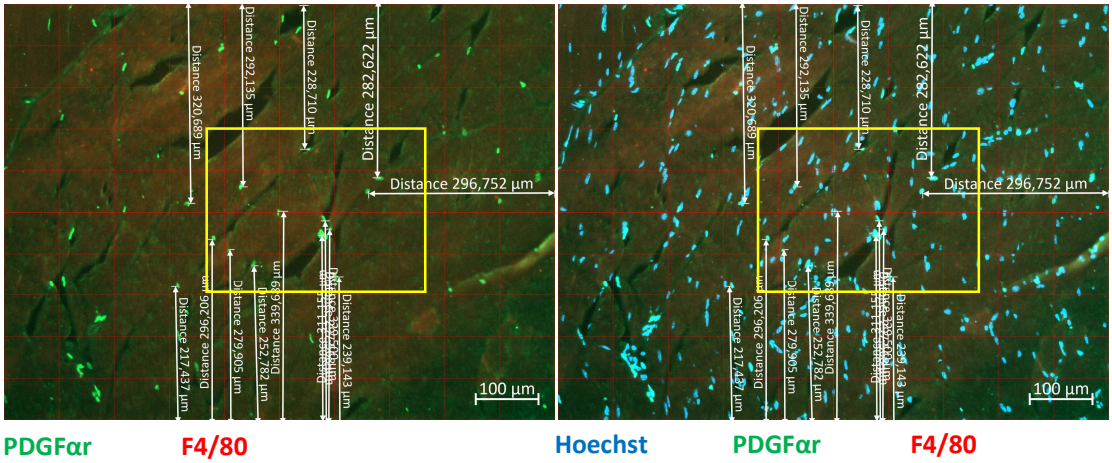

Supplementary Figure 7. Analysis of distance between macrophages and fibro/adipogenic progenitors in muscles. (A) Representative distance analysis between macrophages (MAC: F4/80^{+ve}

cells) and fibro/adipogenic progenitors (FAPs: PDGFαr^{+ve} cells) shown in **Figure 22 A**. The analysis was performed measuring the distance of each macrophage from its closest FAP within the image field. Gastrocnemius section of ~ 18 months old female B6.129S4-PDGFRα$^{tm11(EGFP)Sor/J}$;*mdx*^{4Cv} (Cntr HET) mouse is shown. Scale bar: 20 µm. Staining: anti-F4/80 (red), Hoechst (blue). **(B-C)** Representative distance analysis between fibro/adipogenic progenitors (FAPs: PDGFαr^{+ve} cells) and macrophages (MAC: F4/80^{+ve} cells) shown in **Figure 22 B**. The analysis was performed measuring the distance of each FAP from its closest macrophage within a fixed portion of the image field (100 µm^2, yellow rectangle). If no macrophage was present in the entire image field **(C)**, distance was estimated as the distance between a FAP and the image edge. Gastrocnemius section of ~ 12 months old male B6.129S4-PDGFRα$^{tm11(EGFP)Sor/J}$;*mdx*^{4Cv} (MDX) mouse **(B)** and ~ 18 months old female B6.129S4-PDGFRα$^{tm11(EGFP)Sor/J}$;*mdx*^{4Cv} (Cntr HET) mouse **(C)** are shown. Note that clusters of macrophages and FAPs were observed mostly in the MDX regenerating areas (**B**). Scale bar: 100 µm. Staining: anti-F4/80 (red), Hoechst (blue).

A

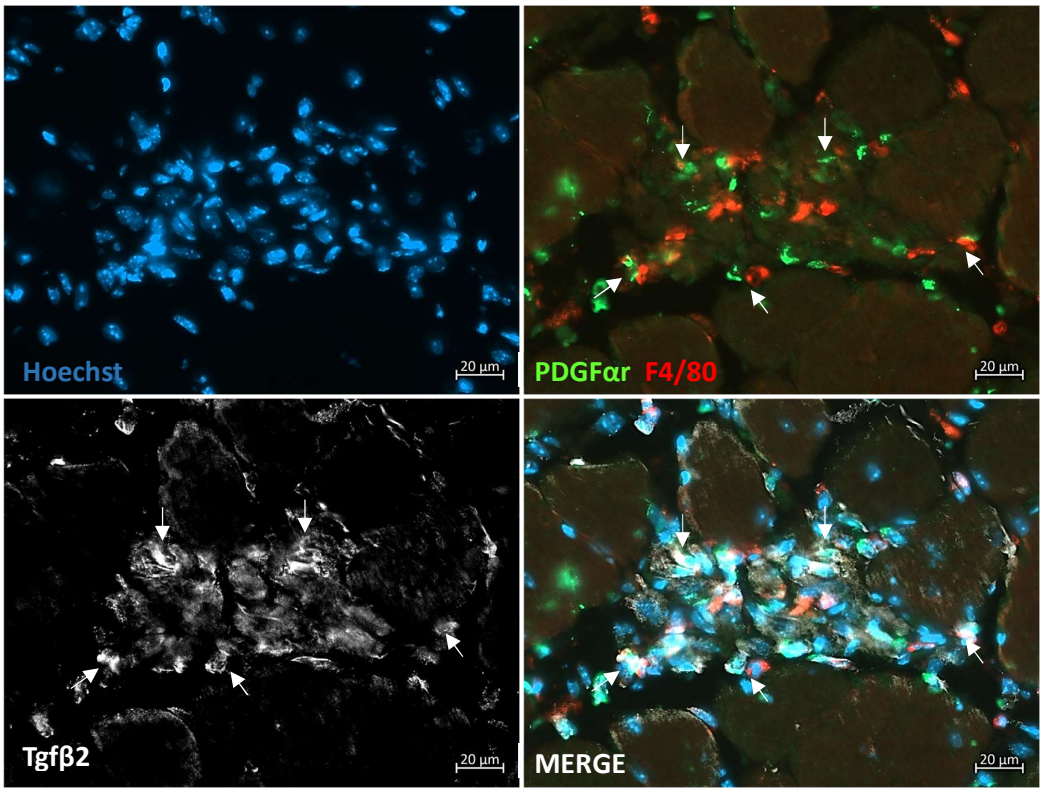

Supplementary Figure 8. Tgfβ2 protein colocalizes with macrophages and FAPs in the dystrophic regenerating areas. (A) Representative immunofluorescence image of a regenerating area of the gastrocnemius of a ~ 18 months old male B6.129S4-PDGFRα$^{tm11(EGFP)Sor/J}$;*mdx*^{4Cv} (MDX) mouse stained with anti-F4/80 (red), anti-Tgfβ2 (white) and Hoechst (blue). White arrows indicate Tgfβ2

signal that colocalizes with macrophages (F4/80^{+ve} cells) and FAPs (PDGFα^{+ve} cells). Scale bar: 20 µm.

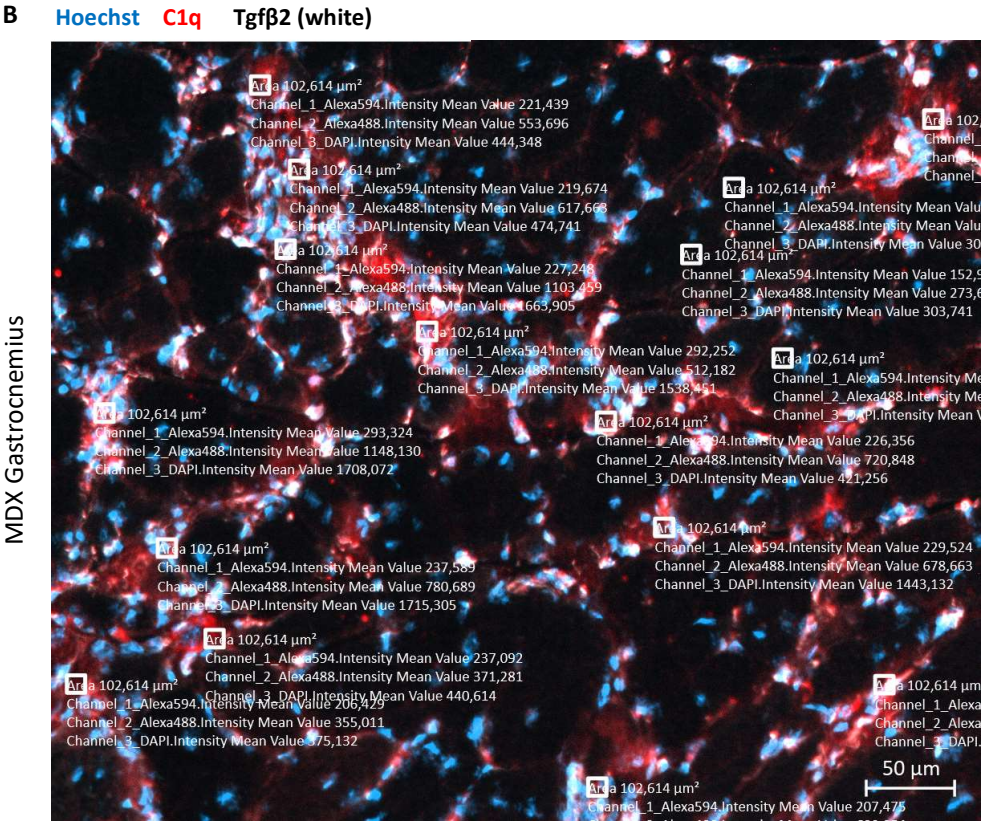

Supplementary Figure 9. Correlation analysis of C1q and Tgfβ2 / Axin2 in dystrophic muscles. Representative pixel quantification analysis shown in **Figure 24 A, B**. Gastrocnemius of ~ 12 months old *mdx*^{4Cv} (MDX) stained with anti-C1q (red), anti-Axin2 (green) and Hoechst (blue) **(A)** (scale bar: 50 µm) or anti-C1q (red), anti-Tgfβ2 (white) and Hoechst (blue) **(B)** (scale bar: 100 µm). 336 areas of 1017 µm^2 (for C1q and Axin2 correlation analysis, 109 or more areas per mouse, 3 mice) or 502 of 102 µm^2 (for C1q and Tgfβ2 correlation analysis, 106 or more areas per mouse, 3 mice) were selected in the regenerating areas and the corresponding mean pixel intensities were quantified. Chanel 1: C1q, chanel 2: Axin2; chanel 3: Hoechst **(A)**; chanel 1: C1q; chanel 2: Tgfβ2; chanel 3: Hoechst **(B)**. The background pixel intensity from sections stained with only the secondary antibody was subtracted. Refer also to Materials and Methods section.

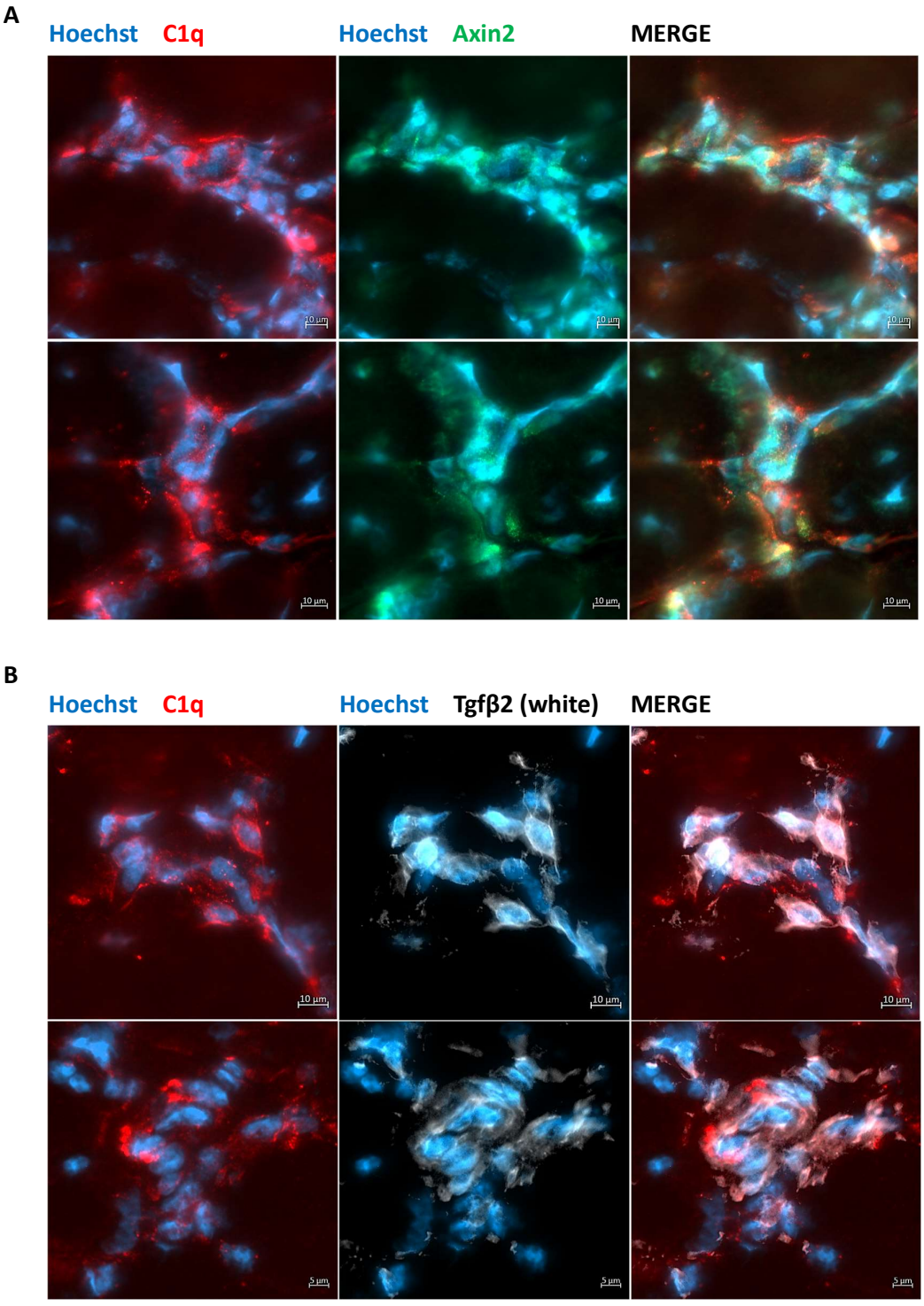

Supplementary Figure 10. Enhanced C1q correlates with an increased Wnt-Tgfβ2 activity in dystrophic muscles. (A) Representative immunofluorescence of gastrocnemius of ~ 12 months old *mdx*^{4Cv} (MDX) stained with anti-C1q (red), anti-Axin2 (green) and Hoechst (blue). Scale bar: 10 µm. **(B)** Representative immunofluorescence of gastrocnemius of ~ 12 months old *mdx*^{4Cv} (MDX) stained

with anti-C1q (red), anti-Tgfβ2 (white) and Hoechst (blue). Scale bar (first to third field): 10 µm; scale bar (fourth field): 5 µm. Refer also to **Figure 24**.

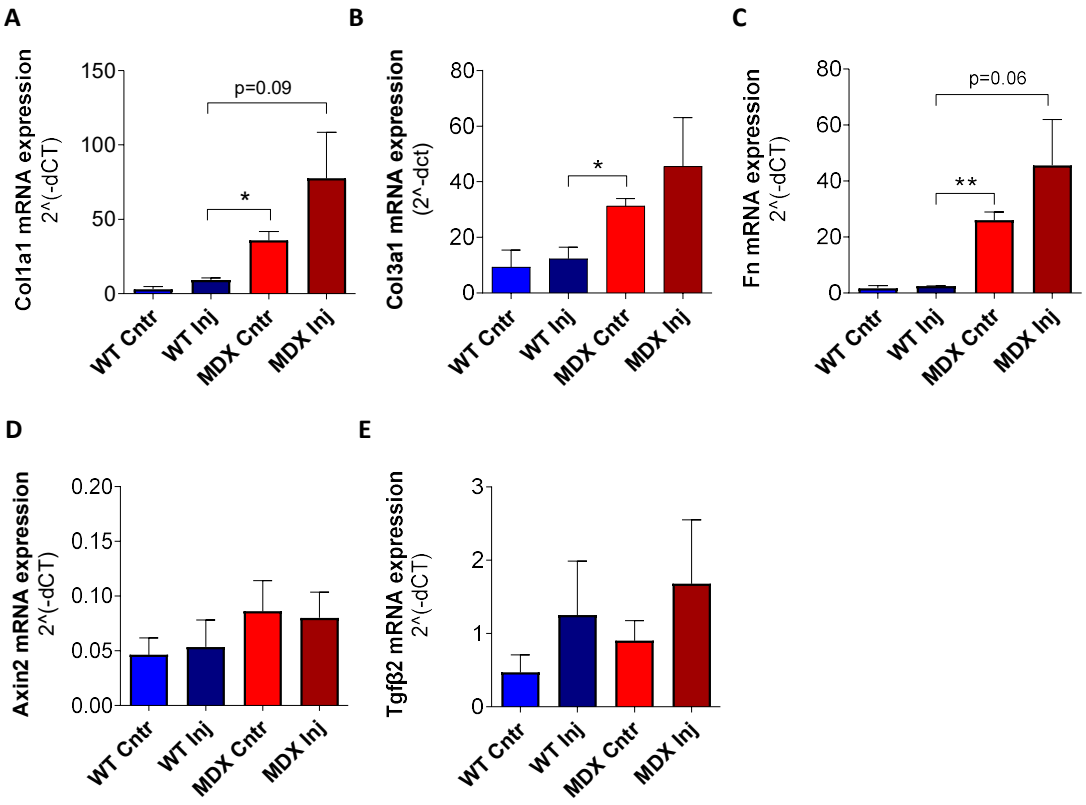

Supplementary Figure 11. Gene expression of canonical Wnt signaling genes and fibrotic genes in the fib-*mdx* satellite cells. (A-D) qPCR analysis of collagen1a1 (**A**), collagen3a1 (**B**), fibronectin (**C**), Axin2 (**D**) and Tgfβ2 (**E**) in SCs FACS isolated from ~ 4 to 6 months old wild type (WT) and *mdx*^{4Cv} (MDX). WT Cntr and MDX Cntr were not injured. WT Inj and MDX Inj were processed as indicated in **Figure 25 A**. Data are expressed as mean with SEM. N=3 except for collagen1a1, collagen3a1 and fibronectin of WT Cntr (N=2). Two-tailed unpaired t-test was applied. $p > 0.05$: ns; $p < 0.05$ (*), < 0.01 (**), < 0.001 (***), < 0.0001 (****).

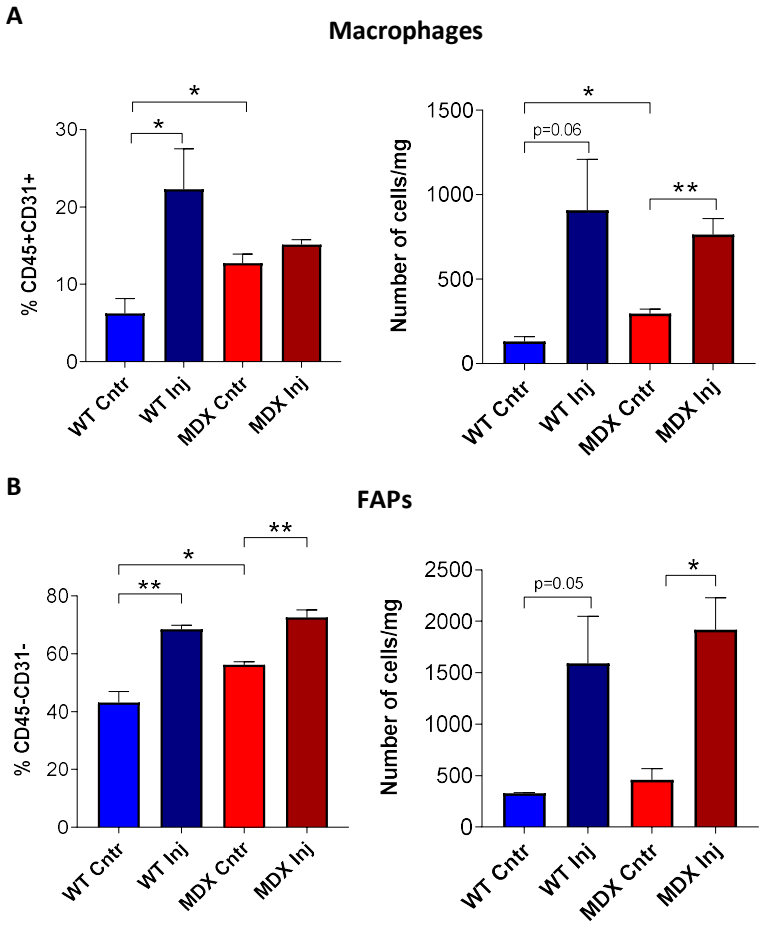

Supplementary Figure 12. Macrophages and fibro/adipogenic progenitors are increased in the fib-*mdx* mouse model compared to the *mdx*^{4Cv}. (A) Quantification of macrophages (CD45^{+ve}F4/80^{+ve}) expressed as percentage of CD45^{+ve}CD31^{+ve} cells **(left)** or as number of cells per mg of tissue **(right)**. **(B)** Quantification of FAPs (CD45^{-ve}CD31^{-ve}Sca1^{+ve}) expressed as percentage of CD45^{+ve}CD31^{+ve} cells **(left)** or as number of cells per mg of tissue **(right)**. Hindlimb muscle from ~ 4 to 6 months old wild type (WT) and *mdx*^{4Cv} (MDX) were analyzed. WT Cntr and MDX Cntr were not injured. WT Inj and MDX Inj were processed as indicated in **Figure 25 A**. Data are expressed as mean with SEM. N=3. Two-tailed unpaired t-test was applied. $p > 0.05$: ns; $p < 0.05$ (*), < 0.01 (**), < 0.001 (***), < 0.0001 (****).

8. References

1. Mukund, K. & Subramaniam, S. Skeletal muscle: A review of molecular structure and function, in health and disease. *Wiley Interdisciplinary Reviews: Systems Biology and Medicine* vol. **12** (2020).

2. Chal, J. & Pourquié, O. Making muscle: Skeletal myogenesis in vivo and in vitro. *Development (Cambridge)* vol. **144** 2104–2122 (2017).

3. Muñoz-Cánoves, P., Neves, J. & Sousa-Victor, P. Understanding muscle regenerative decline with aging: new approaches to bring back youthfulness to aged stem cells. *FEBS J.* **287**, 406–416 (2020).

4. Morgan, J. & Partridge, T. Skeletal muscle in health and disease. *DMM Disease Models and Mechanisms* vol. **13** (2020).

5. Davies, O. G. *et al.* Defining the balance between regeneration and pathological ossification in skeletal muscle following traumatic injury. *Front. Physiol.* **8**, 1–15 (2017).

6. Schofield, R. The relationship between the spleen colony-forming cell and the haemopoietic stem cell. *Blood Cells* **4**, 7–25 (1978).

7. Wosczyna, M. N. & Rando, T. A. A Muscle Stem Cell Support Group: Coordinated Cellular Responses in Muscle Regeneration. *Dev. Cell* **46**, 135–143 (2018).

8. Mashinchian, O., Pisconti, A., Le Moal, E. & Bentzinger, C. F. *The Muscle Stem Cell Niche in Health and Disease*. *Current Topics in Developmental Biology* vol. **126** (2018).

9. Alexander, M. Satellite cell of skeletal muscle fibers. *J. Biophys. Biochem. Cytol.* **9**, 493–495 (1961).

10. Cheung, T. H. & Rando, T. A. Molecular regulation of stem cell quiescence. *Nat. Rev. Mol. Cell Biol.* **14**, 329–340 (2013).

11. Holmberg, J. & Durbeej, M. Laminin-211 in skeletal muscle function. *Cell Adhes. Migr.* **7**, 111–121 (2013).

12. Abou-Khalil, R. *et al.* Autocrine and Paracrine Angiopoietin 1/Tie-2 Signaling Promotes Muscle Satellite Cell Self-Renewal. *Cell Stem Cell* **5**, 298–309 (2009).

13. Christov, C. R. A.-K., Guillaume Bassez, Gregoire Vallet, F.-J. A., Yann Bassaglia, Vasily Shinin, Shahragim Tajbakhsh, B. C. & Gherardi, and R. K. Muscle Satellite Cells and Endothelial Cells: Close Neighbors and Privileged Partners. *Mol. Biol. Cell* **18**, 1397–1409

(2007).

14. Kostallari, E. *et al.* Pericytes in the myovascular niche promote post-natal myofiber growth and satellite cell quiescence. *Dev.* **142**, 1242–1253 (2015).

15. Mourikis, P. *et al.* A Critical Requirement for Notch Signaling in Maintenance of the Quiescent Skeletal Muscle Stem Cell State. *Stem Cells* **30**, 243–252 (2012).

16. Bjornson, C. R. R. *et al.* Notch Signaling Is Necessary to Maintain Quiescence in Adult Muscle Stem Cells. *Stem Cells* **30**, 232–242 (2012).

17. Baghdadi, M. B. *et al.* Reciprocal signalling by Notch–Collagen V–CALCR retains muscle stem cells in their niche. *Nat. 2018 5577707* **557**, 714–718 (2018).

18. Baghdadi, M. B. *et al.* Notch-Induced miR-708 Antagonizes Satellite Cell Migration and Maintains Quiescence. *Cell Stem Cell* **23**, 859-868.e5 (2018).

19. Verma, M. *et al.* Muscle Satellite Cell Cross-Talk with a Vascular Niche Maintains Quiescence via VEGF and Notch Signaling. *Cell Stem Cell* **23**, 530-543.e9 (2018).

20. Gohring, W., Sasaki, T., Heldin, C. H. & Timpl, R. Mapping of the binding of platelet-derived growth factor to distinct domains of the basement membrane proteins BM-40 and perlecan and distinction from the BM-40 collagen-binding epitope. *Eur. J. Biochem.* **255**, 60–66 (1998).

21. Cossu, G. & Tajbakhsh, S. Oriented Cell Divisions and Muscle Satellite Cell Heterogeneity. *Cell* vol. **129** 859–861 (2007).

22. Asfour, H. A., Allouh, M. Z. & Said, R. S. Myogenic regulatory factors: The orchestrators of myogenesis after 30 years of discovery. *Exp. Biol. Med.* **243**, 118–128 (2018).

23. Biressi, S. *et al.* Myf5 expression during fetal myogenesis defines the developmental progenitors of adult satellite cells. *Dev. Biol.* **379**, 195–207 (2013).

24. De Morrée, A. *et al.* Staufen1 inhibits MyoD translation to actively maintain muscle stem cell quiescence. *Proc. Natl. Acad. Sci. U. S. A.* **114**, E8996–E9005 (2017).

25. Valdez, M. R., Richardson, J. A., Klein, W. H. & Olson, E. N. Failure of Myf5 to support myogenic differentiation without myogenin, MyoD, and MRF4. *Dev. Biol.* **219**, 287–298 (2000).

26. Rudnicki, M. A. *et al.* MyoD or Myf-5 is required for the formation of skeletal muscle. *Cell* **75**, 1351–1359 (1993).

27. Hasty, P. *et al.* Muscle deficiency and neonatal death in mice with a targeted mutation in the myogenin gene. *Nature* **364**, 501–506 (1993).

28. Nabeshima, Y. *et al.* Myogenin gene disruption results in perinatal lethality because of severe muscle defect. *Nature* **364**, 532–535 (1993).

29. Ott, M. O., Bober, E., Lyons, G., Arnold, H. & Buckingham, M. Early expression of the myogenic regulatory gene, myf-5, in precursor cells of skeletal muscle in the mouse embryo. *Development* **111**, 1097–1107 (1991).

30. Braun, T., Rudnicki, M. A., Arnold, H. H. & Jaenisch, R. Targeted inactivation of the muscle regulatory gene Myf-5 results in abnormal rib development and perinatal death. *Cell* **71**, 369–382 (1992).

31. Rudnicki, M. A., Braun, T., Hinuma, S. & Jaenisch, R. Inactivation of MyoD in mice leads to up-regulation of the myogenic HLH gene Myf-5 and results in apparently normal muscle development. *Cell* **71**, 383–390 (1992).

32. Hausburg, M. A. *et al.* Post-transcriptional regulation of satellite cell quiescence by TTP-mediated mRNA decay. *Elife* **4**, (2015).

33. Seale, P. *et al.* Pax7 is required for the specification of myogenic satellite cells. *Cell* **102**, 777–786 (2000).

34. Von Maltzahn, J., Jones, A. E., Parks, R. J. & Rudnicki, M. A. Pax7 is critical for the normal function of satellite cells in adult skeletal muscle. *Proc. Natl. Acad. Sci. U. S. A.* **110**, 16474–16479 (2013).

35. Liu, L., Cheung, T. H., Charville, G. W. & Rando, T. A. Isolation of skeletal muscle stem cells by fluorescence-activated cell sorting. *Nat. Protoc.* **10**, 1612–1624 (2015).

36. Nishijo, K. *et al.* Biomarker system for studying muscle, stem cells, and cancer in vivo . *FASEB J.* **23**, 2681–2690 (2009).

37. Sambasivan, R. *et al.* Distinct Regulatory Cascades Govern Extraocular and Pharyngeal Arch Muscle Progenitor Cell Fates. *Dev. Cell* **16**, 810–821 (2009).

38. Lepper, C., Conway, S. J. & Fan, C. M. Adult satellite cells and embryonic muscle progenitors have distinct genetic requirements. *Nature* **460**, 627–631 (2009).

39. Csapo, R., Gumpenberger, M. & Wessner, B. Skeletal Muscle Extracellular Matrix – What Do We Know About Its Composition, Regulation, and Physiological Roles? A Narrative Review. *Front. Physiol.* **11**, 1–15 (2020).

40. Järveläinen, H., Sainio, A., Koulu, M., Wight, T. N. & Penttinen, R. Extracellular matrix molecules: Potential targets in pharmacotherapy. *Pharmacological Reviews* vol. **61** 198–223 (2009).

41. Naba, A. *et al.* The extracellular matrix: Tools and insights for the 'omics' era. *Matrix Biology* vol. **49** 10–24 (2016).

42. McKee, T. J., Perlman, G., Morris, M. & Komarova, S. V. Extracellular matrix composition of connective tissues: a systematic review and meta-analysis. *Sci. Rep.* **9**, 1–15 (2019).

43. Wynn, T. A. Common and unique mechanisms regulate fibrosis in various fibroproliferative diseases. *Journal of Clinical Investigation* vol. **117** 524–529 (2007).

44. Yazdani, S., Bansal, R. & Prakash, J. Drug targeting to myofibroblasts: Implications for fibrosis and cancer. *Advanced Drug Delivery Reviews* vol. **121** 101–116 (2017).

45. Brack, A. S. & Muñoz-Cánoves, P. The ins and outs of muscle stem cell aging. (2016)

46. Joe, A. W. B. *et al.* Muscle injury activates resident fibro/adipogenic progenitors that facilitate myogenesis. *Nat. Cell Biol.* **12**, 153–163 (2010).

47. Uezumi, A., Fukada, S. I., Yamamoto, N., Takeda, S. & Tsuchida, K. Mesenchymal progenitors distinct from satellite cells contribute to ectopic fat cell formation in skeletal muscle. *Nat. Cell Biol.* **12**, 143–152 (2010).

48. Wosczyna, M. N., Biswas, A. A., Cogswell, C. A. & Goldhamer, D. J. Multipotent progenitors resident in the skeletal muscle interstitium exhibit robust BMP-dependent osteogenic activity and mediate heterotopic ossification. *J. Bone Miner. Res.* **27**, 1004–1017 (2012).

49. Uezumi, A., Fukada, S. I., Yamamoto, N., Takeda, S. & Tsuchida, K. Mesenchymal progenitors distinct from satellite cells contribute to ectopic fat cell formation in skeletal muscle. *Nat. Cell Biol.* **12**, 143–152 (2010).

50. Dominici, M. *et al.* Minimal criteria for defining multipotent mesenchymal stromal cells. The International Society for Cellular Therapy position statement. *Cytotherapy* **8**, 315–317 (2006).

51. Sherwood, R. I. *et al.* Isolation of adult mouse myogenic progenitors: Functional heterogeneity of cells within and engrafting skeletal muscle. *Cell* **119**, 543–554 (2004).

52. Mueller, A. A., Van Velthoven, C. T., Fukumoto, K. D., Cheung, T. H. & Rando, T. A. Intronic polyadenylation of PDGFRα in resident stem cells attenuates muscle fibrosis. *Nature* **540**, 276–279 (2016).

53. Trensz, F., Haroun, S., Cloutier, A., Richter, M. V. & Grenier, G. A muscle resident cell population promotes fibrosis in hindlimb skeletal muscles of mdx mice through the Wnt canonical pathway. *Am. J. Physiol. - Cell Physiol.* **299**, (2010).

54. Lemos, D. R. *et al.* Nilotinib reduces muscle fibrosis in chronic muscle injury by promoting

TNF-mediated apoptosis of fibro/adipogenic progenitors. *Nat. Med.* **21**, 786–794 (2015).

55. Murray, P. J. & Wynn, T. A. Protective and pathogenic functions of macrophage subsets. *Nature Reviews Immunology* vol. **11** 723–737 (2011).

56. Theret, M., Mounier, R. & Rossi, F. The origins and non-canonical functions of macrophages in development and regeneration. *Development* **146**, (2019).

57. Juban, G. & Chazaud, B. Metabolic regulation of macrophages during tissue repair: insights from skeletal muscle regeneration. *FEBS Letters* vol. **591** 3007–3021 (2017).

58. Novak, M. L. & Koh, T. J. Macrophage phenotypes during tissue repair. *J. Leukoc. Biol.* **93**, 875–881 (2013).

59. Rigamonti, E., Zordan, P., Sciorati, C., Rovere-Querini, P. & Brunelli, S. Macrophage plasticity in skeletal muscle repair. *Biomed Res. Int.* (2014).

60. Vidal, B. *et al.* Fibrinogen drives dystrophic muscle fibrosis via a TGFβ/alternative macrophage activation pathway. *Genes Dev.* **22**, 1747–1752 (2008).

61. Wang, Y., Wehling-Henricks, M., Samengo, G. & Tidball, J. G. Increases of M2a macrophages and fibrosis in aging muscle are influenced by bone marrow aging and negatively regulated by muscle-derived nitric oxide. *Aging Cell* **14**, 678–688 (2015).

62. Wehling-Henricks, M. *et al.* Arginine Metabolism by Macrophages Promotes Cardiac and Muscle Fibrosis in mdx Muscular Dystrophy. *PLoS One* **5**, e10763 (2010).

63. Tidball, J. G. & Villalta, S. A. Regulatory interactions between muscle and the immune system during muscle regeneration. *American Journal of Physiology - Regulatory Integrative and Comparative Physiology* vol. **298** 1173–1187 (2010).

64. Butterfield, T. A., Best, T. M. & Merrick, M. A. The dual roles of neutrophils and macrophages in inflammation: A critical balance between tissue damage and repair. *Journal of Athletic Training* vol. **41** 457–465 (2006).

65. Fontenot, J. D., Gavin, M. A. & Rudensky, A. Y. Foxp3 programs the development and function of CD4+CD25+ regulatory T cells. *J. Immunol.* **198**, 986–992 (2017).

66. Hori, S., Nomura, T. & Sakaguchi, S. Control of regulatory T cell development by the transcription factor Foxp3. *J. Immunol.* **198**, 981–985 (2017).

67. Kuswanto, W. *et al.* Poor Repair of Skeletal Muscle in Aging Mice Reflects a Defect in Local, Interleukin-33-Dependent Accumulation of Regulatory T Cells. *Immunity* **44**, 355–367 (2016).

68. Burzyn, D. *et al.* A Special Population of regulatory T Cells Potentiates muscle repair. *Cell*

155, 1282–1295 (2013).

69. Panduro, M., Benoist, C. & Mathis, D. Tissue Tregs. *Annual Review of Immunology* vol. **34** 609–633 (2016).

70. Castiglioni, A. *et al.* FOXP3+ T cells recruited to sites of sterile skeletal muscle injury regulate the fate of satellite cells and guide effective tissue regeneration. *PLoS One* **10**, (2015).

71. Cai, B., Spencer, M. J., Nakamura, G., Tseng-Ong, L. & Tidball, J. G. Eosinophilia of dystrophin-deficient muscle is promoted by perforin-mediated cytotoxicity by T cell effectors. *Am. J. Pathol.* **156**, 1789–1796 (2000).

72. Wehling-Henricks, M., Lee, J. J. & Tidball, J. G. Prednisolone decreases cellular adhesion molecules required for inflammatory cell infiltration in dystrophin-deficient skeletal muscle. *Neuromuscul. Disord.* **14**, 483–490 (2004).

73. Wehling-henricks, M. *et al.* Major basic protein-1 promotes fibrosis of dystrophic muscle and attenuates the cellular immune response in muscular dystrophy. *Hum. Mol. Genet.* **17**, 2280–2292 (2008).

74. Schröder, T., Fuchss, J., Schneider, I., Stoltenburg-Didinger, G. & Hanisch, F. Eosinophils in hereditary and inflammatory myopathies. *Acta Myol.* **32**, 148–153 (2013).

75. Sek, A. C. *et al.* Eosinophils Do Not Drive Acute Muscle Pathology in the mdx Mouse Model of Duchenne Muscular Dystrophy. *J. Immunol.* **203**, 476–484 (2019).

76. Heredia, J. E. *et al.* Type 2 innate signals stimulate fibro/adipogenic progenitors to facilitate muscle regeneration. *Cell* **153**, 376–388 (2013).

77. Chapman, M. A., Meza, R. & Lieber, R. L. Skeletal muscle fibroblasts in health and disease. *Differentiation* vol. **92** 108–115 (2016).

78. Richler, C. & Yaffe, D. The in vitro cultivation and differentiation capacities of myogenic cell lines. *Dev. Biol.* **23**, 1–22 (1970).

79. Mathew, S. J. *et al.* Connective tissue fibroblasts and Tcf4 regulate myogenesis. *Development* **138**, 371–384 (2011).

80. Contreras, O., Rossi, F. M. V. & Theret, M. Origins, potency, and heterogeneity of skeletal muscle fibro-adipogenic progenitors—time for new definitions. *Skelet. Muscle 2021 111* **11**, 1–25 (2021).

81. Asahara, T. *et al.* Isolation of putative progenitor endothelial cells for angiogenesis. *Science (80-.).* **275**, 964–967 (1997).

82. Majka, S. M. *et al.* Distinct progenitor populations in skeletal muscle are bone marrow derived and exhibit different cell fates during vascular regeneration. *J. Clin. Invest.* **111**, 71–79 (2003).

83. Emslie-Smith, A. M. & Engel, A. G. Microvascular changes in early and advanced dermatomyositis: A quantitative study. *Ann. Neurol.* **27**, 343–356 (1990).

84. Tatsumi, R., Anderson, J. E., Nevoret, C. J., Halevy, O. & Allen, R. E. HGF/SF is present in normal adult skeletal muscle and is capable of activating satellite cells. *Dev. Biol.* **194**, 114–128 (1998).

85. Bryan, B. A. *et al.* Coordinated Vascular Endothelial Growth Factor Expression and Signaling During Skeletal Myogenic Differentiation. *Mol. Biol. Cell* **19**, 994–1006 (2008).

86. Latroche, C. *et al.* Coupling between Myogenesis and Angiogenesis during Skeletal Muscle Regeneration Is Stimulated by Restorative Macrophages. *Stem Cell Reports* **9**, 2018–2033 (2017).

87. Murray, I. R. *et al.* Skeletal and cardiac muscle pericytes: Functions and therapeutic potential. *Pharmacology and Therapeutics* vol. **171** 65–74 (2017).

88. Tedesco, F. S., Dellavalle, A., Diaz-Manera, J., Messina, G. & Cossu, G. Repairing skeletal muscle: Regenerative potential of skeletal muscle stem cells. *Journal of Clinical Investigation* vol. **120** 11–19 (2010).

89. Mitchell, K. J. *et al.* Identification and characterization of a non-satellite cell muscle resident progenitor during postnatal development. *Nat. Cell Biol.* **12**, 257–266 (2010).

90. Zheng, B. *et al.* Prospective identification of myogenic endothelial cells in human skeletal muscle. *Nat. Biotechnol.* **25**, 1025–1034 (2007).

91. Qu-Petersen, Z. *et al.* Identification of a novel population of muscle stem cells in mice: Potential for muscle regeneration. *J. Cell Biol.* **157**, 851–864 (2002).

92. Torrente, Y. *et al.* Human circulating AC133+ stem cells restore dystrophin expression and ameliorate function in dystrophic skeletal muscle. *J. Clin. Invest.* **114**, 182–195 (2004).

93. Liu, N. *et al.* A Twist2-dependent progenitor cell contributes to adult skeletal muscle. *Nat. Cell Biol.* **19**, 202–213 (2017).

94. Lepper, C., Partridge, T. A. & Fan, C. M. An absolute requirement for pax7-positive satellite cells in acute injury-induced skeletal muscle regeneration. *Development* **138**, 3639–3646 (2011).

95. Murphy, M. M., Lawson, J. A., Mathew, S. J., Hutcheson, D. A. & Kardon, G. Satellite cells,

connective tissue fibroblasts and their interactions are crucial for muscle regeneration. *Development* **138**, 3625–3637 (2011).

96. Sambasivan, R. *et al.* Pax7-expressing satellite cells are indispensable for adult skeletal muscle regeneration. *Development* **138**, 3647–3656 (2011).

97. Biressi, S., Filareto, A. & Rando, T. A. Stem cell therapy for muscular dystrophies. *J. Clin. Invest.* **130**, 5652–5664 (2020).

98. Hardy, D. *et al.* Comparative study of injury models for studying muscle regeneration in mice. *PLoS One* **11**, (2016).

99. Bischoff, R. Interaction between satellite cells and skeletal muscle fibers. *Development* **109**, 943–952 (1990).

100. Caldwell, C. J., Mattey, D. & Weller, R. O. Role of the basement membrane in the regeneration of skeletal muscle. *Neuropathol. Appl. Neurobiol.* **16**, 225–238 (1990).

101. Webster, M. T., Manor, U., Lippincott-Schwartz, J. & Fan, C. M. Intravital Imaging Reveals Ghost Fibers as Architectural Units Guiding Myogenic Progenitors during Regeneration. *Cell Stem Cell* **18**, 243–252 (2016).

102. Engel, A. G. & Biesecker, G. Complement activation in muscle fiber necrosis: Demonstration of the membrane attack complex of complement in necrotic fibers. *Ann. Neurol.* **12**, 289–296 (1982).

103. H N Fernandez, P M Henson, A Otani, T. E. H. Chemotactic response to human C3a and C5a anaphylatoxins. I. Evaluation of C3a and C5a leukotaxis in vitro and under stimulated in vivo conditions. *J Immunol* **120**, 109–15. (1978).

104. Gigli, I. & Nelson, R. A. Complement dependent immune phagocytosis. I. Requirements for C′1, C′4, C′2, C′3. *Exp. Cell Res.* **51**, 45–67 (1968).

105. Morey-Holton, E., Wronski, T. J. & Wronski, T. J. Animal models for simulating weightlessness. (1982).

106. Frenette, J., Cai, B. & Tidball, J. G. Complement activation promotes muscle inflammation during modified muscle use. *Am. J. Pathol.* **156**, 2103–2110 (2000).

107. Mann, C. J. *et al.* Aberrant repair and fibrosis development in skeletal muscle. *Skeletal Muscle* vol. **1** 1–20 (2011).

108. Hindi, S. M. & Kumar, A. Toll-like receptor signalling in regenerative myogenesis: Friend and foe. *Journal of Pathology* vol. **239** 125–128 (2016).

109. Brigitte, M. *et al.* Muscle resident macrophages control the immune cell reaction in a mouse model of notexin-induced myoinjury. *Arthritis Rheum.* **62**, 268–279 (2010).

110. Varga, T. *et al.* Highly Dynamic Transcriptional Signature of Distinct Macrophage Subsets during Sterile Inflammation, Resolution, and Tissue Repair. *J. Immunol.* **196**, 4771–4782 (2016).

111. Saclier, M. *et al.* Differentially activated macrophages orchestrate myogenic precursor cell fate during human skeletal muscle regeneration. *Stem Cells* **31**, 384–396 (2013).

112. Tidball, J. G. & Wehling-Henricks, M. Damage and inflammation in muscular dystrophy: Potential implications and relationships with autoimmune myositis. *Current Opinion in Rheumatology* vol. **17** 707–713 (2005).

113. Lluís, F. *et al.* Urokinase-dependent plasminogen activation is required for efficient skeletal muscle regeneration in vivo. *Blood* **97**, 1703–1711 (2001).

114. Suelves, M. *et al.* Plasmin activity is required for myogenesis in vitro and skeletal muscle regeneration in vivo. *Blood* **99**, 2835–2844 (2002).

115. Lukjanenko, L. *et al.* Loss of fibronectin from the aged stem cell niche affects the regenerative capacity of skeletal muscle in mice. *Nat. Med.* **22**, 897–905 (2016).

116. Urciuolo, A. *et al.* Collagen VI regulates satellite cell self-renewal and muscle regeneration. *Nat. Commun.* **4**, (2013).

117. Fiore, D. *et al.* Pharmacological blockage of fibro/adipogenic progenitor expansion and suppression of regenerative fibrogenesis is associated with impaired skeletal muscle regeneration. *Stem Cell Res.* **17**, 161–169 (2016).

118. Yin, H., Price, F. & Rudnicki, M. A. Satellite cells and the muscle stem cell niche. *Physiol. Rev.* **93**, 23–67 (2013).

119. Chazaud, B. *et al.* Satellite cells attract monocytes and use macrophages as a support to escape apoptosis and enhance muscle growth. *J. Cell Biol.* **163**, 1133–1143 (2003).

120. Londhe, P. & Davie, J. K. Interferon-γ resets muscle cell fate by stimulating the sequential recruitment of JARID2 and PRC2 to promoters to repress myogenesis. *Sci. Signal.* **6**, (2013).

121. Acharyya, S. *et al.* TNF Inhibits Notch-1 in Skeletal Muscle Cells by Ezh2 and DNA Methylation Mediated Repression: Implications in Duchenne Muscular Dystrophy. *PLoS One* **5**, e12479 (2010).

122. Palacios, D. *et al.* TNF/p38α/polycomb signaling to Pax7 locus in satellite cells links

inflammation to the epigenetic control of muscle regeneration. *Cell Stem Cell* **7**, 455–469 (2010).

123. Tonkin, J. *et al.* Monocyte/macrophage-derived IGF-1 orchestrates murine skeletal muscle regeneration and modulates autocrine polarization. *Mol. Ther.* **23**, 1189–1200 (2015).

124. Deng, B., Wehling-Henricks, M., Villalta, S. A., Wang, Y. & Tidball, J. G. IL-10 Triggers Changes in Macrophage Phenotype That Promote Muscle Growth and Regeneration. *J. Immunol.* **189**, 3669–3680 (2012).

125. Luque, E., Peña, J., Martin, P., Jimena, I. & Vaamonde, R. Capillary Supply During Development of Individual Regenerating Muscle Fibers. *Anat. Histol. Embryol. J. Vet. Med. Ser. C* **24**, 87–89 (1995).

126. Rhoads, R. P. *et al.* Satellite cell-mediated angiogenesis in vitro coincides with a functional hypoxia-inducible factor pathway. *Am. J. Physiol. Physiol.* **296**, C1321–C1328 (2009).

127. Birbrair, A. *et al.* Pericytes: Multitasking cells in the regeneration of injured, diseased, and aged skeletal muscle. *Frontiers in Aging Neuroscience* vol. **6** (2014).

128. Abou-Khalil, R., Mounier, R. & Chazaud, B. Regulation of myogenic stem cell behavior by vessel cells: The 'ménage à trois' of satellite cells, periendothelial cells and endothelial cells. *Cell Cycle* vol. **9** 892–896 (2010).

129. Dellavalle, A. *et al.* Pericytes resident in postnatal skeletal muscle differentiate into muscle fibres and generate satellite cells. *Nat. Commun.* **2**, (2011).

130. Lightfoot, A. P., McCormick, R., Nye, G. A. & McArdle, A. Mechanisms of skeletal muscle ageing; Avenues for therapeutic intervention. *Current Opinion in Pharmacology* vol. **16** 116–121 (2014).

131. Goodell, M. A. & Rando, T. A. Stem cells and healthy aging. *Science* vol. **350** 1199–1204 (2015).

132. Brack, A. S., Bildsoe, H. & Hughes, S. M. Evidence that satellite cell decrement contributes to preferential decline in nuclear number from large fibres during murine age-related muscle atrophy. *J. Cell Sci.* **118**, 4813–4821 (2005).

133. Day, K., Shefer, G., Shearer, A. & Yablonka-Reuveni, Z. The depletion of skeletal muscle satellite cells with age is concomitant with reduced capacity of single progenitors to produce reserve progeny. *Dev. Biol.* **340**, 330–343 (2010).

134. Shefer, G., Van de Mark, D. P., Richardson, J. B. & Yablonka-Reuveni, Z. Satellite-cell pool size does matter: Defining the myogenic potency of aging skeletal muscle. *Dev. Biol.* **294**, 50–

66 (2006).

135. Sousa-Victor, P. & Muñoz-Cánoves, P. Regenerative decline of stem cells in sarcopenia. *Molecular Aspects of Medicine* vol. **50** 109–117 (2016).

136. Ponsot, E., Lexell, J. & Kadi, F. Skeletal muscle telomere length is not impaired in healthy physically active old women and men. *Muscle Nerve* **37**, 467–472 (2008).

137. Li, J., Han, S., Cousin, W. & Conboy, I. M. Age-Specific Functional Epigenetic Changes in p21 and p16 in Injury-Activated Satellite Cells. *Stem Cells* **33**, 951–961 (2015).

138. Carlson, B. M. & Faulkner, J. A. Muscle transplantation between young and old rats: Age of host determines recovery. *Am. J. Physiol. - Cell Physiol.* **256**, (1989).

139. Conboy, I. M. *et al.* Rejuvenation of aged progenitor cells by exposure to a young systemic environment. *Nature* **433**, 760–764 (2005).

140. Bernet, J. D. *et al.* P38 MAPK signaling underlies a cell-autonomous loss of stem cell self-renewal in skeletal muscle of aged mice. *Nat. Med.* **20**, 265–271 (2014).

141. Conboy, I. H., Conboy, M. J., Smythe, G. M. & Rando, T. A. Notch-Mediated Restoration of Regenerative Potential to Aged Muscle. *Science (80-.).* **302**, 1575–1577 (2003).

142. Chakkalakal, J. V., Jones, K. M., Basson, M. A. & Brack, A. S. The aged niche disrupts muscle stem cell quiescence. *Nature* **490**, 355–360 (2012).

143. Fuerer, C., Habib, S. J. & Nusse, R. A study on the interactions between heparan sulfate proteoglycans and Wnt proteins. *Dev. Dyn.* **239**, 184–190 (2010).

144. Etienne, J., Liu, C., Skinner, C. M., Conboy, M. J. & Conboy, I. M. Skeletal muscle as an experimental model of choice to study tissue aging and rejuvenation. *Skeletal Muscle* vol. **10** 1–16 (2020).

145. Lukjanenko, L. *et al.* Aging Disrupts Muscle Stem Cell Function by Impairing Matricellular WISP1 Secretion from Fibro-Adipogenic Progenitors. *Cell Stem Cell* **24**, 433-446.e7 (2019).

146. Hearon, C. M. & Dinenno, F. A. Regulation of skeletal muscle blood flow during exercise in ageing humans. *Journal of Physiology* vol. **594** 2261–2273 (2016).

147. Le Moal, E. *et al.* Redox Control of Skeletal Muscle Regeneration. *Antioxidants Redox Signal.* **27**, 276–310 (2017).

148. Furman, D. *et al.* Chronic inflammation in the etiology of disease across the life span. *Nat. Med. 2019 2512* **25**, 1822–1832 (2019).

149. Price, F. D. *et al.* Inhibition of JAK-STAT signaling stimulates adult satellite cell function. *Nat. Med.* **20**, 1174–1181 (2014).

150. Tierney, M. T. *et al.* STAT3 signaling controls satellite cell expansion and skeletal muscle repair. *Nat. Med.* **20**, 1182–1186 (2014).

151. Paliwal, P., Pishesha, N., Wijaya, D. & Conboy, I. M. Age dependent increase in the levels of osteopontin inhibits skeletal muscle regeneration. *Aging (Albany. NY).* **4**, 553–566 (2012).

152. Cui, C. *et al.* Skewed macrophage polarization in aging skeletal muscle. *Aging Cell* **18**, e13032 (2019).

153. Blau, H. M., Cosgrove, B. D. & Ho, A. T. V. The central role of muscle stem cells in regenerative failure with aging. *Nature Medicine* vol. **21** 854–862 (2015).

154. Carlson, M. E., Hsu, M. & Conboy, I. M. Imbalance between pSmad3 and Notch induces CDK inhibitors in old muscle stem cells. *Nature* **454**, 528–532 (2008).

155. Egerman, M. A. *et al.* GDF11 Increases with Age and Inhibits Skeletal Muscle Regeneration. *Cell Metab.* **22**, 164–174 (2015).

156. Carlson, M. E. *et al.* Relative roles of TGF-Î²1 and Wnt in the systemic regulation and aging of satellite cell responses. *Aging Cell* **8**, 676–689 (2009).

157. Elabd, C. *et al.* Oxytocin is an age-specific circulating hormone that is necessary for muscle maintenance and regeneration. *Nat. Commun.* **5**, (2014).

158. Vinel, C. *et al.* The exerkine apelin reverses age-associated sarcopenia. *Nat. Med.* **24**, 1360–1371 (2018).

159. Brack, A. S. *et al.* Increased Wnt signaling during aging alters muscle stem cell fate and increases fibrosis. *Science* **317**, 807–810 (2007).

160. Naito, A. T. *et al.* Complement C1q activates canonical Wnt signaling and promotes aging-related phenotypes. *Cell* **149**, 1298–1313 (2012).

161. Ervasti, J. M. Dystrophin, its interactions with other proteins, and implications for muscular dystrophy. *Biochimica et Biophysica Acta - Molecular Basis of Disease* vol. **1772** 108–117 (2007).

162. Brancaccio, A. A molecular overview of the primary dystroglycanopathies. *J. Cell. Mol. Med.* **23**, 3058–3062 (2019).

163. Brun, C. E., Chevalier, F. P., Dumont, N. A. & Rudnicki, M. A. *The Satellite Cell Niche in Skeletal Muscle*. *Biology and Engineering of Stem Cell Niches* (Elsevier Inc., 2017).

164. Morley, J. E., Thomas, D. R. & Wilson, M. M. G. Cachexia: Pathophysiology and clinical relevance. *American Journal of Clinical Nutrition* vol. **83** 735–743 (2006).

165. Sahenk, Z. & Mendell, J. R. The muscular dystrophies: Distinct pathogenic mechanisms invite novel therapeutic approaches. *Curr. Rheumatol. Rep.* **13**, 199–207 (2011).

166. McArdle, A., Foxley, A., Edwards, R. H. T. & Jackson, M. J. Prostaglandin metabolism in dystrophin-deficient MDX mouse muscle. in *Biochemical Society Transactions* vol. **19** 177S-177S (Portland Press, 1991).

167. Nakagawa, T. *et al.* A prostaglandin D2 metabolite is elevated in the urine of Duchenne muscular dystrophy patients and increases further from 8 years old. *Clin. Chim. Acta* **423**, 10–14 (2013).

168. Villalta, S. A., Rosenberg, A. S. & Bluestone, J. A. The immune system in Duchenne muscular dystrophy: Friend or foe. *Rare Dis.* **3**, e1010966 (2015).

169. Hodgetts, S., Radley, H., Davies, M. & Grounds, M. D. Reduced necrosis of dystrophic muscle by depletion of host neutrophils, or blocking TNFα function with Etanercept in mdx mice. *Neuromuscul. Disord.* **16**, 591–602 (2006).

170. Hussein, M. R. *et al.* The effects of glucocorticoid therapy on the inflammatory and Dendritic cells in muscular dystrophies. *Int. J. Exp. Pathol.* **87**, 451–461 (2006).

171. Serrano, A. L. & Muñoz-Cánoves, P. Fibrosis development in early-onset muscular dystrophies: Mechanisms and translational implications. *Seminars in Cell and Developmental Biology* vol. **64** 181–190 (2017).

172. Alvarez, K., Fadic, R. & Brandan, E. Augmented synthesis and differential localization of heparan sulfate proteoglycans in Duchenne muscular dystrophy. *J. Cell. Biochem.* **85**, 703–713 (2002).

173. Cáceres, S. *et al.* Synthesis of proteoglycans is augmented in dystrophic mdx mouse skeletal muscle. *Eur. J. Cell Biol.* **79**, 173–181 (2000).

174. Vidal, B. *et al.* Amelioration of Duchenne muscular dystrophy in mdx mice by elimination of matrix-associated fibrin-driven inflammation coupled to the α mβ 2 leukocyte integrin receptor. *Hum. Mol. Genet.* **21**, 1989–2004 (2012).

175. Serrano, A. L. & Muñoz-Cánoves, P. Fibrosis development in early-onset muscular dystrophies: Mechanisms and translational implications. *Semin. Cell Dev. Biol.* **64**, 181–190 (2017).

176. Myllylä, R., Myllylä, V. V., Tolonen, U. & Kivirikko, K. I. Changes in Collagen Metabolism in

Diseased Muscle: I. Biochemical Studies. *Arch. Neurol.* **39**, 752–755 (1982).

177. Peltonen, L., Myllylä, R., Tolonen, U. & Myllylä, V. V. Changes in Collagen Metabolism in Diseased Muscle: II. Immunohistochemical Studies. *Arch. Neurol.* **39**, 756–759 (1982).

178. Goldspink, G., Fernandes, K., Williams, P. E. & Wells, D. J. Age-related changes in collagen gene expression in the muscles of mdx dystrophic and normal mice. *Neuromuscul. Disord.* **4**, 183–191 (1994).

179. Contreras, O., Rebolledo, D. L., Oyarzún, J. E., Olguín, H. C. & Brandan, E. Connective tissue cells expressing fibro/adipogenic progenitor markers increase under chronic damage: relevance in fibroblast-myofibroblast differentiation and skeletal muscle fibrosis. *Cell Tissue Res.* **364**, 647–660 (2016).

180. Pessina, P. *et al.* Fibrogenic Cell Plasticity Blunts Tissue Regeneration and Aggravates Muscular Dystrophy. *Stem Cell Reports* **4**, 1046–1060 (2015).

181. Biressi, S., Miyabara, E. H., Gopinath, S. D., Carlig, P. M. M. & Rando, T. A. A Wnt-TGF2 axis induces a fibrogenic program in muscle stem cells from dystrophic mice. *Sci. Transl. Med.* **6**, 1–13 (2014).

182. Blau, H. M., Webster, C. & Pavlath, G. K. Defective myoblasts identified in Duchenne muscular dystrophy. *Proc. Natl. Acad. Sci. U. S. A.* **80**, 4856–4860 (1983).

183. Alexakis, C., Partridge, T. & Bou-Gharios, G. Implication of the satellite cell in dystrophic muscle fibrosis: A self-perpetuating mechanism of collagen overproduction. *Am. J. Physiol. - Cell Physiol.* **293**, (2007).

184. Ionasescu, V. & Ionasescu, R. Increased collagen synthesis by Duchenne myogenic clones. *J. Neurol. Sci.* **54**, 79–87 (1982).

185. Thomas, K., Engler, A. J. & Meyer, G. A. Extracellular matrix regulation in the muscle satellite cell niche. *Connective Tissue Research* vol. **56** 1–8 (2015).

186. Dulauroy, S., Di Carlo, S. E., Langa, F., Eberl, G. & Peduto, L. Lineage tracing and genetic ablation of ADAM12 + perivascular cells identify a major source of profibrotic cells during acute tissue injury. *Nat. Med.* **18**, 1262–1270 (2012).

187. Kharraz, Y., Guerra, J., Pessina, P., Serrano, A. L. & Muñoz-Cánoves, P. Understanding the process of fibrosis in duchenne muscular dystrophy. *BioMed Research International* (2014).

188. Hoffman, E. P., Brown, R. H. & Kunkel, L. M. Dystrophin: The protein product of the duchenne muscular dystrophy locus. *Cell* **51**, 919–928 (1987).

189. Wilson, K. *et al.* Duchenne and Becker Muscular Dystrophies: A Review of Animal Models, Clinical End Points, and Biomarker Quantification. *Toxicologic Pathology* vol. **45** 961–976 (2017).

190. Ervasti, J. M. & Campbell, K. P. A role for the dystrophin-glycoprotein complex as a transmembrane linker between laminin and actin. *J. Cell Biol.* **122**, 809–823 (1993).

191. Rosenberg, A. S. *et al.* Immune-mediated pathology in Duchenne muscular dystrophy. *Science Translational Medicine* vol. **7** 299rv4-299rv4 (2015).

192. Schmalbruch, H. Segmental fibre breakdown and defects of the plasmalemma in diseased human muscles. *Acta Neuropathol.* **33**, 129–141 (1975).

193. Carpenter, S. & Karpati, G. Duchenne Muscular Dystrophy. *Brain* **102**, 147–161 (1979).

194. Chargé, S. B. P. & Rudnicki, M. A. Cellular and Molecular Regulation of Muscle Regeneration. *Physiological Reviews* vol. **84** 209–238 (2004).

195. Mercuri, E., Bönnemann, C. G. & Muntoni, F. Muscular dystrophies. *The Lancet* vol. **394** 2025–2038 (2019).

196. van Deutekom, J. C. *et al.* Local Dystrophin Restoration with Antisense Oligonucleotide PRO051. *N. Engl. J. Med.* **357**, 2677–2686 (2007).

197. McGreevy, J. W., Hakim, C. H., McIntosh, M. A. & Duan, D. Animal models of Duchenne muscular dystrophy: From basic mechanisms to gene therapy. *DMM Disease Models and Mechanisms* vol. **8** 195–213 (2015).

198. Allen, D. G., Whitehead, N. P. & Froehner, S. C. Absence of dystrophin disrupts skeletal muscle signaling: Roles of Ca2+, reactive oxygen species, and nitric oxide in the development of muscular dystrophy. *Physiol. Rev.* **96**, 253–305 (2015).

199. Rando, T. A. The dystrophin-glycoprotein complex, cellular signaling, and the regulation of cell survival in the muscular dystrophies. *Muscle and Nerve* **24**, 1575–1594 (2001).

200. Massagué, J. TGFβ signalling in context. *Nature Reviews Molecular Cell Biology* vol. **13** 616–630 (2012).

201. Girardi, F. & Le Grand, F. Wnt Signaling in Skeletal Muscle Development and Regeneration. in *Progress in Molecular Biology and Translational Science* vol. **153** 157–179 (Elsevier B.V., 2018).

202. Zhou, L. *et al.* Temporal and spatial mRNA expression patterns of TGF-β1, 2, 3 and TβRI, II, III in skeletal muscles of mdx mice. *Neuromuscul. Disord.* **16**, 32–38 (2006).

203. Meng, X. M., Nikolic-Paterson, D. J. & Lan, H. Y. TGF-β: The master regulator of fibrosis. *Nat. Rev. Nephrol.* **12**, 325–338 (2016).

204. Rahman, F. A. & Krause, M. P. PAI-1, the plasminogen system, and skeletal muscle. *International Journal of Molecular Sciences* **21**, 1–22 (2020).

205. Li, Y. *et al.* Transforming Growth Factor-β1 Induces the Differentiation of Myogenic Cells into Fibrotic Cells in Injured Skeletal Muscle: A Key Event in Muscle Fibrogenesis. *Am. J. Pathol.* **164**, 1007–1019 (2004).

206. Olson E. N., Sternberg E., Hu J. S., Spizz G., Wilcox C., Regulation of myogenic differentiation by type beta transforming growth factor. *J. Cell Biol.* **103**, 1799–1805 (1986).

207. Massagué J., Cheifetz S., Endo T. & Nadal-Ginard B. Type beta transforming growth factor is an inhibitor of myogenic differentiation. *Proc. Natl. Acad. Sci. U. S. A.* **83**, 8206–8210 (1986).

208. Girardi, F. *et al.* TGFβ signaling curbs cell fusion and muscle regeneration. *Nat. Commun.* **12**, (2021).

209. Andreetta F. *et al.* Immunomodulation of TGF-beta 1 in mdx mouse inhibits connective tissue proliferation in diaphragm but increases inflammatory response: implications for antifibrotic therapy. *J. Neuroimmunol.* **175**, 77–86 (2006).

210. Chon R.D., *et al.* Angiotensin II type 1 receptor blockade attenuates TGF-beta-induced failure of muscle regeneration in multiple myopathic states. *Nat. Med.* **13**, 204–210 (2007).

211. Nelson, C. A. *et al.* Inhibiting TGF-β Activity Improves Respiratory Function in mdx Mice. *Am. J. Pathol.* **178**, 2611 (2011).

212. Duffield, J. S., Lupher, M., Thannickal, V. J. & Wynn, T. A. Host Responses in Tissue Repair and Fibrosis. *Annu. Rev. Pathol. Mech. Dis.* **8**, 241–276 (2013).

213. Lieber, R. L. & Ward, S. R. Cellular mechanisms of tissue fibrosis. 4. structural and functional consequences of skeletal muscle fibrosis. *Am. J. Physiol. - Cell Physiol.* **305**, (2013).

214. Vial, C. *et al.* Skeletal muscle cells express the profibrotic cytokine connective tissue growth factor (CTGF/CCN2), which induces their dedifferentiation. *J. Cell. Physiol.* **215**, 410–421 (2008).

215. Croce, J. C. & McClay, D. R. Evolution of the Wnt pathways. *Methods in Molecular Biology* vol. **469** 3–18 (2008).

216. Nusse, R. & Varmus, H. Three decades of Wnts: A personal perspective on how a scientific field developed. *EMBO Journal* vol. **31** 2670–2684 (2012).

217. Aberle, H., Bauer, A., Stappert, J., Kispert, A. & Kemler, R. β-catenin is a target for the ubiquitin-proteasome pathway. *EMBO J.* **16**, 3797–3804 (1997).

218. Qu, J., Yue, L., Gao, J. & Yao, H. Perspectives on Wnt signal pathway in the pathogenesis and therapeutics of chronic obstructive pulmonary disease. *Journal of Pharmacology and Experimental Therapeutics* vol. **369** 473–480 (2019).

219. Barker, N. *et al.* Identification of stem cells in small intestine and colon by marker gene Lgr5. *Nature* **449**, 1003–1007 (2007).

220. Hutcheson, D. A., Zhao, J., Merrell, A., Haldar, M. & Kardon, G. Embryonic and fetal limb myogenic cells are derived from developmentally distinct progenitors and have different requirements for β-catenin. *Genes Dev.* **23**, 997–1013 (2009).

221. Piersma, B., Bank, R. A. & Boersema, M. Signaling in fibrosis: TGF-β, WNT, and YAP/TAZ converge. *Frontiers in Medicine* vol. **2** 1 (2015).

222. Reggio, A. *et al.* Adipogenesis of skeletal muscle fibro/adipogenic progenitors is affected by the WNT5a/GSK3/β-catenin axis. *Cell Death Differ.* **27**, 2921–2941 (2020).

223. Doi, R. *et al.* Critical role of Frizzled1 in age-related alterations of Wnt/β-catenin signal in myogenic cells during differentiation. *Genes to Cells* **19**, 287–296 (2014).

224. Tusavitz, S. *et al.* Macrophage-derived Wnt signaling increases endothelial permeability during skeletal muscle injury. *Inflamm. Res.* **69**, 1235–1244 (2020).

225. Giordani, L. *et al.* High-Dimensional Single-Cell Cartography Reveals Novel Skeletal Muscle-Resident Cell Populations. *Mol. Cell* **74**, 609-621.e6 (2019).

226. Contreras, O., Soliman, H., Theret, M., Rossi, F. M. V & Brandan, E. TGF-β-driven downregulation of the Wnt/β-Catenin transcription factor 1 TCF7L2/TCF4 in PDGFRα + fibroblasts 2. *J Cell Sci* **133** (2020)

227. Pessina, P. *et al.* Fibrogenic Cell Plasticity Blunts Tissue Regeneration and Aggravates Muscular Dystrophy. *Stem Cell Reports* **4**, 1046–1060 (2015).

228. Galibert, L. & Merten, O. W. Latest developments in the large-scale production of adeno-associated virus vectors in insect cells toward the treatment of neuromuscular diseases. *Journal of Invertebrate Pathology* vol. **107** (2011).

229. Ramos, J. N. *et al.* Development of Novel Micro-dystrophins with Enhanced Functionality. *Mol. Ther.* **27**, 623–635 (2019).

230. Watchko, J. *et al.* Adeno-associated virus vector-mediated minidystrophin gene therapy

improves dystrophic muscle contractile function in mdx mice. *Hum. Gene Ther.* **13**, 1451–1460 (2002).

231. Le Guiner, C. *et al.* Long-term microdystrophin gene therapy is effective in a canine model of Duchenne muscular dystrophy. *Nat. Commun.* **8**, (2017).

232. Mendell, J. R. *et al.* Dystrophin Immunity in Duchenne's Muscular Dystrophy. *N. Engl. J. Med.* **363**, 1429–1437 (2010).

233. Fortunato, F., Rossi, R., Falzarano, M. S. & Ferlini, A. Innovative Therapeutic Approaches for Duchenne Muscular Dystrophy. *J. Clin. Med.* **10**, 820 (2021).

234. Song, Y. *et al.* Non-immunogenic utrophin gene therapy for the treatment of muscular dystrophy animal models. *Nat. Med.* **25**, 1505–1511 (2019).

235. Chicoine, L. G. *et al.* Vascular delivery of rAAVrh74.MCK.GALGT2 to the gastrocnemius muscle of the rhesus macaque stimulates the expression of dystrophin and laminin α2 surrogates. *Mol. Ther.* **22**, 713–724 (2014).

236. Xu, R., Jia, Y., Zygmunt, D. A. & Martin, P. T. rAAVrh74.MCK.GALGT2 Protects against Loss of Hemodynamic Function in the Aging mdx Mouse Heart. *Mol. Ther.* **27**, 636–649 (2019).

237. Charville, G. W. *et al.* Ex vivo expansion and in vivo self-renewal of human muscle stem cells. *Stem Cell Reports* **5**, 621–632 (2015).

238. Montarras, D. *et al.* Developmental biology: Direct isolation of satellite cells for skeletal muscle regeneration. *Science* **309**, 2064–2067 (2005).

239. England, S. B. *et al.* Very mild muscular dystrophy associated with the deletion of 46% of dystrophin. *Nature* **343**, 180–182 (1990).

240. Nicholson, L. V. B. The 'rescue' of dystrophin synthesis in boys with Duchenne muscular dystrophy. *Neuromuscul. Disord.* **3**, 525–531 (1993).

241. Sherratt, T. G., Vulliamy, T., Dubowitz, V., Sewry, C. A. & Strong, P. N. Exon skipping and translation in patients with frameshift deletions in the dystrophin gene. *Am. J. Hum. Genet.* **53**, 1007–1015 (1993).

242. Scoto, M., Finkel, R., Mercuri, E. & Muntoni, F. Genetic therapies for inherited neuromuscular disorders. *The Lancet Child and Adolescent Health* vol. **2** 600–609 (2018).

243. Lim, K. R., Maruyama, R. & Yokota, T. Eteplirsen in the treatment of Duchenne muscular dystrophy. *Drug Des. Devel. Ther.* vol. **11**, 533–545 (2017).

244. Heo Y.A. Golodirsen: First Approval. *Drugs* **80**, 329–333 (2020).

245. Agboola, F. The Effectiveness and Value of Deflazacort and Exon-Skipping. (2020).

246. Sander, J. D. & Joung, J. K. CRISPR-Cas systems for editing, regulating and targeting genomes. *Nature Biotechnology* vol. **32** 347–350 (2014).

247. Long, C. *et al.* Postnatal genome editing partially restores dystrophin expression in a mouse model of muscular dystrophy. *Science* **351**, 400–403 (2016).

248. Nelson, C. E. *et al.* In vivo genome editing improves muscle function in a mouse model of Duchenne muscular dystrophy. *Science* **351**, 403–407 (2016).

249. El Refaey, M. *et al.* In vivo genome editing restores dystrophin expression and cardiac function in dystrophic mice. *Circ. Res.* **121**, 923–929 (2017).

250. Amoasii, L. *et al.* Gene editing restores dystrophin expression in a canine model of Duchenne muscular dystrophy. *Science* **362**, 86–91 (2018).

251. Hakim, C. H. *et al.* AAV CRISPR editing rescues cardiac and muscle function for 18 months in dystrophic mice. *JCI insight* **3**, (2018).

252. Nelson, C. E. *et al.* Long-term evaluation of AAV-CRISPR genome editing for Duchenne muscular dystrophy. *Nat. Med.* **25**, 427–432 (2019).

253. Ryan N. J. Ataluren: first global approval. *Drugs* **74**, 1709–1714 (2014).

254. Finkel R. S. Read-through strategies for suppression of nonsense mutations in Duchenne/ Becker muscular dystrophy: aminoglycosides and ataluren (PTC124). *J. Child Neurol.* **25**, 1158–1164 (2010).

255. Sheikh O. & Yokota T. Developing DMD therapeutics: a review of the effectiveness of small molecules, stop-codon readthrough, dystrophin gene replacement, and exon-skipping therapies. *Expert Opin. Investig. Drugs* **30**, 167–176 (2021).

256. Guiraud, S. & Davies, K. E. Pharmacological advances for treatment in Duchenne muscular dystrophy. *Current Opinion in Pharmacology* vol. **34** 36–48 (2017).

257. Traynor, K. Deflazacort approved for Duchenne muscular dystrophy. *Am. J. Heal. Pharm.* **74**, 368–368 (2017).

258. Valentine, B. A., Cooper, B. J., de Lahunta, A., O'Quinn, R. & Blue, J. T. Canine X-linked muscular dystrophy. An animal model of Duchenne muscular dystrophy: Clinical studies. *J. Neurol. Sci.* **88**, 69–81 (1988).

259. van Putten, M. *et al.* Mouse models for muscular dystrophies: an overview. *Dis. Model. Mech.* **13**, (2020).

260. Araki, E. *et al.* Targeted disruption of exon 52 in the mouse dystrophin gene induced muscle degeneration similar to that observed in Duchenne muscular dystrophy. *Biochem. Biophys. Res. Commun.* **238**, 492–497 (1997).

261. Cohn, R. D. *et al.* Disruption of Dag1 in differentiated skeletal muscle reveals a role for dystroglycan in muscle regeneration. *Cell* **110**, 639–648 (2002).

262. Veltrop, M. *et al.* A dystrophic Duchenne mouse model for testing human antisense oligonucleotides. *PLoS One* **13**, (2018).

263. Young, C. S., Mokhonova, E., Quinonez, M., Pyle, A. D. & Spencer, M. J. Creation of a Novel Humanized Dystrophic Mouse Model of Duchenne Muscular Dystrophy and Application of a CRISPR/Cas9 Gene Editing Therapy. *J. Neuromuscul. Dis.* **4**, 139 (2017).

264. Egorova, T. V. *et al.* CRISPR/Cas9-generated mouse model of Duchenne muscular dystrophy recapitulating a newly identified large 430 kb deletion in the human DMD gene. *Dis. Model. Mech.* **12**, (2019).

265. Bulfield, G., Siller, W. G., Wight, P. A. L. & Moore, K. J. X chromosome-linked muscular dystrophy (mdx) in the mouse. *Proc. Natl. Acad. Sci. U. S. A.* **81**, 1189–1192 (1984).

266. Coulton, G. R., Morgan, J. E., Patridge, T. A. & Sloper, J. C. The mdx mouse skeletal muscle myopathy: A histological, morphometric and biochemical investigation. *Neuropathol. Appl. Neurobiol.* **14**, 53–70 (1988).

267. Grounds, M. D. Two-tiered hypotheses for Duchenne muscular dystrophy. *Cellular and Molecular Life Sciences* vol. **65** 1621–1625 (2008).

268. Stedman, H. H. *et al.* The mdx mouse diaphragm reproduces the degenerative changes of Duchenne muscular dystrophy. *Nat. 1991 3526335* **352**, 536–539 (1991).

269. Grady, R. M. *et al.* Skeletal and cardiac myopathies in mice lacking utrophin and dystrophin: A model for Duchenne muscular dystrophy. *Cell* **90**, 729–738 (1997).

270. Chandrasekharan, K. *et al.* A human-specific deletion in mouse Cmah increases disease severity in the mdx model of duchenne muscular dystrophy. *Sci. Transl. Med.* **2**, (2010).

271. Wood, C. L. *et al.* A comparison of the bone and growth phenotype of mdx, mdx: Cmah-/- and mdx:Utrn+/- murine models with the C57BL/10 wild-type mouse. *DMM Dis. Model. Mech.* **13**, (2020).

272. Mourkioti, F. *et al.* Role of telomere dysfunction in cardiac failure in Duchenne muscular dystrophy. *Nat. Cell Biol.* **15**, 895–904 (2013).

273. Sacco, A. *et al.* Short telomeres and stem cell exhaustion model duchenne muscular dystrophy in mdx/mTR mice. *Cell* **143**, 1059–1071 (2010).

274. Desguerre, I. *et al.* A new model of experimental fibrosis in hindlimb skeletal muscle of adult mdx mouse mimicking muscular dystrophy. *Muscle and Nerve* **45**, 803–814 (2012).

275. van Putten, M. *et al.* Natural disease history of the D2-mdx mouse model for Duchenne muscular dystrophy. *FASEB J.* **33**, 8110–8124 (2019).

276. Im, W. Bin *et al.* Differential expression of dystrophin isoforms in strains of mdx mice with different mutations. *Hum. Mol. Genet.* **5**, 1149–1153 (1996).

277. Lo, M. W. & Woodruff, T. M. Complement: Bridging the innate and adaptive immune systems in sterile inflammation. *Journal of Leukocyte Biology* vol. **108** 339–351 (2020).

278. Charles A Janeway, J., Travers, P., Walport, M. & Shlomchik, M. J. The complement system and innate immunity. (2001).

279. Stover, C. *et al.* The human gene for mannan-binding lectin-associated serine protease-2 (MASP-2), the effector component of the lectin route of complement activation, is part of a tightly linked gene cluster on chromosome 1p36.2-3. *Genes Immun.* **2**, 119–127 (2001).

280. Arlaud, G. J. *et al.* Structural biology of the C1 complex of complement unveils the mechanisms of its activation and proteolytic activity. *Molecular Immunology* vol. **39** 383–394 (2002).

281. Petry, F. *et al.* The mouse C1q genes are clustered on chromosome 4 and show conservation of gene organization. *Immunogenetics* **43**, 370–376 (1996).

282. Ramshaw, J. A. M., Shah, N. K. & Brodsky, B. Gly-X-Y tripeptide frequencies in collagen: A context for host-guest triple-helical peptides. *J. Struct. Biol.* **122**, 86–91 (1998).

283. Mortensen, S. A. *et al.* Structure and activation of C1, the complex initiating the classical pathway of the complement cascade. *Proc. Natl. Acad. Sci. U. S. A.* **114**, 986–991 (2017).

284. Beveridge, A. J., Wallis, R. & Samani, N. J. A molecular dynamics study of C1r and C1s dimers: Implications for the structure of the C1 complex. *Proteins Struct. Funct. Bioinforma.* **80**, 1987–1997 (2012).

285. Tschopp, J., Villiger, W., Fuchs, H., Kilchherr, E. & Engel, J. Assembly of subcomponents C1r and C1s of first component of complement: Electron microscopic and ultracentrifugal studies.

Proc. Natl. Acad. Sci. U. S. A. **77**, 7014–7018 (1980).

286. Kishore, U. *et al.* C1q and tumor necrosis factor superfamily: Modularity and versatility. *Trends in Immunology* vol. **25** 551–561 (2004).

287. Kemper, C. & Köhl, J. Back to the future – non-canonical functions of complement. *Seminars in Immunology* vol. **37** 1–3 (2018).

288. Hawksworth, O. A., Coulthard, L. G., Mantovani, S. & Woodruff, T. M. Complement in stem cells and development. *Seminars in Immunology* vol. **37** 74–84 (2018).

289. Singh, J., Ahmed, A. & Girardi, G. Role of complement component C1q in the onset of preeclampsia in mice. *Hypertens. (Dallas, Tex. 1979)* **58**, 716–724 (2011).

290. Watanabe, S. *et al.* Serum C1q as a novel biomarker of sarcopenia in older adults. *FASEB J.* **29**, 1003–1010 (2015).

291. Perlmutter, D. H. & Colten, H. R. Molecular immunobiology of complement biosynthesis: a model of single-cell control of effector-inhibitor balance. *Annual review of immunology* vol. **4** 231–251 (1986).

292. Lubbers, R., van Essen, M. F., van Kooten, C. & Trouw, L. A. Production of complement components by cells of the immune system. *Clinical and Experimental Immunology* vol. **188** 183–194 (2017).

293. Legoedec, J., Gasque, P., Jeanne, J. -F & Fontaine, M. Expression of the complement alternative pathway by human myoblasts in vitro: Biosynthesis of C3, factor B, factor H and factor I. *Eur. J. Immunol.* **25**, 3460–3466 (1995).

294. Legoedec, J., Gasque, P., Jeanne, J. F., Scotte, M. & Fontaine, M. Complement classical pathway expression by human skeletal myoblasts in vitro. *Mol. Immunol.* **34**, 735–741 (1997).

295. Horii, N. *et al.* Resistance training prevents muscle fibrosis and atrophy via down-regulation of C1q-induced Wnt signaling in senescent mice. *FASEB J.* **32**, 3547–3559 (2018).

296. Moralez, A., Busby, W. H. & Clemmons, D. Control of insulin-like growth factor binding protein-5 protease synthesis and secretion by human fibroblasts and porcine aortic smooth muscle cells. in *Endocrinology* vol. **144** 2489–2495 (Endocrinology, 2003).

297. Cedzyński, M., Thielens, N. M., Mollnes, T. E. & Vorup-Jensen, T. Editorial: The role of complement in health and disease. *Frontiers in Immunology* vol. **10** 1869 (2019).

298. Lieber, R. L., Schmitz, M. C., Mishra, D. K. & Friden, J. Contractile and cellular remodeling in rabbit skeletal muscle after cyclic eccentric contractions. *J. Appl. Physiol.* **77**, 1926–1934

(1994).

299. Del Rio-Tsonis, K., Tsonis, P. A., Zarkadis, I. K., Tsagas, A. G. & Lambris, J. D. Expression of the Third Component of Complement, C3, in Regenerating Limb Blastema Cells of Urodeles. *J. Immunol.* **161**, (1998).

300. Kimura, Y. *et al.* Expression of Complement 3 and Complement 5 in Newt Limb and Lens Regeneration. *J. Immunol.* **170**, 2331–2339 (2003).

301. Long, K. K., Pavlath, G. K. & Montano, M. Sca-1 influences the innate immune response during skeletal muscle regeneration. *Am. J. Physiol. - Cell Physiol.* **300**, (2011).

302. Kafadar, K. A. *et al.* Sca-1 expression is required for efficient remodeling of the extracellular matrix during skeletal muscle regeneration. *Dev. Biol.* **326**, 47–59 (2009).

303. Zhang, C. *et al.* Complement C3a signaling facilitates skeletal muscle regeneration by regulating monocyte function and trafficking. *Nat. Commun.* **8**, (2017).

304. Rouaud, T. *et al.* Complement C3 of the innate immune system secreted by muscle adipogenic cells promotes myogenic differentiation. *Sci. Rep.* **7**, 1–9 (2017).

305. Cornelio, F. & Dones, I. Muscle fiber degeneration and necrosis in muscular dystrophy and other muscle diseases: Cytochemical and immunocytochemical data. *Ann. Neurol.* **16**, 694–701 (1984).

306. Spuler, S. & Engel, A. G. Unexpected sarcolemmal complement membrane attack complex deposits on nonnecrotic muscle fibers in muscular dystrophies. *Neurology* **50**, 41–46 (1998).

307. Sewry, C. A., Dubowitz, V., Abraha, A., Luzio, J. P. & Campbell, A. K. Immunocytochemical localisation of complement components C8 and C9 in human diseased muscle the role of complement in muscle fibre damage. *J. Neurol. Sci.* **81**, 141–153 (1987).

308. Porter, J. D. *et al.* A chronic inflammatory response dominates the skeletal muscle molecular signature in dystrophin-deficient mdx mice. *Hum. Mol. Genet.* **11**, 263–272 (2002).

309. Pescatori, M. *et al.* Gene expression profiling in the early phases of DMD: a constant molecular signature characterizes DMD muscle from early postnatal life throughout disease progression. *FASEB J.* **21**, 1210–1226 (2007).

310. Liu, H. *et al.* Augmented Wnt signaling in a mammalian model of accelerated aging. *Science (80-.).* **317**, 803–806 (2007).

311. Kikuchi, A., Yamamoto, H. & Kishida, S. Multiplicity of the interactions of Wnt proteins and their receptors. *Cellular Signalling* vol. **19** 659–671 (2007).

312. White, B. D., Nguyen, N. K. K. & Moon, R. T. T. Wnt Signaling: It Gets More Humorous with Age. *Current Biology* vol. **17** (2007).

313. Yabumoto, C. *et al.* Angiotensin II receptor blockade promotes repair of skeletal muscle through down-regulation of aging-promoting C1q expression. *Sci. Rep.* **5**, (2015).

314. Conti, S., Cassis, P. & Benigni, A. Aging and the renin-angiotensin system. *Hypertension* **60**, 878–883 (2012).

315. Benigni, A., Cassis, P. & Remuzzi, G. Angiotensin II revisited: New roles in inflammation, immunology and aging. *EMBO Molecular Medicine* vol. **2** 247–257 (2010).

316. Benigni, A. *et al.* Disruption of the Ang II type 1 receptor promotes longevity in mice. *J. Clin. Invest.* **119**, 524–530 (2009).

317. Okada, K. *et al.* Wnt/β-catenin signaling contributes to skeletal myopathy in heart failure via direct interaction with forkhead box o. *Circ. Hear. Fail.* **8**, 799–808 (2015).

318. Cenacchi, G., Fanin, M., De Giorgi, L. B. & Angelini, C. Ultrastructural changes in dysferlinopathy support defective membrane repair mechanism. *J. Clin. Pathol.* **58**, 190–195 (2005).

319. Gallardo, E. *et al.* Inflammation in dysferlin myopathy: Immunohistochemical characterization of 13 patients. *Neurology* **57**, 2136–2138 (2001).

320. Selcen, D., Stilling, G. & Engel, A. G. The earliest pathologic alterations in dysferlinopathy. *Neurology* **56**, 1472–1481 (2001).

321. Choi, J. H. *et al.* Differential Immunohistological features of inflammatory myopathies and dysferlinopathy. *J. Korean Med. Sci.* **24**, 1015–1023 (2009).

322. Naoki Suzuki, Masashi Aoki, Yuji Hinuma, Toshiaki Takahashi, Yoshiaki Onodera, Aya Ishigaki, Masaaki Kato, Hitoshi Warita, Maki Tateyama, Y. I. Expression profiling with progression of dystrophic change in dysferlin-deficient mice (SJL). *Neurosci Res* **52**, 47–60 (2005).

323. Wenzel, K. *et al.* Increased Susceptibility to Complement Attack due to Down-Regulation of Decay-Accelerating Factor/CD55 in Dysferlin-Deficient Muscular Dystrophy. *J. Immunol.* **175**, 6219–6225 (2005).

324. Han, R. *et al.* Genetic ablation of complement C3 attenuates muscle pathology in dysferlin-deficient mice. *J. Clin. Invest.* **120**, 4366–4374 (2010).

325. Kissel, J. T., Mendell, J. R. & Rammohan, K. W. Microvascular Deposition of Complement

Membrane Attack Complex in Dermatomyositis. *N. Engl. J. Med.* **314**, 329–334 (1986).

326. Whitaker, J. N. & Engel, W. K. Vascular Deposits of Immunoglobulin and Complement in Idiopathic Inflammatory Myopathy. *N. Engl. J. Med.* **286**, 333–338 (1972).

327. Halterman, R. K., Rammohan, K. W., Mendell, J. R. & Kissel, J. T. The Relationship of Complement-Mediated Microvasculopathy to the Histologic Features and Clinical Duration of Disease in Dermatomyositis. *Arch. Neurol.* **48**, 26–30 (1991).

328. Mascaró, J. M. *et al.* Membrane Attack Complex Deposits in Cutaneous Lesions of Dermatomyositis. *Arch. Dermatol.* **131**, 1386–1392 (1995).

329. Burgin, S., Stone, J. H., Shenoy-Bhangle, A. S. & McGuone, D. Case 18-2014. *N. Engl. J. Med.* **370**, 2327–2337 (2014).

330. Jain, A. *et al.* Detection of the membrane attack complex as a diagnostic tool in dermatomyositis. *Acta Neurol. Scand.* **123**, 122–129 (2011).

331. Dalakas, M. C. Immunotherapy of myositis: Issues, concerns and future prospects. *Nature Reviews Rheumatology* vol. **6** 129–137 (2010).

332. Leddy, J. P., Griggs, R. C., Klemperer, M. R. & Frank, M. M. Hereditary complement (C2) deficiency with dermatomyositis. *Am. J. Med.* **58**, 83–91 (1975).

333. Miller, F. W. *et al.* Genome-wide association study identifies HLA 8.1 ancestral haplotype alleles as major genetic risk factors for myositis phenotypes. *Genes Immun.* **16**, 470–480 (2015).

334. Lintner, K. E. *et al.* Gene copy-number variations (CNVs) of complement C4 and C4A deficiency in genetic risk and pathogenesis of juvenile dermatomyositis. *Ann. Rheum. Dis.* **75**, 1599–1606 (2016).

335. Gilhus, N. E. *et al.* Myasthenia gravis. *Nature Reviews Disease Primers* vol. **5** 1–19 (2019).

336. Mantegazza, R., Vanoli, F., Frangiamore, R. & Cavalcante, P. Complement Inhibition for the Treatment of Myasthenia Gravis</p>. *ImmunoTargets Ther.* vol. **9**, 317–331 (2020).

337. Ashizawa, T. & Appel, S. H. Complement-dependent lysis of cultured rat myotubes by myasthenic immunoglobulins. *Neurology* **35**, 1748–1753 (1985).

338. Tüzün, E. *et al.* Circulating Immune Complexes Augment Severity of Antibody-Mediated Myasthenia Gravis in Hypogammaglobulinemic RIIIS/J Mice. *J. Immunol.* **172**, 5743–5752 (2004).

339. Dhillon, S. Eculizumab: A Review in Generalized Myasthenia Gravis. *Drugs* **78**, 367–376

(2018).

340. Weiser, M. R. *et al.* Reperfusion injury of ischemic skeletal muscle is mediated by natural antibody and complement. *J. Exp. Med.* **183**, 2343–2348 (1996).

341. Toomayan, G. A. *et al.* C1-esterase inhibitor and a novel peptide inhibitor improve contractile function in reperfused skeletal muscle. *Microsurgery* **23**, 561–567 (2003).

342. Kyriakides, C. *et al.* Skeletal muscle reperfusion injury is mediated by neutrophils and the complement membrane attack complex. *Am. J. Physiol. - Cell Physiol.* **277**, (1999).

343. Chan, R. K. *et al.* The Differing Roles of the Classical and Mannose-Binding Lectin Complement Pathways in the Events following Skeletal Muscle Ischemia-Reperfusion. *J. Immunol.* **177**, 8080–8085 (2006).

344. Rosenblatt, J. D., Lunt, A. I., Parry, D. J. & Partridge, T. A. Culturing satellite cells from living single muscle fiber explants. *Vitr. Cell. Dev. Biol. - Anim. J. Soc. Vitr. Biol.* **31**, 773–779 (1995).

345. Rando, T. A. & Blau, H. M. Primary mouse myoblast purification, characterization, and transplantation for cell-mediated gene therapy. *J. Cell Biol.* **125**, 1275–1287 (1994).

346. Gibbs, E. M. & Crosbie-Watson, R. H. A simple and low-cost assay for measuring ambulation in mouse models of muscular dystrophy. *J. Vis. Exp.* **2017**, (2017).

347. Aartsma-Rus, A. & Putten, M. van. Assessing Functional Performance in the Mdx Mouse Model. *J. Vis. Exp.* **85**, 51303 (2014).

348. Judson, R. N., Low, M., Eisner, C. & Rossi, F. M. Isolation, culture, and differentiation of Fibro/Adipogenic Progenitors (FAPs) from skeletal muscle. in *Methods in Molecular Biology* vol. **1668** 93–103 (Humana Press Inc., 2017).

349. Chen, H. Z., Tsai, S. Y. & Leone, G. Emerging roles of E2Fs in cancer: An exit from cell cycle control. *Nature Reviews Cancer* vol. **9** 785–797 (2009).

350. Gulati, P., Lemercier, C., Lappin, D., Whaley, K. & Gue, D. Expression of the components and regulatory proteins of the classical pathway of complement in normal and diseased synovium. *Rheumatol. Int.* **14**, 13–19 (1994).

351. Serrano A.L. *et al.* Cellular and molecular mechanisms regulating fibrosis in skeletal muscle repair and disease. *Curr. Top. Dev. Biol.* **96**, 167–201 (2011).

352. Du J. *et al.* Aging increases CCN1 expression leading to muscle senescence. *Am. J. Physiol. Cell Physiol.* **306**, (2014).

353. Reis E.S. *et al.* Applying complement therapeutics to rare diseases. *Clin. Immunol.* **161**, 225–240 (2015).

354. Jager U. *et al.* Inhibition of complement C1s improves severe hemolytic anemia in cold agglutinin disease: a first-in-human trial. *Blood* **133**, 893–901 (2019).

355. Feussner A., Kalina U., Hofmann P., Machnig T. & Henkel G. Biochemical comparison of four commercially available C1 esterase inhibitor concentrates for treatment of hereditary angioedema. *Transfusion* **54**, 2566–2573 (2014).

356. Uezumi A. *et al.* Fibrosis and adipogenesis originate from a common mesenchymal progenitor in skeletal muscle. *J. Cell Sci.* **124**, 3654–3664 (2011).

357. Clevers H. & Nusse R. Wnt/β-catenin signaling and disease. *Cell* **149**, 1192–1205 (2012).